

# **Development of Micro-Computed Tomography for Human Fetal Post- mortem Imaging**

**Mr Ian Craig Simcock**

Student Number: 18121056

Registration Date: 1<sup>st</sup> June 2018

Submitted for the degree of Doctor of Philosophy, PhD

University College London, UCL

London, 2021

## **Students Declaration**

I, Mr Ian Craig Simcock, confirm that the work presented in this thesis is my own. Where information has been derived from other sources, I can confirm that this has been indicated in the thesis.

Date 03 December 2021

# Abstract

Perinatal autopsy is an essential way of assessing the cause of fetal loss during pregnancy. However, parents are reluctant to consent to an invasive autopsy. Modern imaging techniques can offer a non-invasive solution, but most current clinical techniques are unable to offer adequate image resolution for early gestation miscarriages, typically below 20weeks gestation or 300g body weight.

This thesis describes evaluating micro-CT imaging for this purpose, culminating in developing a pragmatic clinical protocol.

Within this thesis, five aspects are evaluated:

1. Scan preparation. The optimal concentration and immersion time for I<sub>2</sub>KI was established, with a formula to predict the immersion time required for full iodination.
2. Imaging parameters. Optimal micro-CT imaging parameters were investigated, comparing the signal-to-noise (SNR) and relative contrast-to-noise ratio (rCNR) across different settings.
3. Patient factors. The effect of demographics/external factors on image quality was evaluated. Maceration was identified as having the greatest detriment to image quality, yet high image quality was attained in the majority of scans. Fetal weight and number of projections were also noted to be positive predictors.
4. Image SNR / rCNR. Assessments were tested across whole fetus organ volumes with imaging parameters defined as 110kV, 200 $\mu$ A, 250ms, 2frames-per-projection, enabling a single anatomical area to be optimally imaged within a clinically relevant timeframe, <30minutes.
5. Parental experience. A pilot study consisting of parents who have experienced a miscarriage was also undertaken. Response to the technique was overwhelmingly positive, with key potential benefits being increased choice and uptake of autopsy investigations with multiple mental health benefits.

Finally, the future direction of this work within the clinical setting is presented. The clinical impact of the research is to be able to offer parents a more acceptable non-invasive imaging investigation following miscarriage.

# Statement of Impact

I have developed and optimised a micro-CT clinical protocol for human fetal post-mortem imaging following early pregnancy loss. Whilst conventional autopsy provides the greatest diagnostic yield for the cause of death in early pregnancy loss, it is the invasive nature of these investigations that makes them unacceptable to most parents, yet non-invasive techniques currently available do not provide good diagnostic accuracy below 20 weeks gestation. This thesis describes a series of experiments to develop a clinical micro-CT protocol. I demonstrate that 2.5% I<sub>2</sub>KI solution can be used to fully iodinate a range of fetal weights (0-300 g), with minimal tissue distortion, and produce an equation to accurately predict the immersion times required prior to imaging. I develop a methodology and a set of clinically appropriate imaging parameters to provide maximal SNR and rCNR and determine the demographics and image quality that predict the image quality of the micro-CT scan. I also show that parents who have experienced a miscarriage are extremely positive about the technique and its ability to provide peace-of-mind, facilitate closure and to possibly provide answers relevant to the cause of death, leading them to fully support its development.

This work has potential benefits for parents, the medical profession and society:

Having experienced a miscarriage, parents may be offered a conventional autopsy, but the majority feel this technique is too invasive. Micro-CT imaging demonstrates a more acceptable alternative to parents with its high-resolution and non-invasive approach. This allows parents the peace-of-mind of being able to fully investigate their loss, in a manner of their choosing, with limited disturbance to the body, whilst providing clinicians with greater knowledge due to increased autopsy uptake. This would equate to better provision of future pregnancy care through increased understanding of the cause of miscarriage.

# Academic Output

The following is a summary of the work and achievements during this doctorate.

## Publications

Peer-reviewed journal articles directly arising from this thesis	11
Peer-reviewed journal articles written during PhD studies	12
Contribution to National professional guidelines	1

## Presentations directly related to this thesis

Invited speaker at International/National conferences and courses	5
Oral presentations at International/National conferences	11
Poster presentations at International/National conferences	3

## Academic Accolades

Prizes and awards	4
Grants	2

# Dissemination of Research

Where I am stated as first author on a publication or conference proceeding/presentation I led the development, completed the micro-CT scanning performed the data collection, analysis and wrote the paper. Where I am listed as a co-author I fully assessed the literature, completed the data collection and micro-CT scanning, and participated fully in the writing of the publication, with a smaller role in the analysis of the data.

## Chapter 1

Hutchinson JC, Shelmerdine SC, Lewis C, Parmenter J, **Simcock IC**, Ward L, Ashworth MT, Chitty LS, Arthurs OJ, Sebire NJ. Minimally invasive perinatal and pediatric autopsy with laparoscopically assisted tissue sampling: feasibility and experience of the MinImAL procedure. *Ultrasound Obstetrics and Gynecology* 2019; Nov;54(5):661-669.

Shelmerdine SC, Hutchinson JC, Lewis C, **Simcock IC**, Sekar T, Sebire NJ, Arthurs OJ. An evidence-based approach to post-mortem perinatal imaging. *Insights in Imaging* 2021; Jul 15;12(1):101.

## Chapter 2

Hutchinson JC, Shelmerdine SC, **Simcock IC**, Sebire NJ, Arthurs OJ. Early clinical applications for imaging at microscopic detail: Microfocus computed tomography (micro-CT). *British Journal of Radiology* 2017; Jul;90(1075): 20170113.

Shelmerdine SC, **Simcock IC**, et al. 3D printing from Microfocus computed tomography (micro-CT) in human specimens: education and future implications. *British Journal of Radiology* 2018; Jun 14:20180306.

### Chapter 3

**Simcock IC**, Hutchinson JC, Shelmerdine SC, Matos JN, Sebire NJ, Fuentes VL, Arthurs OJ. Investigation of optimal sample preparation conditions with potassium triiodide and optimal imaging settings for microfocus computed tomography of excised cat hearts. *American Journal of Veterinary Research* 2020; Apr;81(4):326-333.

Novo Matos J, Garcia-Canadilla P, **Simcock IC**, et al. Micro-computed tomography (micro-CT) for the assessment of myocardial disarray, fibrosis, and ventricular mass in a feline model of hypertrophic cardiomyopathy. *Scientific Reports* 2020 Nov 19;10(1):20169.

Tan TJ, Garcia--Cañadilla P, Bijnens B, Dejea H, Bonnin A, Tran V, Arthurs OJ, **Simcock IC**, Tobon-Geers C, Geers AJ, Comamala JV, Stampanoni M, Rau C, Cook AC. Using micro-CT and X-PCI to visualise coronary morphology and ventriculo-coronary arterial connections in the setting of pulmonary atresia with intact ventricular septum. *Medical Careers Conference, London UK 2018* (poster presentation).

**Simcock IC**, Hutchinson JC, Shelmerdine SC, Novo Matos J, Sebire NJ, Arthurs OJ. Image Optimisation in Micro Computed Tomography for feline hearts. *Tomography for Scientific Advancement Conference, Warwick, UK 2018* (oral presentation).

**Simcock IC**, Shelmerdine SC, Novo Matos J, Sebire NJ, Arthurs OJ. Optimisation of Tissue Preparation for Kidneys in Micro Computed Tomography. *Tomography for Scientific Advancement Conference, Southampton, UK 2019* (oral presentation).

Novo Matos J, Garcia-Canadilla P, **Simcock IC**, et al. Micro-computed tomography (micro-CT) for the assessment of myocardial disarray in a feline model of hypertrophic cardiomyopathy. *Tomography for Scientific Advancement. London, UK 2020* (oral presentation).

Olivares AL, Pons MI, Mill J, Novo Matos J, Garcia P, Cerrada I, Guy A, Hutchinson JC, **Simcock IC**, Arthurs OJ, Cook AC, Luis Fuentes V, Camara O. Shape analysis and computational fluid simulations to assess feline left atrial function and



thrombogenesis. Functional Imaging and Model of the Heart. Stanford University, California, USA 2021 (poster presentation).

#### **Chapter 4**

**Simcock IC**, Shelmerdine SC, Hutchinson JC, Sebire NJ, Arthurs OJ. Tissue preparation optimisation for post-mortem human fetal micro computed tomography. European Congress of Radiology, Vienna, Austria 2019 (oral presentation).

**Simcock IC**, Shelmerdine SC, Sebire NJ, Arthurs OJ. Effect of body weight on iodination for human fetal post-mortem micro-CT imaging. European Congress of Radiology, Vienna, Austria 2020 (oral presentation).

**Simcock IC**, Shelmerdine SC, Langan D, Sebire NJ, Arthurs OJ. Optimisation of Human Post-Mortem Micro-CT Service - Iodination and Image Quality Predictors. International Paediatric Radiology Congress, Rome, Italy 2021 (oral presentation).

#### **Chapter 5**

**Simcock IC**, "Coding Quantitative Data." Academic Involvement Group. Great Ormond Street Hospital, London UK. 2020 (oral presentation).

#### **Chapter 6**

**Simcock IC**, Shelmerdine SC, Hutchinson JC, Sebire NJ, Arthurs OJ. Human fetal whole-body postmortem microfocus computed tomographic imaging. Nature Protocols 2021 May;16(5):2594-2614.

**Simcock IC** "Development of Micro-CT for Human Fetal Post-mortem Imaging". Clinical Academic Careers Evening, Great Ormond Street Hospital, London, UK. 2018. (oral presentation).

**Simcock IC**, Shelmerdine SC, Sebire NJ, Arthurs OJ. Micro-CT of Early Gestation Fetuses: Technique, Tips & Tricks. European Congress of Radiology, Vienna, Austria 2020 (oral presentation).

**Simcock IC** “Guidelines for Imaging Small Fetuses Under 20 Weeks Gestation in Microcomputed Tomography”. Allied Health Professionals in Research. Great Ormond Street Hospital, London UK. 2019. (oral presentation).

**Simcock IC** “Development of a clinical micro-CT service for human fetal post-mortem imaging”. Great Ormond Street Hospital Conference. Great Ormond Street Hospital, London UK. 2021. (oral presentation).

## **Chapter 7**

**Simcock IC**, Shelmerdine SC, Langan D, Sebire NJ, Arthurs OJ. Predictors of image quality for human fetal post-mortem micro-CT. European Congress of Radiology, Vienna, Austria 2020 (oral presentation).

**Simcock IC**, Shelmerdine SC, Langan D, Sebire NJ, Arthurs OJ. Optimisation of Human Post-Mortem Micro-CT Service - Iodination and Image Quality Predictors. International Paediatric Radiology Congress, Rome, Italy 2021 (oral presentation).

## **Chapter 8**

Lewis C, **Simcock IC**, Arthurs OJ. Improving uptake of perinatal autopsy. Current Opinions in Obstetrics and Gynecology 2021. April 1;33(2):129-134.

**Simcock IC**, Lewis C, Shelmerdine SC, Sebire NJ, Arthurs OJ. Focus Group Findings – Parental feedback on micro-CT imaging following miscarriage. National Institute for Health Research Conference, Leeds, UK 2020 (poster presentation).

**Simcock IC**, Lewis C, Shelmerdine SC, Sebire NJ, Arthurs OJ. Knowing the answers gives you hope moving forward: parental views on micro-CT scanning following miscarriage. United Kingdom Imaging and Oncology Conference, Liverpool, UK 2021 (oral presentation).

**Simcock IC**, Lewis C, Shelmerdine SC, Sebire NJ, Arthurs OJ. “I just wanted answers”: parental views on micro-CT scanning following miscarriage. International

Society of Radiographers and Radiographical Technologists World Congress, Dublin Ireland 2021 (oral presentation).

## **Chapter 9**

Shelmerdine SC, Singh M, **Simcock IC**, Calder AD, Ashworth M, Beleza A, Sebire NJ, Arthurs OJ. Characterisation of Bardet Biedl Syndrome by post-mortem microfocus computed tomography (micro-CT). *Ultrasound Obstetrics and Gynecology* 2019 Jan;53(1):132-134.

Shelmerdine SC, **Simcock IC**, Hutchinson JC, Guy A, Ashworth MT, Sebire NJ, Arthurs OJ. Post-mortem microfocus computed tomography for non-invasive autopsies: experience in >250 human fetuses. *American Journal of Obstetrics and Gynecology* 2021 Jan;224(1):103.e1-103.e15.

**Simcock IC**, “Developing Non-invasive Imaging to Investigate Fetal Death.” Biomedical Research Centre / Institute of Child Health Showcase Event, Wellcome Institute, London, UK. 2019 (oral presentation).

## **Other output: promoting AHP / radiographer academic careers**

**Simcock IC**, Reeve R, Burnett C, Costigan C, McNair H, Robinson C, Arthurs OJ. Clinical academic radiographers – A challenging but rewarding career. *Radiography* 2021 (online ahead of print).

**Simcock IC**, “Being an AHP in a Research Hospital.” Chairperson. Great Ormond Street Hospital, London UK. October 2020.

**Simcock IC**, Rose E, Cooper J, Simcock C. Radiographer Career Development: Are we pushing the right buttons? United Kingdom Imaging and Oncology. Liverpool, UK. June 2020 (oral presentation).

**Simcock IC**. Development of Micro-CT for Human Fetal Post-Mortem Imaging. NIHR Great Ormond Street Hospital Biomedical Research Centre Showcase, Wellcome Collection, London, UK. 6<sup>th</sup> March 2019 (oral presentation).

Livermore P, Bichard E, Brind J, Evans J, Handley S, Harniess P, Jewell T, Katchburian I, Kerr-Elliott T, Kim J, Nightingale R, Shkurka E, **Simcock IC**, Sipanoun P, Stewart A. "The importance of peer-support for clinical academics at GOSH". Great Ormond Street Conference, London, UK. 2020 (oral presentation).

Eaton J, **Simcock IC**, Simcock C, Arthurs OJ. "Paediatric Research Radiographers: Great Ormond Street Hospital." United Kingdom Imaging and Oncology, Liverpool, UK. June 2020 (poster presentation).

**Simcock IC**, "Writing and Responding: Sharing experiences of being a reviewer and responding to reviews of papers submitted to peer reviewed journals." Academic Involvement Group, Great Ormond Street Hospital, London, UK. April 2021.

**Simcock IC**, Reeve R, Burnett C, Costigan C, McNair H, Robinson C, Arthurs OJ. Clinical academic careers - Challenges and benefits. International Society of Radiographers and Radiographical Technologists World Congress, Dublin Ireland 2021 (oral presentation).

Bruno C, Moumneh R, Sauvage E, Redaelli A, **Simcock I**, Schievano S, Capelli C, Shroff R. "A computational approach to investigate malfunctions of central venous lines in children". European Society for Paediatric Nephrology, Amsterdam, The Netherlands in September 2021 (poster presentation).

# Acknowledgements

The content of this thesis is the result of three years of study and collaborative work with many individuals who were selfless in sharing their skills and knowledge. Firstly, I would like to thank my PhD supervisors *Dr Owen Arthurs* and *Prof Neil Sebire* who provided me with the encouragement to begin this work and who sustained me with their constant advice and patient perseverance. I would also like to express my thanks to my funder the National Institute for Health Research.

My thanks must also go to the wider multidisciplinary team including *Dr Susan Shelmerdine* (paediatric radiologist), *Dr Ciaran Hutchinson* (paediatric pathologist), *Hannah McGarrick*, *Dasha Alvarez*, *Jade Parmenter*, *Bronya Czarny*, *Vanna Lee* and *Lakiesha Ward* (mortuary staff), *Dr Jose Novos Matos* (veterinary surgeon), *Ruth Bender-Atik* (National Director, Miscarriage Association), *Dr Bennie Smit* and *Dr Oliver Larkin* (Nikon Metrology engineers) and *Dr Xin Kang* (fetal medicine team at Brugmann University Hospital, Belgium) for their support and advice during this work.

I would also like to especially thank *Dr Dean Langan* (statistician) who supervised me in application of the statistical work and *Dr Celine Lewis* (social scientist) who supervised me in the qualitative methodology.

I am blessed to have such a supportive family and will be eternally grateful to my wife, Clare Simcock, for her unflinching support and encouragement throughout this doctorate and my two children, Elliott and Dylan, who always made me realise the importance of relaxing with a game of cricket or football in the garden.

Finally, I would like to thank the parents who consented to their children taking part in this study. They took part in this research at a time of distress so that we can advance the knowledge associated with post-mortem imaging and micro-CT.

# Table of Contents

Student declaration.....	2
Abstract.....	3
Statement of impact.....	5
Academic output.....	6
Dissemination of research .....	7
Acknowledgements .....	13
Figure list .....	22
Table list .....	25
Abbreviations .....	27
Thesis overview .....	29
<b>Chapter 1 Background.....</b>	<b>30</b>
<b>1.1 Overview .....</b>	<b>30</b>
<b>1.2 Miscarriage and stillbirth.....</b>	<b>30</b>
<b>1.3 Conventional autopsy investigations.....</b>	<b>32</b>
<b>1.4 Less-invasive autopsy investigations.....</b>	<b>33</b>
<b>1.5 Non-invasive imaging investigations .....</b>	<b>34</b>
1.5.1 Radiographs .....	34
1.5.2 Computed Tomography .....	35
1.5.3 Magnetic Resonance Imaging .....	36
1.5.4 Ultrasound .....	37
<b>1.6 Conclusion.....</b>	<b>38</b>
<b>Chapter 2 Micro-CT – What is it, how does it work and what can it offer? .....</b>	<b>39</b>
<b>2.1 Overview .....</b>	<b>39</b>
<b>2.2 Computed Tomography.....</b>	<b>39</b>
<b>2.3 Microfocus Computed Tomography.....</b>	<b>42</b>
<b>2.4 How it works .....</b>	<b>43</b>
<b>2.5 Micro-CT setup .....</b>	<b>43</b>
<b>2.6 Nano-CT .....</b>	<b>46</b>
<b>2.7 Phase-contrast imaging .....</b>	<b>47</b>
<b>2.8 Synchrotron imaging .....</b>	<b>48</b>
<b>2.9 Imaging Parameters.....</b>	<b>48</b>

2.9.1	Kilovoltage .....	48
2.9.2	Current.....	49
2.9.3	Exposure time.....	49
2.9.4	Gain.....	50
2.9.5	Frames-per-projection .....	50
<b>2.10</b>	<b>Phantoms.....</b>	<b>51</b>
<b>2.11</b>	<b>Signal to Noise (SNR) and relative Contrast to Noise (rCNR) .....</b>	<b>52</b>
<b>2.12</b>	<b>Micro-CT contrast agents.....</b>	<b>52</b>
2.12.1	Osmium tetroxide .....	53
2.12.2	Phosphotungstic acid .....	53
2.12.3	Potassium tri-iodide.....	54
2.12.4	Preferred contrast for micro-CT of human fetuses within this thesis .	56
<b>2.13</b>	<b>Historical development of micro-CT for post-mortem imaging .....</b>	<b>56</b>
2.13.1	Mouse embryo micro-CT imaging .....	56
2.13.2	Human fetal imaging .....	58
<b>2.14</b>	<b>Conclusion.....</b>	<b>59</b>
<b>2.15</b>	<b>Thesis aims and objectives.....</b>	<b>60</b>
<b>Chapter 3</b>	<b>Assessment of Micro-CT Scanning of Ex-Vivo Animal Organs.....</b>	<b>61</b>
<b>3.1</b>	<b>Overview .....</b>	<b>61</b>
<b>3.2</b>	<b>Experiment 1 – ex-vivo feline cardiac tissue .....</b>	<b>61</b>
<b>3.3</b>	<b>Introduction – previous animal I<sub>2</sub>KI usage.....</b>	<b>61</b>
<b>3.4</b>	<b>Aims .....</b>	<b>62</b>
<b>3.5</b>	<b>Methods .....</b>	<b>62</b>
3.5.1	Tissue Preparation – feline hearts .....	63
3.5.2	Imaging Acquisition – feline hearts .....	65
<b>3.6</b>	<b>Results .....</b>	<b>66</b>
3.6.1	Tissue preparation – feline hearts .....	66
3.6.2	Imaging parameters – feline hearts .....	68
<b>3.7</b>	<b>Discussion .....</b>	<b>73</b>
<b>3.8</b>	<b>Limitations .....</b>	<b>74</b>
<b>3.9</b>	<b>Conclusion.....</b>	<b>75</b>
<b>3.10</b>	<b>Considerations for Future Experiments.....</b>	<b>75</b>
<b>3.11</b>	<b>Experiment 2 – ex-vivo canine renal tissue .....</b>	<b>77</b>
<b>3.12</b>	<b>Introduction .....</b>	<b>77</b>
<b>3.13</b>	<b>Aims .....</b>	<b>77</b>
<b>3.14</b>	<b>Method .....</b>	<b>77</b>

3.14.1	Tissue preparation – canine kidneys .....	78
3.14.2	Iodination and tissue distortion analysis .....	79
<b>3.15</b>	<b>Results .....</b>	<b>83</b>
3.15.1	Tissue iodination – canine kidneys .....	83
3.15.2	Tissue distortion – canine kidneys.....	84
3.15.3	SNR.....	85
3.15.4	rCNR .....	86
<b>3.16</b>	<b>Discussion – canine kidneys .....</b>	<b>86</b>
<b>3.17</b>	<b>Limitations .....</b>	<b>88</b>
<b>3.18</b>	<b>Conclusion.....</b>	<b>88</b>
<b>3.19</b>	<b>Considerations for Future Experiments.....</b>	<b>89</b>
<b>3.20</b>	<b>Summary.....</b>	<b>89</b>
<b>3.21</b>	<b>Key Points.....</b>	<b>89</b>

## Chapter 4 Development of Tissue Preparation of Human Fetuses for Micro-CT Scanning 91

<b>4.1</b>	<b>Overview .....</b>	<b>91</b>
<b>4.2</b>	<b>Introduction – human fetal iodination .....</b>	<b>91</b>
<b>4.3</b>	<b>Experiment 1 – optimal I<sub>2</sub>KI concentration .....</b>	<b>92</b>
<b>4.4</b>	<b>Aims .....</b>	<b>92</b>
<b>4.5</b>	<b>Method .....</b>	<b>92</b>
4.5.1	Study population .....	92
4.5.2	Fetal iodination and scanning parameters .....	94
4.5.3	Fetal Head and abdomen analysis .....	94
<b>4.6</b>	<b>Results .....</b>	<b>95</b>
4.6.1	Tissue distortion .....	95
4.6.2	Tissue iodination.....	97
<b>4.7</b>	<b>Discussion .....</b>	<b>99</b>
4.7.1	Tissue iodination.....	99
4.7.2	Tissue distortion .....	101
<b>4.8</b>	<b>Limitations .....</b>	<b>101</b>
<b>4.9</b>	<b>Conclusion.....</b>	<b>103</b>
<b>4.10</b>	<b>Experiment 2 – larger cohort.....</b>	<b>103</b>
<b>4.11</b>	<b>Aims .....</b>	<b>104</b>
<b>4.12</b>	<b>Method .....</b>	<b>104</b>
4.12.1	Patient selection.....	104
4.12.2	Micro-CT scanning and I <sub>2</sub> KI immersion .....	104



4.12.3	Data analysis.....	105
<b>4.13</b>	<b>Results .....</b>	<b>105</b>
4.13.1	Study population.....	105
4.13.2	Gestational age and immersion time .....	107
4.13.3	Body weight and immersion time.....	108
4.13.4	Gestational age and body weight .....	109
<b>4.14</b>	<b>Discussion .....</b>	<b>109</b>
4.14.1	Gestational age .....	110
4.14.2	Body weight.....	110
4.14.3	Maceration .....	111
<b>4.15</b>	<b>Limitations .....</b>	<b>113</b>
<b>4.16</b>	<b>Conclusion / Summary .....</b>	<b>113</b>
<b>4.17</b>	<b>Key Points.....</b>	<b>114</b>

**Chapter 5 Development of Methodology For Quantitative Assessment Of Imaging Parameters .....** **115**

<b>5.1</b>	<b>Overview .....</b>	<b>115</b>
<b>5.2</b>	<b>Aims .....</b>	<b>115</b>
<b>5.3</b>	<b>Experiment 1 – ROI placement.....</b>	<b>116</b>
5.3.1	Aim .....	116
5.3.2	Background .....	116
5.3.3	Method.....	116
5.3.4	Results.....	118
5.3.5	Discussion .....	120
5.3.6	Conclusion.....	121
<b>5.4</b>	<b>Experiment 2 – Imaging parameter determination .....</b>	<b>122</b>
5.4.1	Background .....	122
5.4.2	Method.....	123
5.4.3	Results.....	124
5.4.4	Discussion .....	126
<b>5.5</b>	<b>Conclusion.....</b>	<b>129</b>
<b>5.6</b>	<b>Experiment 3 – phantom determination.....</b>	<b>130</b>
5.6.1	Background .....	130
5.6.2	Method.....	130
5.6.3	Results.....	131
5.6.4	Discussion .....	132
5.6.5	Conclusion.....	133

<b>5.7</b>	<b>Experiment 4 – Assessment of SNR and rCNR through 2D and 3D analysis</b>	<b>134</b>
5.7.1	Background	134
5.7.2	Method	134
5.7.3	Data analysis	136
5.7.4	Results	137
5.7.5	Discussion	138
5.7.6	Conclusion	141
<b>5.8</b>	<b>Limitations</b>	<b>141</b>
<b>5.9</b>	<b>Considerations for future experiments</b>	<b>142</b>
<b>5.10</b>	<b>Summary of findings</b>	<b>142</b>
 <b>Chapter 6 Quantitative Assessment of Imaging Parameters</b>		<b>144</b>
<b>6.1</b>	<b>Overview</b>	<b>144</b>
<b>6.2</b>	<b>Introduction – imaging parameters</b>	<b>144</b>
<b>6.3</b>	<b>Aims</b>	<b>145</b>
<b>6.4</b>	<b>Method</b>	<b>145</b>
6.4.1	Patient selection	145
6.4.2	Fetal preparation	146
6.4.3	Data analysis	147
<b>6.5</b>	<b>Results</b>	<b>150</b>
6.5.1	Study population	150
6.5.2	SNR and rCNR percentage changes	151
6.5.3	Determination of incremental percentage change as imaging parameters increased	154
6.5.4	Reduction of scanning time	158
6.5.5	Detector saturation elimination	159
<b>6.6</b>	<b>Discussion</b>	<b>162</b>
6.6.1	Maximal imaging parameters	163
6.6.2	Optimising clinical protocols on different micro-CT scanners	163
<b>6.7</b>	<b>Limitations</b>	<b>164</b>
<b>6.8</b>	<b>Conclusion</b>	<b>165</b>
<b>6.9</b>	<b>Summary</b>	<b>165</b>
<b>6.10</b>	<b>Key points</b>	<b>166</b>
 <b>Chapter 7 Evaluation of Image Quality in Human Fetal Post-mortem Micro-CT</b>		<b>167</b>
<b>7.1</b>	<b>Overview</b>	<b>167</b>

<b>7.2</b>	<b>Introduction – image quality</b>	<b>167</b>
<b>7.3</b>	<b>Aims</b>	<b>167</b>
<b>7.4</b>	<b>Methods</b>	<b>168</b>
7.4.1	Patient recruitment	168
7.4.2	Post-mortem micro-CT imaging	170
7.4.3	Demographic data and imaging factors	170
7.4.4	Image analysis	171
7.4.5	Statistical analysis	174
<b>7.5</b>	<b>Results</b>	<b>175</b>
7.5.1	Demographics and imaging parameters	175
7.5.2	Overall image quality assessments	176
7.5.3	Maceration and iodination assessments	177
7.5.4	Image quality predictors	177
<b>7.6</b>	<b>Discussion</b>	<b>181</b>
<b>7.7</b>	<b>Limitations</b>	<b>183</b>
<b>7.8</b>	<b>Conclusion</b>	<b>183</b>
<b>7.9</b>	<b>Summary</b>	<b>183</b>
<b>7.10</b>	<b>Key points</b>	<b>184</b>
<b>Chapter 8 Focus group investigations into early pregnancy loss from the family’s perspective: a pilot study</b>		<b>185</b>
<b>8.1</b>	<b>Overview</b>	<b>185</b>
<b>8.2</b>	<b>Introduction – parental perceptions of autopsy</b>	<b>185</b>
<b>8.3</b>	<b>Aims</b>	<b>186</b>
<b>8.4</b>	<b>Methods</b>	<b>186</b>
8.4.1	Funding	186
8.4.2	Study participants and recruitment	186
8.4.3	Data collection	187
8.4.4	Data handling and analysis	188
<b>8.5</b>	<b>Results</b>	<b>189</b>
8.5.1	Participant recruitment	189
8.5.2	Participant characteristics	190
8.5.3	Findings	192
8.5.4	Internal themes	193
8.5.5	Outer-world benefits of micro-CT	195
8.5.6	Thematic sentences	198
<b>8.6</b>	<b>Discussion</b>	<b>198</b>

8.7	Limitations .....	200
8.8	Conclusion.....	201
8.9	Summary.....	201
8.10	Key points.....	202
<b>Chapter 9 Future Direction for post-mortem micro-CT of human fetuses. ....</b>		<b>203</b>
9.1	Summary of findings .....	203
9.2	How has this technique changed local clinical practice? .....	204
9.3	Limitations of this thesis.....	205
9.3.1	Other imaging techniques and contrast agents .....	205
9.3.2	Qualitative assessment of parental views following post-mortem imaging techniques.....	207
9.3.3	Diagnostic accuracy studies .....	207
9.4	Future clinical integration .....	208
9.5	Future research direction.....	209
9.5.1	Evaluation of the additional diagnostic yield of micro-CT following miscarriage .....	209
9.5.2	Ongoing public, patient involvement and experience .....	212
9.5.3	Ongoing engagement through pregnancy loss charities.....	212
9.6	Conclusion.....	213
<b>10, Appendix 1 Nature Protocols paper .....</b>		<b>214</b>
<b>11, Appendix 2 Ethics .....</b>		<b>215</b>
<b>12, Appendix 3 Post-mortem Examination Consent Form .....</b>		<b>218</b>
<b>13, Appendix 4 Thesis Common Methods .....</b>		<b>230</b>
<b>14, Appendix 5 Data analysis guide.....</b>		<b>239</b>
<b>15, Appendix 6 Focus group recruitment.....</b>		<b>248</b>
<b>References .....</b>		<b>251</b>

# Figure List

## Chapter 1

- 1.1 Differences between standard, less-invasive and minimally-invasive autopsies 34
- 1.2 Appropriateness of post-mortem imaging modalities in relation gestational age and body weight 38

## Chapter 2

- 2.1 Clinical CT scanner in Great Ormond Street Hospital 40
- 2.2 Med-X micro-CT scanner 42
- 2.3 Micro-CT system with fixed SOD and ODD 44
- 2.4 Micro-CT system with flexible SOD and ODD 45
- 2.5 Micro-CT image of feline heart without contrast enhancement 46

## Chapter 3

- 3.1 Phantom containing air, water, ethanol, and wax 64
- 3.2 Serial micro-CT images of a feline heart during iodination 64
- 3.3 Flow diagram for feline cardiac tissue investigations 65
- 3.4 ROI placement within feline cardiac tissue 66
- 3.5 Signal intensity for inner and outer myocardium immersed in 1.25% and 2.5% I<sub>2</sub>KI 67
- 3.6 SNR effects due to changing imaging parameters 71
- 3.7 rCNR effects due to changing imaging parameters 72
- 3.8 ROI placement within canine renal tissue 79
- 3.9 Measurement of canine renal iodination and tissue distortion 81
- 3.10 Serially imaged canine kidneys following immersion in solution 82
- 3.11 Percentage iodination for canine kidneys following immersion in I<sub>2</sub>KI solution 83
- 3.12 Tissue distortion for canine kidneys following immersion in I<sub>2</sub>KI solution 84
- 3.13 SNR effects following immersion in I<sub>2</sub>KI solution 85
- 3.14 rCNR effects following immersion in I<sub>2</sub>KI solution 86

## Chapter 4

4.1	Flow diagram for exclusion criteria	93
4.2	Methodology to measure iodination within the head and body of human fetuses	95
4.3	Head diameter tissue distortion	96
4.4	Comparison of head and abdomen tissue distortion	97
4.5	Serial imaging of fetal heads following immersion in differing I <sub>2</sub> KI concentrations	98
4.6	Iodination effect of immersion in differing I <sub>2</sub> KI concentrations	99
4.7	Maceration effects on diagnostic detail	100
4.8	Compression effects on fetal head	104
4.9	Flow diagram for exclusion criteria for larger iodination study	106
4.10	Linear regression of gestational age vs immersion time	107
4.11	Linear regression of body weight vs immersion time	108
4.12	Linear regression of body weight vs gestational age	109

## Chapter 5

5.1	ROI placement within head, heart, and liver	118
5.2	SNR and rCNR for head, heart, and liver	120
5.3	ROI position within a liver	124
5.4	SNR and rCNR effects of changing imaging parameters	125
5.5	Changing image quality as imaging parameters are altered	126
5.6	Low image quality at exposure time 66ms	127
5.7	ROI within phantom material	131
5.8	rCNR changes as kilovoltage is increased	132
5.9	ROI of whole liver within a single slice	135
5.10	3D segmentation of a complete liver volume	136
5.11	SNR assessments for 3 x small ROI, single liver slice and whole liver volume	137
5.12	rCNR assessments for 3 x small ROI, single liver slice and whole liver volume	138

## Chapter 6

6.1	SNR and rCNR effects with changing imaging parameters	152
-----	---	-----

6.2	Image quality changes with increasing kilovoltage	155
6.3	Image quality changes with increasing kilovoltage	156
6.4	Image quality changes with increasing kilovoltage	157
6.5	Image quality changes with increasing kilovoltage	168
6.6	Optimal imaging parameters demonstrating image quality	161
6.7	Demonstration of detector saturation due to kilovoltage and current	162

## **Chapter 7**

7.1	Flow diagram for time to immersion and iodination time	171
7.2	Iodination descriptions	172
7.3	Bimodal distribution of time to immersion	175
7.4	Image quality scores head vs chest	176

## **Chapter 8**

8.1	Flow diagram for recruitment of study	189
-----	---------------------------------------	-----

## **Chapter 9**

9.1	Clinical micro-CT referrals (2014-2021)	205
9.2	High resolution images from optimised imaging protocol	206
9.3	Flow diagram for future post-mortem micro-CT investigations	211

# Table List

## Chapter 1

1.1 Annual UK birth and death statistics in 2019	31
--	----

## Chapter 2

2.1 Effects on x-ray beam and scan time in changing imaging parameters	51
2.2 Properties of three contrast agents	56

## Chapter 3

3.1 Time to plateau for feline cardiac tissue in 1.25% and 2.5% I <sub>2</sub> KI	68
3.2 Literature review for cardiac micro-CT protocols	70

## Chapter 4

4.1 Demographics of the I <sub>2</sub> KI group's	94
---	----

## Chapter 5

5.1 Imaging factors to compare differing anatomical areas	116
5.2 Effects on x-ray beam and scan time in changing imaging parameters	122
5.3 Imaging parameters for initial investigations to effect of changing imaging parameters	123
5.4 Optimised imaging parameters for investigation of SNR and rCNR effects	128
5.5 Advantages and disadvantages of three segmentation methods	140

## Chapter 6

6.1 Imaging parameters to investigate SNR and rCNR changes in whole fetuses	147
6.2 Descriptions of the maceration criteria by which the axial head and chest images were assessed	149
6.3 Demographics of human fetuses cohort	150
6.4 Maceration scores for the human fetus cohort	151



6.5	Percentage change in SNR and rCNR with changing kilovoltage	155
6.6	Percentage change in SNR and rCNR with changing current	156
6.7	Percentage change in SNR and rCNR with changing exposure time	157
6.8	Percentage change in SNR and rCNR with changing FPP	158
6.9	Steps taken to reduce scanning protocol below 30 minutes	159
6.10	Steps taken to eliminate detector saturation and maximise SNR and rCNR	160
6.11	Previously employed imaging parameters for human fetuses	163

## **Chapter 7**

7.1	Demographics for study cohort	169
7.2	Demonstration of partial and full iodination	173
7.3	Demonstration of image quality rankings	174
7.4	Patient demographics	178
7.5	Tissue preparation	179
7.6	Imaging parameters	180

## **Chapter 8**

8.1	Demographics of focus groups	191
8.2	Categories and codes for micro-Ct imaging for miscarriage	192

# Abbreviations

<b>CHL</b>	Crown-Heel Length
<b>CRL</b>	Crown-Rump Length
<b>CT</b>	Computed Tomography
<b>EPS</b>	Effective Pixel Size
<b>FG</b>	Focus Group
<b>FPP</b>	Frames Per Projection
<b>GOSH</b>	Great Ormond Street Hospital
<b>HC</b>	Head Circumference
<b>I<sub>2</sub></b>	Iodine
<b>I<sub>2</sub>KI</b>	Potassium Tri-Iodide
<b>IUD</b>	Intra Uterine Death
<b>KI</b>	Potassium Iodide
<b>kV</b>	Kilovoltage
<b>LIA</b>	Less-Invasive Autopsy
<b>MIA</b>	Minimally-Invasive Autopsy
<b>Micro-CT</b>	Microfocus Computed Tomography
<b>MRI</b>	Magnetic Resonance Imaging
<b>NIHR</b>	National Institute for Health Research
<b>NHS</b>	National Health Service
<b>ODD</b>	Object-Detector Distance

<b>OT</b>	Osmium Tetroxide
<b>PCI</b>	Phase Contrast Imaging
<b>PMCT</b>	Post-Mortem Computed Tomography
<b>PMMR</b>	Post-Mortem Magnetic Resonance Imaging
<b>PTA</b>	Phosphotungstic Acid
<b>QA</b>	Quality Assurance
<b>rCNR</b>	Relative Contrast-to-noise ratio
<b>ROI</b>	Regions Of Interest
<b>SI</b>	Signal Intensity
<b>SNR</b>	Signal-To-noise Ratio
<b>SOD</b>	Source-Object Distance
<b>TOP</b>	Termination Of Pregnancy
<b>UK</b>	United Kingdom
<b>U/S</b>	Ultrasound
<b>w/v</b>	Weight By Volume

# Thesis overview

This thesis addresses the use of micro-CT for perinatal autopsy as an alternative to conventional autopsy. Prior to this, proof of principle work had demonstrated the ability of micro-CT to provide diagnostic detail in human fetal hearts and whole human fetuses, but the imaging protocol used had not been fully developed to become an efficient & reproducible clinical protocol.

This thesis therefore comprises of 9 chapters, which describes the series of experiments undertaken to develop micro-CT for human fetal post-mortem imaging into an optimised clinical protocol.

Chapter 1 details a literature search describing the development of minimally-invasive imaging techniques for perinatal autopsy, and their strengths and weakness. The need for micro-CT examination is made, against a backdrop of increased parental acceptability of less-invasive investigations.

Chapter 2 provides a detailed description of how micro-CT works, its strengths and weaknesses and the available exogenous contrast agents to demonstrate soft tissue abnormalities. The previous uses of micro-CT are also explained and how this relates to post-mortem imaging. The overall aims and objectives are stated in developing an optimised clinically appropriate protocol for tissue preparation and imaging parameters for whole human fetal micro-CT imaging.

Chapter 3 describes several ex-vivo animal tissue experiments: to optimise the tissue preparation and imaging parameters required for ex-vivo feline cardiac tissue and canine renal tissue. A range of different I<sub>2</sub>KI concentrations were assessed, along with the imaging parameters for kilovoltage, current and exposure time to maximise the SNR and rCNR. Immersion in 2.5% I<sub>2</sub>KI solution for 48 hours provided full iodination, with imaging parameters of 100kV, 150μA and 354ms were found to maximise SNR and rCNR in feline cardiac tissue. Immersion in 2.5% I<sub>2</sub>KI solution for 100 hours was found to provide full iodination with minimal tissue distortion for canine kidney tissue.

Chapter 4 describes experiments to optimise the tissue preparation of human fetuses in terms of tissue distortion and iodination time. The relationship between immersion time, gestational age, and body weight was evaluated to develop a clinical protocol to accurately predict the immersion time required for human fetuses (0-300g body weight) in 2.5% I<sub>2</sub>KI.

Chapter 5 describes the methodology development to evaluate the effect imaging parameters (kilovoltage, current, exposure time and frames per projection (FPP)) have on SNR and rCNR used in Chapter 6. Optimal ROI placement, a maximal range of imaging parameters and appropriate phantom materials were determined. Automated whole organ ROI assessment of the liver, using a 2.5% I<sub>2</sub>KI phantom allowed accurate reproducible assessment of SNR and rCNR.

Chapter 6 describes the experiments to determine the effect imaging parameter changes have on SNR and rCNR for human fetal micro-CT scanning. Imaging parameters of 130 kV, 250  $\mu$ A, 250 ms and 2 FPP provided the optimal clinical protocol.

Chapter 7 describes the effect demographics and imaging parameters have on human fetal micro-CT image quality. High image quality was achievable for most fetuses, with maceration and body weight being strong negative predictors, and number of projections and FPP being the strongest positive predictors of image quality.

Chapter 8 describes an exploratory qualitative study of parental perceptions of micro-CT for non-invasive autopsy. Two focus group of patients who had experienced a miscarriage felt there were multiple benefits of micro-CT: increased autopsy uptake, advancing medical knowledge, engagement with the post-mortem process and mental health benefits through peace-of-mind and facilitating closure. Parents felt strongly that this technique should be more widely available.

Chapter 9 describes how the developed protocol designed within this thesis could be used within the clinical environment and future work. The challenges to its adoption and the advantages it can provide for families and healthcare professions are discussed.

# Chapter 1      **Background**

## **1.1 Overview**

This chapter describes the background for this thesis, the development of non-invasive post-mortem imaging techniques for perinatal autopsy, and their strengths and weaknesses. The need for micro-CT examination is made against a backdrop of increased parental acceptability of less-invasive investigations.

All the work presented in this chapter was undertaken by the author of this thesis. Some of this work has been published in *Ultrasound Obstetrics and Gynecology* in 2019 [1] and *Insights into Imaging* in 2021 [2].

## **1.2 Miscarriage and stillbirth**

Pregnancy loss, either from miscarriage, defined as the loss of a pregnancy before viability at 24 weeks or stillbirth, defined as the death after 24 weeks gestation is a commonly occurring event [3]. In the United Kingdom (UK) it is estimated that 8 babies are stillborn and over 500 babies are miscarried every day, with 1 in 4 pregnancies ending in loss during pregnancy or birth [4, 5]. Few countries publish miscarriage statistics, and since miscarriage commonly occurs at home with 80% occurring before the 12<sup>th</sup> week of gestation [3, 6], collation of accurate pregnancy loss data is difficult. The estimated 23 million miscarriages occurring each year globally is based solely on a calculated 15% total risk of miscarriage [3, 7] with the possibility that the actual number could be far higher.

**Table 1.1 Annual birth and death statistics within the UK for 2019 [4]**

	Number in 2019
Miscarriage	Approx. 187,975
Stillbirth	2763
Live births	712,680

The news that a pregnancy has ended, no matter the time point during pregnancy, can be an extremely traumatic moment in a parent's life, and the way this is dealt with can have repercussions for the future well-being for the family [8]. This event is often unexpected, with only a short time to come to terms with the loss [9] and studies have shown that this can lead to prolonged grief, depression, anxiety and post-traumatic stress regardless of the age of the fetus and is an under researched area of medicine [7, 10-13].

It has also been shown that despite its common occurrence, miscarriage is little understood by both the general public and health care professionals alike [14], with many believing it to be rare, and possibly caused by lifting or previous contraceptive use, as well as the misconception that no treatment is available [14, 15]. These myths can cause mothers to believe they are at fault and stop them seeking help and support, which can lead to their isolation from family, friends, and partners [6, 9].

Gaining information into the cause of the death can give parents a degree of closure on the event, alleviate the emotional worry that may accompany future pregnancies and enable future pregnancies to proceed with reduced emotional trauma [16]. This is an under-researched area, given the undisclosed number of pregnancy losses and potential impact it can have on short- and long-term health [7].

### 1.3 Conventional autopsy investigations

Determining the cause for pregnancy loss is extremely important to parents and medical practitioners [17, 18], with the current standard of care being a standard (invasive) autopsy, also known as a post-mortem. This technique has been used over a long period in history and involves cutting into the body, removing the organs, inspecting them for signs of disease and abnormalities, and taking tissue samples to allow further specialised histopathological investigation and genetic analysis (Figure 1.1) [19]. It can determine the factors that contributed to the death, identify concomitant diseases that may influence future pregnancies, provide a clinical audit, and determine if any iatrogenic factors were present, whilst also assisting in the grieving process for the family [19-22]. It has been shown to provide additional diagnosis or information in 40-70% of perinatal deaths [23-25] with 15–51% of cases not previously been suspected clinically [26-29].

Despite this, parental uptake rates within stillbirth and miscarriage are low at 55% [21] with informed consent required from the mother or both parents before it can proceed due to the parent having sole responsibility for consenting to this investigation [22].

There are many reasons why parents may decline any investigation into their loss including lack of communication about the value of the procedure between professionals and parents and religious beliefs [8]. Broadly speaking, parents dislike the invasive nature of an autopsy: the need to make incisions to examine organs and take tissue samples is not welcomed by parents, and parental uptake is well below the minimum recommended rate of 75% [8, 30-32]. 44% stillbirths, 38% perinatal deaths 25% neonatal deaths [21, 33].

If parents are offered an investigation following a pregnancy loss it is often simply a binary choice for parents of a standard autopsy or no investigation at all.

In 2012 the National Health Service (NHS) England and the Department of Health indicated that one of the key areas of investigation should be to develop additional techniques which investigate into the cause of death whilst minimising the need to cut open the body. This led to the development of a greater choice of investigations to be



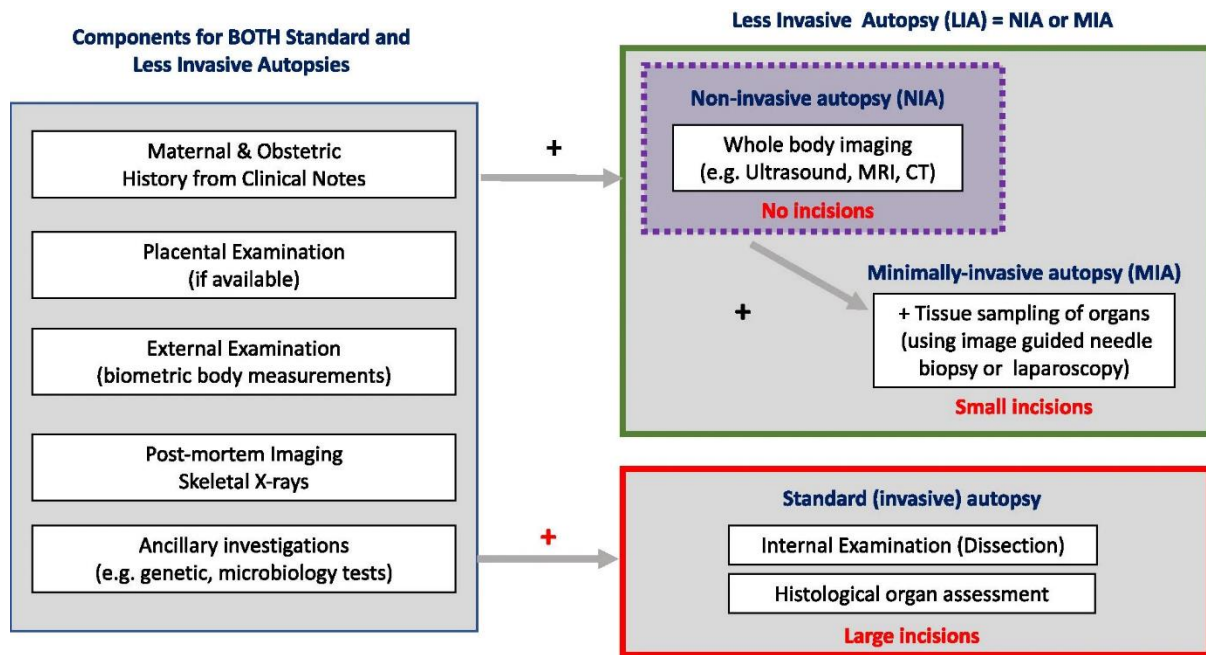
developed including post-mortem imaging with no dissection of the body required, and minimally invasive procedures including image guided biopsies and endoscopic investigations, with limited incisions and is classed as a “less invasive autopsy” (LIA) (Figure 1.1) [22, 32, 34].

#### **1.4 Less-invasive autopsy investigations.**

This term has come to represent procedures where the majority of the invasive internal examination is replaced by post-mortem imaging. Where tissue sampling is required, larger incisions to the body are avoided through the use of endoscopic or percutaneous techniques. These allow histological assessment of these samples and permit genetic testing to be completed [35].

These examinations can be performed “blind” as a percutaneous needle biopsy but demonstrate a poor yield in collecting the correct organ sample of sufficiently intact tissue [36]. Whereas laparoscopic techniques allow visualisation of the organ and tissue sampling area through a small incision in the abdominal wall showing a subsequent increase in the sampling success of over 80% [36, 37]. These techniques where image guided tissues are sampled is also called a “minimally invasive autopsy” (MIA) (Figure 1.1).

These techniques represent a reduction in the degree of invasiveness, with smaller incisions being made but allowing tissue sampling for histopathological assessment. This is more acceptable to parents and allows them to balance their need to protect their child against large incisions yet enabling a more thorough investigation to be completed. Any incision may still be too invasive for some parents [16, 38], therefore there is a need for accurate non-invasive imaging techniques to determine the cause of fetal death during pregnancy.



**Figure 1.1** Different components of standard, less-invasive and minimally-invasive autopsies, reproduced with permission [2]

## 1.5 Non-invasive imaging investigations

A non-invasive autopsy refers to an imaging only technique where no invasive procedures are carried out and is continually being developed within radiology (Figure 1.1) [35, 39, 40]. This can identify anatomical abnormalities, and therefore narrow down syndromes and genetic disorders, which can then be used to identify possible risks for siblings [41, 42]. These imaging practices must be adapted and applied differently for adults, children and fetuses depending on the age and size of the patient [41]. This area of radiology has evolved into its own speciality yet requires collaboration with histopathological services to ensure optimal diagnostic approaches, with advantages seen in earlier and increased identification of fetal abnormalities, and syndromic diseases [33, 43, 44]. Many techniques are now available with specific advantages and disadvantages, ranging from conventional radiographs to cross sectional imaging.

### 1.5.1 Radiographs

Radiographs are two-dimensional images created through the exposure of an object to x-rays. As the x-ray beam passes through the object, the radiation can be absorbed or attenuated. This is determined by the x-ray beams spectral composition as well as

the density and atomic number of the materials within the specimen. Therefore, structures within the body which exhibit a significant difference in their x-ray attenuation characteristics, enable visualisation of these differences, such as bone fractures or air within certain anatomical structures.

Although radiographs are widely available and are performed in most post-mortem investigations to image the skeleton, they provide diagnostically useful information in <1% of cases [35]. Whole fetal radiographs should only be performed in suspected skeletal abnormalities [41, 44-47], and provide only limited information on the soft tissue structures within the body.

### **1.5.2 Computed Tomography**

Computed tomography (CT) is a modality that also uses the attenuation of x-rays to provide information on the structures within the body. The majority of clinical CT scanners in use today are classified as third generation and uses an x-ray source and detector at opposite sides of the body which revolves through 360° whilst the patient is moved through the x-ray beam. This configuration constantly scans the patient in a helical manner, with shortened examination times in comparison to previous generations of clinical CT scanners. It can provide greater detail through the reconstruction of the collected data into 3-dimensional images. It lends itself well to the investigation of the cause of death as it is quick, relatively cheap, and widely available within clinical practice. This makes it widely utilised in the adult post-mortem imaging setting for fracture detection, intracranial pathologies and in medicolegal proceedings [48, 49], but has shown limited utility for fetal and childhood post-mortem imaging.

In cases of fetal death, CT can provide information on abnormalities of the skeletal system and the differential detection of air/fluid within normally aerated organs [44, 50-53]. The main problem in fetal and neonatal imaging is the poor soft-tissue contrast due to the lack of intra-abdominal fat, meaning unenhanced CT has limited diagnostic ability [52, 54]. Exogenous contrast can be delivered and is gaining popularity in the adult post-mortem imaging setting [55], but remains technically challenging in small children and fetuses due to the more challenging venous access [54, 56] with the resulting diagnostic accuracy and yield yet to be confirmed [57]. Imaging the heart is

also feasible following direct cardiac venous access [57], but has not been widely adopted. Low resolution is also associated with this technique in fetuses <20 weeks gestation due to their physical small size [58]. Although, bone detail can be provided after ossification commences, at 8 weeks gestation, it is only useful in specific clinical situations regarding suspected skeletal abnormalities, with the vast majority of uses only diagnostic after 20 weeks gestation [2].

Therefore, although post-mortem CT (PMCT) can provide diagnostic information on the skeleton and lungs, it provides limited soft tissue detail, with low resolution imaging on fetuses <20 weeks gestation.

### **1.5.3 Magnetic Resonance Imaging**

Post-mortem magnetic resonance imaging (PMMR) is a technique that provides excellent detail on the soft tissue structures within the body [41] and has been proven in detecting neurological [33, 52, 59], cardiac [41] and abdominal abnormalities [60], with particular uses in brain imaging prior to conventional autopsy [59]. Studies showing confirmation of the conventional autopsy diagnosis in 60-80% of cases [46, 61] have proven this imaging method to be the primary technique for fetal and perinatal post-mortem imaging [62].

PMMR has specific limitations: Whilst post-mortem results have been shown to be diagnostic at 1.5T in larger (above 500 grams body weight) and older gestation fetuses (>24 weeks), below this range the accuracy of PMMR reduces significantly, with the results relying on sufficient signal being detected at high resolution [44, 63-65]. Poor signal can be overcome in the post-mortem setting with 3D techniques, and longer scanning times (>30 minutes), as there is no movement artefact, but this reduces clinical throughput [62]. Jawad et al., found that fetuses >500g results in high diagnostic accuracy for PMMR in 90% of cases yet this falls to 50% of cases <200g [66].

Whilst higher field strengths, such as 3T PMMR have shown good results in cardiac imaging it is unsure whether this offers considerable improvement over 1.5T in other anatomical areas [42, 64, 67, 68], and although >7T has shown further improvement in image production, it is only currently available within the laboratory setting [69, 70].

Higher field strength MRI does not yet provide sufficiently high diagnostic accuracy below 20 weeks gestation [68]. Although 9.4T increases the diagnostic information available at lower gestational ages and weights through greater spatial resolution and higher tissue contrast [69], it remains an expensive specialist procedure, time consuming with up to 18 hours of scanning required and is extremely rare within a clinical setting.

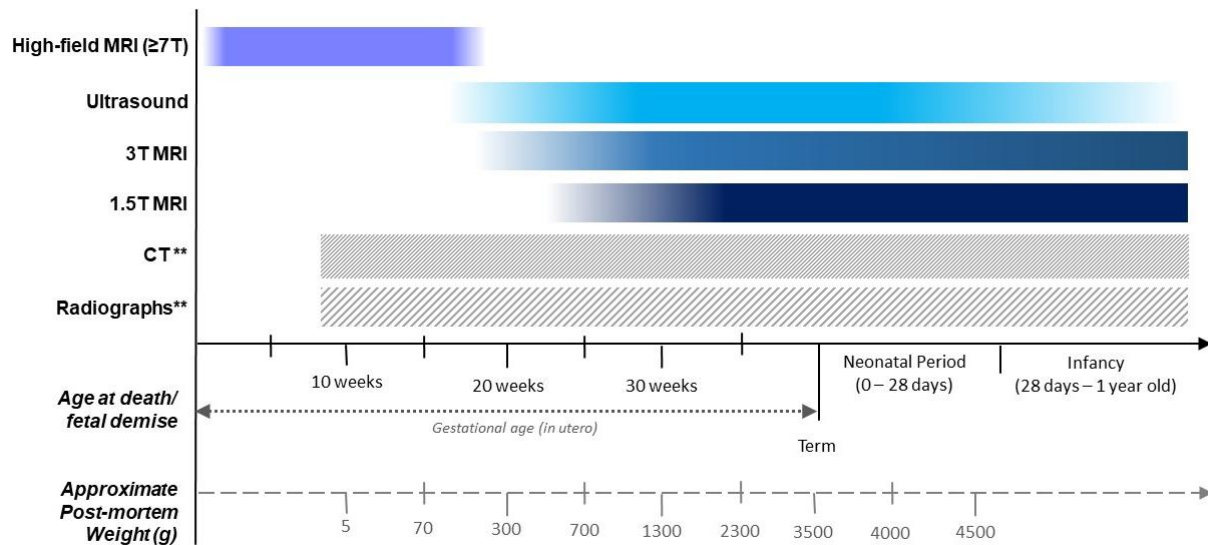
A further limitation for PMMR is the pressure on most imaging centres to perform magnetic resonance imaging (MRI) scans on living patients, often resulting in waiting lists and the required prioritisation of the living over deceased patients. PMMR is also a time-consuming process, requiring up to 2.5 hours scanning time, and consequently requires dedicated resources which may already be under pressure [71].

Overall, although the superior soft tissue definition is better demonstrated than other post-mortem imaging techniques, smaller fetuses suffer from lower diagnostic accuracy due to poor signal and a fixed resolution. Accompanied by a high demand for MRI scanning time for living patients and long examination times, this technique is unsuitable for post-mortem imaging following early pregnancy loss.

#### **1.5.4 Ultrasound**

Ultrasound (U/S) is also a low cost, easily available and non-invasive technique with high concordance rates with autopsy [33, 44, 64]. It is also able to provide diagnostic details on the brain and lungs due to open cranial sutures and the lack of air within the lungs [41]. However it is challenging to determine central nervous system malformations in early gestations (<20 weeks) due to lack of fetal development [65], and is challenging to assess thoracic and cardiac pathologies due to distortion, size of organs and the limit of ultrasound resolution [71, 72]. Ultrasound is also operator dependant and requires specialist training to ensure high diagnostic accuracy [44], with fetal maceration also reducing the ability to provide diagnostic results [71].

Despite these limitations, there is large concordance between ultrasound and PMMR, therefore ultrasound may be used as a triage tool to determine whether a conventional autopsy is required [46]. The lack of sufficiently high resolution for early gestation fetuses restricts its usage within this cohort of patients.



**Figure 1.2 Demonstration of imaging modalities with reference to approximate gestational ages and body weights, adapted with permission from [2].**

## 1.6 Conclusion

Post-mortem radiological investigations have rapidly expanded recently to provide increasing options for parents and professionals alike. Parental acceptance for less-invasive autopsy based on imaging is high. All these techniques require specialist training not only in ensuring correct application of the investigations, but also in understanding the post-mortem changes that can often mimic pathological changes [51, 73].

However, all these techniques have limited diagnostic accuracy below 20 weeks gestation due to either low resolution, poor signal, or limited contrast to noise, (Figure 1.2). This leaves a clear area of investigation for fetuses of <20 weeks gestation that currently has no satisfactory non-invasive imaging technique and demonstrates the need for the work outlined in this PhD.

## **Chapter 2      Micro-CT – What is it, how does it work and what can it offer?**

### **2.1 Overview**

This chapter describes how micro-CT works, its strengths and weaknesses and the available contrast agents to demonstrate soft tissue abnormalities. The previous uses of micro-CT are also explained and how this relates to post-mortem imaging. A suitable contrast agent is also identified for use within this thesis. The overall aims and objectives are stated in developing an optimised clinically appropriate protocol for tissue preparation and imaging parameters for whole human fetal micro-CT.

All the work presented in this chapter was undertaken by the author of this thesis.

A selection of the material included in this chapter has been published in British Journal of Radiology in 2017 [74] and 2018 [75].

### **2.2 Computed Tomography**

Computed tomography (CT) (Figure 2.1) is a clinical procedure where 3D images of the internal structure of the human body can be visualised and has been used as a vital tool within the clinical hospital setting for decades [76].

CT images are possible due to the principle of x-ray attenuation. When x-rays pass through an object, they are either absorbed or attenuated depending on the density and atomic number of the object. The attenuated x-rays are then detected on a photo-sensitive detector array to provide information on the density and atomic number of the object within the x-ray beam.



**Figure 2.1 Clinical CT scanner in Great Ormond Street Hospital for Children**

In CT, the x-ray production and detectors are placed on opposite sides of a circular aperture around which they are rotated. The patient then lies on a bed or gantry which travels through this aperture whilst being exposed to the x-rays. The x-ray beam is then rotated through  $360^\circ$  to attain information of the whole slice of tissue being irradiated from multiple angles. This data is reconstructed using mathematical techniques into 2-dimensional slices/images as the patient is moved incrementally through the aperture until the desired anatomical area has been imaged [77].

Finer “slices” will allow increased resolution of the structures but will also have inherently lower signal-to-noise (SNR) and relative contrast-to-noise ratio (rCNR) due to fewer photons striking the detector cell. These “slices” can then be either viewed in 2-dimensions in the axial plane they were attained in or combined to produce a 3-dimensional image which can be viewed in alternative planes.



Noise in CT scanning is any unwanted change in the signal intensity, in an area where otherwise a homogeneous signal would be seen and is demonstrated by an increased grainy appearance. This can detract from the observer's ability to identify the true signal and make accurate diagnoses. Reducing the noise in any imaging technique provides an improved ability to observe true differences between adjacent structures [78].

The slice thickness can be altered depending on the structures to be imaged, and the scanner capabilities, but is commonly between 1 and 10 mm [79]. The spatial resolution of an image depends on a number of factors including, the x-ray focal spot size, number of projection views per rotation of the x-ray tube, detector cell size and the reconstruction algorithms [80]. Achieving the maximum theoretical resolution may not be possible if a given value of power in Watts, (kilovoltage (kVp) x current ( $\mu$ A)) is required to penetrate a specimen and provide sufficient attenuated x-ray photons to the detectors to produce a diagnostic image. By increasing the power, the spot size is increased and becomes the limiting factor for the minimum resolution possible [80, 81]. Although increased spatial resolution is now possible due to breakthroughs in detector technology, there are still questions over radiation dose efficiency, scanning speed, and the financial cost for this increase in spatial resolution imaging [80].

It is this lack of spatial resolution for clinical CT, combined with a poor soft tissue contrast, due to a lack of fat between the fetal organs, that reduces the diagnostic ability of clinical CT scanners for fetal autopsy. This limits the technique in diagnosing abnormalities in fetuses <24 weeks gestation [64, 82].

Image contrast in CT scanning is the difference in signal intensity between two areas within an image. Low contrast is seen when two areas have a similar signal intensity, making distinguishing one area from another more difficult and can occur when the signal intensity for both areas is either high or low. High contrast is seen when two areas within an image have a much greater difference in signal intensity, making it easier to distinguish the two areas.

Therefore, whilst CT is extremely useful for many clinical applications in larger fetuses through to adulthood, an ability to visualise smaller structures for use within the laboratory setting is not possible and a higher resolution system is required [83-85].

### **2.3 Microfocus Computed Tomography**

Microfocus computed tomography (micro-CT), (Figure 2.2) was first described in 1982 [86] and is a technique that has historically been used in industry and archaeology to image small specimens with a resolution in the order of microns. The development of megapixel charge-coupled device detectors and increases in computer memory and speed allowed this technique to advance swiftly, with increased computing efficiency and higher resolutions [87, 88].



**Figure 2.2 Med-X micro-CT scanner (Nikon Metrology, Tring, UK)**

## **2.4 How it works**

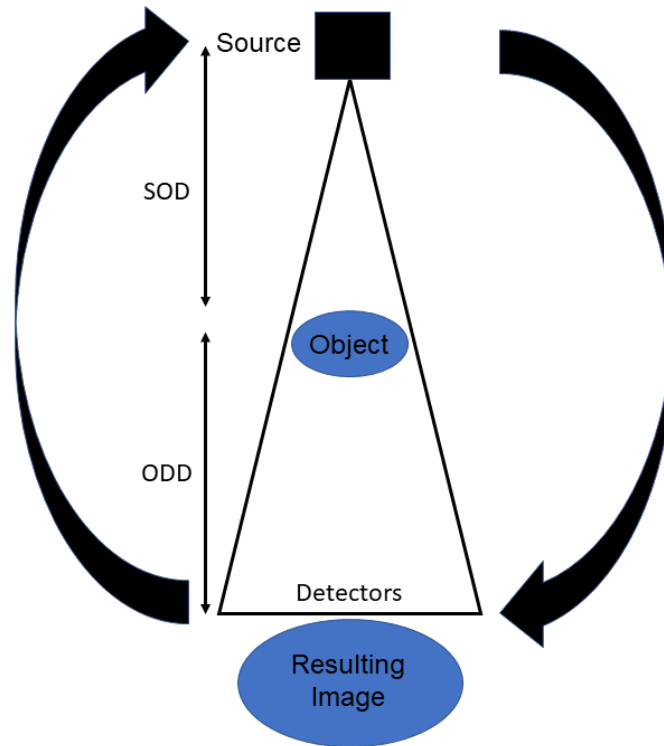
Micro-CT works by emitting electrons from a cathode filament and projecting them onto a target material. Although in theory any material can create x-rays, a dense material with a high atomic number is used to increase the number of x-rays produced. Copper, Silver, Tungsten and Molybdenum are commonly used in many micro-CT scanners. These x-rays are created in multiple directions, but the beam is collimated to restrict the x-rays into the desired cone beam shape. The finer the electron beam, the smaller the spot size of the x-rays allowing a possible higher resolution.

The choice of target material is dependent on the specimen being imaged, the corresponding x-ray spectra required, the rate at which heat can be removed from the x-ray target, and the parameters chosen for the x-ray beam [87]. Due to the higher resolutions attainable by the micro-CT technique the 3-dimensional reconstructions will also have a reduced isotropic voxel size [89]

## **2.5 Micro-CT setup**

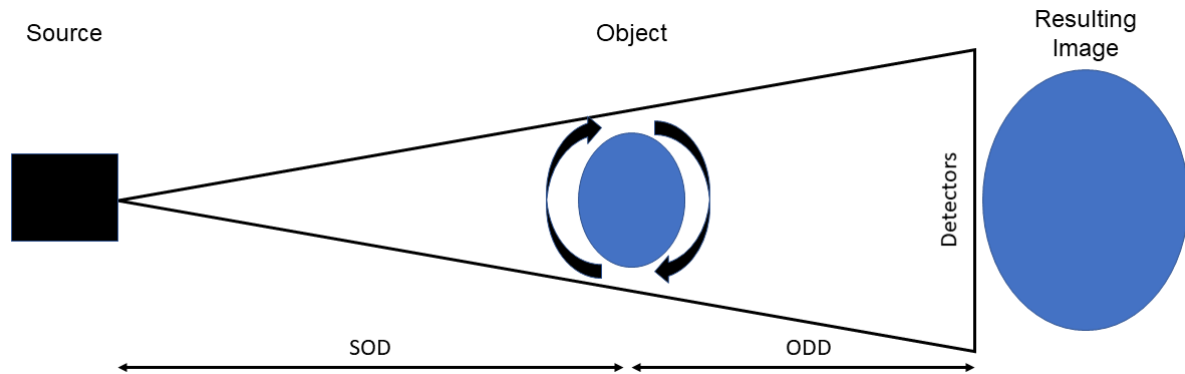
Two micro-CT setups are possible.

Firstly, where the radiation source and x-ray detectors are mounted on a gantry and rotate around the specimen [89, 90], similar to a CT scanner. This setup has a fixed source-object distance (SOD) and object-detector distance (ODD), (Figure 2.3) and is less flexible due to this fixed magnification, and limitations due to the size and shape of the specimen that can be imaged [90].



**Figure 2.3 Micro-CT system with a fixed SOD and ODD resulting in a fixed magnification**

The second setup has the specimen mounted on a turntable, which is rotated independently of the radiation source and x-ray detectors to enable variation of the SOD and the ODD, which in turn allows the geometric magnification level to be varied [89], (Figure 2.4). This is a more flexible system enabling a greater variation of specimen sizes to be optimally imaged, as the specimen can be moved along the x-ray beams axis, to be positioned closer to the x-ray source. This allows increased magnification as the specimen is projected over a greater number of x-ray detector cells [90]. This allows a smaller specimen to be moved closer to the x-ray source, whilst remaining wholly within the cone x-ray beam, thus resulting in a higher magnification and a corresponding higher resolution image.

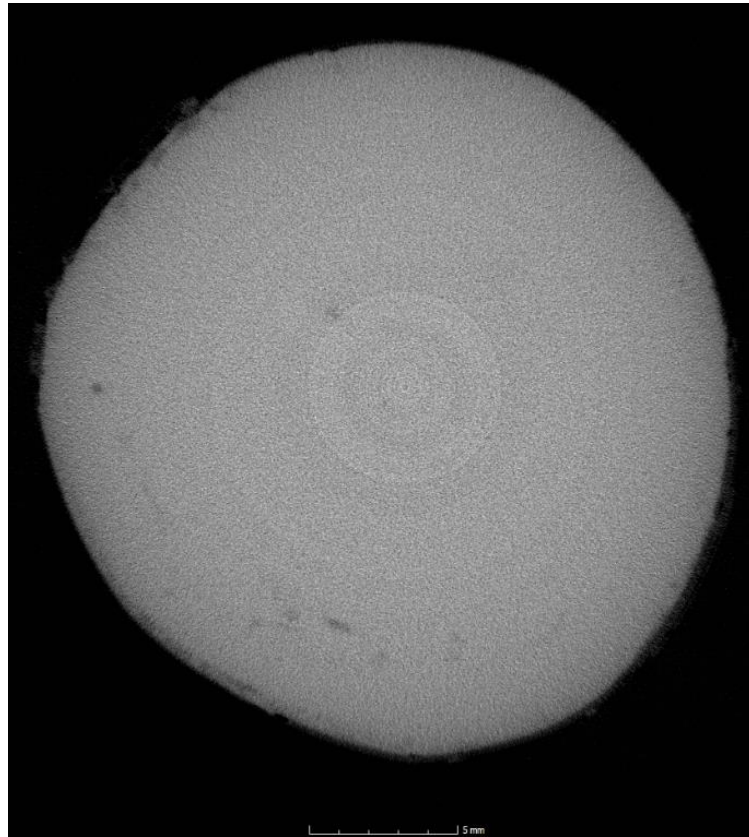


**Figure 2.4 Micro-CT system where the SOD and ODD are variable enabling a more flexible system and a greater range of specimen sizes and magnification options**

Similar to CT, repeated X-rays as the specimen is rotated through 360° allows a series of images to be reconstructed using a modified Feldkamp filtered back-projection algorithm to enable x-ray attenuation information within the scanned volume to be calculated [91]. This enables a 3-dimensional model consisting of isotropic voxels to be created. The numerical value for each of these voxels is a linear x-ray attenuation coefficient and results in 3-dimensional volume of brightness values [92]. The advantages of this isotropic micro-CT imaging system are the ability to view a wide range of specimen sizes flexibly, to achieve microscopical equivalent resolution in any plane with no loss of detail and to enable perception of complicated structures in multiple planes.

Similar to x-ray and CT, micro-CT relies on the differential attenuation of these x-rays by the specimen due to its atomic number and density [92]. It therefore provides excellent signal contrast between soft tissue structures and bone [83]. This allows teeth or calcified bone to be investigated without additional contrast due to the high atomic number of calcium in relation to that of soft tissue structures. This technique has been used extensively to investigate bone density and volume [93], as well as its architecture [94] in a non-destructive manner. A wide range of soft tissues structures attenuate x-rays equally, resulting in little discernible difference evident of the internal structure, (Figure 2.5).

This lack of soft tissue detail can be overcome by the introduction of an exogenous contrast agent.



***Figure 2.5 Micro-CT image of a feline heart with no contrast agent, displaying no internal structures***

## **2.6 Nano-CT**

Nano-CT also uses x-ray emission similar to micro-CT, but instead uses a smaller focal spot size (<400 nm) to achieve superior resolution. This technique also benefits from higher resolution, but is affected by increased imaging time in comparison to micro-CT [95].

Due to the higher resolution that is attainable, this can result in an increased data output [96], however, the field of view is in comparison to micro-CT significantly reduced with the volume inspected correspondingly reduced. Thought should still be given though to the long-term storage solutions as the amount of data created by this x-ray technique is still considerable.

As this technique still utilises the absorption characteristics of a specimen to identify differences between structures, it also requires an exogenous contrast agent and therefore a suitable tissue preparation method.

## **2.7 Phase-contrast imaging**

Phase contrast imaging (PCI) was first described in 1965 [97, 98] and as a technique is able to overcome the limited soft tissue sensitivity to conventional x-ray imaging when detecting the differences in x-ray absorption [99-101].

Instead of measuring the intensity changes in the x-ray beam, this technique measures the resultant phase changes, after passing through a specimen. These angular deflections are more pronounced at the interface between two differing materials, with the deflection varying depending on the structures present [102]. Therefore, this technique does not require any exogenous contrast agent and is thus able to create detailed images equivalent to micro-CT.

This technique is rapidly developing into possible new areas of clinical practice including breast, musculoskeletal, lung, vascular and brain [101]. Intra-operative breast specimen imaging has now been developed to complete a clinical acquisition within a clinically relevant timeframe of less than 30 minutes. This allowed a sensitivity increase of over 50%, when compared to conventional x-ray imaging in this particular area of imaging. [103]. This technique allows an increase in the sensitivity over conventional x-ray imaging, with the ability to detect and determine in 3-dimensions the relationship between the tumour and the surgical specimen margin. This is relevant in providing imaging feedback to the surgeons whilst tumour removal surgery is taking place [103]. However, histopathological methods in tumour detection still provide a higher sensitivity, and availability is currently limited, with few commercially available systems as well as limitations on the current achievable field-of-view.

The main advantage of this technique is that it requires no exogenous contrast agent to visualise the soft tissue structures, eliminating the need to iodinate/prepare the fetus prior to imaging. Immobilisation techniques would still be needed to ensure the un-iodinated fetus would remain still during the image acquisition.

At present, although advances have been made in enabling thicker samples through higher x-ray energies, reduced imaging time, and increases in the sensitivity of PCI, this technique is not currently suitable for human clinical imaging. Further advances may soon make these systems more widely available, with greater flexibility and suitable for a greater range of specimens.

## **2.8 Synchrotron imaging**

Synchrotron imaging can provide exceptional high-resolution imaging of extremely small structures with high contrast-to-noise resolution of sub-cellular levels of detail (<60 nm) [92, 104]. It also uses phase contrast imaging to provide detail on the differences between soft tissue structures, but it requires a particular source of radiation to image the specimens, with few facilities available worldwide [42, 105]. This also increases the cost of this technique [96], indicating that this technique is not suitable for widespread clinical post-mortem imaging.

## **2.9 Imaging Parameters**

Imaging parameters play an important role in the acquisition of diagnostic quality of micro-CT images [85], (Figure 2.1). Key parameters are kilovoltage, current, exposure time, gain and frames-per-projection in the quality of an image and the scan time [85]. In of living organisms the radiation dose must be included in determining the optimal imaging parameters to ensure that sufficient image quality is attained, yet radiation dose is kept as low as reasonably practicable to reduce cancer inducing effects. Radiation dose does not require consideration for post-mortem imaging and the imaging parameters can be manipulated to maximise signal. However, attention must be given to the scan time. To become a wide-reaching clinical practice patients must be able to be imaged with sufficiently signal to create a diagnostic image but be able to be completed within a reasonable time frame.

### **2.9.1 Kilovoltage**

Kilovoltage is the potential applied to the x-ray tube to accelerate electrons from the cathode to the anode, these hit the target producing heat and x-ray photons. These



x-ray photons are dependent on the kilovoltage originally applied to determine their energy.

If the kilovoltage is too low, less x-ray photons are able to penetrate the specimen and reach the detector cells. If the kilovoltage is too high, a larger number of x-ray photons are able to penetrate the specimen possibly causing saturation of the detectors. By selecting the appropriate kilovoltage an image can be produced determined by the atomic number, density, and thickness of the specimen.

Overall, the number of emitted photons varies with roughly with the square of the kVp, hence, although a change in the kilovoltage does not directly change the scan time, a reduction in the kilovoltage will require longer exposure times to enable a sufficient number of x-ray photons to reach the detectors, whereas an increase in the kilovoltage will enable a subsequent reduction in the exposure time.

Kilovoltage also affects image contrast. Higher kilovoltages reduces x-ray attenuation, which enables more photons to pass through a specimen without any interaction, resulting in poorer contrast between differing tissues.

### **2.9.2 Current**

Current is important as it heats up the filament allowing electrons to be released, therefore affecting the number of electrons. This in turn effects how many x-ray photons are created within the x-ray beam. Increasing the current subsequently increases the number of x-ray photons produced. Therefore, as with kilovoltage, a reduction in the current will require longer exposure times to enable a sufficient number of x-ray photons to reach the detectors, whereas an increase in the current will enable a subsequent reduction in the exposure time.

### **2.9.3 Exposure time**

Exposure time is the length of time that the x-ray photons are being created, and therefore affects the amount produced to interact with the specimen and therefore reach the target. Too little causes an increase in the image noise, whereas too long and the detectors will be saturated and not produce an image. This factor also affects the scan time, with an increase in exposure time causing an increase in the scan time.

#### **2.9.4 Gain**

Gain refers to the sensitivity of the detectors and by increasing the gain an increase in both the ability to detect signal and the noise detected is observed. This parameter does not directly affect the scan time.

#### **2.9.5 Frames-per-projection**

During scanning, the specimen is continually rotated through 360°. During this rotation, x-ray production is initiated for a set time as denoted by the exposure time. An optimal number of projections and angles throughout the 360° rotation is determined by the width of the specimen, yet ensuring sufficient data is available to allow isotropic voxels are possible when the 3-dimensional data set is reconstructed.

The frames-per-projection (FPP) identifies the number of exposures that are initiated at each of these angles. Increasing the FPP will increase the signal in relation to the noise with a subsequent increase in the observed image quality.

Frames-per-projection (FPP) is the number of times an image is created at a specific angle within the 360° rotation. Increasing the FPP does not affect the x-ray beam but does affect the scan time by causing a doubling from 1 to 2. This effect on the scan time is observed as it is increased.

Increasing it also enables an increase in the signal to be observed due to the cumulative effect of true signal gained from a specimen within the x-ray beam. However, noise is random and so does not cumulatively increase. Therefore, an increase causes an increase in the signal but not the noise and an increase in the image quality is observed.

Correct selection of these parameters is important to ensure sufficient signal is present with noise reduced to maximise image quality and produce diagnostic quality images.

**Table 2.1 The effects of changing individual imaging parameters on the x-ray beam and scan time**

	Effect on x-ray beam	Effect on scan time
Kilovoltage	Increase causes an increase in the energy of the x-ray photons	Decrease results an increase in scan time
Current	Increase causes an increase in the number of x-ray photons produced	Decrease results an increase in scan time
Exposure Time	Increase causes an increase in the length of time the x-rays are produced for each imaging position	Increase causes an increase in scan time
Gain	Increase causes an increase in the sensitivity of the detectors	None
Frames per Projection	Increase affects the number of times the specimen is exposed in each position throughout 360° of rotation	Increase causes an increase in scan time

## 2.10 Phantoms

Phantoms are used to ensure that data collected over time can be compared and to work accurately they must be filled with a comparable and stable material [106]. Previous phantoms have been constructed from vials of water, air, alcohol, wax, and iodine solutions [70, 84, 106, 107]

By including a phantom material within several imaging datasets, the results can be compared with reference to the measurement of a phantom material.

## **2.11 Signal to Noise (SNR) and relative Contrast to Noise (rCNR)**

SNR and rCNR are important in assessing the image created.

### **SNR**

SNR assesses the signal or meaningful information in comparison to the noise, which is random and detracts from the image itself, and allows for comparison between scan protocols. The higher the SNR, the more improved the image is.

This is calculated by the following equation [108].

$$\text{SNR} = \text{Mean signal} \div \text{standard deviation of the signal}$$

The mean signal refers to the area under investigation, with the standard deviation defined from the equivalent measurement.

### **rCNR**

This can be used to measure image quality and compares the contrast difference between an area of interest and the background, but also considers the variation of the signal in the background as this will impact on the ability to delineate a structure within an image.

It is calculated with the following equation [109].

$$\text{rCNR} = (\text{Mean signal} - \text{Background}) \div \text{Standard deviation of background}$$

The mean signal refers to the area under investigation, with the background identified as an area of a constant solution as defined by the phantom.

## **2.12 Micro-CT contrast agents**

Micro-CT provides high resolution detail, but also requires adjacent structures to be distinguished between to provide information on their size, position, and shape.

Contrast between structures is the inherent property of the sample, but if insufficient differences exist in the attenuation of x-ray photons then an exogenous contrast agent is required to accentuate these differences and provide increased contrast. This section describes the various micro-CT contrast agents that are available and have shown promise in previous biological tissue studies by enhancing soft tissue structures [110].

### **2.12.1 Osmium tetroxide**

Osmium tetroxide (OT) has previously been used in imaging biological specimens, demonstrating high differential densities between tissues [111, 112]. However, several limitations are noted. Epithelial skin layers impair the chemical diffusion of osmium [111] which can delay or even arrest diffusion across these layers, resulting in long preparation times or incomplete contrast enhancement.

Combined with its limited penetration and its inability to penetrate tissue stored in alcohol, means it is only suitable for small specimens several millimetres in depth [92].

It is also highly toxic [113] with damage to the skin, eyes, and respiratory system through incorrect exposure, and is expensive to purchase in relation to other contrast agents. It can also produce tissue deformation resulting in alteration of the original tissue dimension and their relation to adjacent structures [114]. Therefore, the lack of depth penetration and potential toxicity make it unsuitable for human fetal post-mortem imaging.

### **2.12.2 Phosphotungstic acid**

Phosphotungstic Acid (PTA) is a solution containing Tungsten ions [104] and by binding to collagen and fibrin [115], as well as proteins and connective tissue [92], enhances multiple structures within biological tissue. This has previously been used for histology and synchrotron imaging to demonstrate mouse heart anatomy and vasculature [104, 113] with the added advantage of its stability as a solution over several months [114].

However, there are limitations on its ability to penetrate biological tissue, including a very slow penetration over a matter of millimetres [92, 113, 114].

For example, whole mice embryos were fully penetrated with PTA after 4-12 days with an initial diffusion rate of 20µm/h dropping to 10µm/h over the following days [104]. Although, this is sufficient for small specimens (4-6mm diameter), it is unlikely to be suitable for increasing specimen size with longer exposure times.

This lack of penetration has previously been overcome in mice through its use as a perfusion agent within the vessels of a specimen. Although this allowed greater delineation of the vessel walls within the heart than potassium tri-iodide) I<sub>2</sub>KI, it produced a less homogeneous stain within the tissues themselves [113].

Dullin et al., (2017) [104] also reported tissue distortion following exposure to PTA, noting that mice hearts increased in volume by 8.9% after 6 days immersion. This was compared to a volume reduction of 7.1% due to drying during conventional histological examination. Overall, the lack of depth penetration makes PTA unsuitable for human fetal imaging.

### **2.12.3 Potassium tri-iodide**

Potassium tri-iodide (I<sub>2</sub>KI) is the most widely used and perhaps the most suitable of the contrast agents currently available. It is also referred to as Lugol's solution and differentially stains biological tissue and historically consists of double the weight of KI as that of I<sub>2</sub> dissolved in a volume of H<sub>2</sub>O [116].

When the specimen is immersed in a solution of I<sub>2</sub>KI, the iodine diffuses into the tissue over several days with the exact mechanism with which the iodine binds to the complex carbohydrate molecules still unknown [114, 117, 118].

As with all high atomic number molecules, iodine binds to different tissue in varying amounts, allowing differences within the soft tissue structures to be observed [74, 85, 107, 119-122]. It is much cheaper in relation to OT and PTA and is easy to store but must be stored away from light to reduce disassociation of the iodine molecules back out of solution. It is non-toxic and can penetrate to the greatest depth of all the micro-CT biological tissue contrasts, up to several centimetres [110]. Increased tissue differentiation has also been demonstrated in Hounsfield Units when measured within myocardial tissue in comparison to PTA [113].

Another advantage is that if insufficient specimen penetration has occurred, it can be returned to the solution with no negative effects [110, 118], and once penetration has reached the centre of the specimen, further immersion does not result in increased differentiation between structures [92].

Over-iodination leads to tissue distortion, which has been noted following immersion in I<sub>2</sub>KI with longer immersion times [123], and higher concentrations [107, 114, 116] although distortion may stabilise after several days seven days immersion for mice organs [117]. The degree of tissue distortion may also differ according to the tissue imaged, with lung and brain more affected than others [92]. This effect should be investigated further if I<sub>2</sub>KI solution is to be used as a contrast agent.

Further difficulties are encountered regarding precise concentrations of iodine solutions. Lugols solution can be purchased commercially yet may contain differing amounts of iodine (3 - 25%) [113, 116], and there is no recommended standard within the literature. This makes comparing techniques and utilisation of previous investigations to direct future experiments difficult.

Gignac et al., [85] reviewed the I<sub>2</sub>KI literature for a wide variety of specimens, alongside the large range of concentration and immersion times employed. Whilst this displayed the versatility of this contrast, it also highlighted the discrepancy that exists in the work and that a more methodical and open approach is required. They stated that in-depth description of the concentration and immersion times for each specimen type will allow standards for a wide range of specimens to be identified.

**Table 2.2 Properties of three contrast agents**

Contrast Agent	Osmium Tetroxide	Phosphotungstic Acid	Potassium Tri-iodide
Cost	Expensive	Cheap	Cheap
Penetration	Limited (few millimetres)	Limited (few millimetres)	Several centimetres
Toxicity	High	Mild	None
Tissue Distortion	Yes	Yes	Yes

#### **2.12.4 Preferred contrast for micro-CT of human fetuses within this thesis**

The main limitation of OT is its inability to penetrate larger specimens, which has been overcome with PTA through vascular access, however, this approach is challenging within the post-mortem fetal arena due to the size of the specimens.

Tissue distortion occurs with all three contrast agents and is a disadvantage as it may alter the volume, structure, or relationship between adjacent tissues within the body. However, conventional histological preparation also results in tissue distortion, yet should clearly be minimised where possible.

Therefore, as indicated, Table 1.2, I<sub>2</sub>KI is likely to be the most suitable contrast agent for the preparation of human fetal post-mortem micro-CT scanning due to its penetration ability, cost, and low toxicity, as evidenced by its wide usage for multiple biological specimens [85]. However, it is important to achieve a standard notation for the I<sub>2</sub>KI solution concentration which is accessible to a wide range of researchers and clinical staff.

### **2.13 Historical development of micro-CT for post-mortem imaging**

#### **2.13.1 Mouse embryo micro-CT imaging**

Early usage of I<sub>2</sub>KI to iodinate biological tissues was first described by two separate groups. Degenhardt et al., [107] and Metscher [92] who both identified its ability to differentially attenuate the x-ray photons depending on the tissue being imaged



following immersion for several days. They used different concentrations of I<sub>2</sub>KI, with 25% and 10% respectively, although the chemical make-up of this solution is only clearly described by Degenhardt et al., as consisting of 10g KI + 5g I<sub>2</sub> dissolved in 100 ml to create a 100% solution, diluted accordingly.

Degenhardt et al., [107] proceeded to test multiple concentrations of I<sub>2</sub>KI solution on mouse embryos and found that increased concentrations produced better differentiation between structures and more uniform staining, but with increased tissue distortion, which was subsequently confirmed by Metscher [114]. This tissue distortion was also noted in mouse embryos by Wong et al., [123], who reported that further optimisation of the technique was required to minimise distortion in future studies. However, no details of the concentration used in these investigations were given, merely stating that the Lugol's staining protocol was adapted from Metscher and Degenhardt et al.

However, acceptance of tissue distortion occurring is not universally noted, with Dunmore-Buyze et al., using a 25% Lugol's solution with a 3% total Iodine content to iodinate in-vivo mouse hearts, reporting no observable tissue distortion [113]. However, no details are provided on the procedure used to prepare the Lugol's solution used within their investigations.

Adaptation of the technique was subsequently used to identify cardiac anomalies within whole mouse pups using a quoted 25% I<sub>2</sub>KI solution, and a 5% total Iodine content [124]. However, this investigation differed by using formalin to dilute the original I<sub>2</sub>KI solution instead of water to reduce further tissue degeneration following death.

Although I<sub>2</sub>KI staining techniques are now widely accepted with many papers quoting Metscher and Degenhardt et al., for their tissue preparation. Most uses are for small specimens, with Gignac et al., [84] observing that there was no clearly defined methodology for larger specimens [84]. Whilst stating that Degenhardt et al., had achieved highly detailed results, these levels of detail had not been matched in larger specimens and that this was limiting the extended use of the technique. Following experimentation, they describe staining alligator and emu heads in 11.25% I<sub>2</sub>KI

solution (3.75% w/v of I<sub>2</sub>) for several weeks and describe optimal tissue differentiation with full iodination at 2 weeks and 4 weeks respectively, but with oversaturation and subsequent lower tissue differentiation after 4 weeks for alligator heads.

They also state that they considered the higher concentrations of I<sub>2</sub>KI combined with higher x-ray tube voltage to be responsible for the higher image quality and indicate that this should be followed for subsequent investigations. Although previous authors mostly agree that higher concentrations of I<sub>2</sub>KI is responsible for increased tissue distortion, they felt that for larger specimens the increased concentrations and immersion times enabled appropriate iodination, and that greater tissue distortion should be acknowledged as an acceptable disadvantage.

However, the oversaturation they noted due to excessive immersion time had not been previously stated and restricting immersion times should be considered when iodinating valuable specimens to minimise/eliminate this disadvantage.

Gignac et al., [85] extensively reviewed the literature, detailing I<sub>2</sub>KI wide usage as a contrast agent. The large variation in both the concentration of I<sub>2</sub>KI used, immersion times and the description of the solution itself was noted. They state that detailed description of these important steps should be detailed within the literature along with the imaging parameters used for micro-CT examinations to assist future investigators.

### **2.13.2 Human fetal imaging**

Imaging using I<sub>2</sub>KI solution was first described for whole fetuses (gestational age 7 – 17 weeks) and ex-vivo human fetal hearts in 2014, with staining using two concentrations of I<sub>2</sub>KI solution (25% and 50%) for between 48 and 72 hours respectively [125]. This study demonstrated the ability of micro-CT to yield diagnoses for these fetuses and hearts in humans where conventional autopsy or dissection was precluded due to size constraints. Although, these diagnoses could not be confirmed with alternative methods, they provided a detailed digital dataset that could be analysed, archived, and re-evaluated if required. The relatively low cost of the micro-CT scanner was also noted, and the possibility of a post-mortem clinical service first stated.

This was followed by subsequent papers for human fetal ex-vivo cardiac and renal tissue by Hutchinson et al., [121, 122, 126], who adapted the technique used by Degenhardt et al., [107] and demonstrated that this technique demonstrated >90% in identifying fetal abnormalities [126] but used different annotation for the I<sub>2</sub>KI solution, with total iodine content quoted as 63.25mg/ml.

## **2.14 Conclusion**

The ability of micro-CT to non-invasively image a wide range of biological tissue to a high resolution, in the order of several microns, following iodination with I<sub>2</sub>KI solution and the demonstrated proof of principle to identify diagnoses in small numbers of human fetuses makes this a promising technique to further develop for a clinical tool.

Combined with the current low uptake of parents for conventional post-mortem autopsy examinations, due primarily to its invasive nature, further identifies it as an excellent alternative for early pregnancy loss, <20 weeks gestation, of which there is currently no other non-invasive imaging option.

Therefore, it is determined that micro-CT for human fetal post-mortem imaging is a novel technique that requires development and optimisation to be refined into a clinical protocol. To ensure that this is possible, steps must be taken to identify the optimal tissue preparation protocol, identifying the optimal I<sub>2</sub>KI concentration and immersion time, and imaging protocol, identifying the optimal method of fetal positioning and imaging parameters, for a wide range of fetal sizes and gestation.

## **2.15 Thesis aims and objectives**

This thesis sets out to achieve the following aims and objectives.

### **Overall objective of this thesis**

To develop an optimal clinical protocol for scanning post-mortem iodinated whole human fetuses with micro-CT.

### **More detailed aims were as follows:**

**Aim 1:** To determine optimal tissue preparation (concentration and immersion time in I<sub>2</sub>KI solution) for ex-vivo organs and whole human fetuses <24 weeks prior to micro-CT scanning.

**Aim 2:** To identify the relationship between key micro-CT imaging parameters and SNR and rCNR for ex-vivo organs and whole human fetuses.

**Aim 3:** To determine a clinically appropriate micro-CT scanning protocol with optimal SNR and rCNR, within a scan time of less than 30 minutes and to eliminate detector saturation.

**Aim 4:** To determine the relative contributions of fetal demographics and imaging parameters to image quality for post-mortem fetal micro-CT imaging.

**Aim 5:** To qualitatively explore parental opinion of micro-CT following miscarriage, particularly around acceptability, the main benefits, and concerns.

# **Chapter 3      Assessment of Micro-CT Scanning of Ex-Vivo Animal Organs**

## **3.1 Overview**

This chapter describes the investigations that were performed into individual ex-vivo organs. Animal cardiac and renal tissue was empirically assessed across different concentrations of I<sub>2</sub>KI solutions for tissue preparation and a range of imaging acquisition parameters to determine the optimal micro-CT imaging protocol.

The work presented in this chapter was undertaken by the author of this thesis, with organ collection was completed by Dr Jose Novos Matos.

Work from this chapter was published in the American Journal of Veterinary Research, 2020 [127] and Scientific Reports 2020 [128] and presented orally at the Tomography for Scientific Advancement Symposium 2018 [129] and 2020 [130], at the Medical Careers Conference 2018 [131], at the Tomography for Scientific Advancement Symposium 2019 [132], and at the Functional Imaging and Model of the Heart Conference 2021 [133].

## **3.2 Experiment 1 – ex-vivo feline cardiac tissue**

## **3.3 Introduction – previous animal I<sub>2</sub>KI usage**

Micro-CT in conjunction with contrast agent I<sub>2</sub>KI shows promise in the area of both ex-vivo organs and whole-body imaging, but investigations to determine the optimal preparation are required. Although previous cardiac studies had been performed on differing species including human [121], mouse [124] and rabbit [118], most authors reference the work of Degenhardt et al., [107]. In this work they iodinated whole mice embryos to study the cardiac and whole-body anatomy as well as the ability of I<sub>2</sub>KI to penetrate the specimen appropriately. Degenhardt et al., [107] also stated that there was only one other example of similar staining techniques with I<sub>2</sub>KI, that of Metscher et al., [114], but that they both arrived at differing concentrations of solution. Degenhardt et al., [107] also notes that at greater concentrations of I<sub>2</sub>KI solution, an

increased degree of differential enhancement was observed as well as a greater degree of distortion/shrinkage. These investigations are further supported by Gignac and Kley [84]. The importance of assessing whether the size of the tissue being scanned can be adequately iodinated to observe the internal structures and how this changes with regards immersion time and concentration of the solution are made.

After contrast investigation, empirical assessments on a variety of imaging parameters were necessary to develop an optimal imaging protocol as there is a wide discrepancy between various authors, Table 3.2. Imaging parameters have a large effect on the contrast seen within the final images, thus a variety of imaging factors should be investigated to inform on an optimal imaging protocol.

### **3.4 Aims**

**Aim 3-1:** To determine optimal tissue preparation (concentration and immersion time in I<sub>2</sub>KI solution) for ex-vivo feline cardiac specimens as assessed by micro-CT scanning (signal intensity).

**Null hypothesis 3-1:** A change in the tissue preparation (concentration and immersion time in I<sub>2</sub>KI solution) will not alter the image quality (signal intensity) as assessed by micro-CT imaging

**Aim 3-2:** To determine optimal imaging acquisition parameters (kilovoltage, current, exposure time and gain) for feline ex-vivo cardiac specimens assessed by micro-CT scanning (signal intensity).

**Null hypothesis 3-2:** A change in imaging acquisition parameters will have no effect on image quality (signal intensity) of extracted organs when imaged with micro-CT.

### **3.5 Methods**

Seven control excised adult feline hearts were sourced from the control arm of a study into hypertrophic cardiomyopathy [128] (ethical approval URN 2016-1638-3; Appendix 2), with no animals being euthanized and collected specifically for this experiment. This provided organs that were roughly equal in size to a fetus from an

early miscarriage (10-17 g) and allowed experimentation without employing human fetuses.

### **3.5.1 Tissue Preparation – feline hearts**

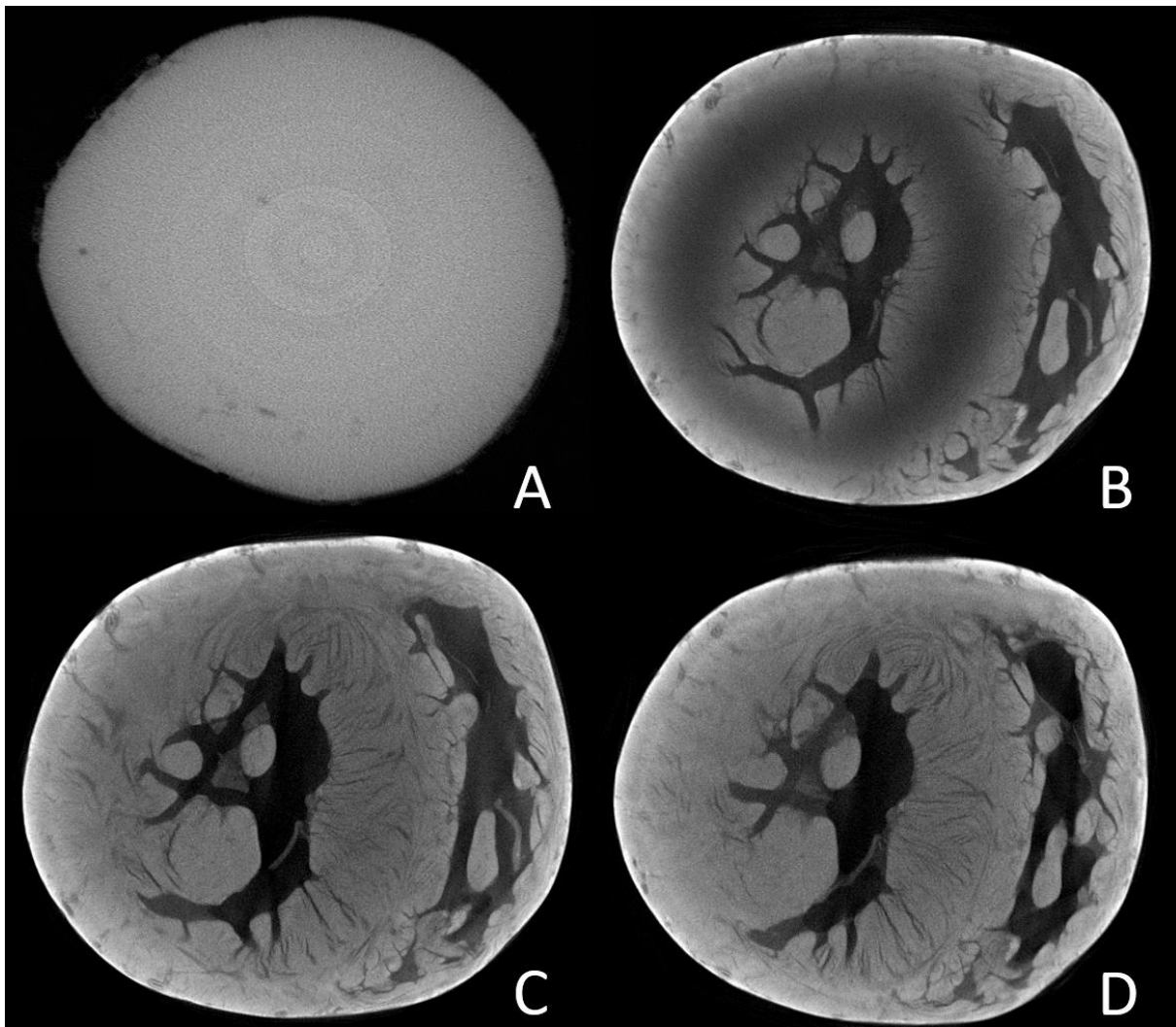
All hearts were previously preserved in a 10% formalin solution immediately after removal, with all hearts being rinsed with water, towel dried and weighed before being immersed in I<sub>2</sub>KI solution. Six feline hearts were split between the two solutions: weight range, 10.8 - 16.8 g at 2.5% I<sub>2</sub>KI solution, 10 – 15 g at 1.25% I<sub>2</sub>KI solution; (Figure 3.3), with explanation of the I<sub>2</sub>KI solution described in Appendix 4. Individual hearts were placed in thirty times the original weight of the organ in millilitres of I<sub>2</sub>KI solution, at room temperature, to ensure that sufficient iodine molecules were present throughout the iodination and were not a limiting factor.

Prior to imaging, the hearts were rinsed with water and towel dried to remove any excess fluid, before being wrapped in Parafilm M (Bemis) to ensure no residual fluid leaked and no movement or desiccation occurred during scanning. Specimens were placed on top of a phantom containing four vials containing air, water, wax, and ethanol (Figure 3.1) and secured in place with parafilm (Appendix 4). These phantoms allowed equivalent measurements to be taken at each scan to allow retrospective choice of standard phantom as necessary. Although this phantom (Figure 3.1) was placed within the x-ray beam and directly scanned, the subsequent data analysis demonstrated that it was not required. Its presence would have allowed any errant values to be investigated, however, it was not required in these experiments. Serial imaging was undertaken at regular time intervals lasting 12 days, (Figure 3.2) [127].

Scans were completed with a Med-X micro-CT scanner (Nikon Metrology, Tring, UK) with a resolution of 30 microns and constant imaging parameters of 100 kV, 150  $\mu$ A, and 15 W, 354 ms, 1 FPP and a gain of 24 dB, equating to an acquisition time of 16 minutes. Importantly, no refreshing of the I<sub>2</sub>KI solution was necessary as the original volume of solution was matched to the individual mass of each heart and was deemed sufficient at thirty times the original weight.



**Figure 3.1** Phantom containing air, water, ethanol, and wax



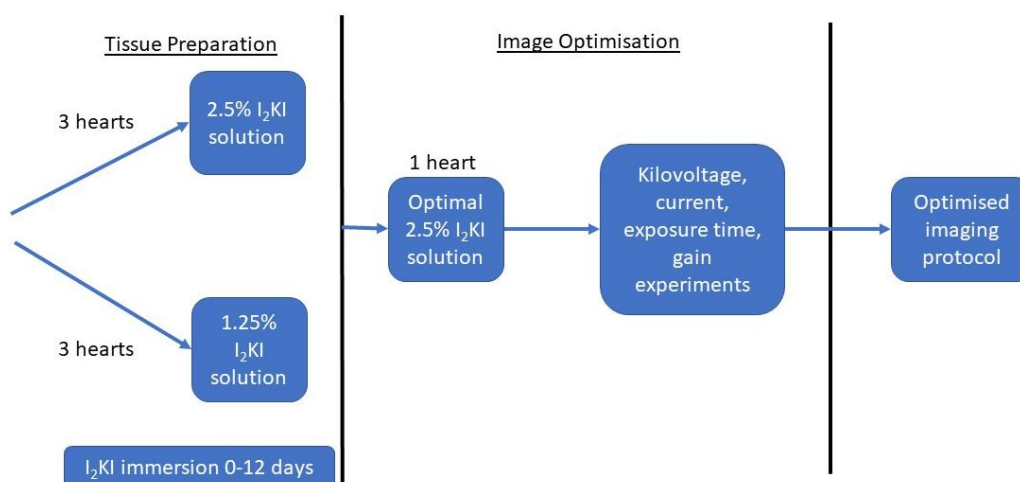
**Figure 3.2** Micro-CT images of a feline heart pre-iodination (A) and following immersion in 2.5%  $I_2KI$  solution for 24 hours (B), 48 hours (C) and 72 hours (D) [121], with permission



### 3.5.2 Imaging Acquisition – feline hearts

Once the tissue preparation experiments were completed, a fresh heart was selected and placed in 2.5% I<sub>2</sub>KI solution as this was deemed optimal for the imaging acquisition experiments (weight 17.6g), investigating the effect kilovoltage, current, exposure time and gain had on SNR and rCNR. The range of parameters included, kilovoltage (50 – 130 kV), current (20 – 220  $\mu$ A), and gain (0-30 dB) with values evenly spread throughout the range as allowed. Exposure time utilised a range of 67 – 500 ms but included measuring the SNR and rCNR at differing currents as this demonstrated a large effect on the maximum exposure times allowed before detector saturation was observed. Therefore, currents of 100 $\mu$ A, 150 $\mu$ A, and 200 $\mu$ A were employed.

Other parameters were kept constant throughout: 1 FPP, Tungsten target and a resolution of 30 microns. As wide a range of factors as possible were selected to allow maximal investigation within the capabilities of the micro-CT scanner. This workflow is illustrated in Figure 3.3.



**Figure 3.3 Flow diagram for the cardiac tissue preparation and image optimisation investigations**

The mean and standard deviation were measured by placing circular ROI within two areas of the myocardium (inner and outer), (Figure 3.4). These ROIs were circular with a diameter of 2 mm, with the inner myocardium ROIs placed along the central portion of the septum equidistant from either ventricle, with the outer ROIs equally spread around the left ventricle.

Three measurements of the signal intensity (SI) values were subsequently recorded in each area, as well as within the air phantom, to calculate SNR and rCNR measures. These repeated measures were evaluated with paired t-tests for statistical significance, following Shapiro-Wilks testing for normal distribution (or “data normality”), that the results followed a ( $p < 0.05$ ; XL Stat).



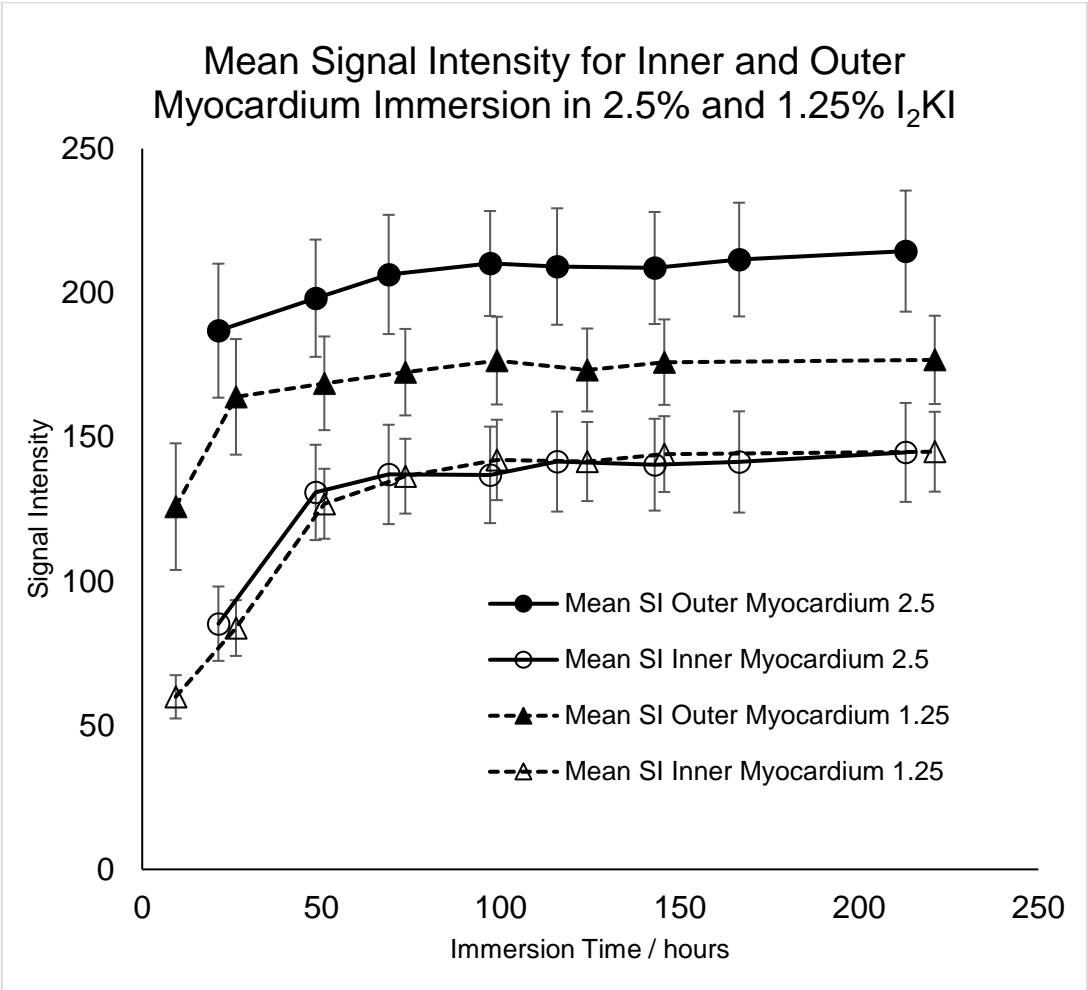
**Figure 3.4 Feline cardiac image showing ROI placement within the inner and outer myocardium**

### **3.6 Results**

#### **3.6.1 Tissue preparation – feline hearts**

Overall, all hearts progressively reached full iodination between 48 and 100 hours, whereupon a plateau was attained, (Figure 3.5). No statistically significant increase was observed in the SI after plateau was attained, although plateau was reached quicker with the 2.5% I<sub>2</sub>KI solution, and the outer myocardium quicker relative to the

inner myocardium. Earliest time to plateau above which only a <5% change in SNR or rCNR was recorded, Table 3.1. Differences between outer and inner SNR also reached plateau within the same time intervals, Table 3.1. Therefore, immersion in 2.5% I<sub>2</sub>KI for 48 hours was taken as the optimal tissue preparation for the imaging parameter optimisation experiment.



**Figure 3.5 Signal intensity graphs for the initial uptake and subsequent plateau for I<sub>2</sub>KI solutions and ROI positions - 1.25% inner (open triangles) and outer (solid triangles) and 2.5% inner (open circles) and outer (solid circles)**

**Table 3.1 Earliest time to plateau and percentage change after plateau for the two I<sub>2</sub>KI solutions**

I <sub>2</sub> KI Concentration		t-test results	Percentage change after time point
		Immersion Time (hours)	
2.5%	Outer	21 - 48	< 4.18
	Inner	48 - 68	< 3.39
	Difference (outer – inner)	21 - 48	-
1.25%	Outer	73 - 99	< 3.48
	Inner	50 - 73	< 2.80
	Difference (outer – inner)	25 - 50	-

### 3.6.2 Imaging parameters – feline hearts

A linear increase was observed for SNR and rCNR as the voltage was increased up to 130kV, (Figure 3.6 and 3.7), with a current of 130  $\mu$ A, exposure time 250 ms, and gain 24 dB (13minute scan time) which was set to allow investigation of a large range of kilovoltage values. When statistically investigated, no significant increase was seen for SNR above 110 kV and CNR above 100 KV, thus a 100 kV was chosen for subsequent experiments.

A linear increase was observed for SNR and rCNR as the current was also increased from 20 - 220  $\mu$ A, (Figure 3.6 and 3.7) with 100 kV as identified from above result, 250 ms, and gain 24 dB (13minute scan time). Thus, 200  $\mu$ A was chosen for subsequent experiments as any further increase in current would result in detector saturation.

To investigate how exposure time affects relative signal intensity and rCNR three current values were used to enable a wider range of exposure times to be investigated, with a constant 100 kV and 24dB. An increase in SNR and rCNR was observed as exposure time was increased, using a constant 100 kV, 100  $\mu$ A and gain 24 dB. Peak

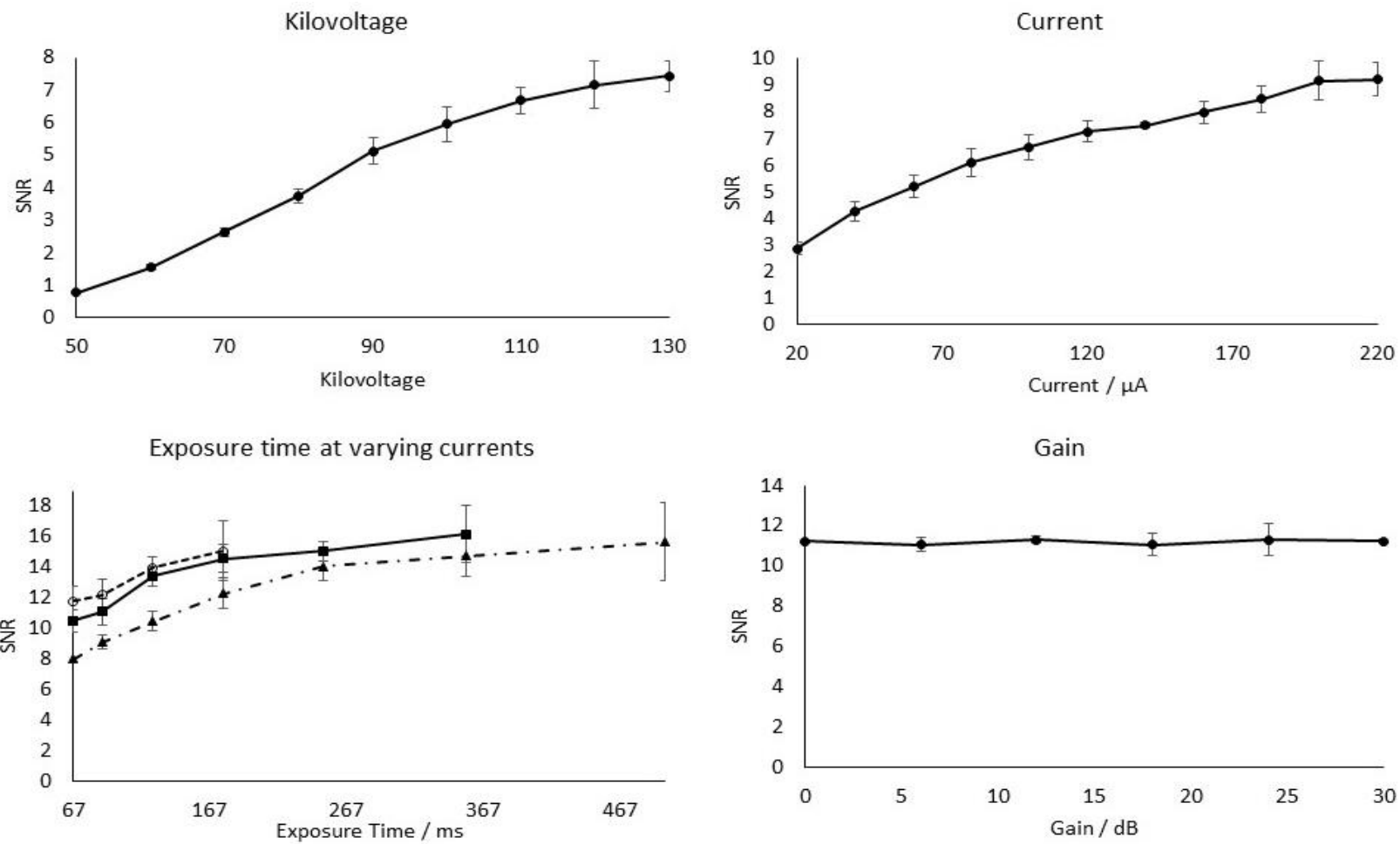
SNR and rCNR were seen at 100  $\mu\text{A}$  and 150  $\mu\text{A}$ , although total peak SNR and rCNR was observed at 500 ms (100  $\mu\text{A}$ ; 15.63 and 41.62; 17 minutes) and 354 ms (150  $\mu\text{A}$ ; 16.16 and 40.54; 12 minutes) respectively, (Figure 3.6 and 3.7). Higher currents (150  $\mu\text{A}$ ) allow shorter scan time (12 vs 17 minutes), therefore, 354 ms was chosen as the exposure time.

SNR or rCNR were not significantly altered by changes to the gain, (Figure 3.6 and 3.7), with constant other imaging parameters, 100 kV, 100  $\mu\text{A}$ , 354 ms and 15 Watts (13-minute scan time). Therefore, changing the gain did not affect SNR or rCNR. From these results, an optimised protocol for feline hearts is presented as the final row in Table 4.2.

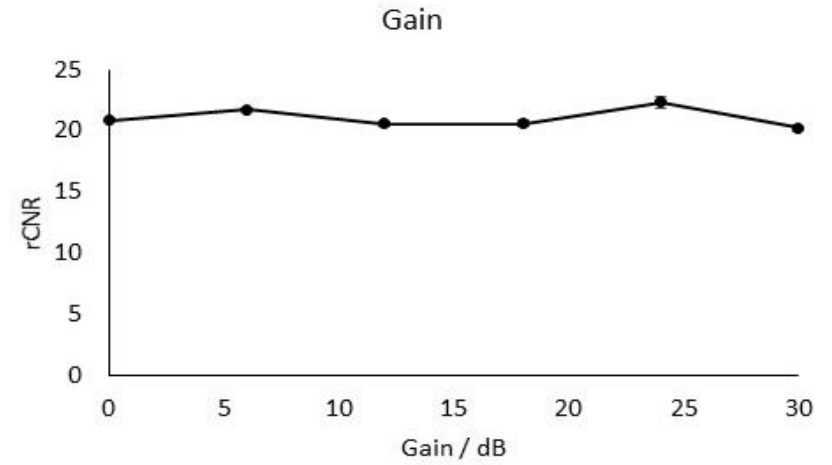
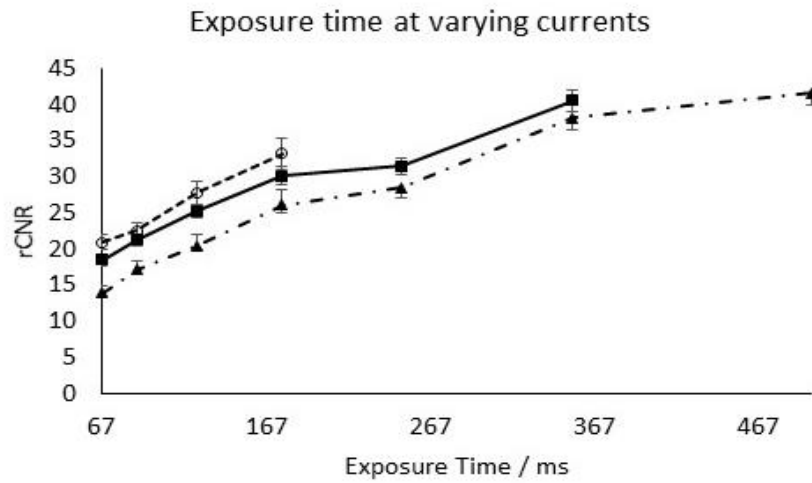
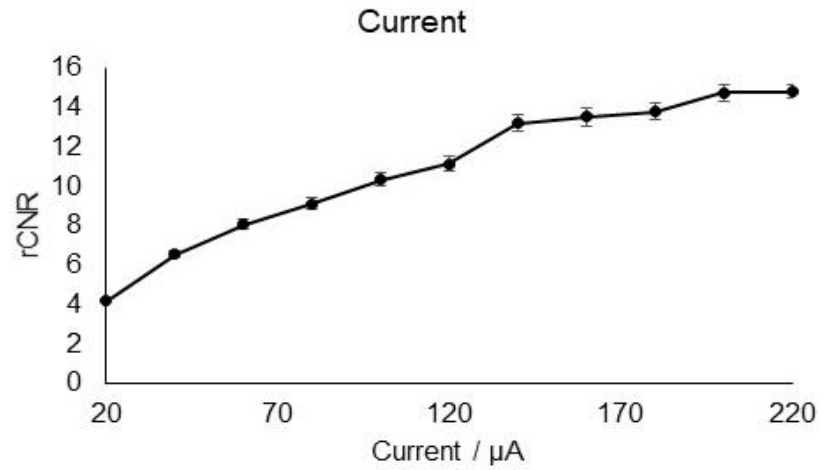
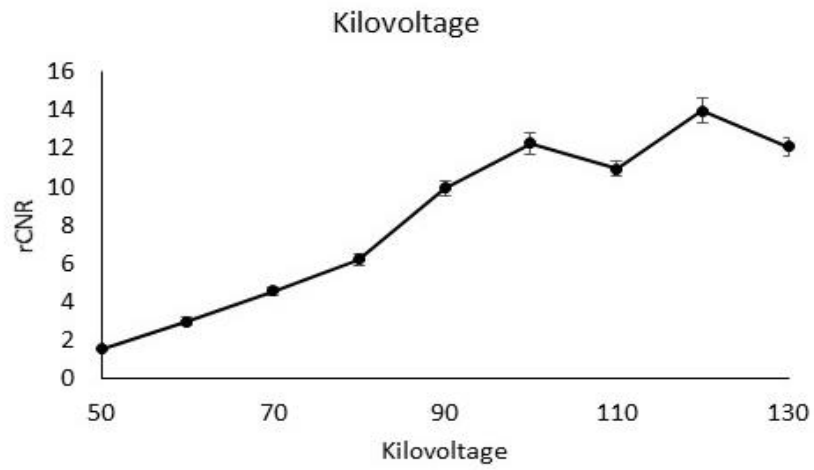
These results are noted to be specific to the micro-CT scanner that was used (Nikon Med-X).

**Table 3.2 Literature review for cardiac micro-CT protocols including this chapter's optimal imaging parameters [127]**

Reference	In situ / Excised	Specimen	Organ Weight (grams)	Number of specimens	I <sub>2</sub> KI solution concentration	Immersion Time (days)	Details of I <sub>2</sub> KI solution	Kilovoltage	Current (μA)	Exposure time (ms)
Aslanidi OV <sup>[134]</sup>	Excised	Adult boxer dog	256	1	7.50%	7	No	150	125	-
Stephenson RS <sup>[118]</sup>	Excised	Adult rat	2.25 – 5.5	4	1.87% - 15%	2	No	130-155	-	-
Stephenson RS <sup>[118]</sup>	Excised	Rabbit	4.1	2	7.5%	3	No	130-155	-	-
Stephenson RS <sup>[118]</sup>	Excised	Rabbit	4.1	2	3.75%	5	No	130-155	-	-
Kim AJ <sup>[124]</sup>	In Situ	Fetal mouse	-	2105	1.25%	2 - 3	Yes	80	100	500 - 800
Hutchinson JC <sup>[121]</sup>	Excised	Fetal human	- 5.3	6	63.25mg/ml	2	Yes	82-125	50-135	500 - 1000
Liu X <sup>[135]</sup>	In Situ	Mouse	0.15 - 0.18	-	0.025 N	-	Yes	-	-	-
Pelizzo G <sup>[136]</sup>	In Situ	Fetal rat	-	29	5%	90	Yes	80	300	300, 1050
<b>This study</b>	<b>Excised</b>	<b>Cat heart</b>	<b>10 – 17.6</b>	<b>7</b>	<b>2.5%</b>	<b>2</b>	<b>Yes</b>	<b>100</b>	<b>150</b>	<b>354</b>



**Figure 3.6 SNR changes as kilovoltage, current, exposure time and gain are independently altered**



**Figure 3.7 rCNR changes as kilovoltage, current, exposure time and gain are independently altered**



### 3.7 Discussion

This study showed that immersion in 2.5% I<sub>2</sub>KI solution for 48 hours, using imaging parameters of 100 kV, 150 μA, and 354 ms gave peak SNR and rCNR for feline cardiac specimens.

rCNR should demonstrate that rCNR grows roughly quadratically with kilovoltage increases and is largely observed until 100 kV, whilst rCNR increases linearly for current and exposure time increases as expected.

This tissue preparation is slightly quicker and uses a lower concentration of I<sub>2</sub>KI than some published investigations: 2.5% compared to 3.75% and 7.5% and shorter immersion times in comparison to some published studies; 2 days compared to 5 and 7 days for ex-vivo rabbit and dog hearts, Table 3.2. The literature demonstrates that a trade-off between longer immersion in lower concentrations is often required, and therefore a lower signal gradient across the tissue is seen. This approach would minimise I<sub>2</sub>KI immersion, thus minimising morphological distortion [85, 107, 121, 137].

Using I<sub>2</sub>KI as a micro-CT soft tissue contrast agent is dependent on diffusion of iodine molecules into the tissue, which has been shown to bind to the muscle cells glycogen [114, 118]. Depending on the type of tissue, iodine penetrates into different tissues to varying degrees. As with all high atomic number molecules, iodine attenuates x-ray photons depending on its concentration within a tissue, and it is this difference in iodine penetration that produces differences in the tissue contrast seen [119]. Micro-CT of soft tissue structures is a new avenue for this technology and although there exists an array of published data regarding I<sub>2</sub>KI solution strengths (e.g. from 0.3% [92] to 25% [138]) and immersion times (e.g. 30 minutes [114] to 7 weeks [138]) for differing sizes and tissue types, in addition to the cardiac literature review, Table 3.2, providing confounding information for the researcher to follow. The terminology that is published on this subject also confounds uptake of the technique and accurate comparison between researchers with the terminology of "Lugol's solution", usually interpreted as a weight of I<sub>2</sub> with double that of KI dissolved in water, but no exact values of often given. Some authors state that a 5% Lugol's solution is taken as "full strength" [116]. Different authors also use the annotation of total solute weight per volume (w/v), or a

percentage of I<sub>2</sub> alone or occasionally no solution details. By attempting to simplify this description in our methodology, our method may be used or adapted as required.

We found an optimised protocol using a lower voltage, lower exposure time and higher current compared to most published excised cardiac micro-CT protocols [118, 121, 134]. This could be due to a difference in the specimen size or scanner capability. This work will add collectively to the studies of previous authors [118, 121, 134] and is applicable to excised feline cardiac specimens or specimens of a similar size and nature but may need to be adapted to other organs.

Maximal imaging parameters were not possible for all parameters under investigation, as this would result in detector saturation so identification of 100 kV, 150  $\mu$ A and 354 ms, enabled maximal SNR and rCNR for these imaging parameters whilst not resulting in detector saturation. Comparison with clinical CT scanning was not completed due to large differences in the technique between micro-CT post-mortem imaging and clinical CT including, the equipment itself, the importance of dose reduction for living patients, extended micro-CT scanning times, and differing contrast methods.

Therefore, null hypotheses 3.1 and 3.2 are rejected as changes within the concentration of I<sub>2</sub>KI and kilovoltage, current and exposure time will alter the signal seen within the cardiac specimens. The null hypothesis has been accepted regarding gain (that alterations to gain does not alter the signal intensity of the micro-CT images).

### **3.8 Limitations**

There are several limitations associated with this study. Firstly, measurements were not completed earlier than 12 hours for 2.5% I<sub>2</sub>KI solution, after which a high signal intensity was already recorded. Earlier measurement would develop a greater understanding of the signal intensity increases for different concentrations.

Secondly, no measurements were completed for tissue distortion in these investigations, yet this is a known effect of immersion in I<sub>2</sub>KI solution. This is an important consideration as this may affect the anatomical structure and reduce the reliability of the results. The effect concentration has on tissue distortion may influence the choice of I<sub>2</sub>KI solution and future investigations should consider this effect.

Thirdly, no higher concentration of I<sub>2</sub>KI solution were tested for cardiac tissue. Increased concentration may increase the signal intensity of the tissues further but may also increase tissue distortion.

### **3.9 Conclusion**

Immersion in 2.5% I<sub>2</sub>KI solution for 48 hours and using imaging parameters of 100 kV, 150  $\mu$ A, and 354 ms gave maximal SNR and rCNR for feline cardiac tissue and provides an optimised micro-CT imaging protocol for tissue preparation and imaging parameters for feline cardiac specimens using I<sub>2</sub>KI contrast media.

These experiments can be used as a basis for developing future protocols on a wider range of ex-vivo specimens with modifications as to the size and tissue type as this knowledge is developed.

### **3.10 Considerations for Future Experiments**

Several important points originated from this work to improve data collection and analysis for future investigations.

Firstly, collecting data earlier than 12 hours will enable a greater understanding of the earlier iodination and rate of diffusion when it is expected to be at its greatest, thereby allowing a more comprehensive analysis of the iodination process. This could be completed for future experiments if iodination is also swift. The small size and swift uptake of the iodine may have been particular to cardiac tissue and may not apply to larger or more complex structures as seen in whole human fetuses.

Secondly, tissue distortion is an important consideration as this may affect the morphological structure of the specimen itself, especially where multiple tissue types are present in whole fetuses, as differential distortion may change the relationship of organs [117]. Therefore, tissue distortion should be measured in future experiments.

Thirdly, gain should be discounted from future investigations as it did not change throughout the experiments. Inclusion of FPP should be investigated as it is the number of images that is taken at each angle as the specimen is rotated. This factor

has a large effect on scan time and signal and can result in increased SNR and rCNR but at a cost of increased scan time.

Fourthly, although maximal image quality should be aimed for, manipulation of the imaging parameters may reduce scanning time and image quality but still provide images of diagnostic quality. Therefore, investigations to determine the imaging parameters that affect image quality should be completed to provide insights into targeted manipulation of imaging parameters. This could provide a time efficient scanning protocol for clinical practice.

Fifthly, higher concentrations of I<sub>2</sub>KI solution should be investigated with regards iodination and tissue distortion. This may result in higher signal intensities with possible faster iodination times yet could also increase tissue distortion.

Sixthly, the number of frames per projections (FPP) should be investigated with regards to SNR and rCNR. This imaging parameter is recognised as causing an increase in both the SNR and rCNR. Any increase in the FPP will also result in an increase in the scan time. Therefore, it is an important factor in developing a clinically relevant scanning protocol.

### **3.11 Experiment 2 – ex-vivo canine renal tissue**

#### **3.12 Introduction**

The aim of these investigations was to utilise the data from ex-vivo feline cardiac micro-CT optimisation and determine an optimal protocol for ex-vivo canine renal tissue, with comparison to the previous investigations particularly regarding enhancement [123] and tissue distortion [117].

#### **3.13 Aims**

**Aim 3-3:** To determine optimal tissue preparation (concentration and immersion time in I<sub>2</sub>KI solution) for canine ex-vivo renal specimens as assessed by micro-CT scanning (signal intensity, tissue distortion).

**Null hypothesis 3-3:** A change in the tissue preparation (concentration and immersion time in I<sub>2</sub>KI solution) will have no effect on image quality (signal intensity, tissue distortion) of ex-vivo renal tissue when imaged with micro-CT.

#### **3.14 Method**

Ten control canine kidneys were collected (URN 2018 1818-2) from the Royal Veterinary College, University of London due to their availability following natural death with a single kidney from each animal not being required for further analysis at autopsy. These were chosen to also be equivalent size to an early miscarried fetus, but with different internal structures than the feline heart, to form a comparison.

Based on the earlier results in this chapter concentrations of 2.5% and 5.0% were selected to observe whether an increase in the I<sub>2</sub>KI concentration would produce an increase in the optimal iodination protocol. The organs were split according to weight into 2 groups to ensure that equivalent weighted specimens were divided equally between the two concentrations of I<sub>2</sub>KI solution (weight range, 16.8 - 89.1 g at 2.5% I<sub>2</sub>KI solution, 12.5 – 89.1 g at 5% I<sub>2</sub>KI solution).

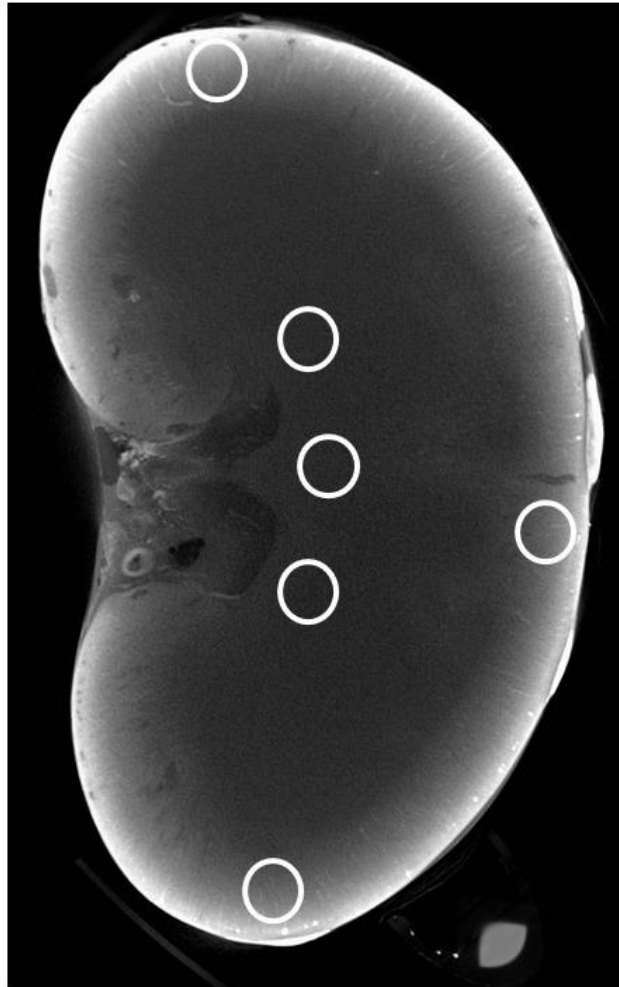
### **3.14.1 Tissue preparation – canine kidneys**

All kidneys were preserved in a 10% formaldehyde solution immediately after removal, and prior to being immersed in their respective I<sub>2</sub>KI solutions were rinsed with water, towel dried and weighed. The I<sub>2</sub>KI solution was prepared as described in Appendix 4 but using stronger concentrations (2.5% and 5%). Ten canine Kidneys were split between these two solutions (weight range, 16.8 - 89.1 g at 2.5% I<sub>2</sub>KI solution, 12.5 – 89.1 g at 5% I<sub>2</sub>KI solution).

Five times the original weight of the organ in millilitres was used, reduced from thirty times the weight used for the cardiac experiments, as these were larger specimens requiring larger volumes of solution.

Prior to imaging, the kidneys were prepared and positioned as described for the cardiac specimens atop the phantom. Circular ROIs (5 mm diameter) were placed equidistant from each other within the renal medulla. These circular ROI were also placed within the renal cortex at the superior, inferior, and posterior part of the kidney, 2 mm away from the edge of the kidney to eliminate any artefact from free iodinated fluid that may collect beneath the parafilm wrapping (Figure 3.8). Measurement of the ROIs was completed after 120 hours to ensure accuracy in repeated measures, with alignment of the datasets completed using anatomical variation and individual vessels/defects to accurately position the ROIs and ensure continuity.

Equivalent circular ROIs were also placed within the air phantom as per the cardiac specimens to calculate SNR and rCNR measurements. Serial imaging was undertaken at intervals at approximately 12, 24, 48, 72, and 100 hours, with further imaging at 24 days (Figure 3.10). All imaging parameters were kept constant for the experiments and were selected to ensure assessment of the I<sub>2</sub>KI penetration could be completed, whilst reducing the time spent out of solution. Scans were completed with a Med-X micro-CT scanner (Nikon Metrology, Tring, UK) at a resolution of 50 microns and imaging parameters of 100 kV, 150  $\mu$ A, 15 W, 354 ms, 1 FPP and a gain of 24 dB, equating to an acquisition time of 16 minutes. Importantly, it was not necessary to refresh the I<sub>2</sub>KI solution as the original volume of solution was matched to the individual mass of each kidney and did not limit iodination.



***Figure 3.8 Three ROI were placed in the renal cortex and medulla respectively***

### **3.14.2 Iodination and tissue distortion analysis**

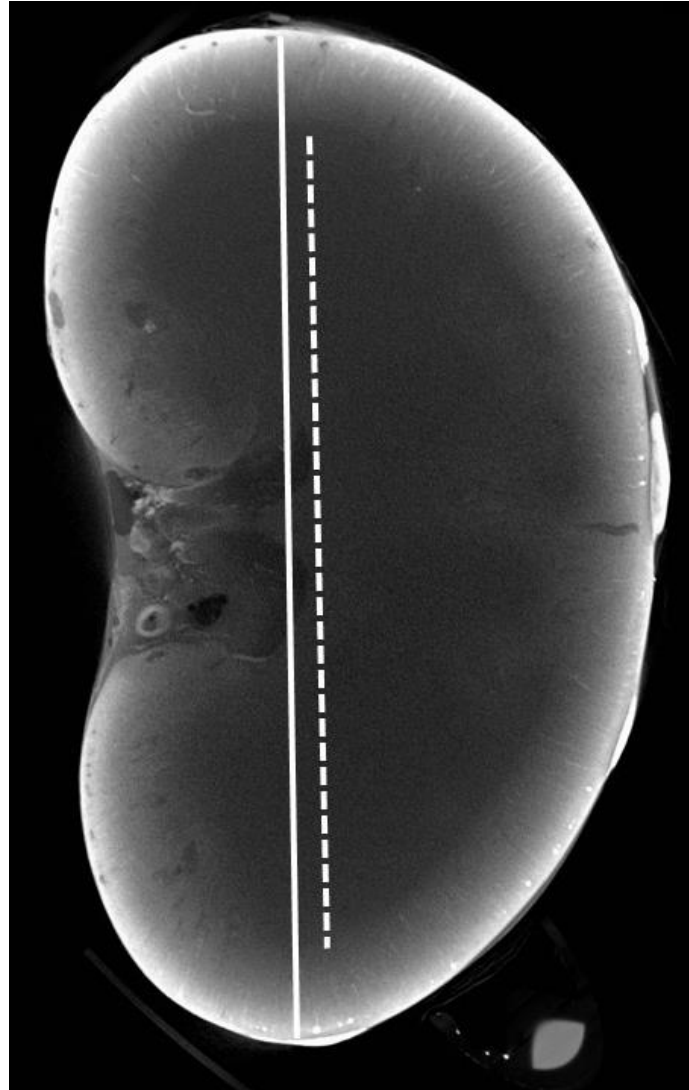
Subjective measurements were taken along a sagittal midline plane for each kidney ensuring that an equivalent slice was chosen for each specimen at each timepoint. This ensured that the time to full iodination was measured as the centre of the organ would require the furthest diffusion distance. The un-iodinated distance was determined by the darker area within this slice, where no anatomy could be identified due to a lack of contrast media. Measurements were completed by a single person with reference made to all timepoints to ensure measurements was completed in an equivalent position (Figure 3.9).

Although measurement of the portion of renal tissue iodinated was completed by a single investigator, equivalence of measurement was completed through the

identification of anatomical variation and vessels within the kidneys to accurately identify the correct measurement plane.

Identification of the iodinated and un-iodinated portion of renal tissue was completed using visual assessment of this border to determine the ratio of iodination. Assessment of the iodinated portion of the kidney could have been completed using absolute Hounsfield units measured along a plane, enabling an increase in the Hounsfield units to indicate iodination having occurred. However, this was deemed unnecessarily complicated as it was simple to visualise the border between the iodinated and un-iodinated tissue and as the main outcome of the investigation was to identify the time taken to full iodination. This was easily identified once internal detail was observed within the central portion of the kidney.





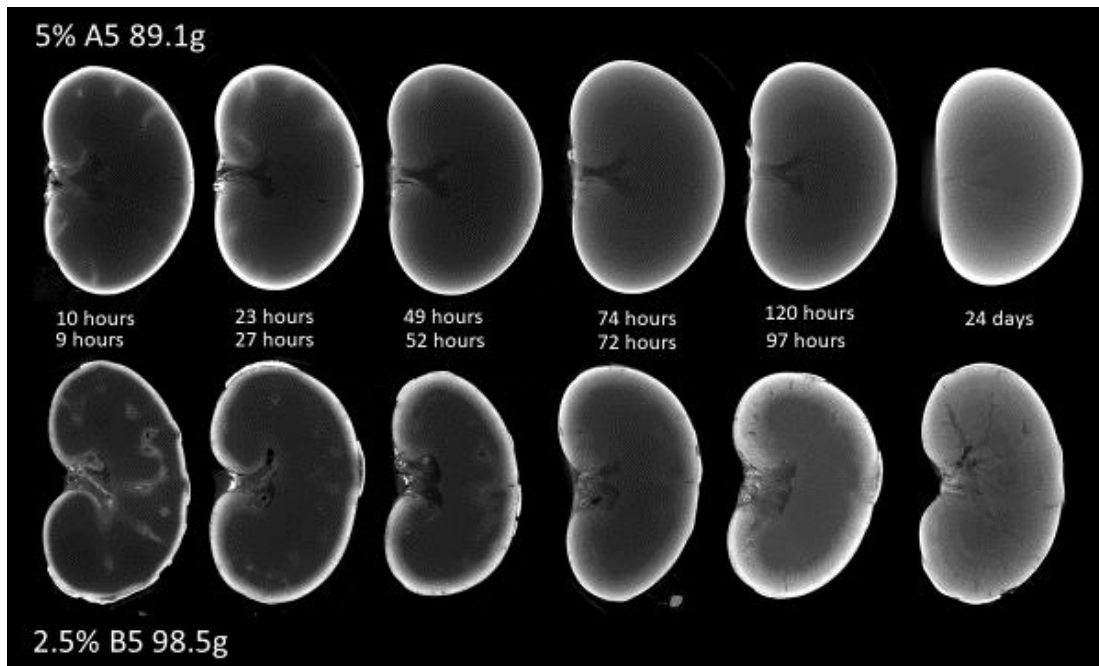
**Figure 3.9 Measurements of total kidney diameter (solid line) and un-iodinated distance (dotted line)**

Calculations to identify the percentage un-iodinated kidney diameter were completed at each timepoint using the following equation,

$$\text{Iodination (\%)} = \left( \frac{\text{Un - iodinated diameter in sagittal plane}}{\text{Total diameter in sagittal plane}} \right) \times 100$$

Calculations to identify the tissue distortion at each timepoint were calculated using the following equation,

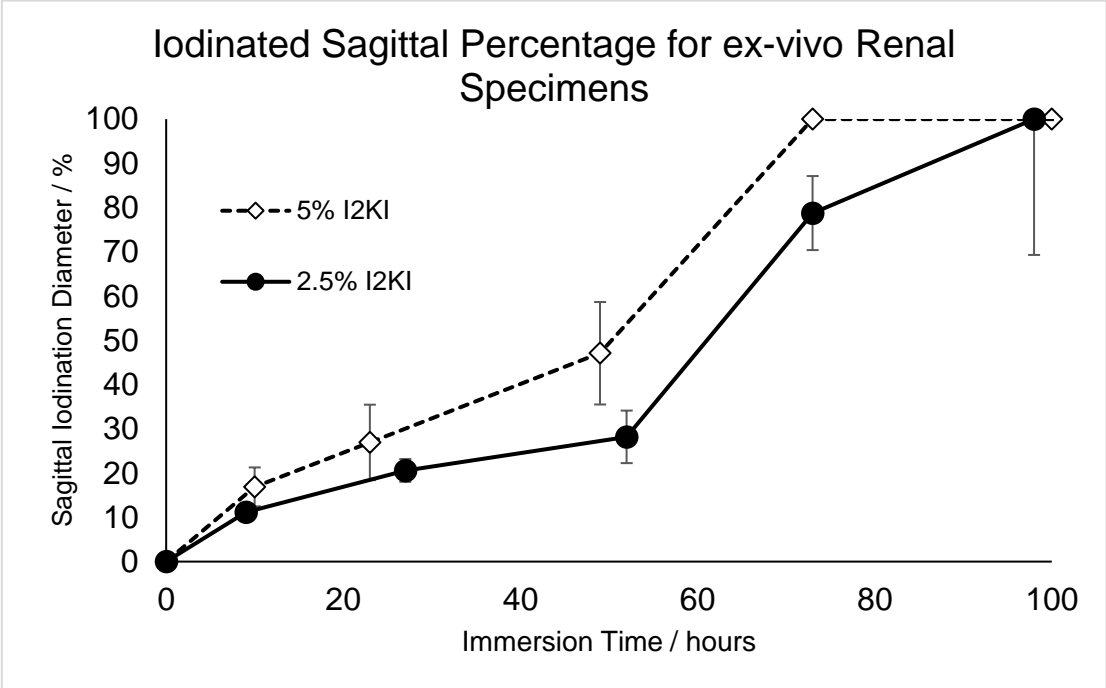
$$\begin{aligned} \text{Tissue distortion (mm)} \\ = \text{Initial sagittal diameter} - \text{sagittal diameter at timepoint} \end{aligned}$$



**Figure 3.10** Serial imaged kidneys (weight 89.1g and 98.5g) following immersion in different I<sub>2</sub>KI concentrations showing an increase in internal detail as immersion time increases

3.15 Results

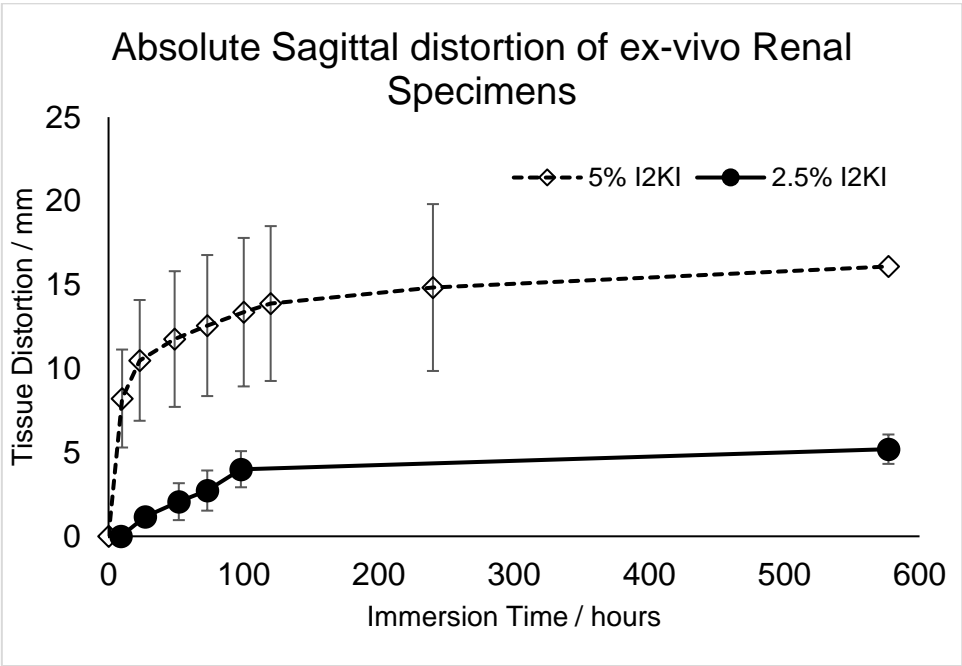
3.15.1 Tissue iodination – canine kidneys



**Figure 3.11 Mean percentage iodination of canine kidneys measured in the sagittal plane showing faster iodination for 5% I<sub>2</sub>KI solution than 2.5%**

Overall, all kidneys progressively reached full iodination between 0 and 100 hours with a faster rate seen for 5% I<sub>2</sub>KI solution, after which a plateau was noted. Mean maximal iodination was seen at 73 hours at 5% I<sub>2</sub>KI and 100 hours at 2.5% I<sub>2</sub>KI, (Figure 3.11).

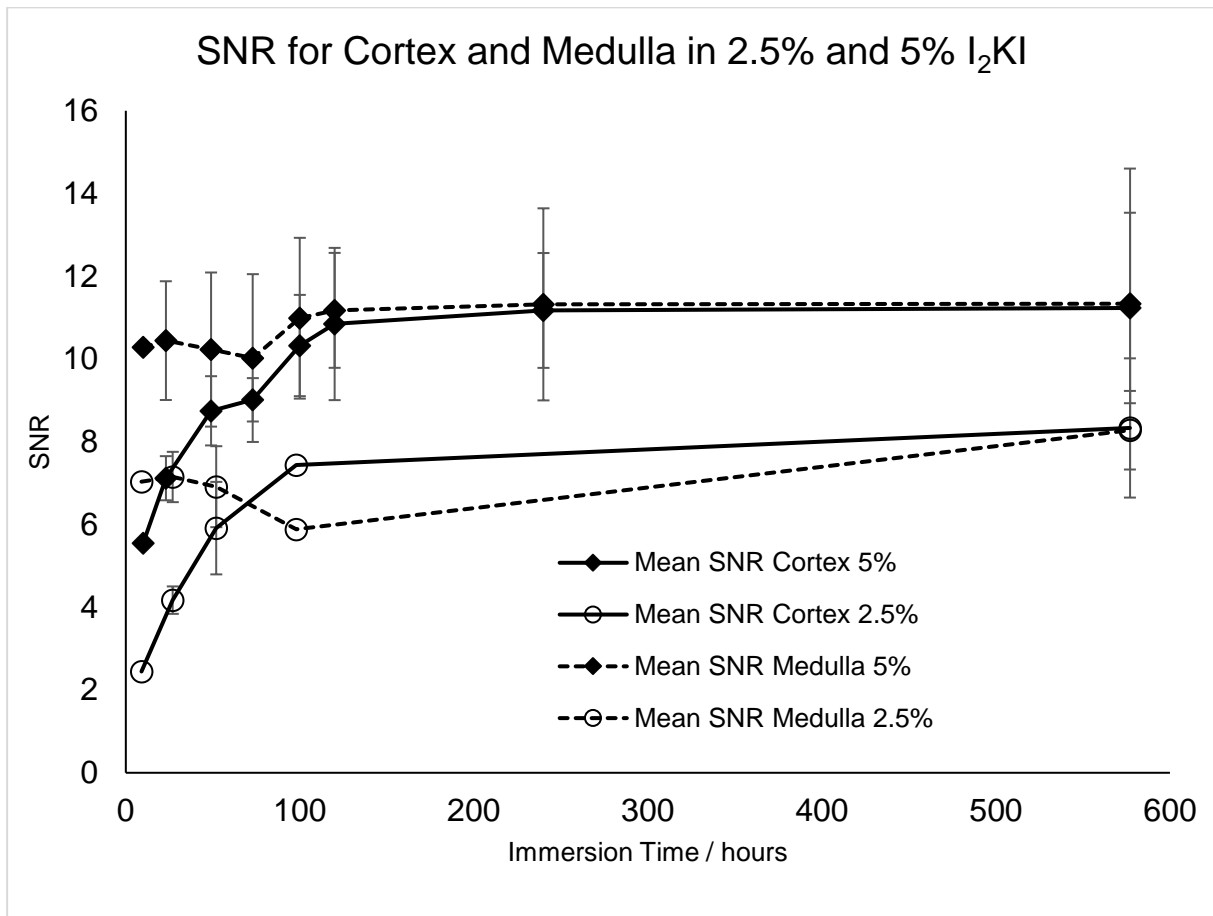
3.15.2 Tissue distortion – canine kidneys



**Figure 3.12 Demonstration of increased tissue distortion for both I<sub>2</sub>KI solution, with increased distortion overall for 5% I<sub>2</sub>KI**

Overall, all kidneys distorted due to immersion in their respective I<sub>2</sub>KI solutions, with a greater distortion seen in the 5% solution, but with the rate of distortion decreasing for both solutions after 100 hours, (Figure 3.12). Over three times the amount of tissue distortion is seen with the 5% I<sub>2</sub>KI solution at all time points when compared to the 2.5% solution.

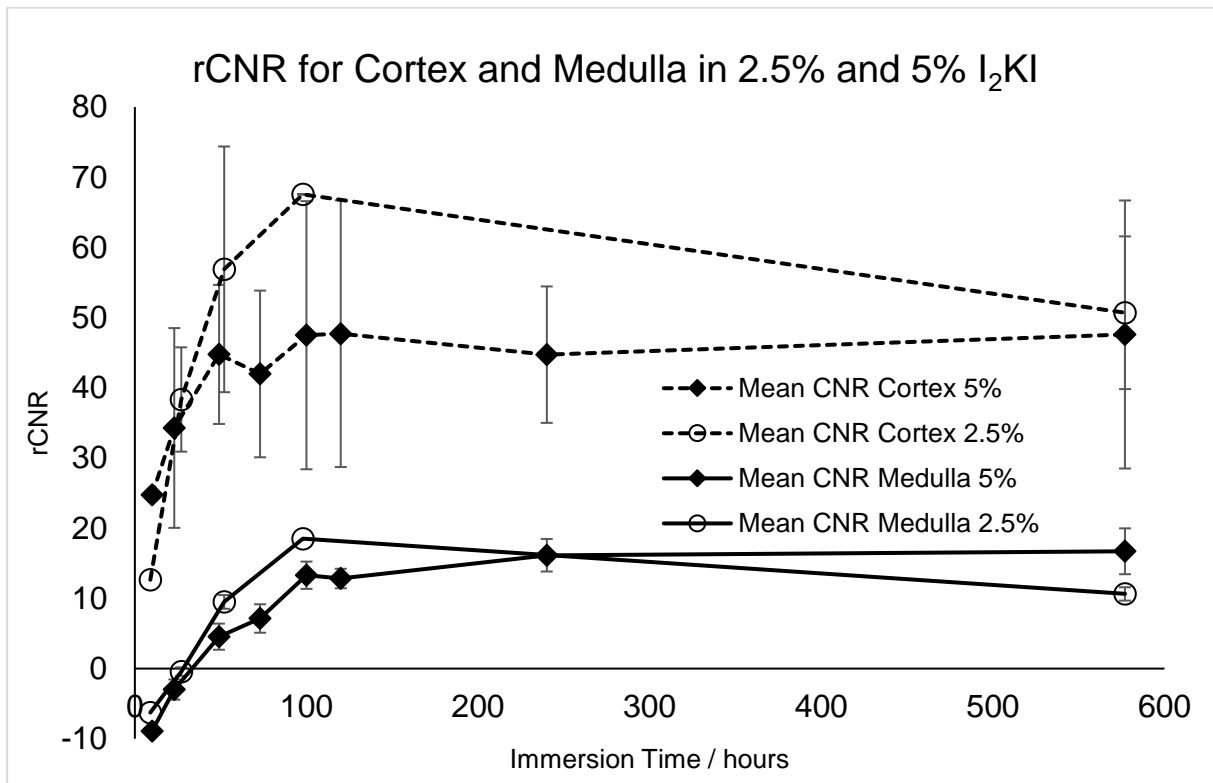
### 3.15.3 SNR



**Figure 3.13** SNR changes in the medulla and cortex of canine kidneys following immersion in 2.5% and 5% I<sub>2</sub>KI solution

Overall, there was a greater SNR seen in the medulla and the cortex for the 5% I<sub>2</sub>KI solution than for the 2.5% throughout the time range to 577 hours, (Figure 3.13). The rate of SNR increase within the cortex was greatest up to 120 hours, after which a plateau was observed. Within the medulla the SNR remained relatively stable for both concentrations of I<sub>2</sub>KI solution.

### 3.15.4 rCNR



**Figure 3.14** rCNR changes in the medulla and cortex of canine kidneys showing equivalent increases after immersion in 2.5% and 5% in I<sub>2</sub>KI solution

Overall, rCNR increases for both the cortex and medulla between 0 and 100 hours and remains relatively stable after this timepoint, with a slight decrease for 2.5%. Within the medulla the rCNR is comparable between the two concentrations of I<sub>2</sub>KI, with a large standard deviation noted. The rCNR for the cortex initially increases to a greater extent for the 2.5% I<sub>2</sub>KI solution when compared to the 5%, although after 577 hours the rCNR is comparable between the two solutions, (Figure 3.14).

### 3.16 Discussion – canine kidneys

These investigations show that 5% I<sub>2</sub>KI solution gave faster iodination for ex-vivo canine kidneys (72 hours compared to 100 hours for 2.5%), it also resulted in significantly increased tissue distortion.

This quicker iodination would allow scanning of renal specimens a day earlier and would be a clinically significant improvement.

The time to iodinate the renal specimens are also one to two days longer than the time to fully iodinate the cardiac specimens. The capsule that exists around a kidney may be inhibiting the diffusion of the iodine from the solution into the tissue and shows the importance of this work to quantify a range of differing tissues for publication, which can then act as a guide to future researchers.

It was also noted that I<sub>2</sub>KI solution five times the specimen weight, in comparison to 30 times for the cardiac investigations, was still sufficient to achieve full iodination. This amount of I<sub>2</sub>KI solution will be sufficient to ensure iodine molecules are not a limiting factor when iodinating other ex-vivo tissue and whole fetuses.

Tissue distortion was three times greater with 5% than 2.5% I<sub>2</sub>KI solution and is an important consideration when determining the optimal I<sub>2</sub>KI concentration. Within complex structures containing multiple tissue types, differential distortion could cause misalignment between structures after iodination [84, 107, 117].

Although distortion is observed with both solutions, the time taken to full iodination with 5% is only 27 hours longer, whereas the distortion is greatly increased. Overall, 2.5% I<sub>2</sub>KI solution displays a good compromise between efficient iodination and reduction of tissue distortion.

When interpreting the SNR and rCNR results the optimal solution choice is less clear. Although there is an increase in the SNR throughout the experiments for the higher 5% I<sub>2</sub>KI solution, rCNR, although increasing initially at a greater rate for the renal cortex in 2.5% I<sub>2</sub>KI reaches equivalent values with 5% I<sub>2</sub>KI solution after 577 hours. This indicates that, as expected, the introduction of an increased concentration of I<sub>2</sub>KI results in enhanced SNR although this greater signal does not translate to greater differentiation in the rCNR of the images. This may be due to external factors as the 5% I<sub>2</sub>KI specimens were scanned several weeks later and although kept under the same conditions. The specimens may have degraded due to room temperature or

inadequacy of the formaldehyde fixative they were stored in, although this is unlikely as formalin solution should have negated any further breakdown of the tissue.

The reduction in the 2.5% cortex rCNR at 577 hours to reach equivalent values with 5% could be explained by the reduced number of iodine molecules within the 2.5% solution. After an initial rCNR rise within the cortex this is reduced at 577 hours as the number of iodine molecules is spread throughout the whole kidney, causing a reduction within the rCNR cortex values.

Therefore, the null hypothesis 3-3, can be rejected.

### **3.17 Limitations**

The main limitation to these experiments was the maceration noted within several of the kidneys.

Maceration is a subjective process which describes tissue changes due to extended periods of time spent immersed in fluid, and to the breakdown of tissue within a cell following its death, causing the release of enzymes to breakdown the tissue itself [139].

This may have caused degradation of the specimens and therefore have affected the SNR and rCNR or iodination efficiency through an alteration of the tissue structure affecting the tissue distortion or iodination processes. Although the formalin within the solution should arrest this process, this may have occurred in-vivo or prior to initial extraction. Maceration would then have caused the breakdown in the barriers between structures and cells and allowed quicker iodination.

### **3.18 Conclusion**

Immersion in 2.5% I<sub>2</sub>KI for 100 hours is the optimal protocol for ex-vivo canine renal specimens. This allows for the minimal degree of tissue distortion and an efficient tissue preparation protocol prior to imaging by micro-CT. This compares with feline cardiac samples which had an optimal immersion time of 48 hours in 2.5% I<sub>2</sub>KI.



### **3.19 Considerations for Future Experiments**

The tissue distortion investigations provided an insight into the large difference that is seen by a doubling of the concentration of the I<sub>2</sub>KI solution and tissue distortion may be a significant factor in optimising whole body fetal imaging.

A greater range of I<sub>2</sub>KI concentrations should be trialled to detail comparable tissue specimens in a more complex structural system as seen with a cartilaginous skeleton in fetal specimens.

Additional phantom vials containing iodinated solution should also be included in future studies to enable equivalent SI values to the tissue under investigation to be assessed when calculating SNR and rCNR. This may also indicate any aberrant values seen with the micro-CT scanning and inform as to any errors.

### **3.20 Summary**

In summary, this chapter developed a methodology which assessed the iodination process, imaging acquisition technique and corresponding tissue distortion. This provides a robust methodology and approximate starting parameters which can be used as a basis for future investigations regarding whole human fetuses undergoing micro-CT scanning.

### **3.21 Key Points**

- Immersion in 2.5% I<sub>2</sub>KI solution for 48 hours can optimally iodinate a range of feline cardiac specimens.
- Immersion in 2.5% I<sub>2</sub>KI for 100 hours can optimally iodinate a range of canine ex-vivo renal specimens and minimise tissue distortion.
- Imaging parameters of 100 kV, 150  $\mu$ A, and 354 ms give maximal SNR and rCNR for feline cardiac tissue and provides an optimised micro-CT imaging protocol.
- Differing tissue distortion results were observed for differing concentrations of I<sub>2</sub>KI solution and this will be important to assess for whole human fetuses.

- Further work to assess the tissue distortion effect of differing I<sub>2</sub>KI concentrations should be carried out for ex-vivo organs and whole fetuses.
- Qualitative assessments of the image quality may provide insight into the diagnostic ability of a range of imaging parameters in comparison to SNR, rCNR and scanning time.

# **Chapter 4      Development of Tissue Preparation of Human Fetuses for Micro-CT Scanning**

## **4.1 Overview**

This chapter describes the investigations for tissue preparation of whole human fetuses prior to micro-CT scanning. Tissue distortion and iodination time are assessed across different concentrations of I<sub>2</sub>KI solutions, followed by a larger analysis using the optimal concentration in clinical practice.

The work presented in this chapter was undertaken by the author of this thesis. Human fetuses were recruited by our Belgian collaborators, Dr Xin Kang.

Work from this chapter was presented orally at European Congress of Radiology (2019 and 2020) [140, 141] and has been accepted for the International Paediatric Radiology Congress (2021) [142].

## **4.2 Introduction – human fetal iodination**

Iodinated micro-CT serves as a suitable tissue contrast to image the internal structures of ex-vivo organs to a high resolution [107, 121, 125].

In earlier chapters, immersion in 2.5% I<sub>2</sub>KI concentration for 48 hours produced full iodination for extracted feline hearts, yet immersion for 100 hours was required for full iodination with minimal tissue distortion for canine kidneys, demonstrating the variation in iodination times for different tissues.

Two small studies have demonstrated micro-CT scanning of human fetuses following full iodination using an equivalent I<sub>2</sub>KI solution to Degenhardt et al., [107]. Although they investigated a relatively small number of fetuses (n=7 and n=20, gestational age 7 – 17 weeks and 11 – 21 weeks), with no information on fetal weight, they demonstrated high diagnostic accuracy (92%) in fetuses <22 weeks gestation and equivalent information as would be provided with conventional autopsy [125, 126].

Therefore, the precise iodination protocol for whole human fetuses is yet to be established regarding tissue immersion time, iodine concentration, and upper and lower size limits for whole human fetal specimens [125].

To address this, two experiments were carried out. First, fifteen fetuses of different sizes were placed in different concentrations of iodine, to determine optimal timing, concentration, and potential side effects. Secondly, a larger study of using these optimal parameters in clinical practice was completed to generate a “real-world” formula for iodine preparation to be used in clinical practice.

### **4.3 Experiment 1 – optimal I<sub>2</sub>KI concentration**

#### **4.4 Aims**

**Aim 4-1:** To determine optimal tissue preparation (concentration and immersion time in I<sub>2</sub>KI solution) and image quality (tissue distortion) as assessed by micro-CT of whole human fetuses.

**Null hypothesis 4-1:** A change in the tissue preparation (concentration and immersion time in I<sub>2</sub>KI solution) will have no effect on image quality (tissue distortion) of whole human fetuses when imaged with micro-CT.

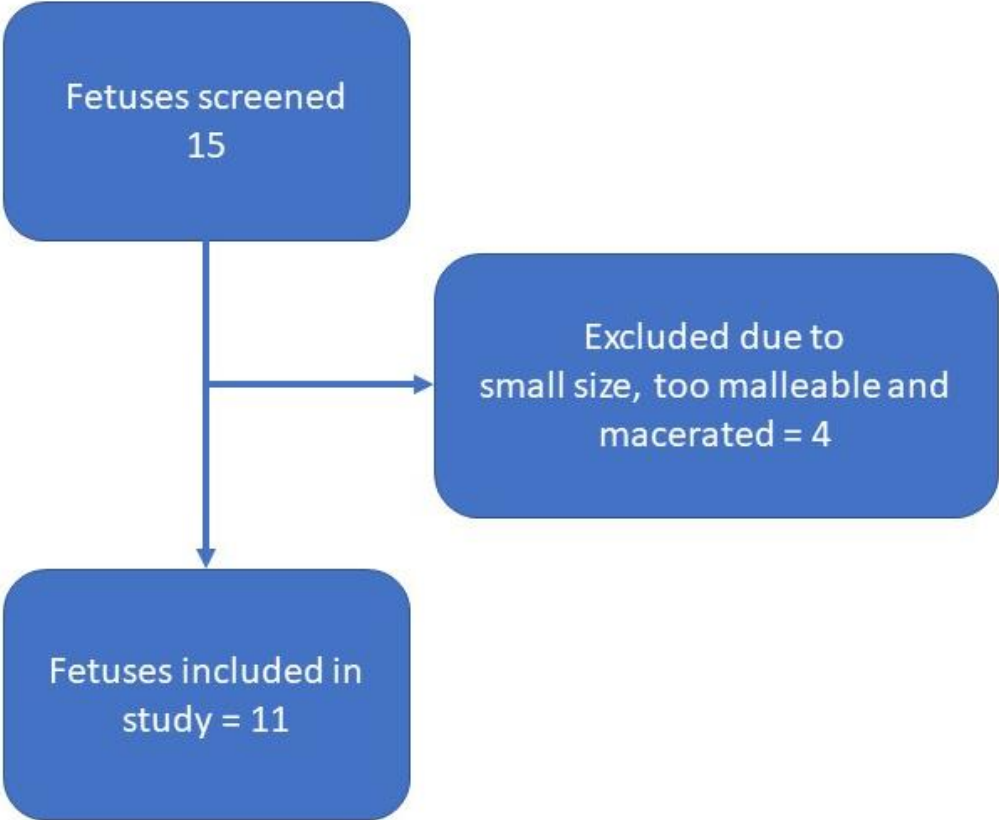
#### **4.5 Method**

Fifteen miscarried fetuses were collected as a single cohort from our Belgian collaborator (XC) to complete a study determining the accuracy of micro-CT post-mortem scanning and conventional autopsy. Ethical approval was obtained (REC Reference Number 17/WS/0089 and CE2015/81). All samples were handled according to the Human Tissue Act (2004), with written parental consent for post-mortem micro-CT imaging and the use of tissue in research following fully informed consent procedures.

##### **4.5.1 Study population**

Fetuses were excluded if their heads were deemed too malleable to accurately immobilise without manually altering the diameter. Fetuses were also excluded if they

were fully iodinated before the first post-iodination scanning time point due to their excessively small size (<5mm diameter), or displayed external severe maceration, (Figure 4.1).



**Figure 4.1** Flow diagram for the exclusion criteria

The fetuses were placed in order of gestational age (9 – 20 weeks) and divided evenly into 4 groups to ensure an even spread of size and weight for each group, before being assigned a concentration of I<sub>2</sub>KI solution, Table 4.1. No other considerations were considered as no previous scanning or clinical information was attained.

**Table 4.1 Demographics of the I<sub>2</sub>KI groups**

	I <sub>2</sub> KI concentration	Head diameters / mm	Mean / mm	Gestational age / weeks	Mean gestational age / weeks
Group A	1.25%	12, 22, 25	19.6	14, 15, 20	16.3
Group B	2.50%	24, 25, 30	26.3	13, 14, 15	14
Group C	3.75%	11, 25	18	14, 17	15.5
Group D	5.00%	16, 17, 22	15	14, 15, 18	12.3

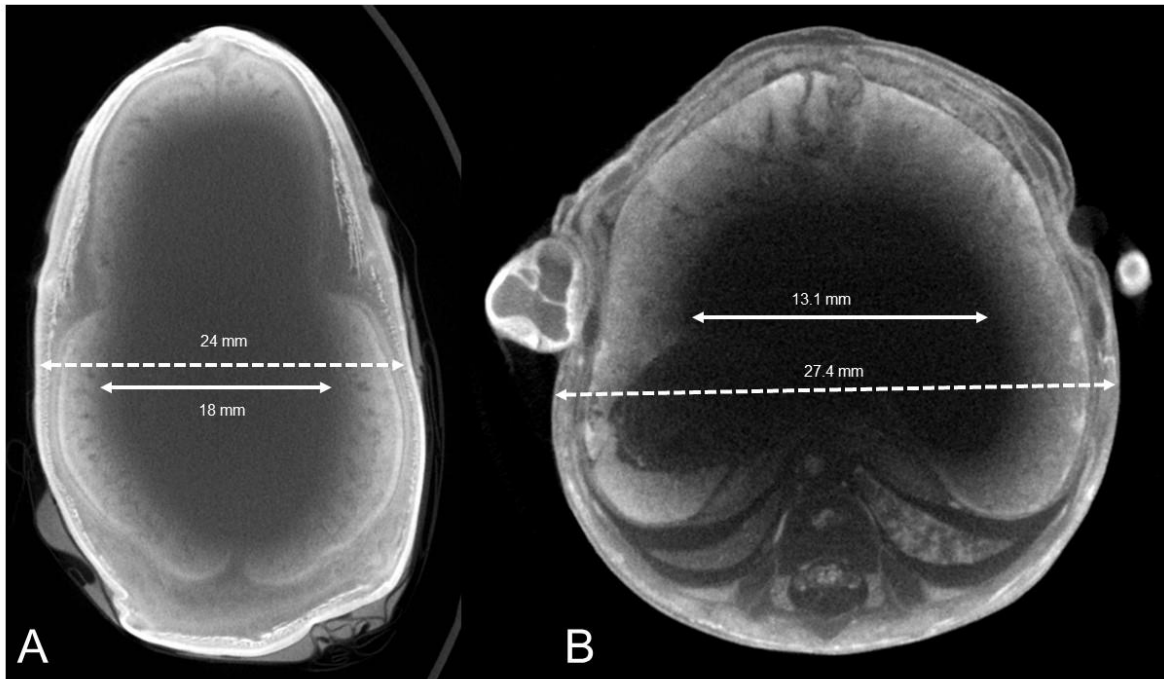
#### **4.5.2 Fetal iodination and scanning parameters**

Immediately, after collection the fetuses were stored in 10% formalin, to arrest further autolysis of the tissues. Excess formalin was removed via rinsing with water prior to iodination. Each fetus was placed in 1 litre of their respective I<sub>2</sub>KI solutions, ensuring that the I<sub>2</sub>KI volume was not a limiting factor in the iodination process. All fetuses were scanned every 12 to 72 hours using positioning described in Appendix 4, with limited timepoints up to 41 days depending on availability of the scanner and staffing. Imaging factors were kept constant for the experiment; 100 kV, 150  $\mu$ A, 354 ms, 15 W and 1 FPP with a scan time of approximately 15 minutes for each fetus per data timepoint. The magnification factor was optimised for each individual fetus and maintained throughout all subsequent imaging time points. The fetuses were returned to the I<sub>2</sub>KI solution immediately after each scan. The data was analysed using VGStudio Max 3.4 (Heidelberg, Germany) with measurements of head diameter and iodine penetration collected and entered in an Excel spreadsheet (Microsoft Corp, Redmond WA, USA).

#### **4.5.3 Fetal Head and abdomen analysis**

The head and abdomen are typically the largest diameter body parts and would therefore take the longest to iodinate for each fetus, based on diffusion distance, and would also demonstrate the largest tissue distortion in comparison to other areas such as the chest. An axial slice through the head and abdomen was identified on serial images to determine total diameter and un-iodinated diameter at this point at each

timepoint. The un-iodinated diameter was determined by the darker area within this slice, where no anatomy could be identified due to a lack of contrast media, (Figure 4.2). Ratio of tissue iodination was calculated to enable comparisons between different fetal sizes and gestations with regard iodination time.



**Figure 4.2** Examples of measurements for the head (A) and abdomen (B) to determine the un-iodinated diameter (dashed line) and full anatomical diameter (solid line)

## 4.6 Results

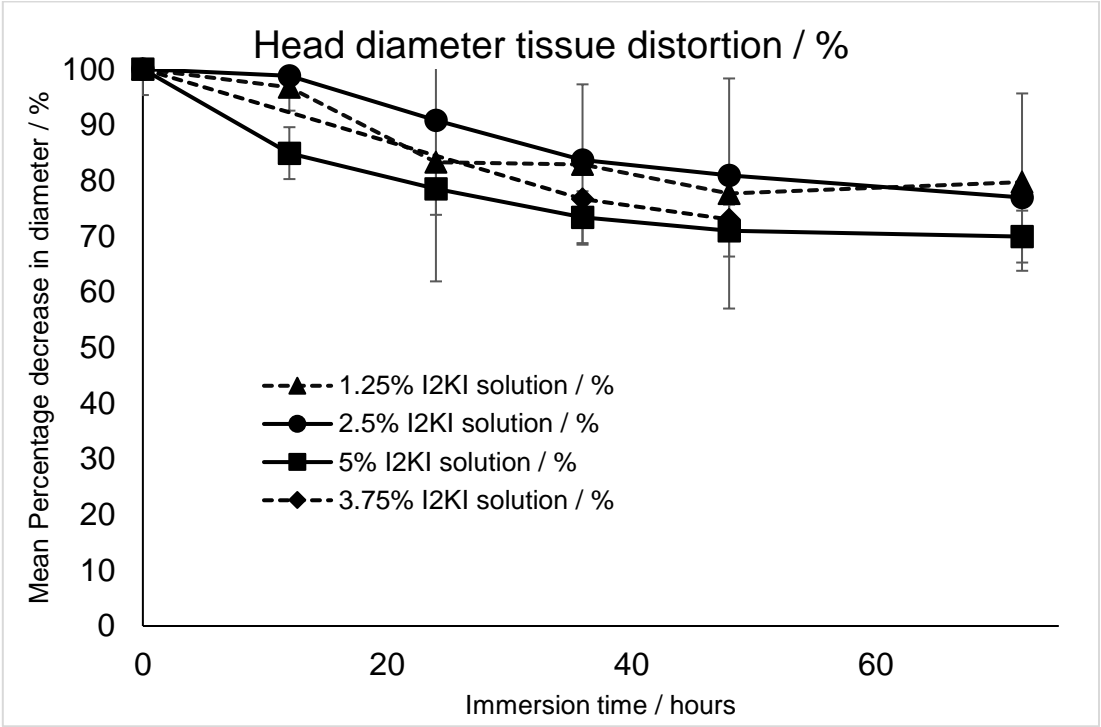
### 4.6.1 Tissue distortion

Head diameter tissue distortion was calculated as a percentage of the original diameter, (Figure 4.3).

All I<sub>2</sub>KI concentrations resulted in a reduction of the head diameter, with a greater reduction seen for the 3.75% and 5% than for 1.25% and 2.5% I<sub>2</sub>KI solutions, (Figure 4.3). Up to 72 hours, a greater reduction in head diameter was observed for all I<sub>2</sub>KI concentrations with a greatly reduced rate after this time, observed by a plateauing of tissue distortion.

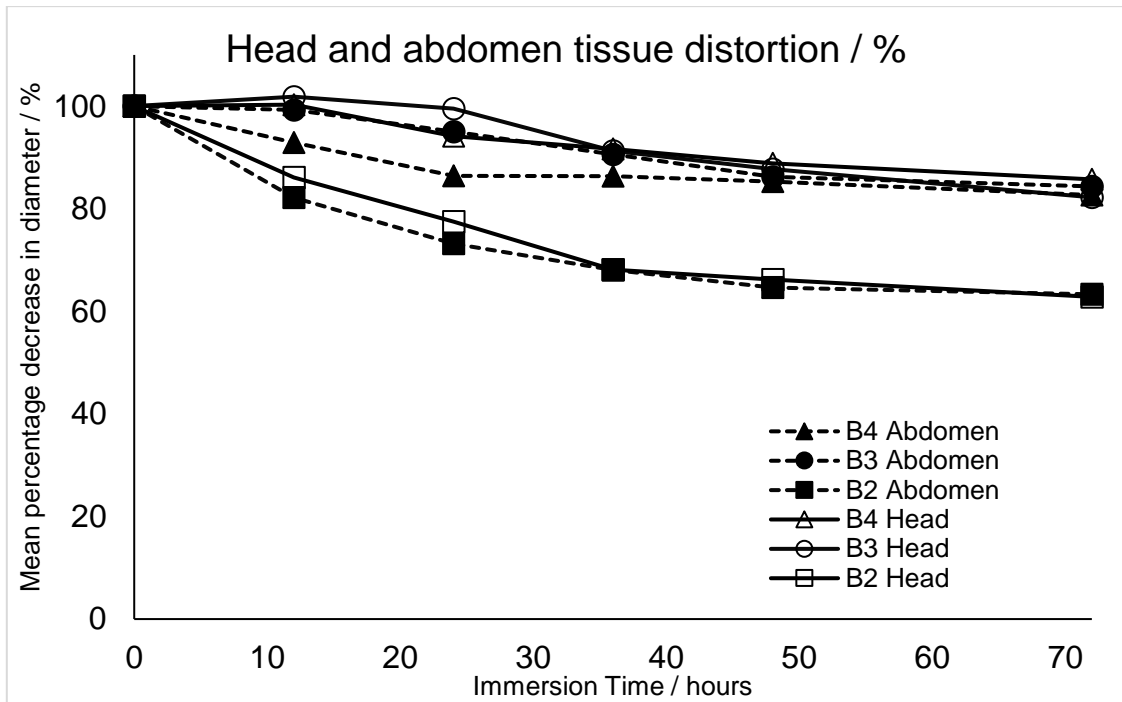
These findings were replicated for the abdomen, with individual fetuses demonstrating equivalent tissue distortion for both head and abdominal diameter as demonstrated for

2.5% I<sub>2</sub>KI solution, (Figure 4.4). There are large standard deviations associated with tissue distortion for each I<sub>2</sub>KI concentration, so although no statistical significance can be derived, trends are seen. It is envisaged that equivalent results of tissue distortion for the anatomical areas of head and abdomen would be replicated for other concentrations of I<sub>2</sub>KI used within this chapter. However, this was only tested with the fetuses immersed in 2.5% I<sub>2</sub>KI solution.



**Figure 4.3 Mean percentage head diameter reduces for all 4 concentrations of I<sub>2</sub>KI, but is greater for 3.75% and 5% than for 1.25% and 2.5%**

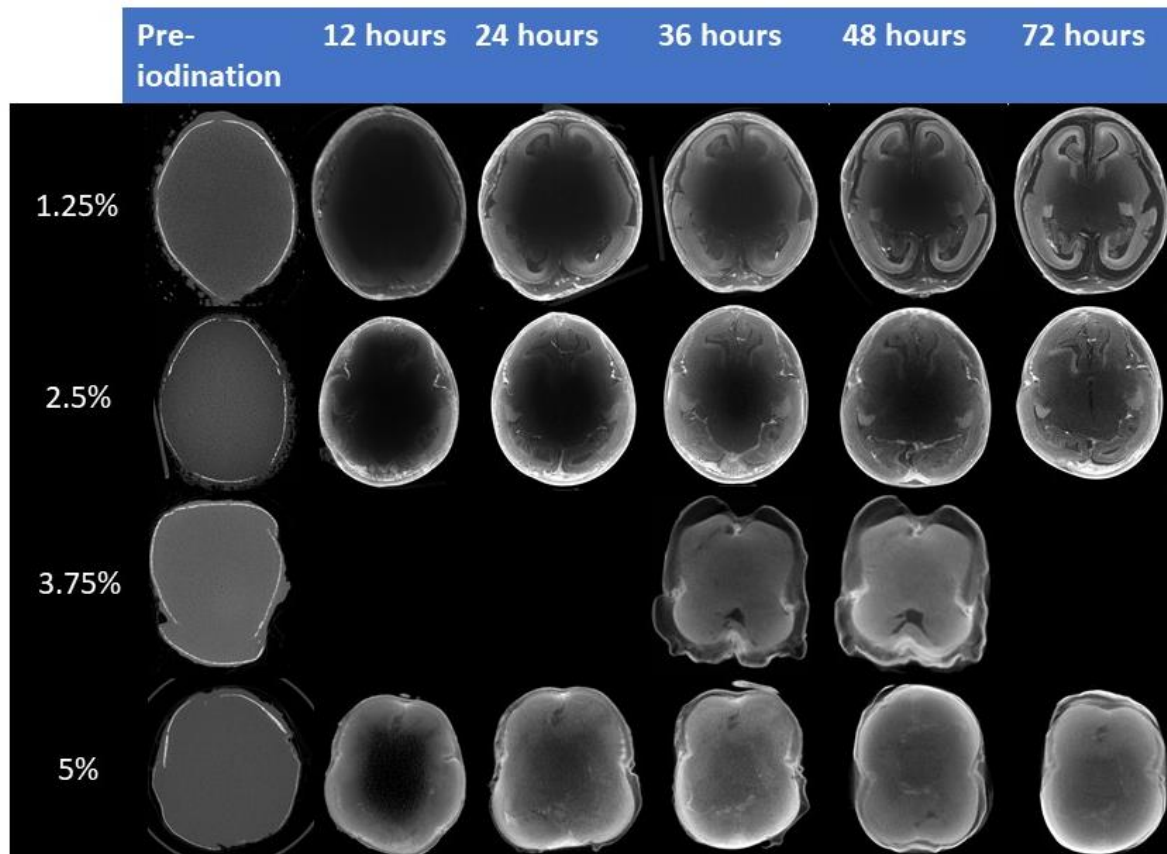




**Figure 4.4** Equivalent percentages of tissue distortion for head (solid line) and abdomen (dashed line) are observed following immersion in 2.5% I<sub>2</sub>KI solution

#### 4.6.2 Tissue iodination

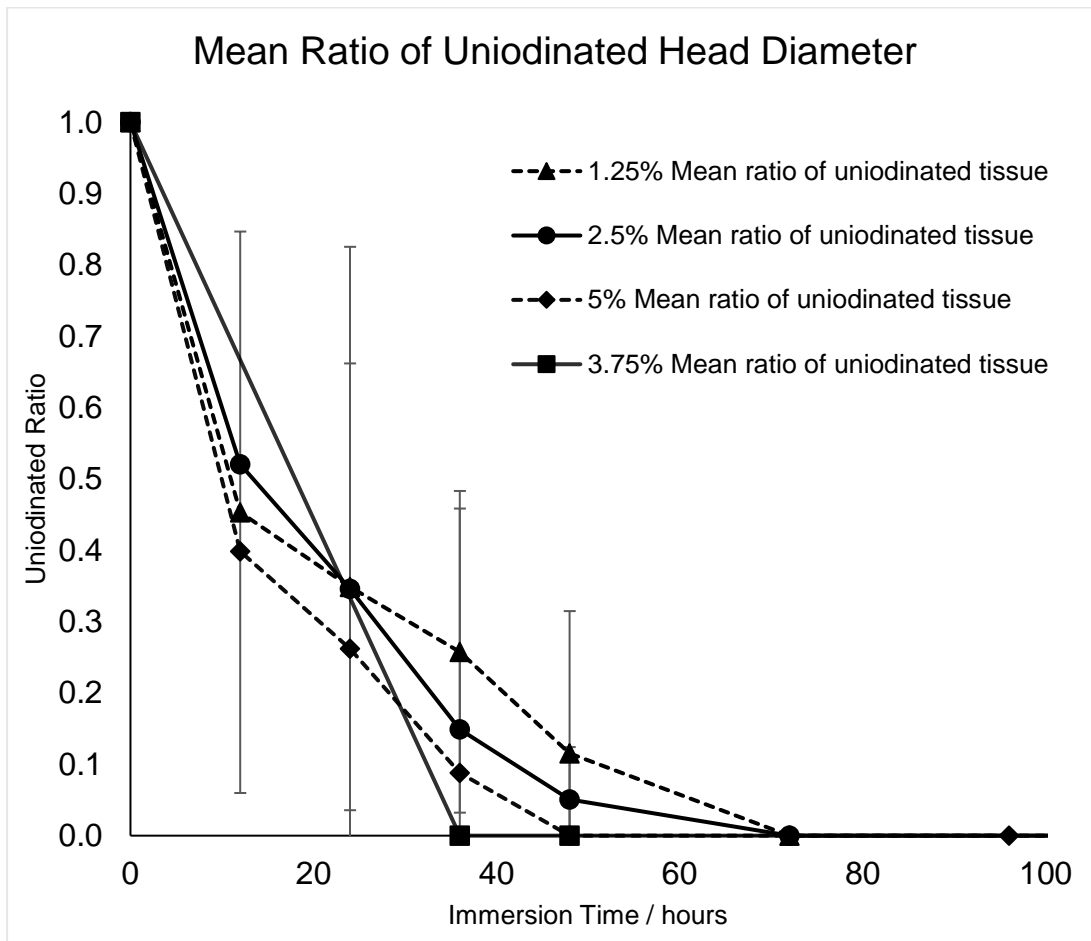
Figure 4.5 shows serial images as immersion time increases up to 72 hours for 1.25%, 2.5% and 5%, with 3.75% imaged at less time points. Gradual iodination can be seen as the cranial structures progressively become visible starting from the edge of the head and progressing towards the centre until full iodination is reached.



**Figure 4.5 Micro-CT images of four fetuses placed in differing concentrations of I<sub>2</sub>KI showing cranial structures becoming more visible with increasing immersion time**

As immersion time increases, the ratio of mean un-iodinated head diameter is reduced, (Figure 4.6), with 3.75% showing full iodination by 36 hours, 5% by 48 hours and 1.25% and 2.5% after 72 hours, Figure 4.5. Occasionally on later scanning timepoints, due to the greater contrast enhancement towards the periphery of the head, darker areas are noted within the central portion of the anatomy. However, this does not necessarily demonstrate non-iodinated areas and once image contrast levels are adjusted, anatomical details are visible both at the centre and periphery of the head, indicating full iodination has occurred. These checks were completed at each timepoint to assess whether this had occurred.

Although no statistical significance can be derived, a trend of increased rate of iodination is observed at the start of immersion in I<sub>2</sub>KI, which reduces over time.



**Figure 4.6 Un-iodinated head diameter reduces at differing rates depending on the I<sub>2</sub>KI concentration quickest iodination 3.75%, followed by 5% and equivalent times for 1.25% and 2.5%**

#### 4.7 Discussion

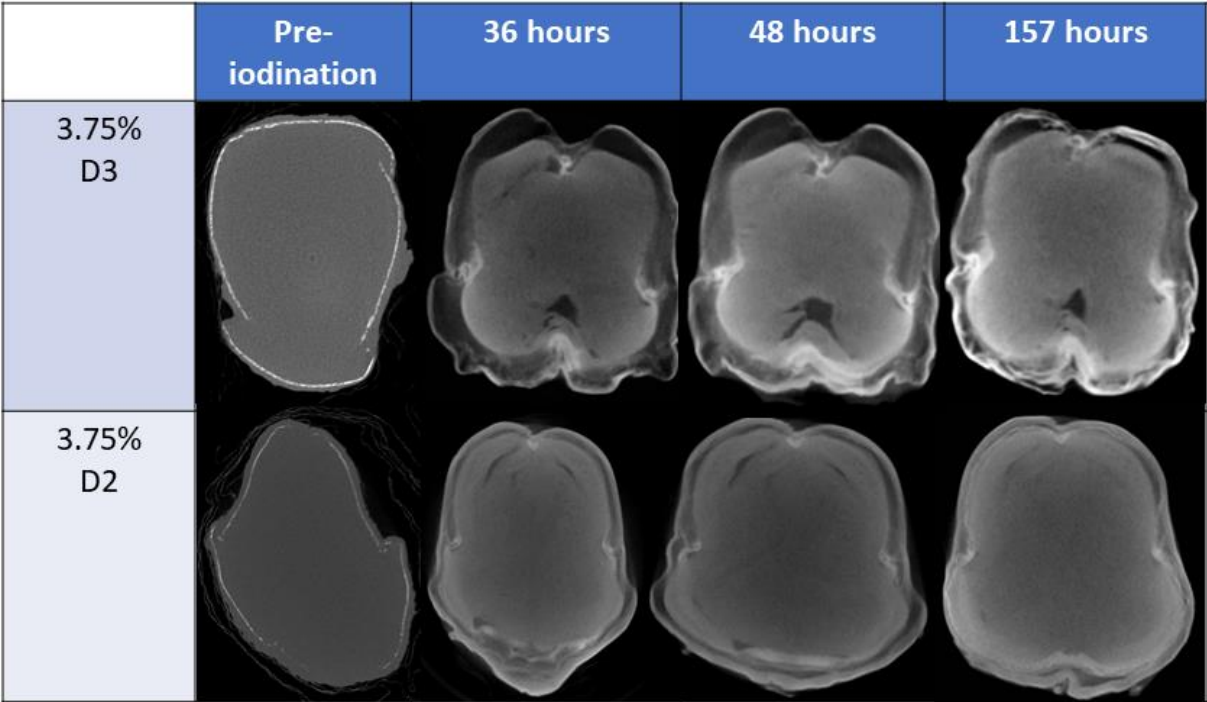
These preliminary results from 11 fetuses show iodination time is reduced with increasing I<sub>2</sub>KI concentration (3.75% and 5%), with full iodination occurring for all solutions after 72 hours. Tissue distortion occurred for all I<sub>2</sub>KI solutions, with reduced tissue distortion for the 1.25% and 2.5% concentrations when compared to 3.75% and 5% concentrations.

##### 4.7.1 Tissue iodination

3.75% was the iodine concentration which gave quickest iodination for all four groups displaying full iodination by 72 hours. 1.25% and 2.5% had the slowest rate, followed by 5%, but there are large overlapping confidence intervals for all four groups.

Although 3.75% I<sub>2</sub>KI resulted in the fastest iodination time, all fetuses within this group demonstrated severe internal maceration, (Figure 4.6) thereby not allowing assessment of non-macerated cases within the 3.75% group. Although the effect that increasing maceration would have on the iodination process was not tested here, it could be predicted that increasing maceration would increase the speed of iodination due to the breakdown of cellular borders and loss of intercellular space, resulting in fewer barriers to diffusion, as observed within the renal experiments, Chapter 3. The internal structure of the brain of these fetuses being clearly non-diagnostic, (Figure 4.7). This may be the cause of the reduced iodination time for the 3.75% I<sub>2</sub>KI group. Two further cases were also noted with one each in the 2.5% and 5% groups and removed from the assessments. However, there were sufficient cases remaining within all other groups, apart from 3.75%, to continue the subsequent analysis.

Ideally, this would have been repeated in a larger group, but there was limited patient consent for this iodination experimentation from the cohort recruited in Belgium to investigate these techniques, therefore further recruitment was not possible. On this basis, the 3.75% I<sub>2</sub>KI group were excluded from the final analysis.



**Figure 4.7 Maceration results in a loss of detail throughout the iodination process, with D2 and D3 demonstrating different fetuses placed within the 3.75% I<sub>2</sub>KI group**

Overall, the observed trends of increased concentration and reduced iodination times agrees with the literature [107, 114, 117, 123]. Our results for the rates of iodination show 1.25% and 2.5% to be slower to achieve full iodination, but that this was still achieved within 72 hours.

#### **4.7.2 Tissue distortion**

All I<sub>2</sub>KI concentrations resulted in a reduction of the head diameter, with a greater reduction seen for the 3.75% and 5% than for 1.25% and 2.5% I<sub>2</sub>KI solutions. The rate of tissue distortion was highest for all I<sub>2</sub>KI concentrations for the first 72 hours, after which the rate of reduction in head diameter reduced for those fetuses measured after this time (1.25%, 2.5% and 5%), (Figure 4.3).

It is proposed that dehydration of the tissue will occur following immersion in I<sub>2</sub>KI solution, and these results initially seem to support this proposition. A reduction in this effect is observed by a reduction in the I<sub>2</sub>KI concentration [107, 114, 116, 117, 123]. The plateau effect of tissue distortion over time has also been noted following several days immersion in mouse organs [117] and in the experiments in Chapter 3 regarding canine kidneys. To optimise the preservation of fetal anatomy for diagnostic purposes, tissue preparation phase for whole human fetuses tissue distortion should be minimised. This data therefore indicates a concentration of 1.25% or 2.5% I<sub>2</sub>KI solution would be ideal to limit tissue distortion. Whilst this may extend the immersion time required to achieve full iodination, the plateauing of the tissue distortion indicates that extended immersion does not result in further tissue distortion.

Therefore, 2.5% I<sub>2</sub>KI solution with its equivalent tissue distortion to 1.25% I<sub>2</sub>KI solution, combined with the negligible increase in iodination time when compared to 5% I<sub>2</sub>KI solution, should be used to iodinate whole human fetuses.

Therefore, the null hypothesis 4-1 can be rejected. A greater number of time points and specimens would have allowed a more detailed analysis.

#### **4.8 Limitations**

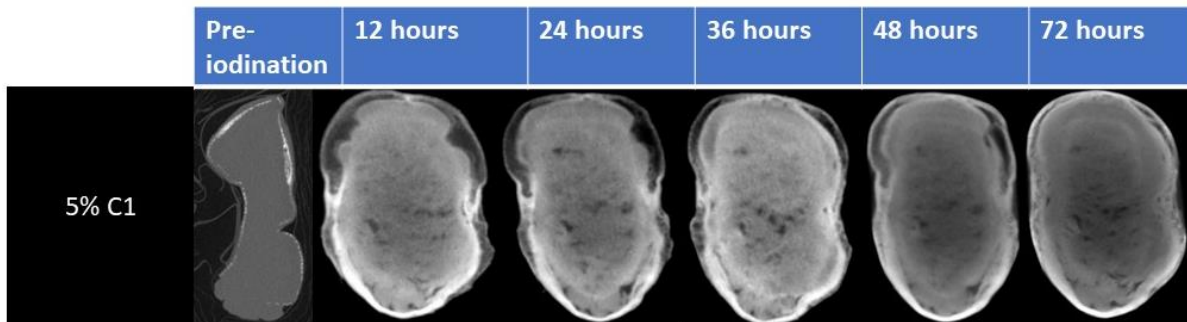
There are several limitations to this study.

Firstly, many fetuses were excluded due to small size and high degree of maceration, resulting in only 2 – 3 specimens in each category. Unfortunately, all fetuses in the 3.75% group were macerated and therefore excluded from further analysis. Although it would have been advantageous to repeat this concentration, this was not possible due to a limited time for recruitment into the tissue iodination assessment. Access to further fetuses was therefore not possible and the 3.75% I<sub>2</sub>KI group were excluded from the analysis.

Secondly, manipulation of the diameter and shape of the head was possible during immobilisation which could have affected tissue distortion. Firm parafilm wrapping was required to ensure no movement during scanning but could cause deformation of the fetus affecting the accuracy of the experiment, (Figure 4.8). It was also noted that the fetuses became less malleable as the iodination process progressed, which is important to note for technical development, as this will minimise deformation of the fetuses following full iodination.

Thirdly, greater detail in the demographics for each fetus and group should have been recorded including, fetal size, body weight, fetal weight, mode of pregnancy loss, and individual fetal measurements prior to immersion within the I<sub>2</sub>KI solution. This would have allowed greater interrogation of the results to determine their effect on tissue distortion and iodination times and it should be taken into account in future research.

Body weight would also have been a more suitable demographic to distribute the fetuses more evenly between the four groups. This is due to gestational age continuing to increase despite a pregnancy loss having occurred until delivery of the fetus, whereas body weight does not alter once the pregnancy loss has occurred and more accurately reflects the fetuses stage of development.



**Figure 4.8 Compression of the fetal head causing errors within subsequent measurements, with C1 being the lowest gestational age within this group**

#### 4.9 Conclusion

In conclusion to minimise tissue distortion and to achieve full iodination in fetal heads of 29mm diameter or less, 2.5% I<sub>2</sub>KI solution should be used, and should be fully iodinated within 72 hours. This should be validated in a larger cohort.

#### 4.10 Experiment 2 – larger cohort

Although the technique has been shown to be applicable to whole human fetuses [74, 125], an optimised tissue preparation protocol has not yet been fully developed and these preliminary investigations show a greater depth of empirical data within this area is required.

Firstly, although trends can be described from this preliminary data, further investigations require a larger number of fetuses to produce more statistically significant results.

Therefore, a larger range of fetal sizes should be immersed within a solution of 2.5% I<sub>2</sub>KI solution to identify the relationship between iodination time and fetal body weight and gestational age. These demographics are chosen as they are independent of individual anatomical areas. This would allow predictions to be made as to the time required for full iodination for a wider range of fetuses as part of a clinical protocol.

## **4.11 Aims**

**Aim 4-2:** To determine whether there is a relationship between immersion time in 2.5% I<sub>2</sub>KI solution and gestational age and body weight

**Null hypothesis 4-2:** Demographics including gestational age and body weight will not correlate with the immersion time for full iodination of human fetuses.

## **4.12 Method**

### **4.12.1 Patient selection**

Consecutive, unselected fetuses below 300g body weight with parental consent for post-mortem micro-CT imaging were prospectively included over a 1-year period between October 2019 – October 2020. It had been identified that above 300 g required more than 2 weeks immersion in I<sub>2</sub>KI solution and that this was deemed too long for some parents. Consent was obtained prior to clinical and research micro-CT scanning using the consent forms developed by GOSH (Appendix 3).

Exclusion criteria included any fetuses where staff absence delayed the examination time. Absence of scanning staff would cause prolonged immersion times where the imaging may have been able to be completed at an earlier date. Also excluded was where the fetus was immersed in insufficient or incorrect concentrations of I<sub>2</sub>KI solution or where an anatomical abnormality affected iodine perfusion, such as a body wall defect.

Note was made of the fetal post-mortem body weight prior to immersion (grams) and gestational age according to the antenatal notes (weeks), which was rounded up to whole weeks.

### **4.12.2 Micro-CT scanning and I<sub>2</sub>KI immersion**

Fetuses were immersed in 2.5% I<sub>2</sub>KI solution and scanned on either a XTH225 ST or Med-X micro-CT scanner (Nikon Metrology, Tring, UK), depending on availability, at regular intervals every three days due to scanning staff availability until full iodination was observed. Although this may have caused a slight increase in the scanning times, this was a practical solution for this large number of patients. Both scanners are equal



in their ability to produce diagnostic images and although there are differences in the detectors installed, this did not influence the determination of full-iodination.

All micro-CT scans were completed as described in Appendix 4. Initial scanning was performed with a range of imaging parameters (100 - 130kv, 150 - 250 $\mu$ A, 250ms and 1FPP), depending on the size of fetus to allow rapid assessment of the extent of fetal iodination in <10 minutes. The end-point of complete iodination was determined when all anatomical regions were visible due to contrast enhancement. If any fetal anatomy was deemed incomplete iodination the fetus was replaced within the I<sub>2</sub>KI solution and scanning repeated at a later time point.

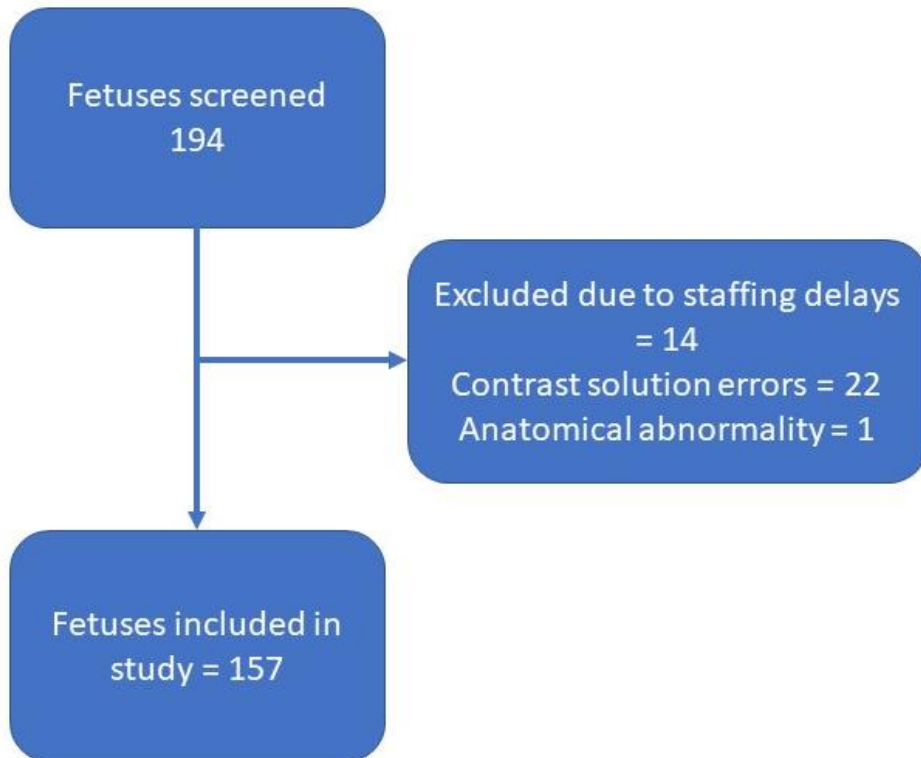
#### **4.12.3 Data analysis**

Data including gestational age, body weight, and the dates of immersion in I<sub>2</sub>KI solution and micro-CT scanning was recorded with the full iodination time calculated using Microsoft Excel version 365 (Microsoft Corp, Redmond WA, USA). Simple linear regression analysis was completed for immersion time against both gestational age and weight.

### **4.13 Results**

#### **4.13.1 Study population**

194 fetuses were referred for micro-CT scanning, with exclusions shown in Figure 4.9 and a total of 157 fetuses included in the study, body weight 5 – 298g, (89 at 0-100 g, 38 at 101-200 g, 30 at 201-300 g) and gestational age 12 – 34 weeks.



**Figure 4.9 Exclusion criteria flow diagram**

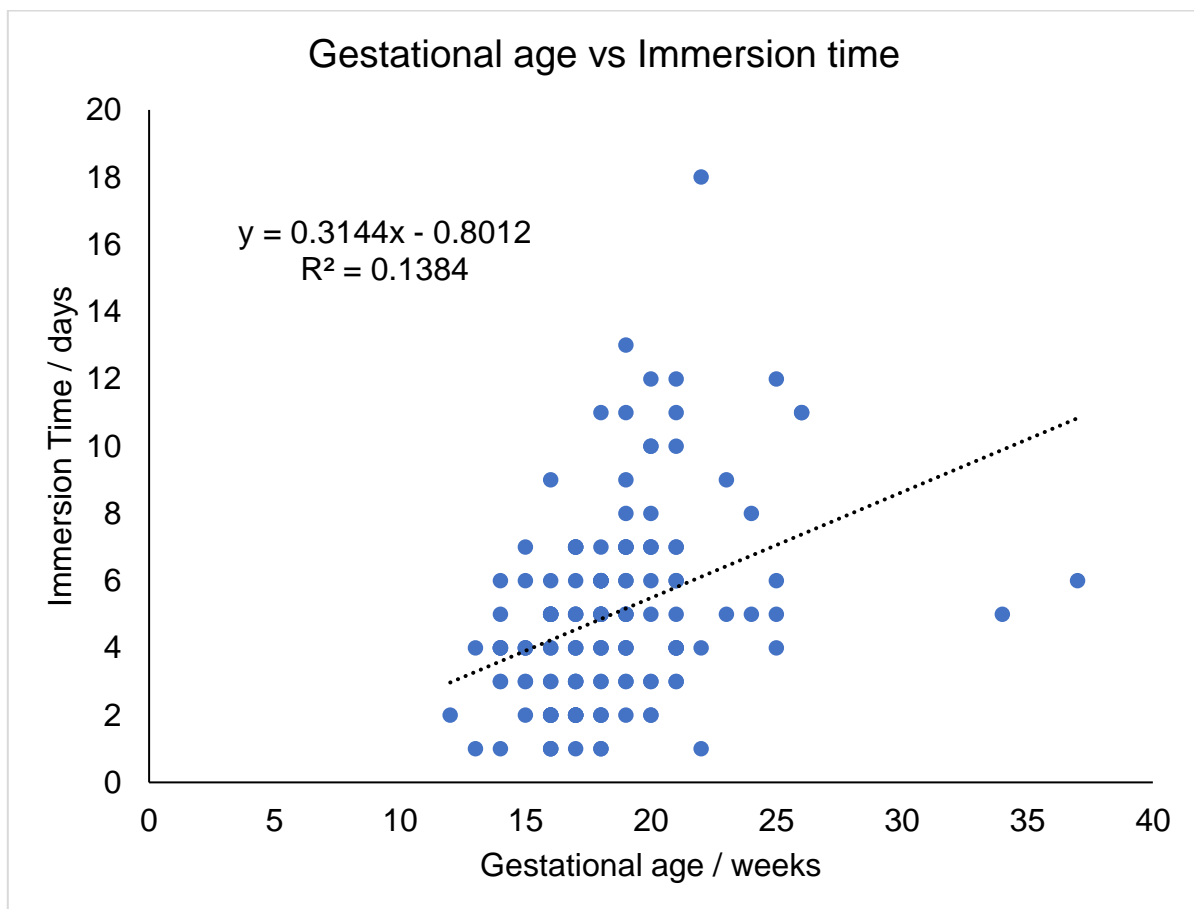
#### 4.13.2 Gestational age and immersion time

Simple linear regression analysis comparing gestational age and iodination time resulted in an  $r^2$  value of 0.1384 and a line of best fit, (Figure 4.10),

$$\text{Immersion time} = (0.3144 \times \text{gestational age (weeks)}) - 0.8012$$

This can be approximated to:

$$\text{Immersion time} = (0.31 \times \text{gestational age (weeks)}) - 0.8$$



**Figure 4.10 Simple linear regression analysis of gestational age and immersion time displaying an  $r^2$  value of 0.1384, determining gestational age as a poor predictor of immersion time**

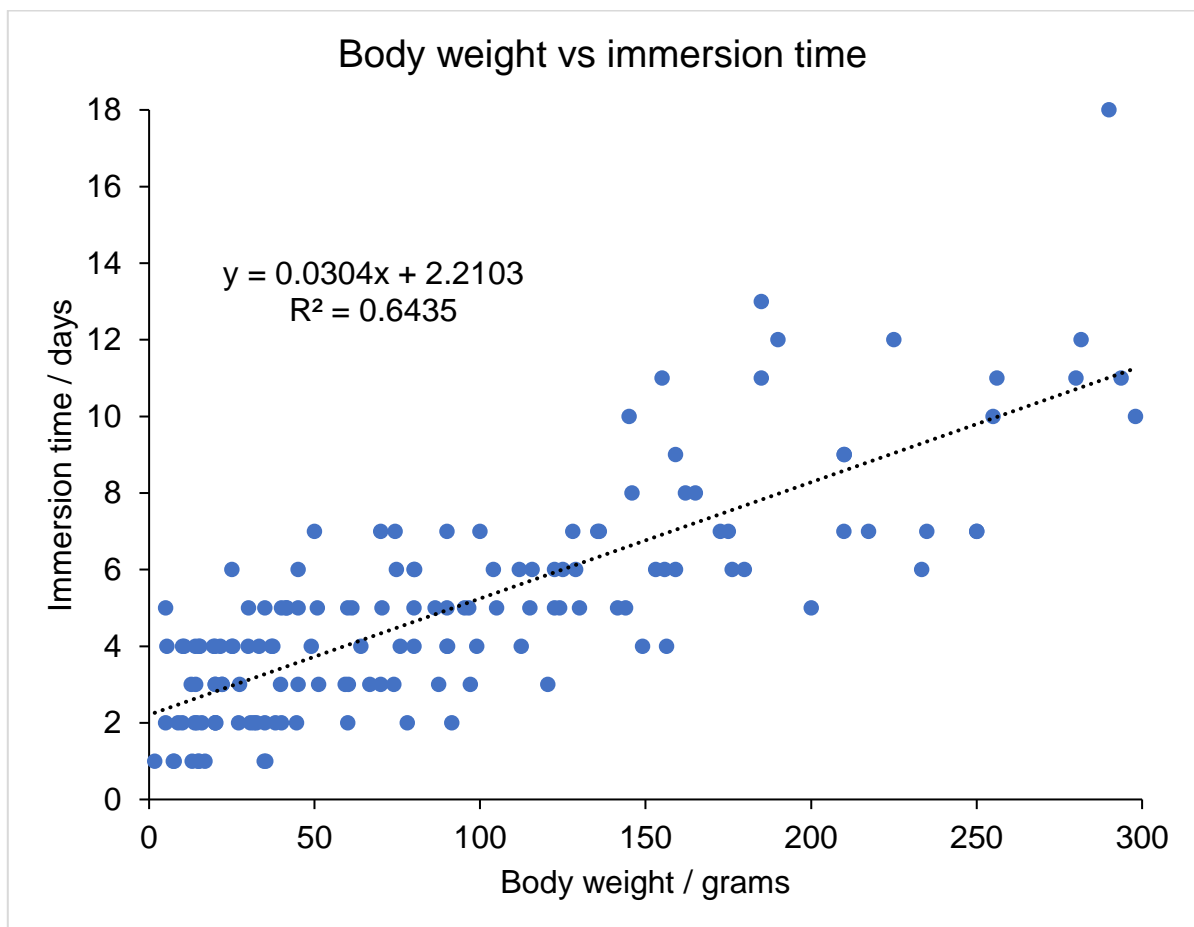
### 4.13.3 Body weight and immersion time

Simple linear regression analysis was completed comparing body weight and iodination time resulted in an  $r^2$  value of 0.6435 and a line of best fit, (Figure 4.11)

$$\text{Immersion time} = (0.0304 \times \text{body weight}) - 2.2103$$

This can be approximated to:

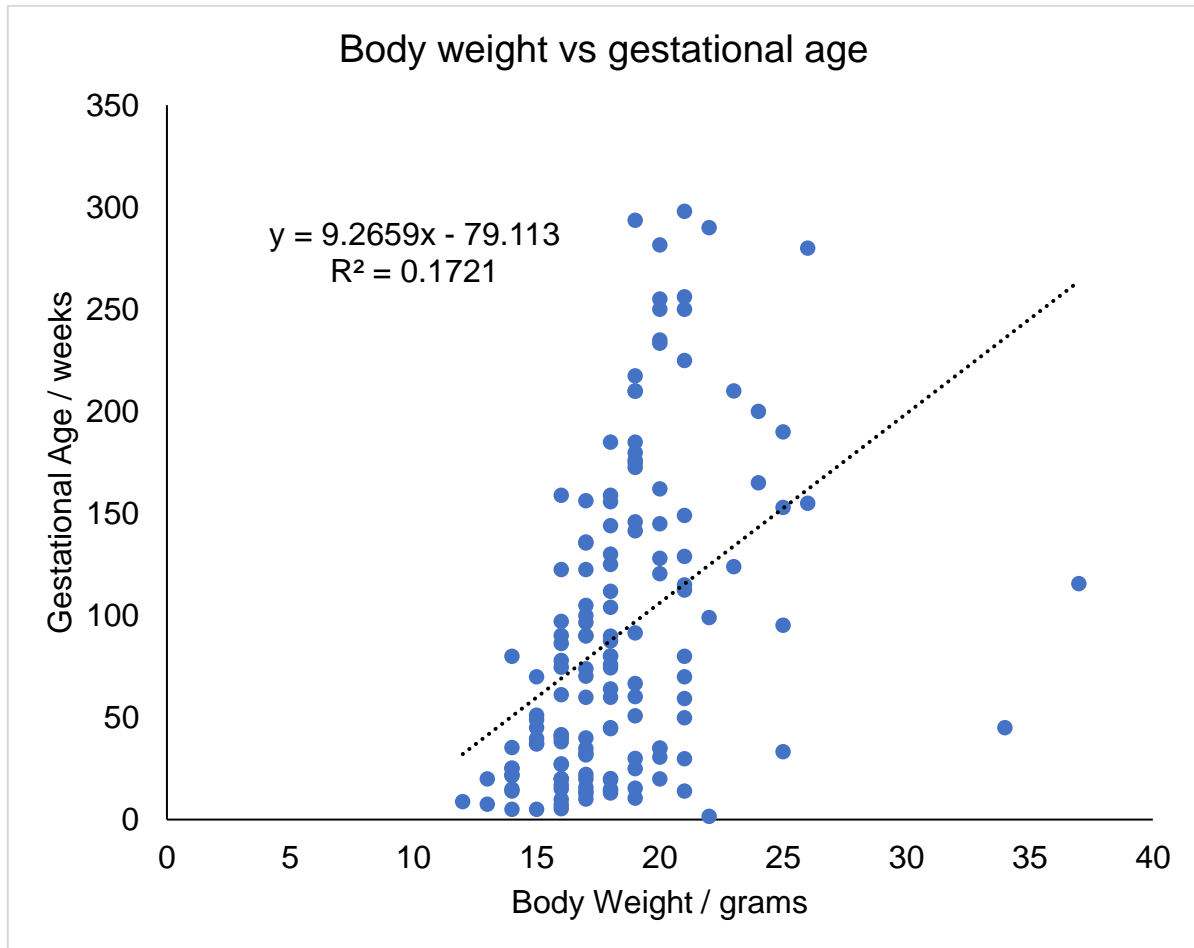
$$\text{Immersion time (days)} = (0.03 \times \text{body weight (grams)}) - 2.2$$



**Figure 4.11 Simple linear regression analysis of body weight and immersion time displaying an  $r^2$  value of 0.6435, determining body weight as a better predictor of immersion time**

#### 4.13.4 Gestational age and body weight

Simple linear regression analysis comparing gestational age and iodination time resulted in a poor  $r^2$  value of 0.1721 and a line of best fit, (Figure 4.12).



**Figure 4.12 Simple linear regression analysis of gestational age and body weight displaying an  $r^2$  value of 0.1721, demonstrating that gestational age is a poor predictor of body weight**

#### 4.14 Discussion

This study has shown that body weight (rather than gestational age) is a better predictor of the iodination immersion time with an  $r^2$  value 0.63. The formula  $\text{Time (days)} = 0.03 \times \text{Weight (g)} + 2.2$  can be used to predict the immersion time required in 2.5%  $\text{I}_2\text{KI}$  solution for whole human fetuses.

Compared to other studies evaluating iodination times for human fetuses [125, 126], this study evaluated the largest cohort (n=157) and was the only study to include weight in its analysis as well as gestational age. These studies were not specifically developing a protocol to predict the immersion time required for full iodination, but instead showing proof of principle and diagnostic accuracy of the micro-CT scanning technique in comparison to conventional autopsy.

#### **4.14.1 Gestational age**

Whilst age is often quoted on referrals for post-mortem investigations, it can be an inaccurate representation of the size of the fetus. Following a miscarriage, time can pass before this event is medically recognised. This creates a mismatch between fetal size (which stops with death) and gestational age (which advances with time), with gestational age becoming increasingly poorly correlated with fetal size. Additionally, some organs are preserved preferentially to other following intrauterine death [143].

Furthermore, the data showed a larger range of body weights (2 – 298 g) in comparison to a smaller range of gestational ages, with the majority within 12-26 weeks, (Figure 4.9). The non-linear association between gestational age and body weight demonstrates this mismatch between gestational ages and weights for these patients.

#### **4.14.2 Body weight**

In comparison, body weight is directly determined by the composition of the remaining fetal anatomy and is easily measured. The relatively high  $r^2$  value (0.6435) indicates that body weight is a good predictor of iodination time and can provide an accurate prediction of the time required for full iodination. Specimen weight is an important variable of iodination speed as larger specimens require greater exposure [85]. This experimental information can be used to determine a clinical service and conveyed to the parents during consent for a more accurate assessment of the time required for the clinical examination.

Although this analysis, (Figure 4.11), shows patients either side of the linear regression line of best fit, these variations of full iodination time differences could be due to a variety of effects.

Although body weight was shown to be a better predictor than gestational age, this weight could be distributed differently depending on the shape of the fetus. This could result in for example, a larger than normal head with only a small body and cause an increase in the time required for iodination. Although this scenario may be encountered in conditions such as intra-uterine growth restriction, this is still rarely seen clinically. This situation could then be identified visually upon examination of the fetus or from the patients notes, prior to immersion in the I<sub>2</sub>KI solution. An extended immersion time could then be advised in these small proportion of cases.

If not identified prior to immersion, a partially-iodinated scan will result, indicating further immersion is required and additional scanning at a later date should take place once fully-iodinated to ensure full visualisation of the anatomy.

Although, diameter measurements of the head or abdomen could have been included in the analysis to examine their influence in determining a more accurate estimation of immersion time required, these are not routine measurements taken by the mortuary and would have required discussion and teaching to collate accurate and repeatable measurements, to eliminate possible error.

Therefore, with the small number of fetuses this affects in clinical practice and the difficulties in collating additional non-routine measurements of the head or abdomen, it was decided that body weight offered a practical solution to the prediction of immersion time required. These observations will allow staff completing the consent procedure to assess the immersion time using the equation and knowledge acquired on expected body shapes.

All fetuses included in the study did fully iodinate, even after an extended immersion time, demonstrating the technique as a practical solution for this wide range of fetal weights.

#### **4.14.3 Maceration**

Maceration describes changes that occur secondary to intrauterine fetal retention following fetal death and tissue autolysis [139], including skin slippage, blistering, discolouration, and overlapping of the skull bones. Maceration was not recorded for

this investigation. Although this data was not formally tested here, further investigations using the pathological maceration scale to assess the fetus prior to immersion in I<sub>2</sub>KI solution and a comparison to the iodination time could be completed to determine whether it caused a change to the iodination time.

Although no data exists within the literature, maceration may speed up the iodination process due to a breakdown in the tissues by removing barriers to the diffusion of iodine molecules, (i.e., reduction of the intercellular space and homogenisation of body tissues). This would possibly result in a reduction in the iodination time, allowing earlier micro-CT scanning. Although fetal maceration reduces the amount of information available for clinical diagnosis, the ability to investigate the cause of death for the family should not be undervalued, even if no clinical information is available following this non-invasive procedure, as it allows parents to feel that they have investigated their loss fully [37, 144-148].

Although, repeated scanning every three days was completed on individual fetuses to determine the earliest iodination time, a decrease in the time between scans would have allowed a more accurate assessment of the immersion time equation. However, it was impractical to complete for this large cohort every 24 hours due to staff capable of scanning availability. Therefore, a pragmatic approach was taken, with scanning completed at regular intervals for the wide range of fetal ages and weights when staffing allowed. Due to the large number and range of fetuses included in this study it is felt that this provides a strong argument for the accuracy of the formula in calculating the immersion time required. Accuracy could have been further improved had scanning been completed more regularly.

To fully iodinate an increased range of fetal weights in micro-CT within a clinically acceptable timeframe, techniques to increase the diffusion speed and distance may be required to iodinate without causing distortion of the fetus through increased I<sub>2</sub>KI concentrations.

Improvements to the technique could be achieved by exerting pressure to the fetus once fully immersed or through agitation of the fetus and solution to increase



penetration and iodination speed, but these experiments were beyond the time frame of this PhD.

This data shows that immersion time can be more accurately predicted using body weight than gestational age. Therefore, the null hypothesis 4-2 is rejected.

#### **4.15 Limitations**

There are several limitations associated with this study.

Firstly, although a large range of body weights were observed, further studies could be completed to investigate how long increased body weights take to fully iodinate. If the regression line continues above 300g, larger fetuses could still be iodinated within 2 weeks, increasing the range of possible fetal sizes within this timeframe.

Secondly, maceration status was not recorded. These assessments require specialist training in paediatric or obstetrics and remains a subjective assessment once it is established. This may increase or decrease the time required for iodination but may increase the accuracy of the protocol. By including all fetuses regardless of their maceration status, a real-world approach was taken which is relevant to clinical practice where fetuses with a range of maceration will be referred.

Thirdly, although tissue distortion has been noted as an artefact of immersion in I<sub>2</sub>KI solution previously [107, 114, 116, 123], it was demonstrated that 2.5% produced minimal distortion in comparison to other concentrations earlier in this chapter. Therefore, this was not completed but is noted as an unavoidable effect, which should be minimised as has been achieved within this thesis.

#### **4.16 Conclusion / Summary**

Body weight is a good predictor of immersion time required in 2.5% I<sub>2</sub>KI solution for full iodination of whole human fetuses. The equation  $\text{Time (days)} = (0.03 \times \text{body weight}) - 2.2$  should be used to predict the immersion time required for clinical micro-CT cases, allowing accurate timeframes to be predicted for healthcare professionals and parents during the consent procedure. It further develops the tissue preparation phase of the

micro-CT protocol, delivering clear guidance to clinical staff in developing this examination for clinical use.

#### **4.17 Key Points**

- Immersion in 2.5% I<sub>2</sub>KI solution can fully iodinate the majority of fetal cases up to 300 g within 14 days.
- Body weight is a good predictor of the required immersion time in 2.5% I<sub>2</sub>KI to fully iodinate whole human fetuses, using the formula  
Immersion time (days) = (0.03 x body weight (grams)) – 2.2
- Tissue distortion is minimised by using lower concentrations.
- Further work to develop methods of increasing the diffusion speed of the I<sub>2</sub>KI solution may result in increased efficiencies and a greater range of weights being applicable to micro-CT scanning.

# **Chapter 5      Development      of      Methodology      For**

## **Quantitative Assessment Of Imaging Parameters**

### **5.1 Overview**

This chapter develops the methodology to investigate the effect imaging parameters has on the image quality of micro-CT images for iodinated human fetuses.

The work presented in this chapter was undertaken by the author of this thesis, with statistical and coding advice provided by Dr Alessandro Felder. Work from this chapter has been presented orally at Academic Involvement Group, GOSH (2020) [149].

### **5.2 Aims**

The main aim of this chapter is to develop a reproducible method for gaining accurate SNR and rCNR measurements for human fetal post-mortem micro-CT imaging.

Therefore, a series of four investigations is described indicating key decisions that were taken to develop this methodology including,

- ROI placement
- Range of imaging parameters
- Use of phantom material
- Method of ROI and 2D or 3D assessment

### 5.3 Experiment 1 – ROI placement

#### 5.3.1 Aim

The main aim of experiment 1 was to determine the most suitable anatomical organ for investigation of the SNR and rCNR as the imaging parameters are altered.

#### 5.3.2 Background

The human fetus consists of a wide range of organs and tissues with a corresponding range of signal intensities depending on the tissue being imaged. To ensure comparable analysis of the imaging parameters, the optimal organ should be identified to provide a consistent area for analysis. This will allow evaluation of the image quality between individual fetuses following assessment of the SNR and rCNR.

When comparing the image quality, ROI will need to be placed within the organ, allowing maximal sampling of the signal intensities. It is envisaged that an easily identifiable and large organ should be chosen to enable suitable ROI placement. Therefore, three organs were initially identified as being suitable, brain, heart, and liver.

#### 5.3.3 Method

A single fetus was sited within the x-ray cone beam of a Med-X micro-CT scanner (Nikon Metrology, Tring, UK) and immobilised as previously described, Appendix 4, along with a small cylindrical phantom containing air which was included within the x-ray beam. Individual acquisitions were obtained using a range of kilovoltage values, with all other imaging factors remaining constant, Table 5.1.

	Kilovoltage / kV	Current / $\mu$ A	Exposure Time / ms	FPP	Scan Time / minutes
Kilovoltage Experiment	50 – 150	200	125	1	4

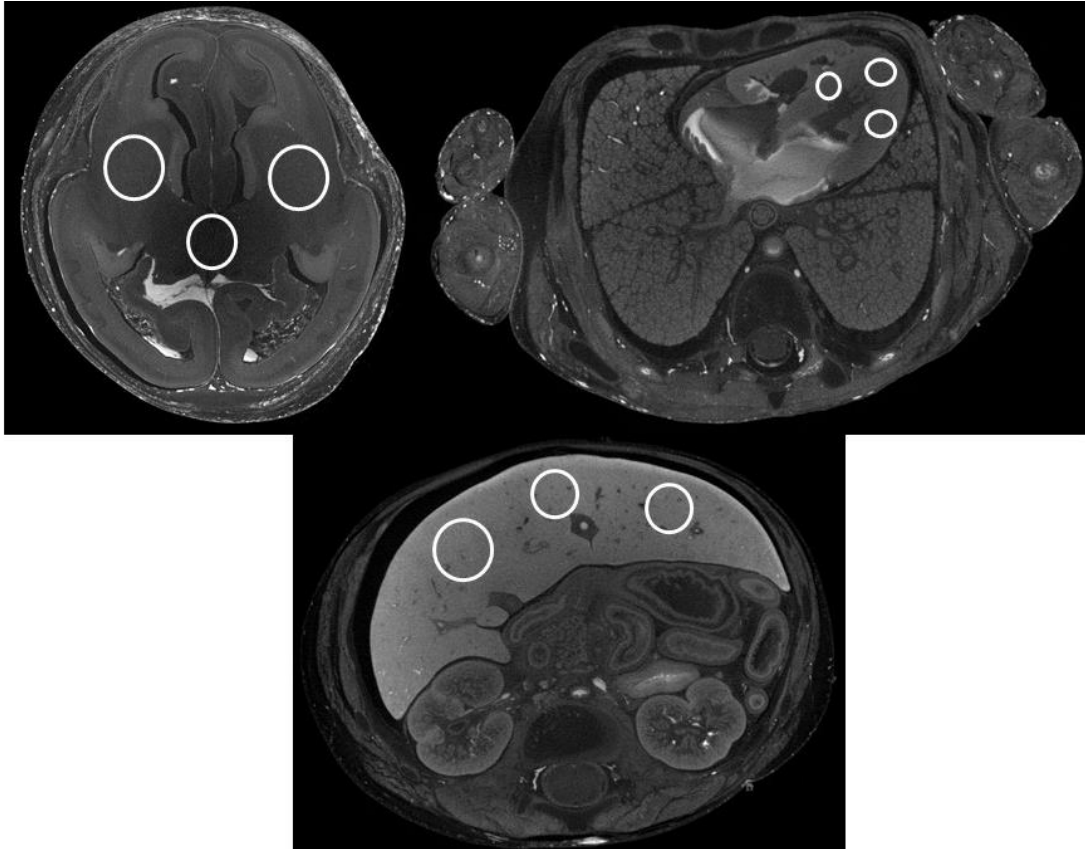
**Table 5.1 Imaging factors used to compare the SNR and rCNR of brain, cardiac and liver tissue.**

All images were reconstructed using VGStudio Max software 3.4 (Heidelberg, Germany) with equivalent single axial slices of all three organs identified: mid-brain, 4-

chamber view of the heart and midpoint of the liver. Three ROI were placed within each organ maximising their size and placement to the homogenous tissue available within each organ to maximise the amount of tissue measured, (Figure 5.1).

The ROI were placed as indicated in figure 5.1, in the axial plane and with the following diameters. Individual ROI were placed within areas of the brain, centrally in the massa intermedia (2 mm), and two laterally to the lateral ventricles (2.5 mm). Individual ROI were placed within the cardiac myocardium, centrally on the ventricular septum (1 mm), at the apex of the heart (1 mm) and at the midway point of the lateral left ventricular myocardium (1 mm). Three ROI were placed within the liver equidistant from each other on a midway through the liver in the axial plane and sited 1 mm from the anterior edge of the liver (3 mm).

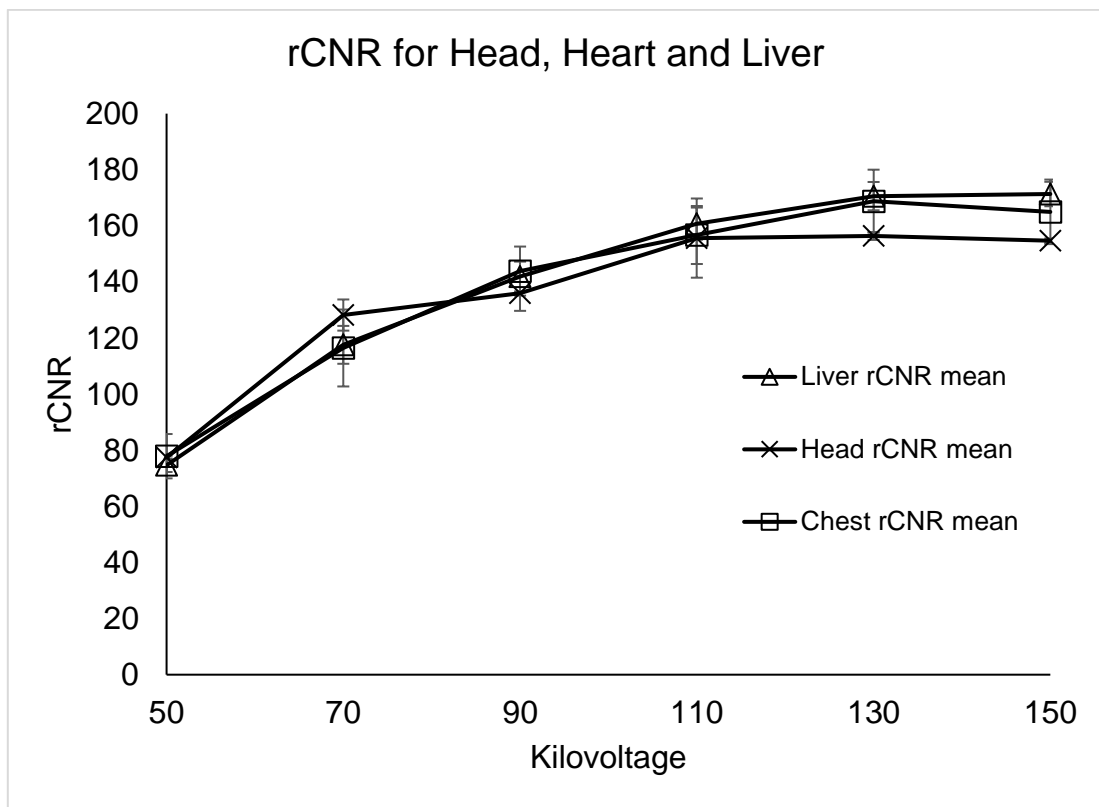
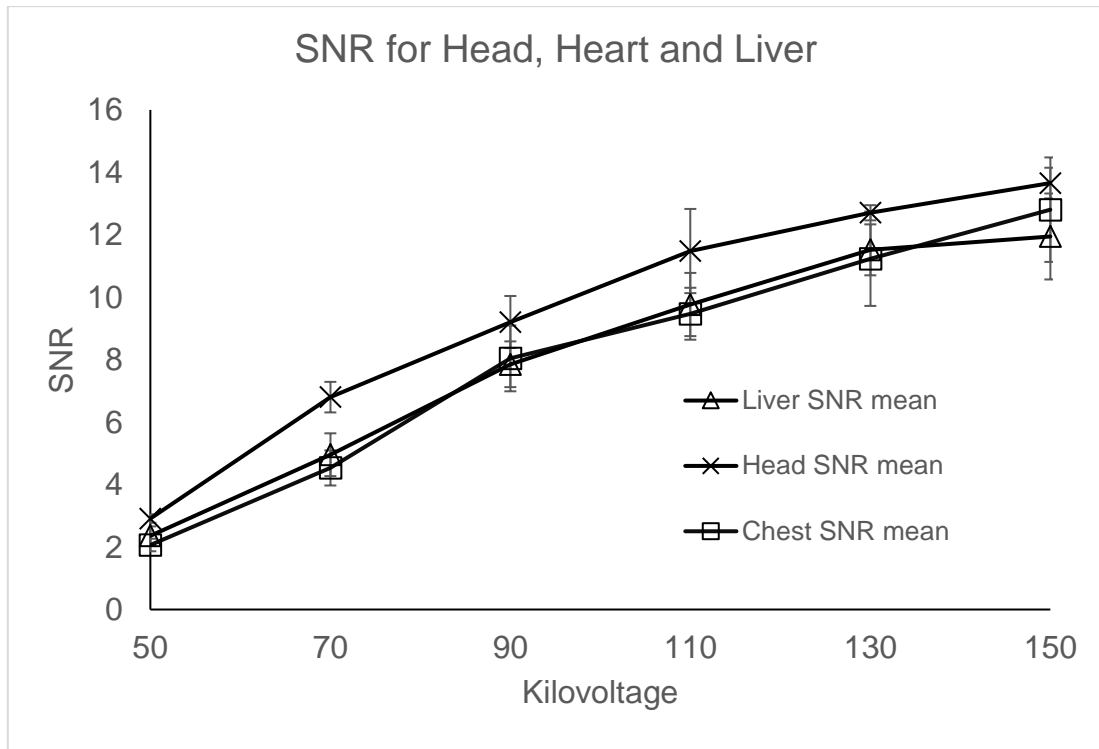
A single ROI was also placed midway through the air phantom. Note was made of the mean signal intensities and standard deviations to calculate the SNR and rCNR for each organ.



***Figure 5.1 Placement of ROI in brain, cardiac and liver tissue to assess the mean signal intensity. ROI placement was optimised to maximise the amount of homogenous tissue and avoidance of vessels, ventricles, and organ edge***

#### **5.3.4 Results**

SNR and rCNR increased equally for all three anatomical areas as kilovoltage increased with slightly increased SNR values observed for the brain, (Figure 5.2).



**Figure 5.2** Equivalent increases for SNR and rCNR as kilovoltage was increased were observed for the brain (cross), heart (square) and liver (triangle) tissue, with slightly raised values of SNR being observed for the brain

### 5.3.5 Discussion

This experiment showed that SNR and rCNR increases were noted for all three anatomical areas.

Slightly increased SNR and rCNR values for the brain in comparison to the liver and heart were observed due to an inherently higher signal intensity and lower standard deviation.

Therefore, all three demonstrate equivalent changes in image quality as kilovoltage is increased and would therefore be suitable for SNR and rCNR assessments. However, a choice is required to standardise data collection, with the following factors considered.

When an organ has large discrepancies in signal intensity, perhaps produced by vessels or alternative tissue within a small area, incorrect placement of the ROI can produce inaccuracies. Therefore, signal homogeneity is an advantage in allowing a larger area to be analysed without changes due to anatomical structures being included in the analysis, e.g., blood vessels, ventricles, or other organs within a structure, gall bladder.

The heart muscle is relatively homogeneous due to the small size of the vessels penetrating the muscle itself. In comparison the liver has much larger vessels, but are mainly positioned centrally, whereas the brain has a larger difference between multiple tissues including grey and white matter, ventricles, and blood vessels, with little homogeneous tissue.

Larger organs allow for increased ROI, allowing greater sampling, providing tissue homogeneity is high and allows for heterogeneous signal to be avoided. This is linked to the homogeneity of the organ and offers the advantage of larger areas to be analysed providing a more informed analysis without inclusion of other structures as detailed previously. Whilst the liver and brain are both relatively large organs within the body, the cardiac muscle is much smaller offering limited placement.

Organs that span the width of the body allow representative sampling from a wide positional range within the body. This variation could account for differences in



iodination, with increased signal at the periphery of the body and lower towards the centre often observed. Whilst the liver and brain span the whole body axially, the majority of the cardiac muscle lies at the periphery.

The liver is relatively homogeneous, albeit with some large vessels easily avoided towards the central portion and spans the width of the body. This makes it the most suitable organ to measure SNR and rCNR changes.

### **5.3.6 Conclusion**

As no clear advantage is observed between the brain, liver, or cardiac muscle through objective testing of SNR and rCNR, a subjective approach choice must be made to identify the most appropriate organ. Therefore, the liver is deemed the most suitable organ to determine image quality changes for SNR and rCNR as imaging parameters are altered as it is relatively homogeneous, is large to allow sufficiently large ROI placement and spans the bodies width, allowing a fuller assessment of the changes observed during imaging parameter changes.

## 5.4 Experiment 2 – Imaging parameter determination

The main aim of experiment 2 was to establish optimal imaging parameters to observe the image quality changes through SNR and rCNR measurement.

Investigating a wider range of imaging parameters will provide a greater understanding of the relationship between these imaging parameters and their effect on image quality.

### 5.4.1 Background

Four imaging parameters (kilovoltage, current, exposure time and FPP) were chosen for investigation due to their effect on the SNR and rCNR of the micro-CT images through their effect on the x-ray beams properties. Exposure time and FPP also affect the scanning time of a protocol, with implications on the clinical applicability of the protocol, Table 5.2. Therefore, thought should be given to the effect this has on image quality at the expense of scan time.

**Table 5.2** *The effects of changing individual imaging parameters on the x-ray beam and scan time*

	Effect on x-ray beam	Effect on imaging time
Kilovoltage	Increase causes an increase in the energy of the x-ray photons	None
Current	Increase causes an increase in the number of x-ray photons produced	None
Exposure Time	Increase causes an increase in the length of time the x-rays are produced for each imaging position	Increase causes an increase in scan time
Frames per Projection	Increase affects the number of times the specimen is exposed in each position throughout 360° of rotation	Increase causes an increase in scan time

### 5.4.2 Method

The fetus was positioned and immobilised as previously described within a cone x-ray beam allowing the inclusion of a cylindrical air phantom.

Each imaging parameter experiment was performed once on a single fetus throughout the specified ranges, with other parameters unchanged, Table 5.2.

**Table 5.3 Imaging parameters for experiment 2, with shading displaying the range of imaging parameters under investigation**

	Kilovoltage / kV	Current / $\mu$ A	Exposure Time / ms	FPP	Scan Time / minutes
Kilovoltage Experiment	50 – 150	200	125	1	4
Current Experiment	100	50 – 400	125	1	4
Exposure Time Experiment	100	100	67 – 500	1	1 – 17
FPP Experiment	100	200	125	1 – 4	10-40

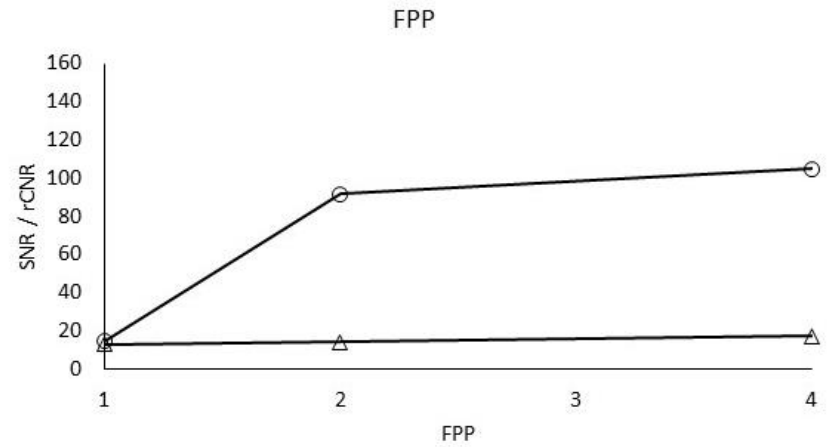
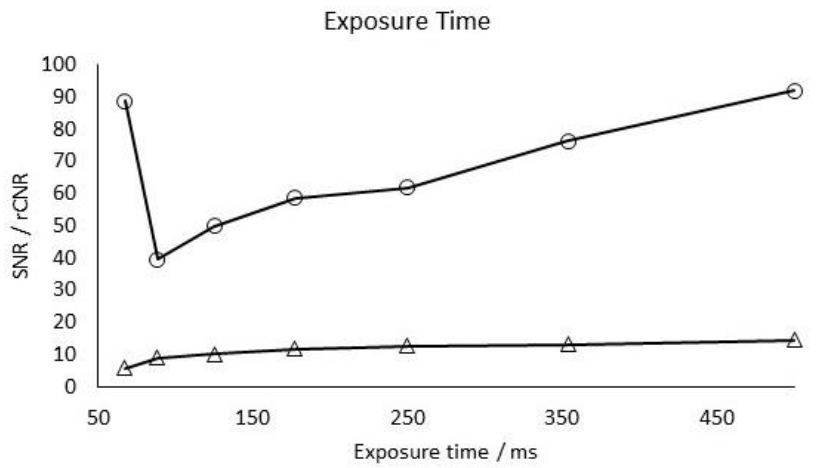
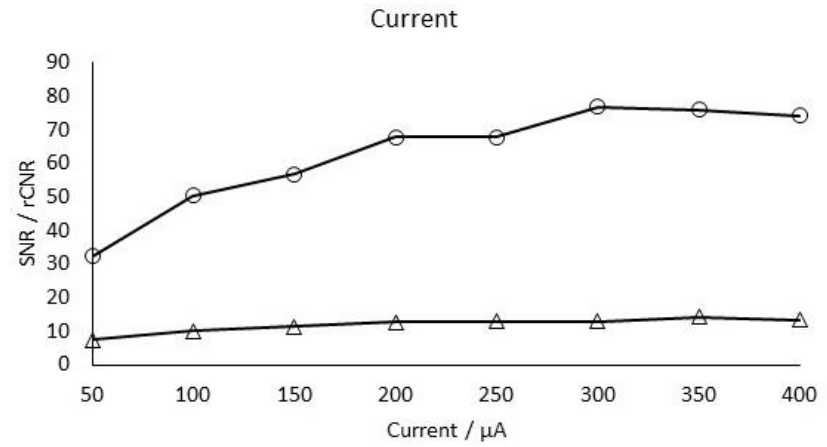
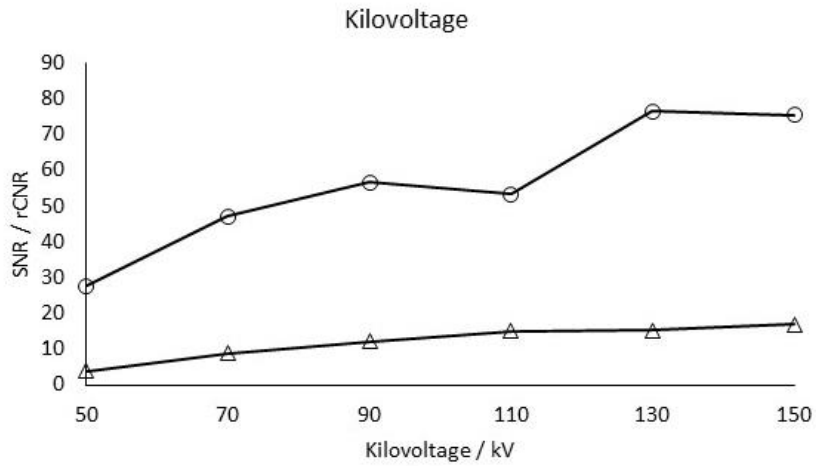
An equivalent axial slice through the liver was identified for all imaging datasets. Three ROI were drawn at the midpoint of the organ, ensuring sufficient distance from the edge of the liver, minimising the amount of heterogenous tissue included, (Figure 5.3). A single ROI was drawn in the mid-point of the air phantom to allow calculation of the SNR and rCNR.



***Figure 5.3 Three ROI were positioned within the liver to maximise size and minimise contamination from heterogenous signal***

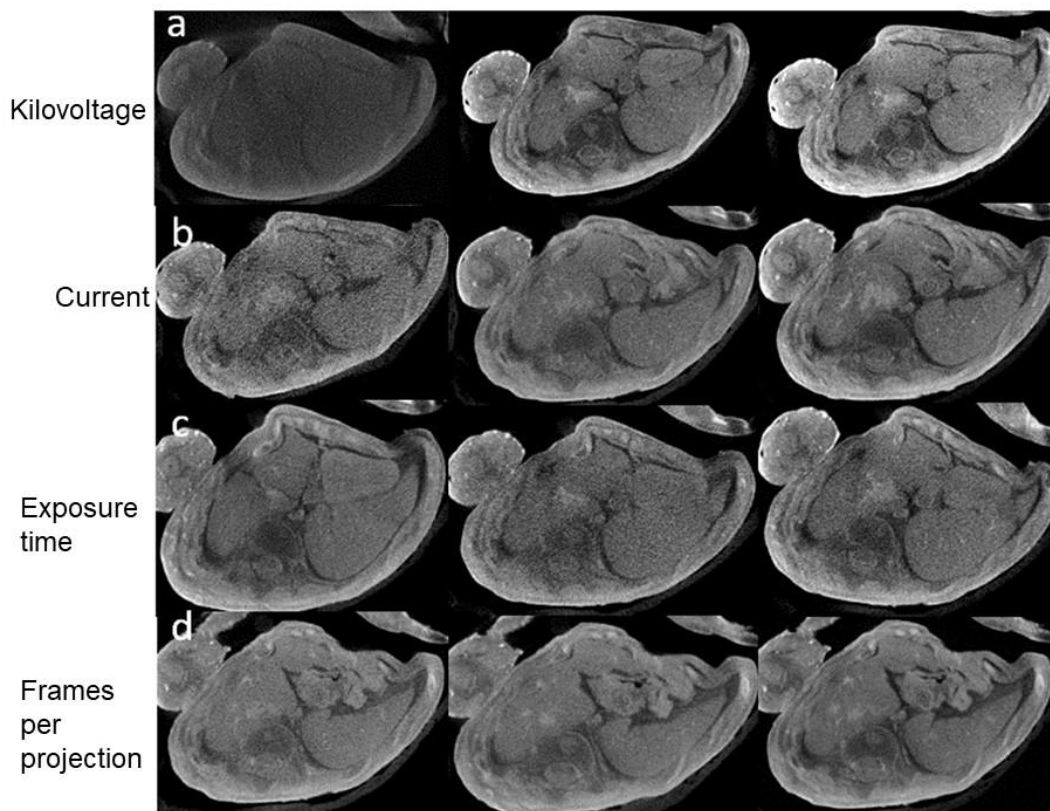
### **5.4.3 Results**

Both SNR and rCNR increased linearly as all 4 imaging parameters were increased, with SNR increasing at a reduced rate in comparison to rCNR, as demonstrated by kilovoltage, (Figure 5.4).



**Figure 5.4** Increasing SNR (triangles) and rCNR (circles) are observed as all imaging parameters are increased

Images were reconstructed for all investigations and increasing image quality was noted as all four imaging parameters were increased, (Figure 5.5).



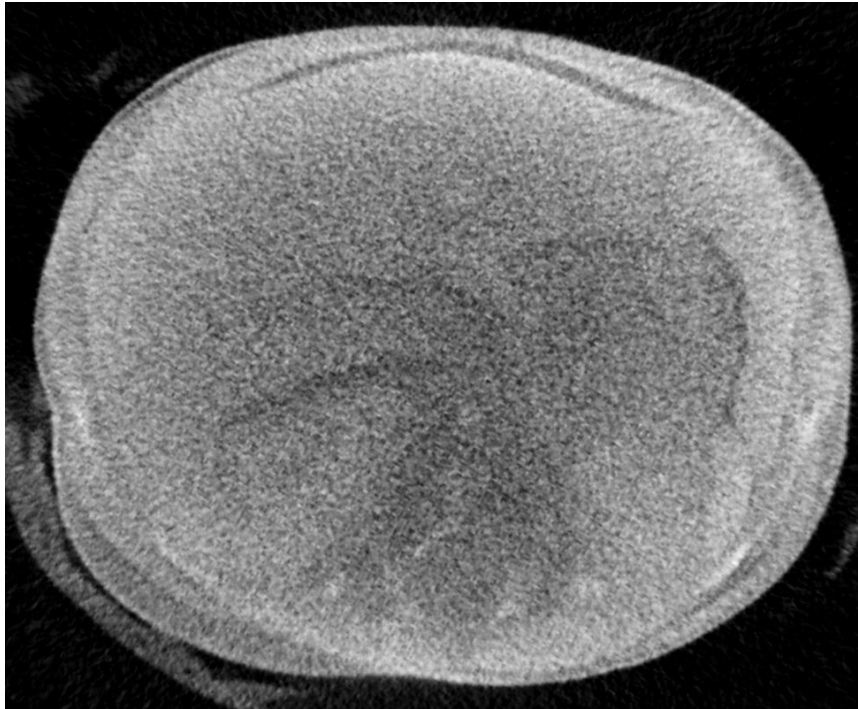
**Figure 5.5** Equivalent axial slices of the fetal chest demonstrate increasing image quality as all four imaging parameters are increased. (a) kV 50, 90, 130. (b) Current 50, 150, 250 $\mu$ A. (c) Exposure time 150, 250, 354ms. (d) FPP 1, 2, 4

#### 5.4.4 Discussion

This experiment shows that image quality as measured by SNR, rCNR increased significantly as all four imaging parameters was increased, in a single fetus.

The lower rate of rCNR increase at 110 kV, 250  $\mu$ A and 4 FPP may be due to inaccurate ROI placement at these values as these were placed manually by the investigator, scanner error in the acquisition of the micro-CT data or variation in the values seen for this individual fetus. This indicates that a greater number of fetuses should be examined to reduce any error that may be observed from sampling completed using a single fetus and that a method of repeatably selecting the equivalent area is required to minimise any error.

The higher rCNR for exposure time 66ms was due to a much larger mean signal intensity within the liver, than seen for all other exposure times and was due to an extremely low-quality image. The high level of noise is easily demonstrable (Figure 5.6) which is not representative of high image quality as observed in the rCNR values and was possibly due to inaccurate placement of the ROI, (Figure 5.4).



***Figure 5.6 Low image quality is observed at 66ms exposure time which does not correspond to the calculated high rCNR***

Although these investigations demonstrated the effect of imaging parameter change, the ranges for kilovoltage, current and exposure time, although approaching, did not fully maximise the micro-CT detector load to 90% of possible signal. However, increasing the imaging parameter under investigation will cause detector saturation. Therefore, imaging parameters, not directly being tested could be increased, increasing image quality across all the images, and aiding anatomical identification and ROI placement.

Increases in the FPP range were also possible without subsequent increase in detector load, but the tested range was already greater than the value quoted previously within the literature [125, 126]. Although increases in FPP, increase SNR and rCNR, they also increase the scan time, and whilst a maximal range should be tested to determine

the optimal imaging parameters, increasing the range above 4 would further double the scanning time from 40 to 80 minutes making it less clinically appropriate for a single imaging acquisition. Hence, a range of 1-4 was deemed clinically appropriate as the longer the scan time the more impractical the scanning protocol becomes with regard future clinical practice.

Therefore, the following imaging parameters were utilised to investigate their effect on image quality, Table 5.4 and demonstrates the increase in parameters not under investigation yet allowing the detector saturation to achieve a 90% of maximum value to increase the SNR and rCNR further. This will maximise the parameter range under investigation whilst also allowing maximal image quality. Factors increased include:

Kilovoltage investigation - current increased from 200 to 230  $\mu$ A.

Current investigation – exposure time increased from 125 to 177 ms.

Exposure time investigation – current increased from 100 to 120  $\mu$ A.

FPP investigation – No changes required.

**Table 5.4 Optimised imaging parameters for all subsequent imaging parameter experiments**

	Kilovoltage / kV	Current / $\mu$ A	Exposure Time / ms	FPP	Scan Time / minutes
Kilovoltage Experiment	50 – 150	230	125	1	4
Current Experiment	100	50 – 400	177	1	4
Exposure Time Experiment	100	120	67 – 500	1	1 – 17
FPP Experiment	100	200	125	1 – 4	10 – 40



## **5.5 Conclusion**

The range of imaging parameters were optimised to investigate the effect of altering the kilovoltage, current, exposure time and FPP on SNR and rCNR and offered the widest possible range on a Med-X micro-CT scanner (Nikon Metrology, Tring, UK).

## **5.6 Experiment 3 – phantom determination**

The main aim of experiment 3 was to identify the most suitable phantom material from water, wax, ethanol, air and 1.25% and 2.5% I<sub>2</sub>KI solution.

### **5.6.1 Background**

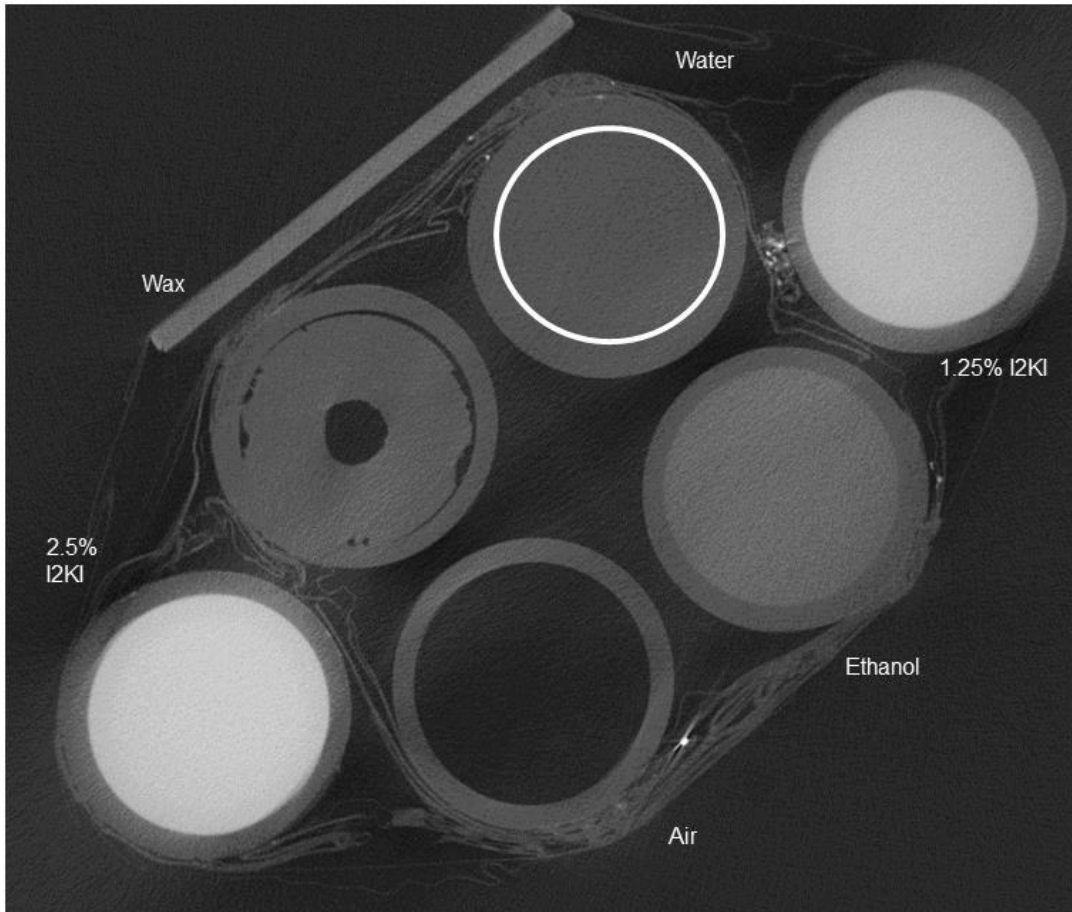
Signal intensity and standard deviation values of a standardised material are required to calculate the rCNR and is therefore defined as a phantom material.

Choice of material is important as it should ideally be of a similar signal intensity to the material under investigation and must remain constant throughout all experimentation, whilst the phantom should also be suitably sized to be positioned alongside the fetus within the x-ray beam, whilst not affecting image quality.

Therefore, the suitability of a variety of phantom materials were investigated.

### **5.6.2 Method**

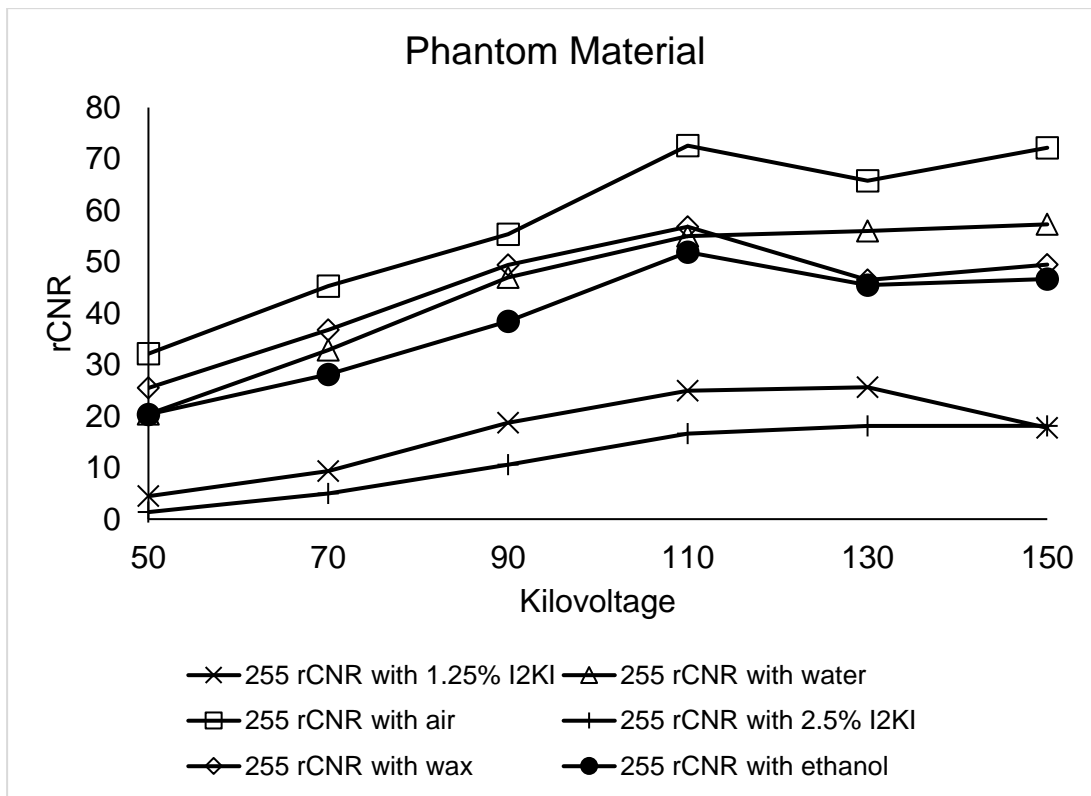
A single fetus was scanned using the range of kilovoltage imaging parameters established in experiment 2. A phantom consisting of 6 small vials, containing water, wax, ethanol, air and 1.25% and 2.5% I<sub>2</sub>KI solution was placed within the primary x-ray beam during data collection. Three ROI of diameter 4 mm were drawn axially within the liver as previously described in experiment 1 and three spread throughout the midpoint of each phantom material, (Figure 5.7) and averaged to calculate mean values. Note was made of the mean signal intensities and standard deviation for all phantom materials and the liver to calculate the rCNR.



**Figure 5.7** Single circular ROI were drawn at the midpoint of each phantom material at each kilovoltage as indicated by water phantom

### 5.6.3 Results

rCNR increased as kilovoltage was increased for all phantom materials tested, (Figure 5.8). Higher rCNR values were observed for the air, wax, water, and ethanol phantoms than for the I<sub>2</sub>KI solutions.



**Figure 5.8** Equivalent rCNR increases are observed as the kilovoltage is increased for all phantom materials

#### 5.6.4 Discussion

Equivalent and increasing rCNR values were observed for all phantom materials as kilovoltage was increased.

Although there were differences in the size of the rCNR values for the various phantom materials, all demonstrated equivalent rCNR increases as kilovoltage was increased from 0 – 110 kV. After 110 kV there followed a lower rate of increase for water, 2.5% I<sub>2</sub>KI and a slight decrease for air, wax, ethanol and 1.25% I<sub>2</sub>KI. This is likely affected by the approach of detector saturation. The primary function of the phantom is to allow a change in the rCNR to be identified whilst the imaging parameters are altered. This was possible for all phantom materials tested here and therefore, deemed suitable for rCNR evaluation. No minimum rCNR values were excluded as all values were above zero as all would be capable of determining the rCNR values of individual fetuses.

However, a single material is required to ensure comparisons can be made; thus, other factors should be used to select the phantom material. It would be relevant to select a

phantom material with similar atomic properties to the specimen under investigation as this would provide similar attenuation during imaging parameter alteration. The iodinated fetus will have a relatively high atomic number when compared to air, ethanol, wax, and water, whilst being closer in signal to the two I<sub>2</sub>KI phantom, in particular the higher values observed in the 2.5% I<sub>2</sub>KI phantom. Therefore, it is reasonable for the 2.5% I<sub>2</sub>KI phantom to be selected for future analysis of rCNR.

This is a subjective approach to determining the most appropriate phantom material. However, it does demonstrate that all six materials produced a similar effect, and that by choosing the phantom with similar characteristics to those potentially demonstrated by the fetuses does allow comparisons to be made. However, more in-depth assessment of phantom measurements was beyond the remit of this thesis.

As the 6-vial phantom takes up little room and has no discernible effect on the imaging, it was decided to continue to place all 6-vials alongside the fetus during the research to allow any future investigations the opportunity for further investigation of phantom materials.

### **5.6.5 Conclusion**

I<sub>2</sub>KI 2.5% solution is to be used as a phantom material throughout future SNR and rCNR calculations due to its similar atomic number and signal intensities to iodinated human fetuses.

## **5.7 Experiment 4 – Assessment of SNR and rCNR through 2D and 3D analysis**

The main aim of experiment 4 was to determine the most appropriate method of ROI selection to assess the SNR and rCNR of the liver.

### **5.7.1 Background**

Evaluation of large areas of anatomy will provide greater insight into the image quality of a micro-CT scan for a given organ, and increased sampling also increases the amount of heterogenous signal if extended to a complete organ. Investigations should be completed to assess whether evaluation of a whole organ affects the assessment of the imaging parameters, and comparisons of the SNR and rCNR employing different 2D and 3D methods will identify the most suitable data collection method.

### **5.7.2 Method**

Six fetuses were individually scanned as previously described alongside a phantom containing 2.5% I<sub>2</sub>KI solution, using the kilovoltage range previously optimised in Experiment 1, Table 5.4.

ROI placement for all three methods was completed on a high image quality dataset for each fetus to ensure accuracy using the following three methods.

#### **Individual multiple small 2D ROI**

A slice midway through the liver was identified for each fetus containing minimal vessels and a large homogeneous area. Three ROI were manually positioned for each dataset in equivalent slices for each fetus, (Figure 5.3).

#### **Complete Single Slice ROI**

Each complete fetal dataset was exported as a stack of contiguous tif images and imported into Image-J [150]. An equivalent axial fetal slice was selected to the previous method for each fetus and the visible liver segmented and saved as a mask, (Figure 5.9). This mask was applied to all datasets for the individual fetus, allowing automated calculation of the mean signal intensity and standard deviation, through which SNR

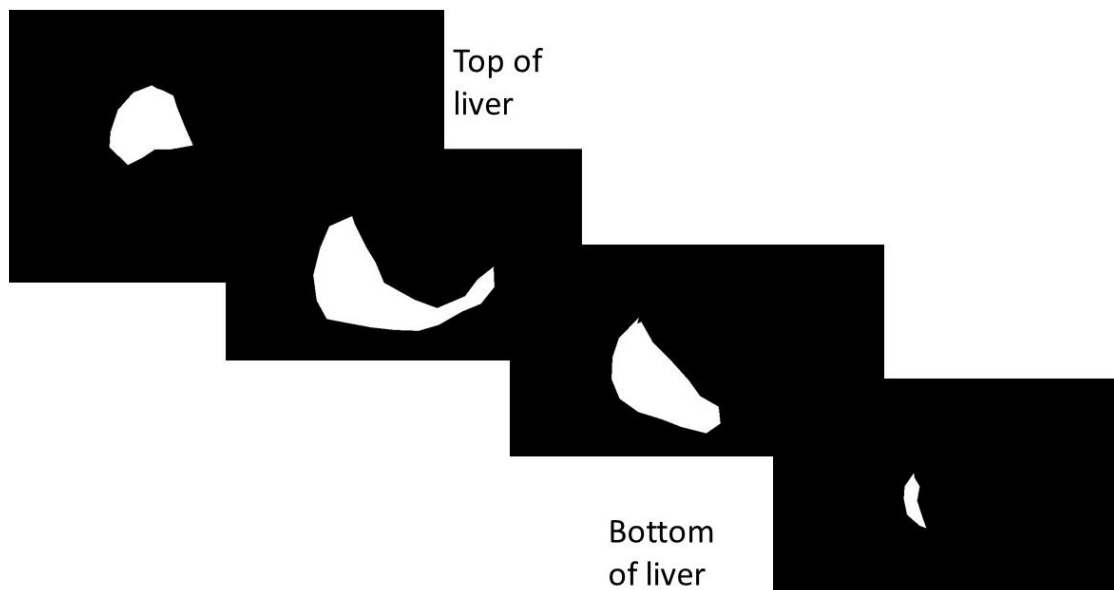
and rCNR was calculated. Detailed Image-J segmentation was completed, Appendix 5.



***Figure 5.9 Demonstration of a complete liver single slice ROI***

### **3D Organ Selection**

Each complete fetal dataset was exported as a stack of contiguous tif images and imported into Image-J [150]. Manual segmentation of every tenth slice throughout the liver was followed by interpolation to fully segment the complete liver volume. Checks were completed to ensure accuracy, with the resulting volume saved as a mask, (Figure 5.10). Detailed Image-J segmentation was completed, Appendix 5. This was completed for all fetuses and applied independently to the imaging parameter datasets to calculate SNR and rCNR was calculated.



**Figure 5.10 Liver images allowing complete organ 3D assessment of the SNR and rCNR**

### **Phantom**

ROI were placed within the 2.5% I<sub>2</sub>KI phantom using each of the above 3 methods to correspond with the specific segmentation technique.

Note was made of the mean signal intensities and standard deviations for all imaging parameters, with automated collection for the complete single slice and 3D organ selection, Appendix 5.

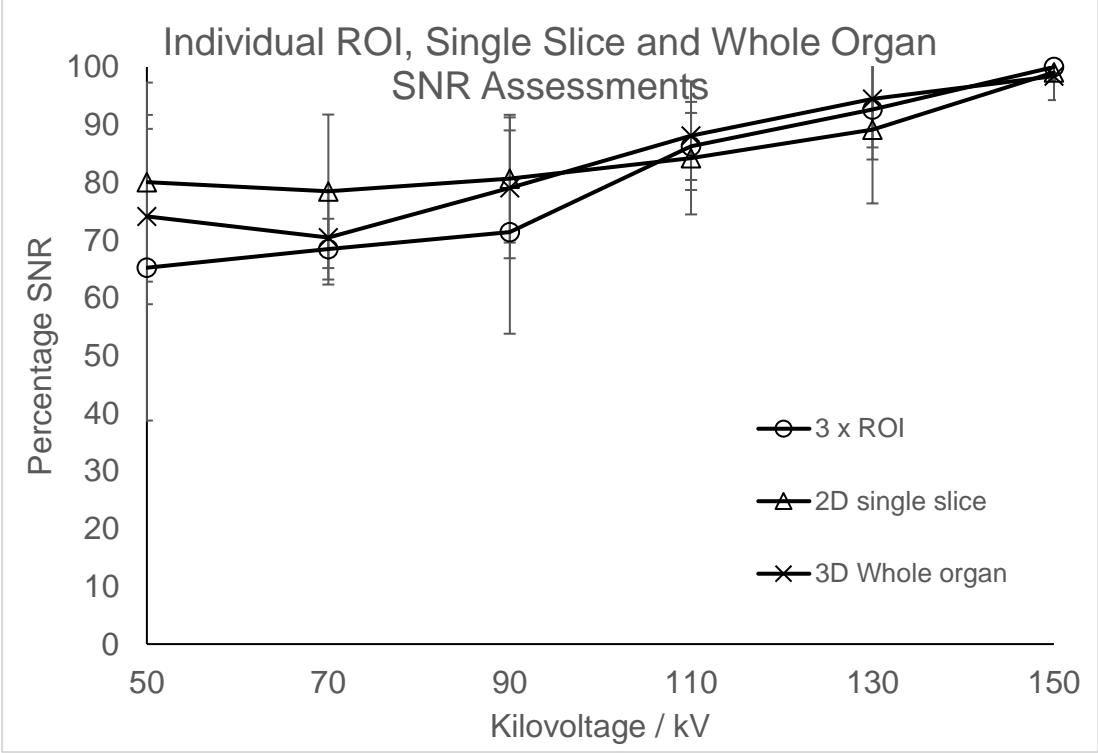
### **5.7.3 Data analysis**

Due to inherent signal intensity differences between individual fetuses, the maximum percentage of SNR and rCNR for each fetus was identified. Measurement of the range of SNR and rCNR were compared to the individual maximal values to determine a relative percentage value. These were then combined to produce an overall percentage value for all the fetuses investigated. Evaluating these differences on individual fetuses before combining them allowed inter-fetal comparisons to be made. The mean and standard deviation for both SNR and rCNR was subsequently calculated for all six fetuses.

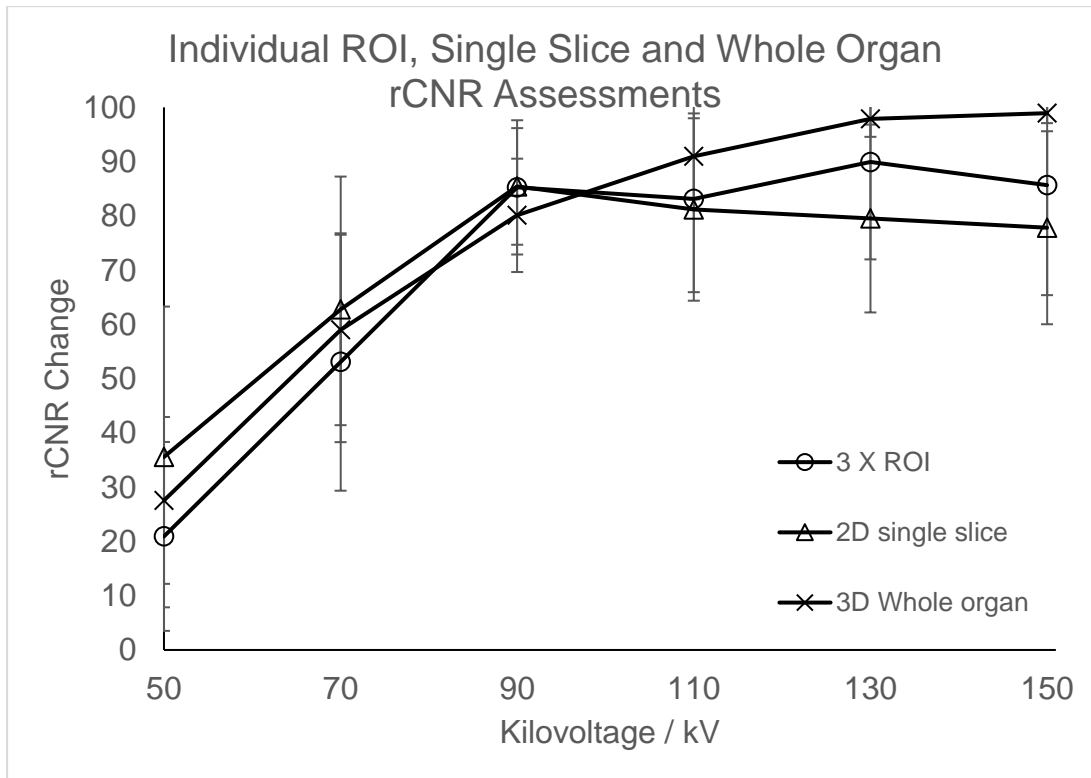


**5.7.4 Results**

All three methods of ROI placement demonstrated increasing SNR and rCNR as kilovoltage was increased, (Figure 5.11 and 5.12).



**Figure 5.11 Three methods of ROI assessment demonstrating equivalent increasing SNR as kilovoltage is increased**



**Figure 5.12** Three methods of ROI assessment demonstrating overall increasing rCNR as kilovoltage is increased

### 5.7.5 Discussion

This experiment demonstrated all three methodologies resulted in equivalent SNR and rCNR increases as kilovoltage was increased.

The most appropriate method was sought. Factors to be considered were,

- Repeatability of ROI placement
- Reduction of abnormal signal
- Efficiency of methodology

#### 5.7.5.1 Repeatability of ROI placement

Accurate repeat placement of ROI within multiple datasets is important to ensure accuracy. Manually, this is challenging to complete accurately, whereas automated placement through the application of a mask enables accuracy in repeated placement, providing the fetus has not moved during imaging.

#### *5.7.5.2 Reduction of abnormal signal*

Placement of individual ROI within a liver slice will allow greater control over avoidance of heterogenous signal and eliminate the error associated with heterogenous signal. No difference was observed between the three methods with inclusion of abnormal signal for the whole single slice and 3D method, and thus all three methods were deemed suitable with regard to heterogenous signal inclusion.

#### *5.7.5.3 Efficiency*

Manual segmentation of equivalent slices for 3 ROI is time consuming to complete accurately. Detailed segmentation of a mask once completed allows automated collection of data over both a single slice and whole liver, thus increasing the efficacy of these methods. Assistance was received from Dr Alessandro Felder (Research Software Development, UCL, UK) to complete the coding required for the automated data analysis, which allows significant increases in the efficiency of the data analysis which is essential for accuracy in large datasets. Comparisons of the three methods are detailed in Table 5.5.

**Table 5.5 Advantages and disadvantages of each ROI methodology**

Method of analysis	Advantages	Disadvantages
Multiple 2D ROI within a single slice	<p>No specialist software or training required</p> <p>Able to be completed on most software packages</p> <p>Quick to assess</p>	<p>Difficult to replicate accurately.</p> <p>Representative of small area</p> <p>Time consuming to replicate in multiple acquisitions</p> <p>May include abnormal areas of anatomy (vessels or errant signal)</p> <p>Dependant on slice and area chosen for ROI</p>
Single whole organ slice	<p>Easier to draw around whole organ due to clear deliniation of organ edge</p> <p>Easier to replicate in other experiments</p> <p>More representative than multiple ROI</p>	<p>Dependant on slice chosen</p> <p>May include abnormal areas of anatomy (vessels or errant signal)</p>
Multiple slice whole organ selection	<p>Easier to draw around whole organ due to clear deliniation of organ edge</p> <p>Whole organ assessment possible</p> <p>More representative than multiple ROI and single slice</p>	<p>Time consuming to repeat in multiple slices</p> <p>May include abnormal areas of anatomy (vessels or errant signal)</p>

Therefore, to ensure accurate and repeatable data analysis with the minimum of user interaction and maximum time efficiency, it is believed the automated approach of data analysis should be used. Assessment of a complete organ in 3D equates to a slight increase in the data analysis step yet enables a more in-depth analysis of the complete organ, removing the error that may be caused by incorrect slice selection.

Therefore, a 3D whole organ approach is the preferred method of choice for continued SNR and rCNR assessment.

### **5.7.6 Conclusion**

The methodology for data collection should be 3D whole organ assessment using a mask to ensure high repeatability of the ROI selection, with increased efficiency possible through automation of the data analysis.

## **5.8 Limitations**

This chapter has defined a methodology to determine the SNR and rCNR as individual imaging parameters are altered. Decisions about the methodology were developed to allow a thorough investigation on a larger cohort of fetuses, but there are several limitations to this work.

Firstly, only a small number of fetuses were investigated during each experiment. Variation in the results of individual fetuses was observed during individual experimentation, but this work was completed to develop a methodology and not to assess the overall SNR and rCNR results. Analysis of a greater number of fetuses will increase the confidence in the results.

Secondly, the work was optimised for usage on a single micro-CT scanner (Med-X, Nikon Metrology, Tring, UK), with a high degree of manipulation of the imaging parameters allowed with this scanner, enabling a wide parameter range to be investigated. Although it is recognised that alternative scanners may vary in the ability to manipulate these individual imaging parameters. These development steps are considered appropriate to alternative micro-CT scanners and could be used to develop individualised methodologies for differing specimens.

Thirdly, data collection for each fetus will require several hours to complete these investigations will be completed within a single day, allowing the fetus to undergo the described testing and clinical scanning, with no subsequent delay in completion of the scan. By fully investigating the effect each imaging parameter has on image quality, an optimised clinical protocol which will be applicable to the scanning of human fetuses for post-mortem imaging can be developed. This will maximise image quality and

reduce repeat imaging through unsuitable imaging parameters for clinically diagnostic scanning.

## **5.9 Considerations for future experiments**

The methodology developed within this chapter should be applied to a greater number of fetuses to ascertain how each individual imaging parameter (kilovoltage, current, exposure time and FPP) affects the SNR and rCNR.

Analysis should be completed to determine which imaging parameter has the greatest effect on the SNR and rCNR. This would allow priority to be given to optimising these imaging parameters for a clinical protocol, thus maximising image quality.

Analysis should also be completed to determine the effect exposure time and FPP has on the SNR and rCNR in relation to scanning time. Whilst the priority of any diagnostic imaging is to ensure accurate diagnosis, if this can be completed in a more efficient manner with reduced scanning times, this will aid the integration of the technique into clinical practice.

This data analysis will allow the quantification of these imaging parameters and result in a clinically appropriate scanning protocol.

## **5.10 Summary of findings**

These experiments have developed a methodology that will assess the effect kilovoltage, current, exposure time and FPP has on the image quality of human fetal post-mortem imaging through the depiction of SNR and rCNR.

- An optimised imaging parameter range was identified for the Med-X micro-CT scanner (Nikon Metrology, Tring, UK) to be used in subsequent investigations within this thesis.
  - Kilovoltage 50 - 150kV

- Current 50 - 400 $\mu$ A
  - Exposure Time 66 – 500ms
  - FPP 1 – 4
- 
- The liver was identified as the most suitable organ to assess the image quality due to its position within the body, large size and relative homogeneity.
  - The most appropriate choice of phantom material to assess the rCNR was identified as 2.5% I<sub>2</sub>KI solution due to its similarity to the signal intensity of iodinated fetal tissue.
  - The method of ROI depiction and subsequent data analysis should be a 3D whole organ assessment using automated data analysis enabling increased accuracy and repeatable data assessment.

# **Chapter 6 Quantitative Assessment of Imaging Parameters**

## **6.1 Overview**

This chapter investigates the effect of imaging parameters (kilovoltage, current, exposure time and FPP) have on the SNR and rCNR of human fetuses using the methodology developed in chapter 5. It determines the optimal imaging parameters for a micro-CT protocol with maximal SNR and rCNR, without detector saturation achievable in <30 minutes on a Med-X micro-CT scanner (Nikon Metrology, Tring, UK).

The work presented in this chapter was undertaken by the author of this thesis, with statistical and coding advice provided by Alessandro Felder.

Work from this chapter was published in Nature Protocols 2021 [90] and presented orally at the Clinical Academic Careers Evening (2018) [151], Allied Health Professionals in Research (2019) [152], European Congress of Radiology (2020) [153], and Great Ormond Street Hospital Conference (2021) [154].

## **6.2 Introduction – imaging parameters**

The four main imaging factors that have a direct impact on the x-ray beam, in terms of beam energy and number of x-ray photons, as well as on the scanning time, are kilovoltage, current, exposure time and FPP [85], Table 5.2.

Regarding kilovoltage, current and exposure time, too low imaging parameters will result in insufficient x-ray photons reaching the detectors, resulting in low SNR and rCNR. Too high imaging parameters results in detector saturation. However, these effects do not correspond to FPP. Careful manipulation of the imaging parameters is important to achieve maximal SNR and rCNR without resulting in detector saturation [85].

Scanning time is also directly affected by the exposure time and FPP or indirectly by the kilovoltage and current. Although high SNR and rCNR are significant in ensuring



diagnostic images, being able to produce images within a clinically appropriate time frame is essential for the uptake of the defined protocol within a clinical setting. This is a fine balance between maximal SNR and rCNR and excessively long scanning times [85]. Within this thesis a clinical micro-CT protocol is defined as three acquisitions; a whole-body scan to assess iodination status and image all areas of the fetus, and two separate head and torso acquisitions at higher resolution. The head and torso are important as these are the sites of greatest clinical importance to determine fetal abnormalities. Therefore, three complete data sets should be completed for each fetus.

To become a clinically relevant technique, achieving complete fetal scanning within 90 minutes would allow multiple fetuses to be scanned within a day, i.e., a target time of 30 minutes per acquisition.

### **6.3 Aims**

**Aim 6-1:** To determine a clinically appropriate micro-CT scanning protocol with maximal SNR and rCNR, a scan time of less than 30 minutes and to eliminate detector saturation.

**Null hypothesis 6-1:** Kilovoltage, current, exposure time and FPP have no effect on SNR and rCNR.

### **6.4 Method**

#### **6.4.1 Patient selection**

Consecutive, unselected fetuses, <300g, with parental consent for post-mortem micro-CT imaging were prospectively included over 16 months between December 2019 – March 2021. Exclusion criteria included any fetuses where maceration made the liver difficult to segment accurately, had been exposed to incorrect I<sub>2</sub>KI solution, had an abnormality of the liver, or weighed >300g.

Ethical approval was acquired (NHS Health Research Authority, ethics approval ID: 13/LO/1494, 17/WS/0089 and CE2015/81) and all samples were handled in accordance with the Human Tissue Act (2004). Written parental consent for post-

mortem micro-CT imaging and the use of tissue in research following fully informed consent procedures.

#### **6.4.2 Fetal preparation**

Fetuses were initially received by the GOSH mortuary and refrigerated at 4°C whilst assessments were carried out to ensure micro-CT was appropriately requested and consented.

Fetuses were immersed in 2.5% I<sub>2</sub>KI solution for several days as determined from the equation developed in chapter 6.

$$\text{Immersion time (days)} = (0.03 \times \text{body weight (grams)}) - 2.2$$

Once fully iodinated a clinical scan was completed to assess liver imaging, with fetuses excluded from further analysis if identification of the liver boundary was not possible.

The fetuses and phantom containing 2.5% I<sub>2</sub>KI solution were positioned and immobilised as described in Appendix 4, positioned within the x-ray cone beam, and scanned using a Med-X micro-CT scanner (Nikon Metrology, Tring, UK) for a range of imaging acquisitions, Table 6.1. This range was maximised by limiting other imaging parameters, thus widening the range tested. Equivalent positioning for all acquisitions of a single fetus allowed automated data analysis as defined in chapter 5. A high-resolution acquisition was acquired, enabling greater segmentation accuracy of the liver and 2.5% I<sub>2</sub>KI phantom segmentation for a mask which was then applied to all subsequent datasets as described in chapter 5.

**Table 6.1 Imaging parameters used in the investigations**

	Kilovoltage / kV	Current / $\mu$ A	Exposure Time / ms	FPP	Scan Time / minutes
Kilovoltage Experiment	50 – 150	230	125	1	4
Current Experiment	100	50 – 400	177	1	4
Exposure Time Experiment	100	120	67 – 500	1	1 – 17
FPP Experiment	100	200	125	1 – 4	5 – 22
Hi-resolution acquisition	130	150	250	2	30

All acquisitions were anonymised, securely archived, and 3-D volumes created using VGStudio Max 3.4 software (Heidelberg, Germany).

### 6.4.3 Data analysis

Mean signal intensities and standard deviations were collected for liver and phantom for each dataset, enabling SNR and rCNR to be calculated. Inter-fetal differences in organ iodination, anatomy and pathology prevented direct comparisons of SNR and rCNR. Therefore, maximal SNR and rCNR for kilovoltage, current, exposure time and FPP, for each fetus was measured. Data from all eleven fetuses were combined to determine mean percentage of SNR and rCNR for each imaging parameter.

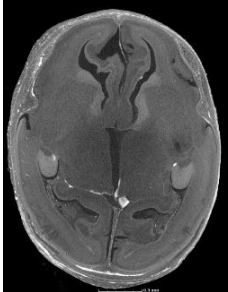
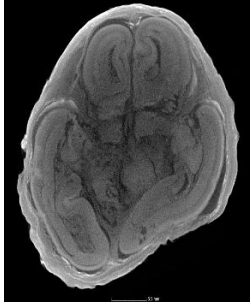
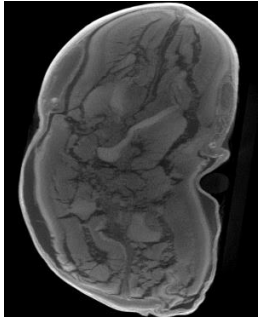
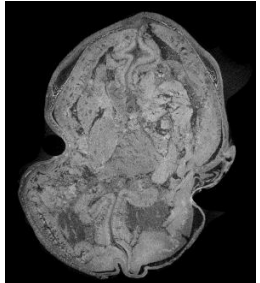
Optimal SNR and rCNR was predefined as the point above which no further (<5%) increase could be achieved. The effect of reducing exposure time and FPP was measured to achieve a <30-minute scan time.

However, for some variables, too high imaging parameters produced detector saturation. Therefore, the effect of reducing kilovoltage and current was also recorded until detector saturation was eliminated, maintaining the SNR and rCNR as high as possible.

Two specialist paediatric radiologists subjectively assessed the degree of maceration score for micro-CT based on previously published ratings (0 = no maceration, 3 severe/established maceration) [155, 156], using the indications indicated in Table 6.2

Pathological maceration was derived at external examination and was based on several physical indications being definitive for maceration having taken place, including skin slippage, skin and cord discolouration, cranial collapse, level of mummification on external examination [155, 157, 158].

**Table 6.2 Descriptions of the maceration criteria by which the axial head and chest images were assessed**

Maceration Score	Maceration	Maceration description	Head images
0	None	No maceration evident	
1	Mild	Mild cracking and distortion but images diagnostic	
2	Moderate	Moderate disruption with reduction in normal tissue planes, limited diagnosis	
3	Severe	Severe maceration, non-diagnostic with severely distorted internal anatomy	

## 6.5 Results

### 6.5.1 Study population

Eleven fetuses (5 males, 6 females) were recruited for the study from a possible 243 referred to the micro-CT clinical service during the 16-month period, with a range of demographics, Table 6.3 and a range of maceration scores, Table 6.4.

**Table 6.3 Demographic information for the study cohort**

	Mean	Median	Range
Gestational age / weeks	18.6	19	13 – 25
Body weight / grams	156.5	205	15 – 299
Iodination time / days	8.7	7	3 – 17
Crown rump length / cm	13.0	14.5	6.9 – 16.5
Crown heel length / cm	17.3	18.2	8.7 – 23.5
Head circumference / cm	12.7	12.6	6.1 – 24.3

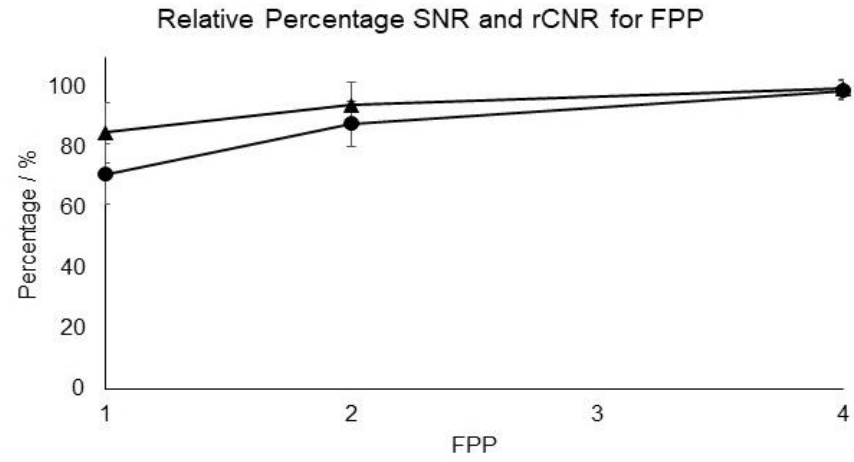
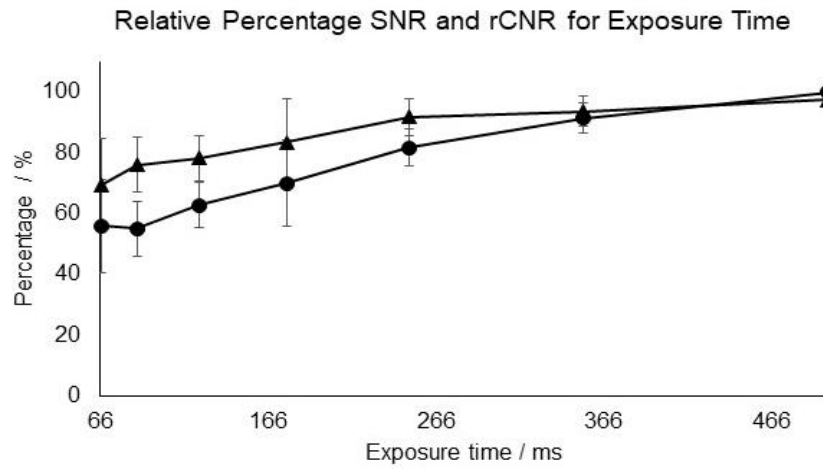
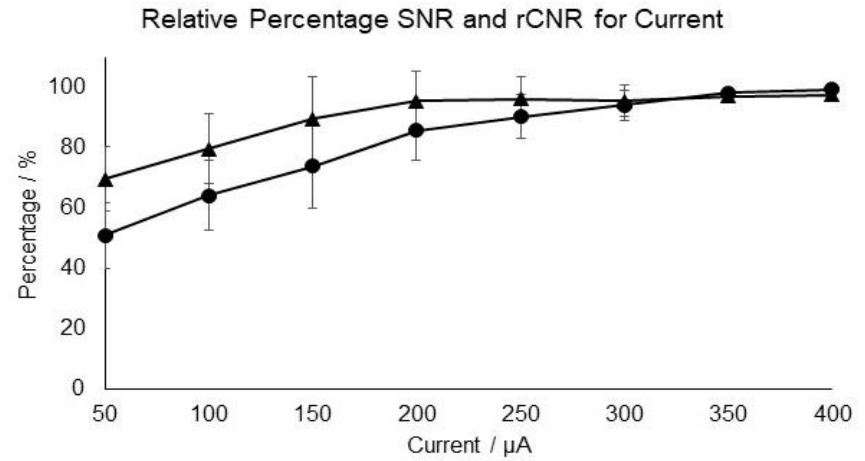
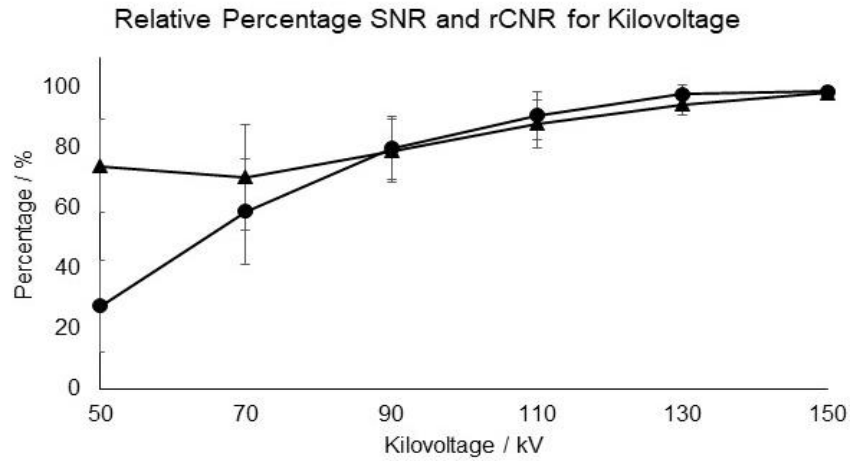
**Table 6.4 Pathological and micro-CT maceration score for the study cohort**

	None	Mild	Moderate	Severe
Pathology score	5	3	1	2
Micro-CT score	4	5	0	2

### **6.5.2 SNR and rCNR percentage changes**

SNR and rCNR increased curvilinearly with all imaging parameters, with greater increases observed throughout the range for rCNR than SNR, (Figure 6.1). The results differ in their comparison to chapter 5 as only a single fetus was analysed to identify the appropriate methodology for objective assessment of SNR and rCNR.

However, in chapter 6, eleven fetuses were included in the analysis and due to inter-fetal differences in enhancement following I<sub>2</sub>KI immersion, a method was required to combine the analysis of multiple fetuses. Therefore, relative maximal percentages for individual fetuses were calculated and combined to allow an overall assessment of the change in relative percentage as imaging parameters are altered.



**Figure 6.1** Relative percentages of SNR (triangles) and rCNR (circles) all increased as all four imaging parameters were increased with error bars depicting the standard deviation



#### *6.5.2.1 Kilovoltage*

An increase in both SNR and rCNR was noted as kilovoltage was increased.

There was no increase in SNR between 50-70kV after which a continual increase was observed, with maximal SNR seen at 150kV.

Although rCNR increased throughout the whole range, there was a steeper increase in rCNR between 50 - 90kV after which the rate of increase slowed with maximal rCNR was observed at 150kV. This slowing in the rate of increase is due to the detectors approaching saturation.

#### *6.5.2.2 Current*

An increase in both SNR and rCNR was noted as current was increased.

There was a constant increase in SNR as current was increased from 50–200 $\mu$ A, after which SNR remained consistently high up to the maximum tested value of 400 $\mu$ A.

Although rCNR increased throughout the tested range of 50 $\mu$ A to 400 $\mu$ A, there was a greater increase seen from 50–200 $\mu$ A after which the rate of increase was smaller up to the maximum tested value of 400 $\mu$ A. This slowing in the rate of increase is due to the detectors approaching saturation.

#### *6.5.2.3 Exposure Time*

An increase in both SNR and rCNR was noted as exposure time was increased.

There was a greater increase in SNR from 66-250ms, after which the rate of increase was smaller up to the maximum tested value of 500ms.

There was a reduction in rCNR from 66-88ms after which there was a continual increase in rCNR up to the maximal tested value of 500ms. This slowing in the rate of increase is due to the detectors approaching saturation.

#### *6.5.2.4 FPP*

An increase in both SNR and rCNR was noted as FPP was increased.

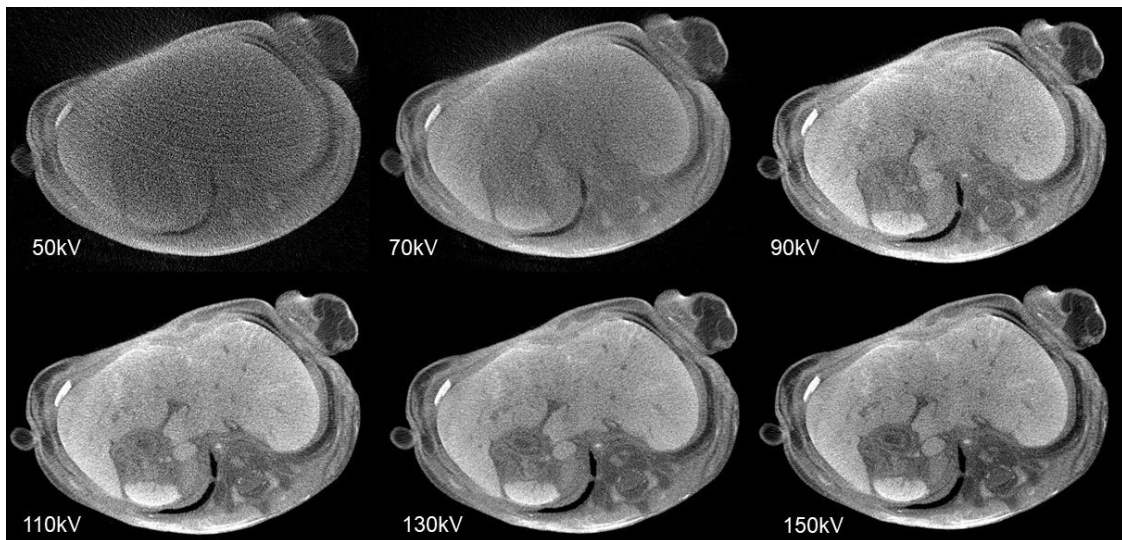
There was a greater increase in both SNR rCNR from 1-2FPP, after which the rate of increase reduced up to the maximum tested value of 4FPP.

### **6.5.3 Determination of incremental percentage change as imaging parameters increased**

Although all imaging parameters increased up to the maximum tested values, there was only incremental (<5%) increase towards the upper limits, (Table 6.3 to 6.6) and (Figures 6.1 to 6.4).

**Table 6.5 Percentage SNR and rCNR change <5% occurs at 130kV, thereby determining the optimal kilovoltage**

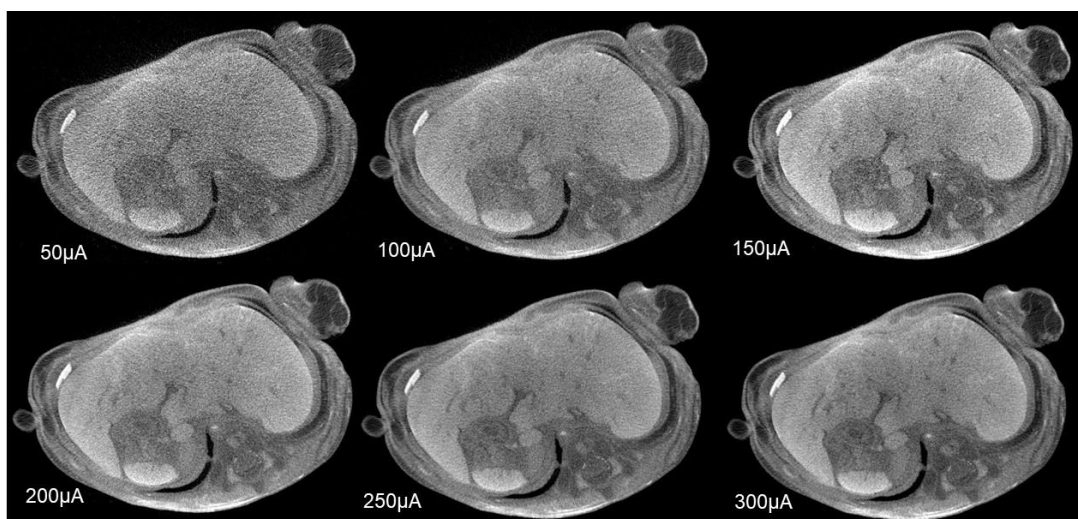
Kilovoltage	Percentage SNR	Percentage SNR change	Percentage rCNR	Percentage rCNR change
50	74.1	0.0	27.6	0.0
70	70.5	-5.2	59.0	53.3
90	79.1	10.9	80.1	26.4
110	88.1	10.2	91.0	11.9
130	94.5	6.8	97.9	7.1
150	98.4	4.0	98.9	1.0



**Figure 6.2 Increasing image quality is noted as the kilovoltage is increased from 50 to 150 kV**

**Table 6.6 Percentage SNR and rCNR change <5% occurs at 300 $\mu$ A, thereby determining the optimal current**

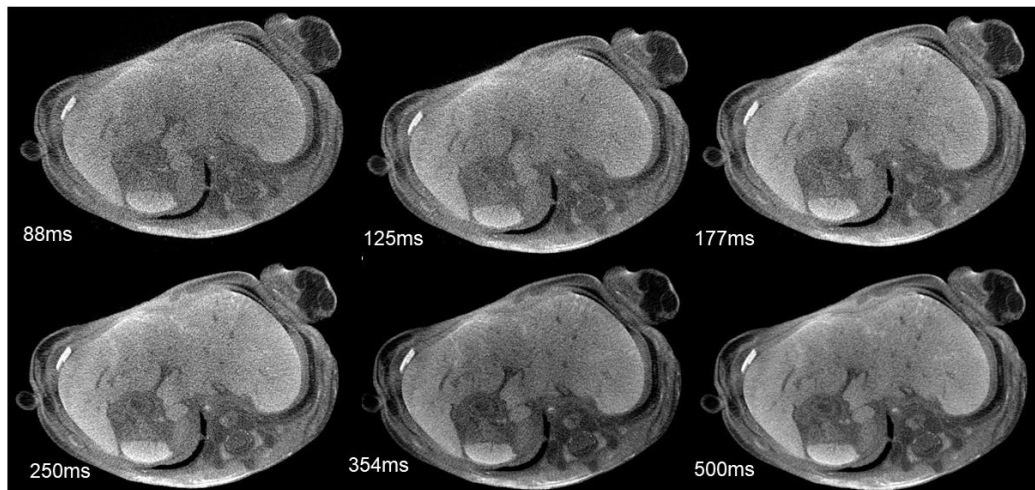
Current	Percentage SNR	Percentage SNR change	Percentage rCNR	Percentage rCNR change
50	69.8	0.0	51.0	0.0
100	79.7	12.5	64.3	20.7
150	89.8	11.2	74.1	13.3
200	95.7	6.2	85.9	13.7
250	96.3	0.7	90.5	5.1
300	95.8	-0.6	94.3	4.0
350	97.3	1.6	98.5	4.3
400	97.8	0.5	99.6	1.1



**Figure 6.3 Increasing image quality is noted as the current is increased from 50 to 300 $\mu$ A**

**Table 6.7 Percentage SNR and rCNR change <5% occurs at 500ms, thereby determining the optimal exposure time**

Exposure time	Percentage SNR	Percentage SNR change	Percentage rCNR	Percentage rCNR change
67	69.5	0.0	56.0	0.0
88	76.1	8.7	55.1	-1.7
125	78.3	2.7	62.7	12.2
177	83.6	6.4	70.0	10.4
250	91.8	8.9	81.8	14.4
354	93.7	2.0	91.5	10.6
500	97.5	3.9	100.0	8.5



**Figure 6.4 Increasing image quality is noted as the exposure time is increased from 88 to 500ms**

**Table 6.8 Percentage SNR and rCNR change <5% occurs at 4FPP, thereby determining the optimal FPP**

FPP	Percentage SNR	Percentage SNR change	Percentage rCNR	Percentage rCNR change
1	85.1	0.0	71.4	0.0
2	94.3	9.7	88.2	19.0
4	99.7	5.4	99.0	11.0



**Figure 6.5 Increasing image quality is noted as the FPP is increased from 1 to 4 FPP**

Therefore, 130 kV, 250  $\mu$ A, 500 ms and 4 FPP was identified as yielding maximal SNR and rCNR where further increase would yield <5% increase in SNR and rCNR. These imaging parameters are not practical as they result in detector saturation and require reducing to below 30 minutes scanning time provide an appropriate clinical protocol.

#### **6.5.4 Reduction of scanning time**

These maximal imaging parameters combine to a scanning time of >30 minutes. Therefore, three reductions in exposure time and FPP were required to achieve a scanning time of 26 minutes whilst minimising reductions in SNR and rCNR, Table 6.9.

**Table 6.9 Demonstration of the exposure time and FPP reductions to minimise SNR and rCNR loss, whilst reducing a scanning time from 104 to <30 minutes**

	Kilovoltage / kV	Current / $\mu$ A	Exposure time / ms	FPP	Scanning time / minutes
Maximal SNR and rCNR protocol	130	300	500	4	104
This protocol is >30 minutes scanning time, therefore reductions in exposure time and FPP required					
Reducing scanning time steps (loss in SNR and rCNR / %)			354ms (SNR -4.0% rCNR -9.3%)		74
			250ms (SNR -2.0% rCNR -11.8%)		52
				2 FPP (SNR -5.6% rCNR -12.3%)	26
Scanning protocol <30 minutes	130	300	250	2	26

### 6.5.5 Detector saturation elimination

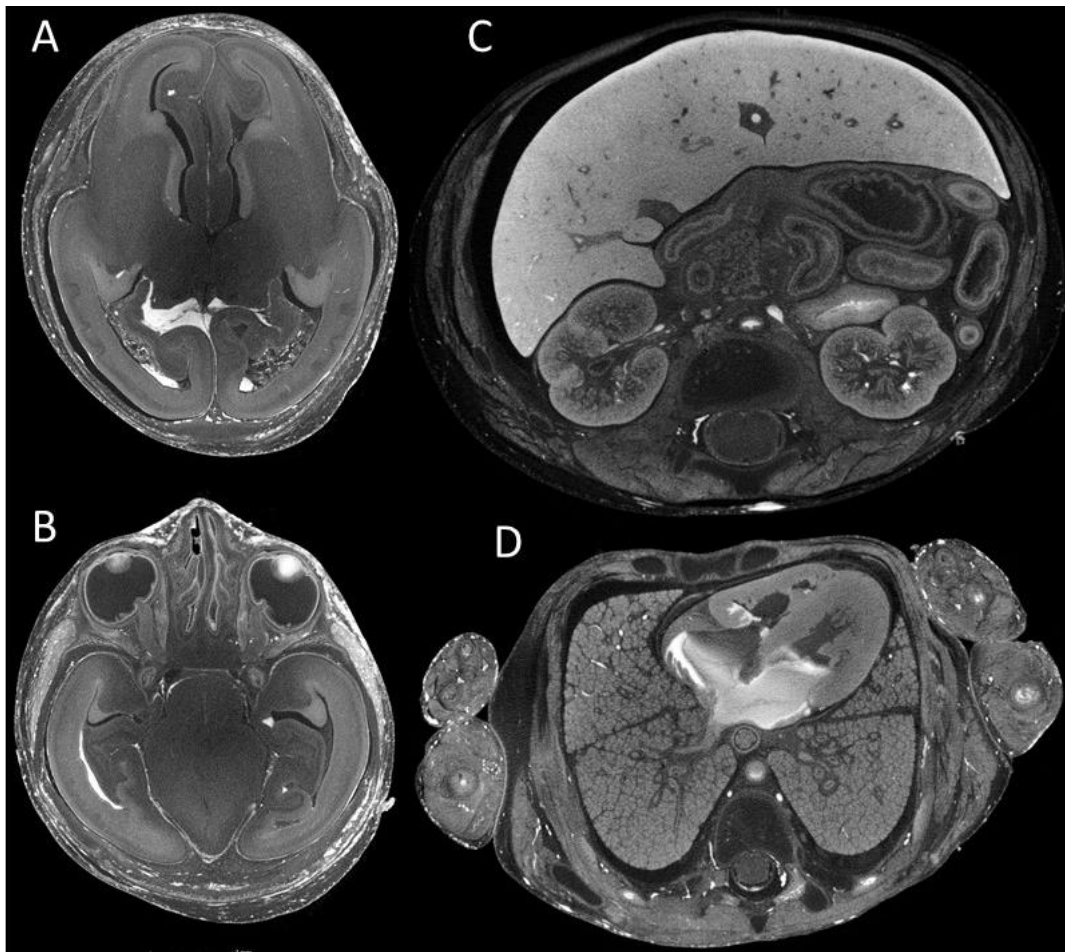
The scanning protocol of 130 kV, 300  $\mu$ A, 250 ms and 2 FPP although clinically appropriate at <30minutes scanning time, still resulted in detector saturation. Therefore, reductions in kilovoltage, current and exposure time were required to reduce detector load, Table 6.10.

**Table 6.10 Demonstration of the kilovoltage, current and exposure time reductions to minimise SNR and rCNR loss whilst eliminating detector saturation**

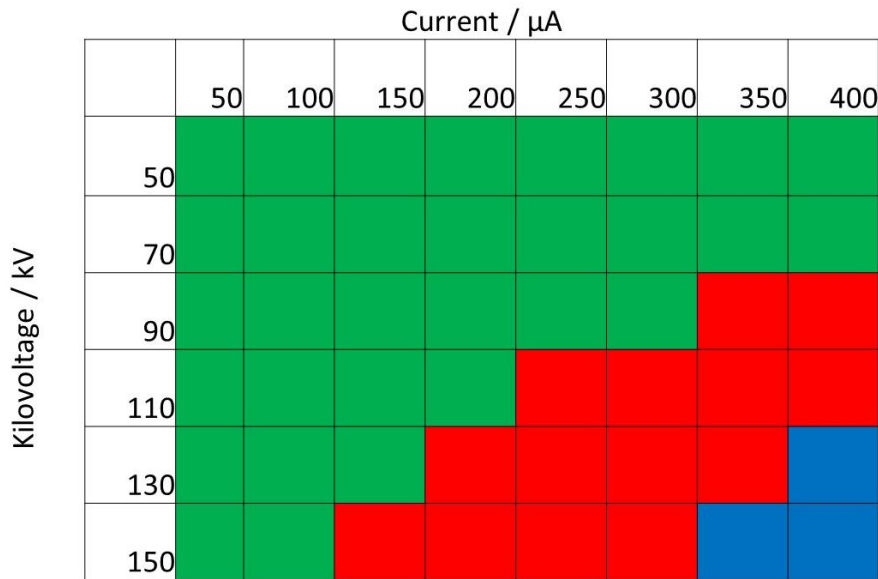
	Kilovoltage / kV	Current / $\mu$ A	Exposure time / ms	FPP	Scanning time / minutes
Scanning protocol <30 minutes	130	300	250	2	26
Reducing detector load steps (loss in SNR and rCNR / %)		250 $\mu$ A (SNR -0.6%, rCNR -4.1%)		2	26
	110kV (SNR -7.2%, rCNR -7.6%)			2	26
		200 $\mu$ A (SNR - 6.6%, rCNR - 15.9%)		2	26
Final protocol	110kV	200	250	2	26
Estimated overall SNR and rCNR of maximum / %	SNR 90% rCNR 92%	SNR 97.9% rCNR 86.3%	SNR 94.2% rCNR 81.8%	SNR 94.6% rCNR 89%	

This resulted in a clinically appropriate micro-CT protocol of <30 minutes, (Figure 6.6), and no detector saturation as demonstrated, (Figure 6.7).





**Figure 6.6** High SNR and rCNR is noted visually with high resolution axial images of the brain (A and B), abdomen (C) and chest (D) using the clinically appropriate micro-CT protocol as defined by this chapter



**Figure 6.7 Demonstration of imaging parameters with no detector saturation (green), detector saturation (red) and >50Watts blocked for scanner safety (blue) with an exposure time of 250ms**

## 6.6 Discussion

This study has defined the imaging parameters of 110 kV, 200  $\mu\text{A}$ , 250 ms and 2 FPP as clinically appropriate for human fetal post-mortem imaging using a Med-X scanner (Nikon Metrology, Tring, UK) with a scanning time of 26 minutes and no detector saturation.

This protocol was possible for a range of body weights (15 – 299 g), gestational ages (13 – 25 weeks) and maceration scores, Table 6.3 and 6.4.

A larger range of imaging parameters was evaluated than previously stated within the literature for human fetuses except for exposure time. An exposure time of 1050 ms (Table 6.9) would equate to a scanning time of 109 minutes, which would not be appropriate for a clinical service.

**Table 6.11 Previously used micro-CT imaging parameters for iodinated human fetuses**

	Kilovoltage / kVp	Current / $\mu$ A	Exposure Time / ms	FPP
Lombardi et al., (2014) [125]	80	300-313	65, 300, 1050	-
Hutchinson et al., (2018) [126]	80 – 110	87 – 180	250 - 354	1

### 6.6.1 Maximal imaging parameters

This experiment intended to achieve the maximal SNR and rCNR possible in a 30-minute scan without reaching detector saturation. Reductions from maximal individual imaging parameters were necessary to stay within these requirements. Employing the maximal parameters for three clinical scans would equate to over 5 hours per patient, with consequent effect on clinical throughput.

The best imaging parameters within 30 minutes was 130 kV, 300  $\mu$ A, 250 ms and 2 FPP, but this was not possible due to detector saturation. Further reductions to reduce detector saturation, whilst maintaining a high SNR and rCNR resulted in a protocol of 110 kV, 200  $\mu$ A, 250 ms and 2 FPP. This achieved the aim a scanning time of <30 minutes, elimination of detector saturation, (Figure 6.7), and maintaining a high SNR and rCNR, (Figure 6.6), which is key in providing an appropriate protocol [85].

### 6.6.2 Optimising clinical protocols on different micro-CT scanners

Micro-CT scanners differ depending on multiple variables including their detectors, object-to-detector distance, and filament and this methodology demonstrates the steps to maximise alternative clinical protocols which should be completed to optimise new areas of scanning [85].

Previously, values of 80kV and 140kV have shown maximal rCNR [79, 159] with iodinated contrast. These differences relate to the different scenarios from vials of iodine contrast in micro-CT to in-vivo humans in clinical CT and indicate the differences in optimal values required for differing imaging scenarios.

Adaptation of these imaging factors is also possible for alternative micro-CT scanners. If detector saturation is reached with 110 kV, 200  $\mu$ A, 250 ms and 2 FPP, a reduction in kilovoltage, current and exposure time will alleviate this issue. It has been shown in (Figure 6.1) that small reductions in the upper values of all imaging parameters are important in maintaining a high SNR and rCNR. Whereas the lower levels of the investigated range result in greater loss in SNR and rCNR.

Therefore, this protocol defines a starting range for alternative scanners and demonstrates the importance of defining the imaging parameters during publication, to build on current knowledge and offer future researchers' direction to optimise the SNR and rCNR for other investigations [84, 85].

## **6.7 Limitations**

There are several limitations associated with this study.

Firstly, each micro-CT scanner will differ and require slight adjustment to the imaging parameters to optimise image quality and negate detector saturation. These investigations provide a guide for imaging parameters, demonstrate the relationship between them and SNR and rCNR and provide a methodology to determine maximal imaging parameters on alternative micro-CT scanners.

Secondly, only eleven fetuses were used in the analysis, there were difficulties in recruiting due to lack of parental consent. Although this is a relatively small number, the small standard deviations noted with percentage change indicate a high agreement between these fetuses in relation to the SNR and rCNR and therefore provide suitable direction, (Figure 6.1).

Thirdly, the methodology did not allow the SNR and rCNR between the four imaging parameters to be directly compared. Although this could have been achieved, it would have reduced the range tested for each imaging parameter. Therefore, this method provided insights into a greater tested range for each imaging parameter.

Fourthly, kilovoltage and current could have been tested for a greater number of imaging parameter data points than every 20kV and 50 $\mu$ A, although this would have

significantly increased the data collection time. The results obtained demonstrate a small standard deviation and a high agreement between individual fetuses.

Fifthly, only objective measurements of SNR and rCNR were included in assessing the optimal imaging parameters. No subjective assessments were included examining the image quality as assessed by radiologists who will be interpreting the images to identify structural anomalies. It could be reasoned that individual observers may prefer alternative parameters to provide varying levels of image contrast. However, optimal image quality, as achievable within 30 minutes scanning time was identified, and this would provide optimal SNR and rCNR which would prove suitable for the vast majority of observers. Therefore, these objective assessments were deemed suitable, though further subjective assessments could be completed in the future.

## **6.8 Conclusion**

A clinically appropriate and optimised scanning protocol for human fetuses following iodination within a solution of 2.5% I<sub>2</sub>KI on the Med-X (Nikon Metrology, Tring, UK) micro-CT scanner of 110 kV, 200  $\mu$ A, 250 ms and 2 FPP will provide optimal SNR and rCNR with a clinically efficient scanning time of 1 hour 18 minutes per fetus.

This ensures maximal SNR and rCNR within a clinically relevant scanning time of <1.5 hours per fetus.

## **6.9 Summary**

In summary, increasing SNR and rCNR were observed as kilovoltage, current, exposure time and FPP all increased. The imaging parameters able to demonstrate maximal SNR and rCNR values were not appropriate due to detector saturation and scanning time. Therefore, a balance between maximising image quality whilst maintaining an appropriate scanning time ensures that micro-CT of human fetuses is clinically appropriate. This chapter provides a methodology that is applicable to a wide variety of scanning applications and an imaging parameter starting point for other micro-CT similar scanners that is not previously demonstrated.

## 6.10 Key points

- Increases in kilovoltage, current, exposure time and FPP all result in increasing SNR and rCNR.
- Increases in SNR and rCNR reduce as the imaging parameters are increased.
- A small reduction in maximal SNR and rCNR through controlled reduction in kilovoltage, current, exposure time and FPP will result in a more clinically appropriate and optimised scanning protocol.

# Chapter 7 Evaluation of Image Quality in Human Fetal Post-mortem Micro-CT

## 7.1 Overview

This chapter assesses the effect fetal demographics and imaging parameters have on image quality, to identify the strongest negative and positive predictors from a retrospective analysis of 258 clinical micro-CT scans.

The work presented in this chapter was undertaken by the author of this thesis, with statistical advice provided by Dr Dean Langan (statistician). Image quality assessments were completed by Dr Owen Arthurs and Dr Susan Shelmerdine.

Work from this chapter was presented orally at European Congress of Radiology (2020) [142], and International Paediatric Radiology Congress (2021) [141], and has been submitted as a journal paper to BMC Medical Imaging.

## 7.2 Introduction – image quality

The effect that four imaging parameters (kilovoltage, current, exposure time and FPP) have on the SNR and rCNR was examined in chapter 6, with an optimised clinical protocol developed.

The effect of fetal demographics and other non-imaging parameters on micro-CT image quality [71] has not yet been investigated fully.

To address these effects, a retrospective analysis of micro-CT data was performed to identify the image quality associated with a wide range of demographics and imaging parameters.

## 7.3 Aims

**Aim 7-1:** To determine the relative contributions of fetal demographic and imaging parameters to image quality of post-mortem fetal micro-CT imaging.

**Null hypothesis 7-1:** There are no demographics or imaging parameters which have a significant effect on image quality of whole post-mortem micro-CT of human fetuses.

## **7.4 Methods**

### **7.4.1 Patient recruitment**

Consecutive unselected fetuses under 350g body weight over an 18-month period (January 2017 to November 2019) underwent whole body micro-CT imaging.

Ethical approval was acquired (NHS Health Research Authority, ethics approval ID: 13/LO/1494, 17/WS/0089 and CE2015/81) and all samples were handled in accordance with the Human Tissue Act (2004). Written parental consent for post-mortem micro-CT imaging and the use of tissue in research following fully informed consent procedures.

Prior to imaging, all fetuses were stored in the hospital mortuary and refrigerated at 4°C whilst suitable consent was determined and the suitability of individual fetuses assessed with all fetuses <350g body weight referred to our service included in this study.

Fetuses were immersed in a solution of 2.5% I<sub>2</sub>KI (2 -13 days) to allow full iodination through diffusion of the contrast to the centre of the fetus according to established protocols described in Chapter 6 [90]. The demographics and imaging parameters are listed in Table 7.1.



**Table 7.1 Study cohort demographic data and imaging parameter range**

	<b>N</b>	<b>Min</b>	<b>Max</b>	<b>Mean</b>	<b>SD</b>	<b>Median</b>	<b>Lower Qu</b>	<b>Upper Qu</b>	
Gestational Age (weeks)	258	11	24	16.0	2.50	16.0	14.0	17.8	
Post Mortem Interval (days)	258	0	48	14.1	5.21	13	11.0	17.0	
Crown Rump Length (cm)	258	4.0	18.6	10.4	2.92	10	8.0	12.5	
Crown Heel Length (cm) (missing = 1)	257	5.7	26.2	14.3	4.25	14.1	11.0	17.4	
Head Circumference (cm)	258	4.1	16.9	9.60	2.91	9.3	7.2	11.9	
Post Mortem Weight (g)	258	2.6	350.0	64.8	63.4	41.7	20.5	94.1	
Time to Immersion (missing = 69)	≤10 days	62	1	10	3.48	2.49	3	1	5
	> 10 days	127	11	19	16.2	1.80	16	15	18
Time Iodinated (days) (missing = 69)	189	1	14	8.80	2.55	9.0	8.0	10.0	
Kilovoltage	258	60	160	106	14.7	100	100	120	
Current (μA)	258	78	400	142	44.6	130	120	150	
Power (Watts)	258	7	40	15	4.9	14	12	17	
Projections	258	1351	3141	2716	440	2808	2431	3141	

#### **7.4.2 Post-mortem micro-CT imaging**

Micro-CT scanning was completed using one of two micro-CT scanners depending on machine availability (model: Med-X or XTH 225-ST; Nikon Metrology, Tring, UK). An initial whole fetal test scan was completed for each fetus to assess full iodination with a further two micro-CT studies performed once full iodination was attained to enable the highest resolution and magnification imaging possible for the two areas of diagnostic interest: a head study, and a combined chest abdomen pelvis study [160].

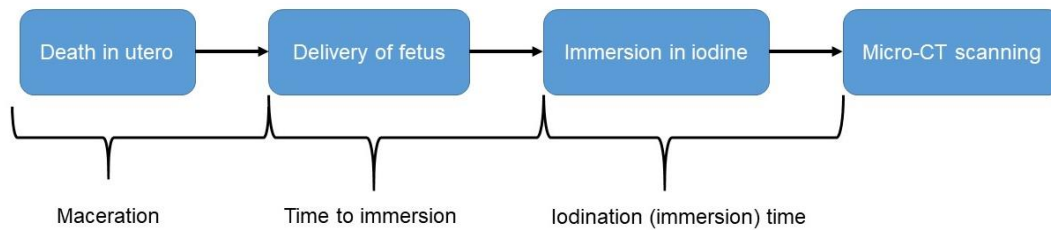
Fetuses were secured within the scanner using foam supports, moisture absorbent wrapping material and Parafilm M (Bemis, Oshkosh, USA) to ensure mechanical stability [90]. Projection images acquired by the scanner were reconstructed using modified Feldkamp filtered back-projection algorithms with CTPro3D software (Nikon Metrology, Tring, UK) and post processed using VGStudio Max 3.4 (Volume Graphics GmbH, Heidelberg, Germany). Isotropic voxel sizes varied according to specimen size and magnification, ranging from 11.6  $\mu\text{m}$  to 89.3  $\mu\text{m}$ . All images were acquired with beam hardening correction 0.5, no noise reduction median filter or tube filtration.

#### **7.4.3 Demographic data and imaging factors**

Demographical data included gestational age (weeks), post-mortem weight (g), post-mortem interval (days), mode of death, and three fetal measurements in centimetres (crown-rump length (CRL), crown-heel length (CHL) and head circumference (HC) as well as whether an abnormality was detected by micro-CT (yes / no).

The timings between delivery and imaging were recorded as in Figure 7.1:

- 1, Time to immersion (defined as the time from birth to placement in I<sub>2</sub>KI solution) and
- 2, Iodination time (defined as the time spent in I<sub>2</sub>KI solution prior to micro-CT imaging).



**Figure 7.1** Flow diagram identifying the Time to immersion and Iodination time

Two specialist paediatric radiologists subjectively assessed the degree of maceration at external examination for the whole body, and derived a single score for each fetus, based on previously published ratings (0 = no maceration, 3 severe/established maceration) [155, 156], and is based on several physical indications being definitive for maceration having taken place, including skin slippage, skin and cord discolouration, cranial collapse, level of mummification on external examination [155, 157, 158].

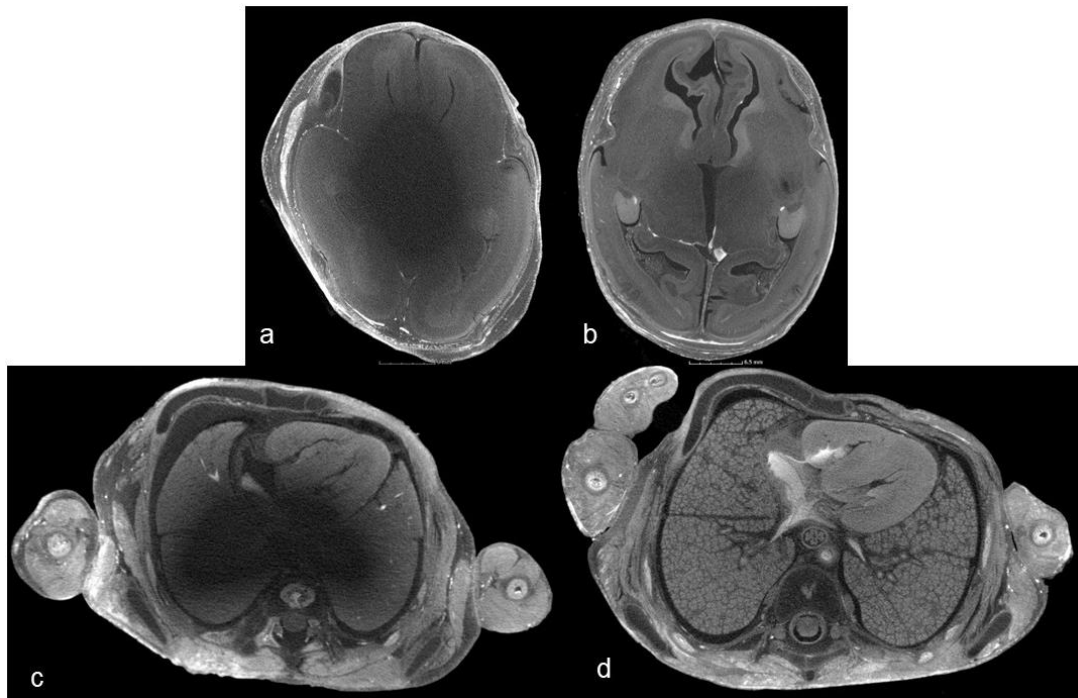
Imaging parameters were recorded for the head and chest/abdomen/pelvis examinations and fell within the following ranges: kilovoltage (60 – 160 kilovolts), current (78 – 400  $\mu$ A), exposure time (125 – 1000 milliseconds), FPP (1 – 4) projections (1066 – 3141) and effective pixel size (EPS) (11.6 – 89.3 microns).

#### 7.4.4 Image analysis

Image quality assessments were completed independently by two board-certified paediatric radiologists, with 5 years and 16 years specialist post-mortem radiology experience. All images were anonymised, and observers were blinded to the clinical history and pathological assessments.

Image quality assessments were made on 2 selected axial images per fetus, one through the head at the level of the mid-brain, and one through the thorax at the level of the heart, providing a 4-chamber cardiac view. Each radiologist provided three different subjective image quality assessments:

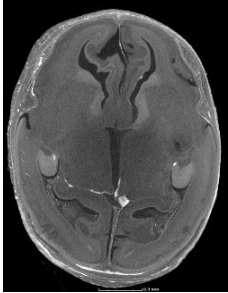
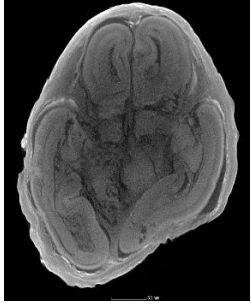
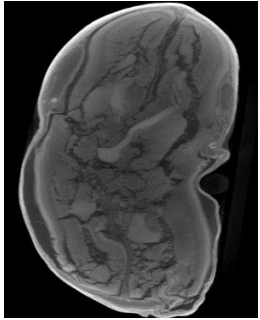
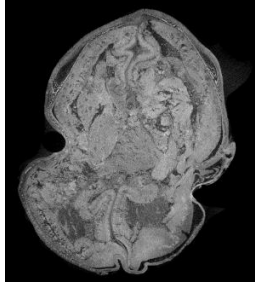
- (i) **Full iodination** (yes, diagnostic / no, non-diagnostic), Figure 7.2.



**Figure 7.2** Axial micro-CT images acquired through the head (a,b) and chest (c,d) demonstrating incomplete (a, c) and complete (b, d) iodination

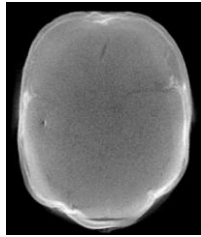
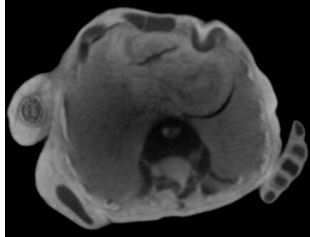
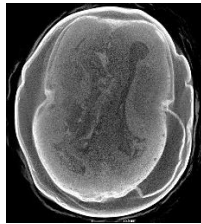

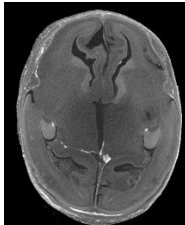
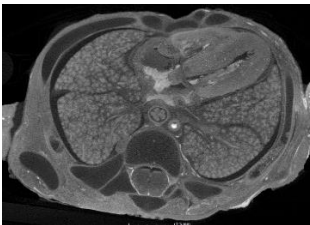
- (ii) **Imaging maceration score** – demonstrating differing degrees of maceration from none, to mild, moderate, and severe, Table 7.2.

**Table 7.2 Descriptions of the maceration criteria by which the axial head and chest images were assessed**

Maceration Score	Maceration	Maceration description	Head images
0	None	No maceration evident	
1	Mild	Mild cracking and distortion but images diagnostic	
2	Moderate	Moderate disruption with reduction in normal tissue planes, limited diagnosis	
3	Severe	Severe maceration, non-diagnostic with severely distorted internal anatomy	

- (iii) **Image quality score** – demonstrating differing levels of image quality from poor, to moderate and high, Table 7.3.

**Table 7.3 Descriptions of the image quality assessment criteria by which the axial head and chest images were assessed**

Image Quality Score	Image Quality	Image Quality Description	Head Images	Chest Images
0 -3	Poor	Very grainy images, loss of normal tissue planes		
4-6	Moderate	Some graininess perceptible, but major structures and tissue planes unaffected		
7-10	High	Imperceptible graininess in image, excellent detail		

#### 7.4.5 Statistical analysis

Descriptive statistics were calculated for baseline demographics, tissue preparation variables and image parameters. Inter- and intra-rater reliability was investigated through the kappa statistic (with linear weights) for maceration score and summary statistics (median, IQR) presented for the differences between image quality ratings. The average ratings between the two radiologist readers for image quality (the primary outcome) and maceration score were used as the final analysed outcome.

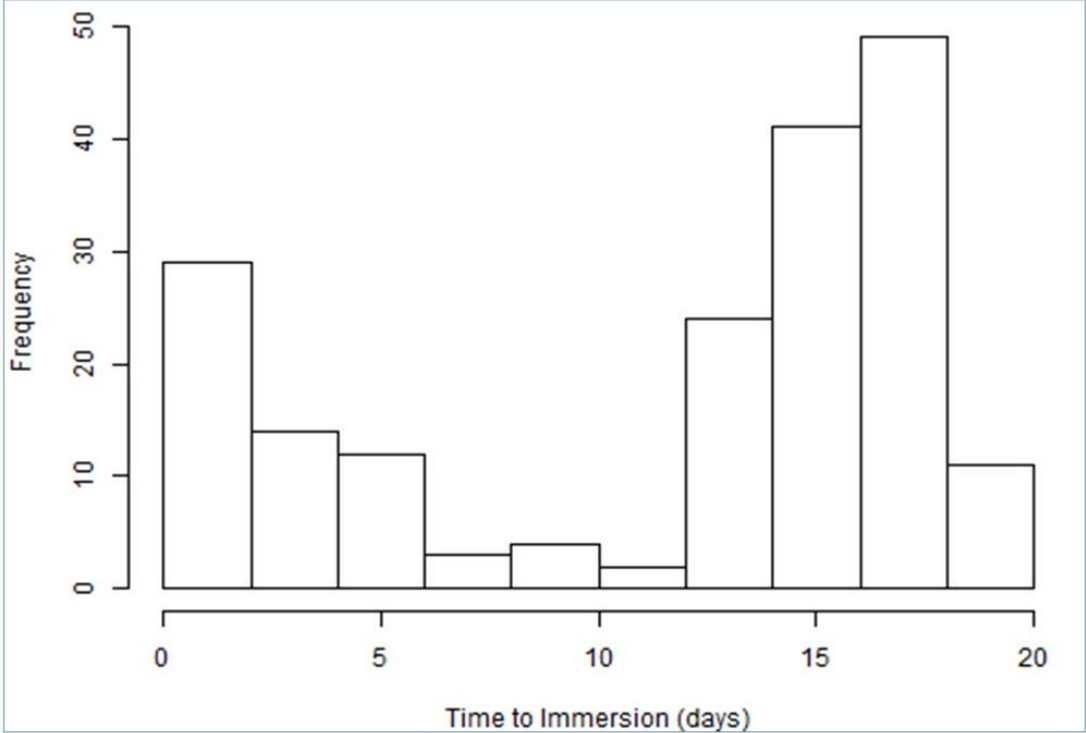
Simple and multivariable linear regression models were fitted for the outcome variables of image quality and perceived maceration score, separately for head and chest

images. Baseline demographics, tissue preparation variables and image parameters were considered as predictor variables in these models. A forward and backward model selection approach was adopted to minimise the model fit statistic AIC to choose the final multivariable models. All analyses were carried out in R (version 3.6.1).

## 7.5 Results

### 7.5.1 Demographics and imaging parameters

258 fetuses underwent micro-CT with a median post-mortem weight 41.7g (range 2.6 - 350), mean gestational age of 16 weeks (range 11 – 24). Further demographic data is provided in Table 7.1. The time to immersion showed a bimodal distribution with peaks <10 days (median 3) and >10 days (median 16 days), (Figure 7.4).



**Figure 7.3 Bimodal distribution of time to immersion across the fetuses included in our cohort**

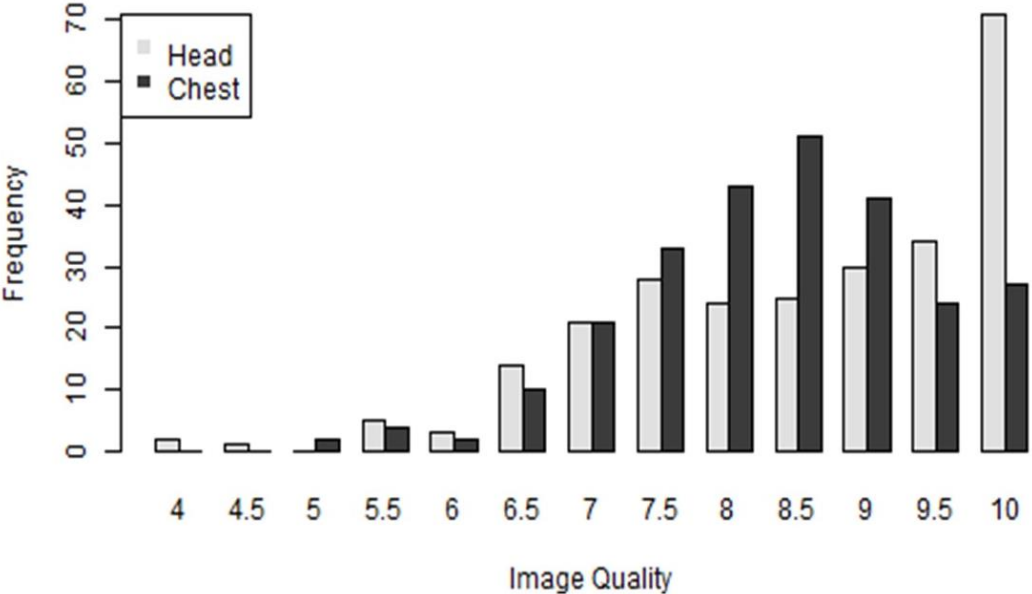
Approximately a quarter (68/258, 26.5%) of cases showed significant abnormality on micro-CT [160]. The commonest imaging indication was miscarriage 157/258 (60.9%),

followed by termination of pregnancy (TOP) 69/258 (26.7%) and intrauterine death (IUD) 32/258 (12.4%).

The range of imaging parameters used were the same for head and chest imaging (Table 10.1) with minor differences between examination areas in <5% of cases (kilovoltage (kV), current, exposure time, power), apart from number of projections and estimated pixel size which varied to a greater extent due to anatomical area size (Table 7.1).

**7.5.2 Overall image quality assessments**

An image quality score of greater than 6.5 was recorded in 247/258 (95.8%) head and 251/258 (97.3%) chest imaging (i.e., 497/516 (95.9%) images overall). Image quality scores were higher for head (median= 9, range 4 – 10) than for chest (median=8.5, range 5 – 10; p<0.001; Figure 7.4).



**Figure 7.4 Greater image quality was noted in the head in comparison to the chest**

Complete agreement between the two observers was seen in 51.2% (132/258) head images and 36% (93/258) chest images with mean score used as “image quality” for the results. There was an interrater variability of -0.16 (SD = 0.99) with one reporter (SS) scoring slightly higher for image quality.



### **7.5.3 Maceration and iodination assessments**

250/258 (96.9%) of all cases were classed as fully iodinated with high agreement of iodination status for heads 250/258 (96.8%) and chest 252/258 (97.6%).

Imaging of the brain scored higher for maceration than the chest. In just over a quarter of brain imaging cases (69/258, 26.7%) the highest maceration imaging score of 3 was provided, compared to only 3/258 (1.2%) chest images. There was an acceptable inter-rater agreement for the maceration score, with weighted Kappa = 0.56 (95% CI 0.49 - 0.63,  $p < 0.001$ ).

Pathologists at external examination recorded that over half of all fetuses (133/258, 51.6%) were severely macerated (i.e., score 3); a minority (14/258 (5.4%) as moderately macerated (i.e., score 2) or mildly macerated (i.e., score 1, 30/258, 11.6%) and approximately a third (81/258, 31.4%) as not macerated.

There was agreement of maceration score on micro-CT images and pathological assessment (within  $\pm 0.5$ ) for the head in 150/258 (58.1%), and chest in 107/258 (41.5%), with micro-CT images predominantly scoring less severe maceration in 64/25 (24.8%) head and 138/258 (53.5%) chest imaging than external assessment.

### **7.5.4 Image quality predictors**

The main predictor of image quality for both head and chest were the pathological score of maceration, with a more severe maceration score associated with lower image quality ( $p < 0.001$ ), although this only accounted for 6.6% of the variation for head imaging and 11.6% for chest imaging. Increasing body weight was also negatively associated with image quality in the adjusted models ( $p < 0.001$  head,  $p = 0.003$  chest), but not in unadjusted models.

The main imaging parameter predictor of the image quality score was the number of projections acquired, which was positively associated with image quality in both head and chest models. A greater image quality score was also positively associated with FPP (for 2 frames, as opposed to 1 or 4 frames) in both head ( $p < 0.081$ ) and chest ( $p < 0.001$ ) images, Table 7.4 - 7.6 (Abbreviations OR: Odds ratio, CI: confidence interval).

**Table 7.4 Patient demographics**

Patient Demographics	Head Images							Chest Images						
	Unadjusted				Adjusted			Unadjusted				Adjusted		
	OR	95% CI	p-value	R <sup>2</sup> (%)	OR	95% CI	p-value	OR	95% CI	p-value	R <sup>2</sup>	OR	95% CI	p-value
Gestational Age (weeks)	- 0.014	-0.079, 0.052	0.678	0.1	0.076	-0.000, 0.152	0.050	-0.062	-0.113, - 0.010	0.020	2.1	-	-	-
Post Mortem Interval (days)	- 0.008	-0.039, 0.024	0.638	0.1	-	-	-	-0.005	-0.030, 0.020	0.685	0.1	-	-	-
Crown Rump Length (cm)	0.004	-0.052, 0.060	0.891	0.0	-	-	-	-0.034	-0.078, 0.011	0.138	0.9	-	-	-
Crown Heel Length (cm)	0.012	-0.027, 0.050	0.549	0.1	-	-	-	-0.018	-0.049, 0.013	0.254	0.5	-	-	-
Head Circumference (cm)	0.021	-0.035, 0.077	0.464	0.2	-	-	-	-0.005	-0.050, 0.040	0.822	0.0	-	-	-
Post Mortem Weight (100 g)	- 0.004	-0.263, 0.255	0.976	0.0	-0.716	-1.074, -0.357	<0.001	-0.029	-0.235, 0.178	0.785	0.0	-0.337	-0.550, -0.114	0.003

**Table 7.5 Maceration was the main predictor of image quality. Higher body weight and time to immersion was also negatively associated with image quality**

Tissue Preparation		Head Images							Chest Images						
		Unadjusted				Adjusted			Unadjusted				Adjusted		
		OR	95% CI	p-value	R <sup>2</sup> (%)	OR	95% CI	p-value	OR	95% CI	p-value	R <sup>2</sup>	OR	95% CI	p-value
Ab on Micro-CT (ref = no)	Yes	0.232	-0.139, 0.602	0.220	0.6	-	-	-	0.367	0.073, 0.660	0.015	2.6	-	-	-
Mode of Death (ref = IUD)	Miscarriage	0.619	0.126, 1.110	0.014		0.469	-0.003, 0.940	0.051	0.219	-0.170, 0.608	0.269		-0.112	-0.480, 0.256	0.548
	TOP	1.170	0.623, 1.710	<0.001	6.9	0.826	0.253, 1.400	0.005	0.895	0.466, 1.320	<0.001	9.3	0.326	-0.122, 0.775	0.152
Maceration Score (autopsy, ref = 0)	1	-0.410	-0.956, 0.136	0.140		-0.523	-1.027, -0.020	0.042	-0.450	-0.874, -0.026	0.038		-0.616	-1.003, -0.229	0.001
	2	-1.110	-1.85, -0.376	0.003		-0.931	-1.652, -0.211	0.012	-0.655	-1.230, -0.081	0.026		-0.815	-1.370, -0.260	0.004
	3	-0.690	-1.050, -0.330	<0.001	6.6	-0.592	-1.048, -0.136	0.011	-0.815	-1.090, -0.535	<0.001	11.6	-0.830	-1.158, -0.500	<0.001
Time to Immersion (days)		-0.006	-0.037, 0.024	0.694	0.1	-	-	-	-0.024	-0.046, -0.001	0.039	2.3	-	-	-
Time Iodinated (days)		0.036	-0.040, 0.111	0.357	0.5	-	-	-	0.038	-0.018, 0.094	0.186	0.9	-	-	-

**Table 7.6 The number of projections was the main imaging parameter associated with higher image quality scores**

Imaging Parameters		Head Images						Chest Images							
		Unadjusted				Adjusted		Unadjusted				Adjusted			
		OR	95% CI	p-value	R <sup>2</sup> (%)	OR	95% CI	p-value	OR	95% CI	p-value	R <sup>2</sup>	OR	95% CI	p-value
Kilovoltage (per 100)		-0.095	-1.210, 1.020	0.867	0.0	-	-	-	0.373	-0.516, 1.260	0.410	0.3	-	-	-
Current (100 µA)		0.060	-0.295, 0.415	0.740	0.0	-	-	-	-0.170	-0.463, 0.123	0.254	0.5	-	-	-
Power (10 Watts)		0.054	-0.273, 0.381	0.744	0.0	-	-	-	-0.099	-0.367, 0.169	0.469	0.2	-0.289	-0.548, -0.029	0.029
Projections (100 s)		0.095	0.065, 0.126	<0.001	12.8	0.102	0.070, 0.134	<0.001	0.060	0.031, 0.088	<0.001	6.0	0.044	0.015, 0.072	0.002
EPS (100 microns)		-2.150	-3.310, -0.982	<0.001	4.9	-	-	-	-1.650	-2.590, -0.701	<0.001	4.4	-	-	-
Exposure time (100 milliseconds)		0.048	-0.075, 0.170	0.445	0.2	-	-	-	0.071	-0.027, 0.168	0.153	0.8	0.074	-0.022, 0.170	0.132
FPP (ref = 1)	2	0.332	-0.041, 0.706	0.081		-	-	-	0.600	0.291, 0.909	<0.001		0.639	0.341, 0.937	<0.001
	4	0.093	-1.210, 1.020	0.869	1.3	-	-	-	-0.453	-1.270, 0.360	0.273	7.3	0.178	-0.566, 0.921	0.638
Target (ref = Mo)	W	0.165	-0.383, 0.713	0.554	0.1	-	-	-	0.447	0.015, 0.879	0.043	1.6	0.358	-0.058, 0.774	0.091

## 7.6 Discussion

This study has shown a high image quality score (of over 6.5) was achieved in the majority (247/258, 96%) of fetal head and chest micro-CT studies across a range of body weights. The strongest negative predictor of final image quality was the extent of fetal maceration, with decreasing image quality also associated with increasing body weight. The strongest imaging parameter predictors for image quality were the number of FPP and EPS.

There was some discrepancy between micro-CT imaging assessment and pathological visual assessment of the extent of fetal maceration, where pathological maceration assessment was a better predictor of poor micro-CT image quality, although poor image quality was only found in 4.1% of fetuses overall. This means that good micro-CT image quality was achieved in the majority of cases despite several severely macerated fetuses being included in the cohort. This demonstrates that this technique can still produce high quality imaging and increase the widespread use of micro-CT in macerated cases. This would allow micro-CT to be used as a triage tool to determine which cases might be best suited for further pathological evaluation.

Whilst image quality was focussed on in these investigations, maceration has been shown to render up to 50% of imaging non-diagnostic, in particular for the brain [160] and heart [71, 161]. However, analysis of macerated cases at conventional autopsy is equally challenging and the ability of micro-CT to provide high quality imaging non-invasively may assist in maintaining the internal and external structure of the fetus intact and allow some level of information to be obtained. This is especially useful in the brain, where maceration often causes little information from conventional autopsy procedures. Further optimisation of micro-CT may also provide greater diagnostic yield in future.

Image quality was also rated as consistently higher for head than chest imaging. This is likely due to intrinsic differences in image quality related to anatomical shapes and ensuring full inclusion within the imaging detectors: spherical objects (such as the head) can be positioned closer to the X-ray source, enabling lower EPS, whereas more elongated shapes (such as the body) require positioning further away, enforcing a

higher EPS to achieve optimal coverage. This causes an increased number of projections, optimised by the scanner automatically, related to object diameter of for the head in comparison to the body, which would explain both higher image quality for the head and a negative association between increased EPS and image quality.

A few fetuses which were imaged using more FPP chest (4/258) 2.7%, head 6/258 (2.3%), and also yielded higher image quality, which is to be expected with increased signal to noise as demonstrated by Chapter 6, although these scans take significantly longer, as scan time is the sum of exposure time, FPP and number of projections. Although 2 FPP was shown to be statistically significant, 4 FPP was not. This can be explained by the small number of examinations that employed 4 FPP. To investigate the effect 4 FPP has on image quality more accurately would require a greater number of examinations with 4 FPP.

Body weight was negatively associated with image quality with a higher image quality rating overall for head when compared to chest images. Both these results can be explained by lower weight fetuses and smaller anatomical areas (particularly heads), resulting in a lower EPS and a higher resolution micro-CT image. Lower body weights and fetuses below 20 weeks gestation have significantly poorer diagnostic accuracy and image quality using other post-mortem techniques, MRI [66] and Ultrasound [161], and should be diverted to micro-CT. Together, these factors combined further demonstrate the importance of the development of a clinical micro-CT protocol.

A bimodal time-to-immersion pattern was observed in our patient demographics, which likely represents the differences between referral centres and their respective consent procedures. Access to the micro-CT service can be expedited where full parental consent is given on referral, but delays are encountered if further information is required, resulting in two peaks at median 3 and 16 days, (Figure 7.3). This could also explain why TOP was a statistically significant positive predictor for image quality when compared to miscarriage, as these cases are likely to be referred more rapidly, and with minimal maceration. Since this analysis was completed, dedicated consent procedures at all referring centres have been adopted to reduce these delays and improve both parent and professionals understanding of the procedures.

These investigations have shown that micro-CT can generate high quality imaging in small, macerated fetuses where perinatal autopsy is known to present considerable logistical challenges. It also offers an attractive alternative to those parents who do not consent to invasive autopsy and is likely to increase the uptake of post-mortem investigations [8, 16, 37, 38]. This further demonstrates the opportunity to offer a broader range of post-mortem techniques on an individualised basis with the ability to triage those cases in whom invasive autopsy will be most useful. Formal autopsy will be of most use where post-mortem investigations and antenatal imaging findings are not concordant [46], although it should be noted that following fetal loss below 18 weeks gestation it is unlikely that detailed antenatal ultrasound will have been performed.

## **7.7 Limitations**

The main limitation was the retrospective nature of this study, where we used a relatively narrow range of imaging parameters, limited by machine capability. Chapter 7 analysed the widest range of imaging factors possible for the Med-X micro-CT scanner (Nikon Metrology, Tring, UK) and determined the impact individual imaging parameters have on SNR and rCNR. Therefore, this study offers a real-world example of the consecutive cases referred to a clinical micro-CT unit and provided data to allow adoption of several of the key points from these results into clinical practice.

## **7.8 Conclusion**

High micro-CT fetal image quality is achievable following early pregnancy loss despite maceration, with higher resolution achievable in smaller fetuses, when conventional autopsy is challenging. These factors further demonstrate the requirement for a clinical micro-CT imaging service, which will address the demonstrated need for less invasive autopsy methods.

## **7.9 Summary**

In summary, although maceration (strong negative predictor) was detrimental to image quality, high image quality was still attainable in the overwhelming majority of micro-

CT scans. Fetal weight was a weaker positive predictor of image quality due to increasing EPS and number of projections.

### **7.10 Key points**

- High image quality was still possible despite the presence of maceration.
- Strongest negative predictor for image quality was maceration.
- Strongest imaging parameters for image quality was EPS and number of projections.
- Body weight was negatively associated with image quality due to its association with a lower EPS.
- Head imaging reported higher image quality due to smaller EPS being possible in general.



## **Chapter 8      Focus group investigations into early pregnancy loss from the family’s perspective: a pilot study**

### **8.1 Overview**

This chapter presents an exploratory qualitative study into parental views of post-mortem micro-CT imaging. Two focus groups consisting of parents following a miscarriage were conducted to determine parental views towards micro-CT. It shows that parents felt overwhelmingly positive about the technique and brought out key themes, in particular greater choice, increased uptake, and mental health benefits.

The work presented in this chapter was undertaken by the author of this thesis, with qualitative analysis and assistance in leading the focus groups provided by Dr Celine Lewis (Social scientist). Recruitment was done through the Miscarriage Association.

Work from this chapter was published in *Opinions in Obstetrics and Gynecology* (2021) [162] and has been submitted for publication at *BMC Medical Imaging*. It has also been presented orally at the NIHR Conference 2020 [163], United Kingdom Imaging and Oncology (2020) [164], and International Society of Radiographers and Radiographical Technologists World Congress (2021) [165].

### **8.2 Introduction – parental perceptions of autopsy**

Multiple investigations have been completed on the reasons why parents’ consent to an autopsy, including determining future risk of recurrence, to advance medical knowledge, to provide “closure” or to rule out self-blame [144-146, 166, 167]. Equally, there are documented reasons parents may decline autopsy investigations, including wanting to protect their baby from further harm, poor communication between professionals and parents and a dislike of the invasiveness of the procedure, with education and socio-economic status also playing a role in the decision-making [8, 16, 168].

It is this invasive nature of conventional autopsy and the lack of alternative non-invasive techniques for early pregnancy loss (<22 weeks), that has led to the continued development of non-invasive imaging techniques including micro-CT. By developing an understanding of the reasons why parents' consent or decline the differing autopsy techniques now available better provision can be targeted to this underserved group.

Therefore, by undertaking this pilot study I aimed to understand the applicability of the micro-CT technique and to better direct research into post-mortem imaging techniques in the future with parents' voices at its centre.

### **8.3 Aims**

**Aim 8-1:** Using thematic analysis to explore parental opinion of micro-CT following miscarriage, particularly around acceptability, the main benefits, and concerns.

This is qualitative research and therefore does not require a null hypothesis.

### **8.4 Methods**

#### **8.4.1 Funding**

This investigation was funded by a National Institute for Health Research, Research Design Service – London “Enabling Involvement” Award (£350).

#### **8.4.2 Study participants and recruitment**

Participation in the focus groups was advertised via the “Miscarriage Association” Facebook account (San Jose, USA) and by email to the London and Home Counties support and media volunteers of the “Miscarriage Association” who had expressed an interest in participating in research during January 2020. Potential participants confirmed their interest and their preferred dates and times via email, with the focus groups completed on the 7<sup>th</sup> and 9<sup>th</sup> March 2020.

Both male and female parents who had experienced a miscarriage and were able to attend a central London site for a face-to-face focus group meeting. There was no limit on the time since the miscarriage event or whether they had experience of micro-CT imaging as a post-mortem investigation for miscarriage. Exclusion criteria included

any parents who were greater than 2 hours travel away from the Institute of Child Health, as reimbursement would likely exceed the grant allowance.

Participants were offered a variety of days and times for the study to maximise uptake. Reimbursement of travel costs and a gift voucher of £10 was made available for their time.

All documentation and questionnaires were checked by the Miscarriage Association to ensure clear plain English was used and suitable terminology to ensure complete understanding by the participants.

### **8.4.3 Data collection**

Prior to the focus groups, participants were sent background information (Appendix 6) on the processes undertaken during conventional autopsies and potential supplementary imaging techniques, including micro-CT. A brief explanation of the intended topics for discussion at the focus group meeting was included. Parents were free to decline participation at any time leading up to the meeting and contact details for the research team were available should additional support or information be required.

Written consent was provided by all participants, allowing for the audio-recording of the focus group discussions, and for use of anonymised quotes in subsequent research papers and reports, and participants demographics. General reflections were collected by a male research radiographer with 3 years' experience of post-mortem imaging techniques (ICS-thesis author) and a female social scientist with 15 years' experience in conducting and analysing qualitative interviews (Dr C. Lewis). The focus group meetings lasted approximately 1.5 hours each and took part in a neutrally decorated university conference room, rather than within the hospital, to avoid triggering any untoward emotional memories of the miscarriage. Both researchers wore casual clothing, rather than uniform, to set the scene for an open and supportive discussion environment.

Intended topics for discussion were pre-planned prior to the focus group through a multidisciplinary team collaboration – comprising of the research radiographer, two

consultant radiologists, a social scientist and patient support advocates from the Miscarriage Association (Wakefield, UK). Key areas for exploration included: assessing parental acceptability of micro-CT imaging, the perceived benefits, and concerns about this technique as described by parents.

During the focus groups, the research radiographer delivered a short presentation depicting the micro-CT imaging technique. This included details of both existing post-mortem imaging techniques and micro-CT, and their advantages, and limitations for miscarriage investigation. Details of the staining preparation required for micro-CT and examples of anonymised human fetal micro-CT images were also included. At the end of the presentation, the participants had the opportunity to ask questions about the procedure.

A group discussion was then performed using open-ended questions to determine parental views. The discussion topics were informed by parental attitudes towards post-mortem investigations from the current literature and previously conducted work [8, 37, 38].

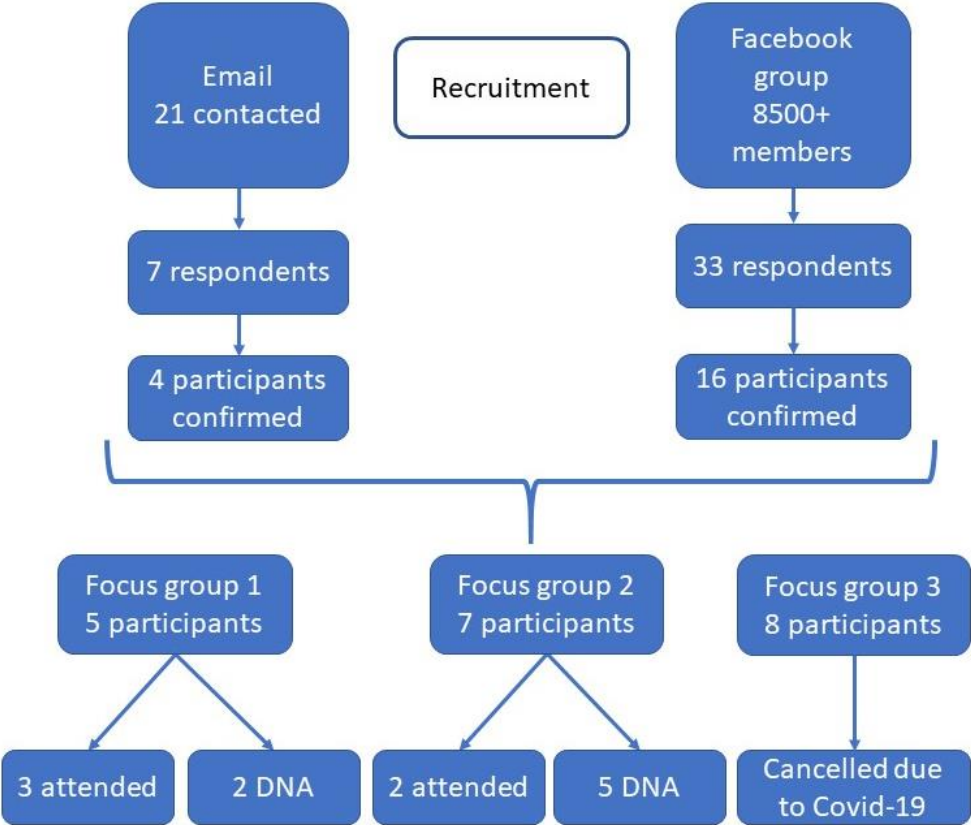
#### **8.4.4 Data handling and analysis**

The focus groups were audio-recorded with a digital voice recorder and transcribed verbatim, with ICS checking the transcription for completeness. Data were analysed using thematic analysis [169]. A codebook approach was used which combined a structured approach, with codes initially identified through the literature and topic guide (a deductive approach) alongside developing codes directly from the data (an inductive approach). Initially, both researchers involved in the focus group meetings independently read both transcripts and developed a coding framework. These were then discussed, and the coding framework amended with some codes split, combined, and renamed. ICS then re-read through the transcripts with the amended framework and developed a set of categories that pulled similar codes together. The codes and categories were discussed between the researchers with subsequent reorganisation of the codes and categories. Transcripts were then read through a final time to check the relevant data had been coded appropriately. In the final stages of analysis, some minor changes were made to the wording of the categories and an overarching theme identified.

**8.5 Results**

**8.5.1 Participant recruitment**

Twenty-one participants were initially contacted via email as part of the London and home counties support and media volunteers. Adverts were also posted on the Miscarriage Association Facebook (San Jose, USA) social media private group (over 8500 members). A total of 41 participants initially responded to take part in the research, with 20 confirming their availability. A further 7 participants did not attend on the day, with one focus group of 8 participants being cancelled due to the Covid-19 pandemic. Therefore, 5 participants attended across 2 focus groups in March 2020, (Figure 8.1).



**Figure 8.1 Flow diagram of the recruitment process**

### **8.5.2 Participant characteristics**

All participants were female, with an undergraduate university degree education or higher, had experienced at least 1 miscarriage and none had experienced a conventional (i.e., 'invasive') or imaging (i.e., 'non-invasive') based post-mortem investigation at time of miscarriage, Table 9.1.

Two participants had been offered post-mortem investigations following their miscarriage; one accepted chromosomal analysis and one declined conventional autopsy, but later regretted this decision after experiencing further miscarriages. She indicated that the information she may have received from the autopsy may have been of some help. No participants were offered post-mortem imaging investigations as part of this study.

**Table 8.1 Demographics of focus group participants**

Participant	Gender	Age	Ethnicity	Number of miscarriages	Number of stillbirths	Investigation following pregnancy loss offered	Autopsy selected
1	F	40	Mixed	2	0	Chromosomal analysis	N
2	F	38	Black / African	8	0	N	N
3	F	33	Mixed	2	0	N	N
4	F	34	White	2	0	N	N
5	F	35	Latin American	1	0	N	N

### 8.5.3 Findings

The overarching theme summarising parental perceptions of micro-CT was that there are multiple advantages to providing micro-CT post-mortem imaging techniques to parents who have experienced miscarriage.

Within this theme identified two key categories were identified:

- 1) inner world benefits of micro-CT,
- 2) outer world benefits of micro-CT.

Further sub-themes were developed with participants' quotes used to highlight these, Table 8.2.

**Table 8.2 Categories and codes identified as important factors around micro-CT post-mortem imaging**

Sub-groups	Sub-themes
Inner-world benefits of micro-CT	Fulfilling parental role through protection and care of the baby
	Contributing to knowledge through research
	Choice and increased investigational options
	Hope for the future
	Conventional autopsy attitudes
Outer-world benefits of micro-CT	High-resolution imaging for early gestation fetuses
	Non-invasive imaging
	Micro-CT staining information during consent
	Access to micro-CT and increased choice for parents



## 8.5.4 Internal themes

### 8.5.4.1 *Fulfilling parental role through continued protection and care of the baby*

Participants felt that the non-invasive nature of micro-CT could allow parents to fulfil their parental responsibility by investigating the cause of the loss whilst at the same time providing protection and care to the fetus.

“you don’t necessarily want any more harm done, because you’re still, in some cases, some parents are still quite protective of that fetus” – FG1

Participants also felt that being able to image the baby using micro-CT independently from the mother helped reaffirm the loss of a human being, even at such an early stage of the pregnancy, which some parents found comforting.

“because at such early stage sometimes you haven’t told a lot of people so, you know, you do think oh was it actually a baby, was it, you know, so it’s amazing to kind of see that image, you know, because you don’t feel crazy anymore.” – FG2

“so actually, I think in a way it’s quite nice because it’s being treated like it’s a baby.” -FG2

Reaffirming the loss as a baby and treating it accordingly could potentially have mental health benefits for the parents and provide comfort. A degree of closure may also be gained by fulfilling their parental responsibilities through investigating their loss to the best of their abilities in having chosen the “best possible” care given to their baby.

### 8.5.4.2 *Contributing to knowledge through research*

The value of micro-CT in contributing to our understanding of miscarriage was discussed. Participants felt that being able to contribute to research following a miscarriage could enable something positive to come from a negative experience.

“so, if I knew that obviously out of this something that was very upsetting, there was some type of good going to happen from it, then I wouldn’t actually mind” – FG1

“.... I think you need answers and if there’s a way to get the answers, that’s great. We need more information, more – we want to know why it happens really.” – FG2

Contributing to an increase in the knowledge surrounding miscarriage could provide benefits both personally and to the knowledge base.

#### *8.5.4.3 Choice and Increased Investigation Options*

Participants acknowledged that another benefit of micro-CT was that it added to the choice of investigations available to parents following a miscarriage.

“...better than “OK do you want an autopsy or not’. So, it’s just offering something a bit more for the parents.” – FG1

“And to have that technology there because, at the moment, with early miscarriage it’s more investigations of the mum.” – FG2

Increasing parental choice could be empowering as it enables parents to have some direct control over the level of investigation and protection they desire for their baby in a situation where it can feel that there is no control available.

#### *8.5.4.4 Hope for the future*

The availability of micro-CT to provide answers and alleviate parents’ fear of future pregnancies was mentioned.

“for your mental health – and also not being so fearful of the next pregnancy as well, because potentially if something was found and is fixable in some shape or form then it, yeah, kind of prepares – you’re in preparation for the next one to be able to get.” -FG1

“You know, so it’s quite invasive for the mum, you know, but actually a lot of the problems sometimes might just be the development and then it would stop the mum from blaming themselves, you know, to have the answers that actually it’s not you, you know, it’s just something that’s happened, you know, you haven’t done anything wrong, you didn’t run for the train too fast or, you know, something so silly!” – FG2

This could provide some comfort for parents going forwards and enable them to move on. In addition, some participants also highlighted the potential for micro-CT to provide answers and therefore prevent mothers' blaming themselves for the loss.

#### *8.5.4.5 Conventional autopsy attitudes*

One participant also stated that she would have accepted a conventional autopsy had it been offered.

“So, yeah, I would. I think I would have either of them offered to me, if either of them was offered and if it was all good, yeah. So, I know it's slightly different feelings!” – FG1

“I personally regret not having an autopsy now because for my nineteen weeks that was baby no.3 and I just presumed that once that happened, because I got pregnant so easily, it would be fine, but now I'm on, or I've had miscarriage no.8 and I still haven't got the full answers.” – FG1

The feeling of regret through not investigating a miscarriage is demonstrated and can have mental health consequences. By increasing the choice of examinations available, more acceptable procedures can be made available to parents who consider conventional autopsy as unacceptable.

### **8.5.5 Outer-world benefits of micro-CT**

#### *8.5.5.1 High-resolution imaging for early gestation fetuses*

The high-resolution of the technique and the ability to image early gestational fetuses from the first trimester were mentioned as a positive impact of the micro-CT technique.

“the understanding of how clear you can actually see and what you can see.” – FG1

“I think the amount of imagery, the amount of detail that you're managing to get obviously is a lot better than an autopsy.” – FG1

“It is so impressive how detailed they are, like, when they are so tiny and you can see so many of the organs and, yeah, I'm really impressed.” – FG2

“So, first trimester losses. Wow, that’s impressive.” - FG1

Providing highly detailed images for earlier pregnancy loss could potentially provide comfort to parents by helping them appreciate their loss as a baby rather than a fetus.

#### 8.5.5.2 *Non-invasive imaging*

Participants felt that the ability to provide answers as to the loss of the pregnancy in a non-invasive manner was important.

“I think you need answers and if there’s a way to get the answers, that’s great. We need more information, more – we want to know why it happens really.” – FG2

“that they’re not having to be cut open and you’re getting the data that you need to potentially find some answers” – FG1

“I just couldn’t bear the thought because I just thought do you know what, he’s been through enough, I don’t want him being cut open. But if something like this was available, I would have jumped at the chance.” – FG1

“really because it’s not invasive, ..... So, I’ve got an idea of, ..... What that kind of procedure is, whereas an autopsy just seems so much scarier.” – FG1

“Yeah, I think as an alternative to what is done at the moment, it’s much better to know that your baby’s not going to be cut and that you’re going to see so clearly what was inside the baby and how long it developed.” – FG2

The non-invasive approach of micro-CT was universally acknowledged by participants as an important factor in acceptability. One participant even stated that this would have changed their mind, and that they would have chosen further investigation.

#### *8.5.5.3 Micro-CT staining information during consent*

Participants expressed that the temporary alteration of skin tone during preparation for micro-CT may influence parental choice of the technique, and that returning the babies skin tone to its original colour would be important for some participants.

“I think if the parents are made aware then they’re waiting for it and then you know if you said to me and I didn’t know the colouration – there’ll be a potentially staining of the baby, I would always imagine it to be worse than what it actually is. Yeah, I don’t think the staining would bother me either.”  
– FG1

“No, it wouldn’t to me. I think it’s a personal thing but, to me, it wouldn’t.” – FG2

“I think getting back to close to the real colour, I think it would be important.” – FG2

Recognising the skin tone change through iodination may affect the uptake of the procedure for some parents and this is important in highlighting a potential barrier to the technique. All participants stated that this would not have discouraged them personally. It demonstrates that parents require full information of the process to enable informed choices to be made.

#### *8.5.5.4 Access to micro-CT and increased choice for parents*

Participants believed that they and other parents would be willing to pay for a micro-CT service if it allowed them access to the technology. They spoke of frustration that only following multiple miscarriages were investigations prioritised in the current clinical service.

They universally expressed that had micro-CT been available at the time of their miscarriage they would have chosen it.

“It would definitely be something, you know, something we were thinking about, we were lucky enough to then go on and have a baby but, you know, it’s definitely something I think people would pay for.” – FG2

“But I know there’s plenty of women that would pay for that if it was available, you know, but also changing the...but, you know, at the moment, as I say, they go three, unless you’ve had more than three early miscarriages, they don’t really do anything, which I can understand, but it’s quite difficult. So, yeah, it’s kind of changing that as well if the technology’s there then you can do it.” – FG2

“Yeah, I think it’s really amazing, I think it can help a lot of women, definitely, and men!” – FG2

Expression of willingness to pay for and choose the micro-CT technique demonstrates the universally positive attitude amongst the participants and their belief that such a clinical service needs to be widely available.

### **8.5.6 Thematic sentences**

Thematic analysis of the focus groups allowed two thematic sentences to be developed:

1. The investigation of miscarriage through micro-CT was perceived as having several parent centric benefits around peace-of-mind, control and facilitating closure.
2. Micro-CT was perceived to have service and societal benefits around finding answers through non-invasive imaging following miscarriage.

## **8.6 Discussion**

In this explorative qualitative study, parental perceptions of post-mortem micro-CT imaging following a miscarriage were positive overall. In particular, the main perceived benefits centred around peace-of-mind, facilitating closure, and providing some answers to why the miscarriage had occurred, matching general parental perceptions of autopsy [8, 13, 144-148, 166, 167, 170, 171], and increasing acceptability of non-invasive autopsy techniques [8, 16, 37, 38, 162, 172].

The non-invasive approach of micro-CT imaging resonated with the focus group participants. They felt it would result in a higher uptake in autopsy investigations, as it

would allow parents to accept some form of autopsy whilst also providing comfort in knowing that their baby was not suffering further harm. This ability to provide respectful care was important to our focus group participants and was previously highlighted in studies looking at benefits of less-invasive autopsy [13, 31, 145-148, 173]. Any increase in the uptake of autopsy investigations from the current low level is likely to be beneficial for families, hospitals, society and policy-makers [8, 16, 37, 38].

The high-resolution imaging also resonated with participants by recognising their early pregnancy loss as a baby rather than a fetus. They felt that the ability to visualise individual organs in such small fetuses to a recognisable degree of detail, was important in providing comfort for parents and increasing the likelihood of engaging with the post-mortem investigation process, in keeping with previous studies [32, 146].

Participants stated that the need for answers concerning the pregnancy loss was important, and that micro-CT can address this need. Micro-CT can provide diagnostic information to determine the cause of pregnancy loss [8, 64, 65, 74, 75, 126, 160, 174], across a wide range of gestational ages (7 – 22 weeks) [126, 175] and fetal weights (2 – 350 grams) [160], which are not adequately served by clinical MRI imaging below 500 grams [44, 64, 66].

Participants also stated that micro-CT allowed acceptable investigations to be completed and could reduce the blame felt by the parents. Even when there was no definitive result as to why the pregnancy was lost, it may allow the parents a degree of closure for their loss and to feel that they had fully investigated the death, thus having a positive impact on parental mental health [37, 144-148]. One participant stated that she had regretted declining a conventional autopsy following multiple miscarriages, in line with literature reporting that most parents who consent to autopsy find it helpful [166], whilst those who decline investigations often express regret [13, 171].

The universally positive response of parents from our focus groups was that they would have accepted a micro-CT investigation had it been offered to them. The ability to provide knowledge resonated with the participants not just on a personal level, but also altruistically, which is a significant motivator for parental consent [144, 148, 167, 170,

171, 173]. Importantly, the participants did not consider the temporary discoloration to be a significant barrier to micro-CT uptake, providing sufficient information was given during consent by a health professional who thoroughly understood the procedure [166, 170].

There are no other studies currently in the literature that have assessed parental acceptability of micro-CT imaging for fetal loss, but these results match parental acceptance of other post-mortem imaging investigations (e.g., PMMR) which is high [8, 16, 37, 38, 162, 176]. Key important factors for parents raised in those studies were invasiveness, communication, respectful care, contribution to research and awareness of the techniques, which were also raised within our study and demonstrates the applicability of micro-CT for use as a non-invasive post-mortem imaging technique.

## **8.7 Limitations**

There are several limitations associated with this study.

Firstly, only a small number of participants took part with none having first-hand experience of the micro-CT imaging process during their miscarriage. Given the relatively new micro-CT imaging service, few parents were available who would have first-hand experience of micro-CT imaging, but the feedback remains useful.

Secondly, the study coincided with the onset of the global Covid-19 pandemic, which was largely responsible for the high non-attendance rate. Despite this, these preliminary results are representative of general parental attitudes, as the data matches the wider literature on less-invasive post-mortem imaging techniques.

Although online virtual meetings would have been possible and have become popular as a data collection method in the past year, this was not the experience at the time. Due to the sensitive nature of this research topic, these discussions would have best been conducted in person in a quiet dedicated space with on-site bereavement support, should any emotional distress arise. On-line data collection will be considered for further studies, to extend the reach of the study population and to allow a wider



audience to attend who may be reluctant to travel or cannot due to on-going Covid-19 restrictions or personal circumstances.

Thirdly, there could be debate whether focus groups or interviews offer the optimum method of data collection. Whilst interviews could offer a greater depth of discussion for individual cases, focus groups successfully developed full conversations around the micro-CT technique.

Fourthly, participants religion should have been recorded as this may have an effect on the choice of investigation as Judaism and Islam dictates that the body should not be cut and that it should be buried within a day. These factors will have an effect on parents choosing micro-CT scanning as it takes several days for iodination to occur yet prohibits any cutting of the body. This demographic should be recorded for future investigations.

## **8.8 Conclusion**

Micro-CT is perceived to be a useful post-mortem imaging technique by parents who have experienced a miscarriage. Our focus group indicated that the key potential benefits were in providing a greater range of choices for parents following early pregnancy loss, increasing the uptake of autopsy in general, and multiple mental health benefits. Further parental involvement including those who have directly experienced the technique should be the next step in developing this patient-centred clinical service.

## **8.9 Summary**

In summary, the response of participants to the micro-CT technique was overwhelmingly positive. The results from this exploratory preliminary study corresponded to larger investigations of less-invasive autopsy techniques and their acceptability. This study provides validation for further work within this area to ensure that the micro-CT technique is further developed. This will increase accessibility for post-mortem imaging techniques where no other alternative imaging tool currently exists.

## 8.10 Key points

The focus groups analysis indicated several key points that development of a clinical micro-CT service would provide.

- Non-invasive approach would allow for increased uptake of post-mortem investigations, increasing individual and overall medical knowledge.
- Mental health advantages for parents through increased care and protection being provided through the non-invasive approach of micro-CT.
- The high-resolution imaging of micro-CT can help recognise the early pregnancy loss as a baby and could provide comfort to parents.
- There was an overall positive response to the micro-CT technique with all participants stating they would have consented to the procedure if offered to them.
- Micro-CT allows greater parental investigational choice for early pregnancy loss.
- Importance of staining information delivered to the parents during the consenting procedure.

## Chapter 9      Future Direction for post-mortem micro-CT of human fetuses.

### Overview

This chapter summarises the work completed as part of this doctoral thesis. It describes how this work has changed clinical practice within Great Ormond Street Hospital and discusses the limitations of this work, with future direction of this work and clinical integration.

Work from this chapter was published in *Ultrasound Obstetrics and Gynecology* (2019) [175] and *American Journal of Obstetrics and Gynecology* (2021) [160]. It has also been presented orally at the Biomedical Research Centre / Institute of Child Health Showcase Event (2019) [177].

### 9.1 Summary of findings

The overall aim of this thesis was to develop an optimal clinical protocol for scanning post-mortem iodinated whole human fetuses with micro-CT. This was achieved and has been published as a clinical protocol [90].

More detailed aims were as follows:

**Aim 1:** To determine optimal tissue preparation (concentration and immersion time in I<sub>2</sub>KI solution) for ex-vivo organs and whole human fetuses <24 weeks prior to micro-CT scanning.

A relationship between iodine immersion time and fetal body weight was found for human fetal tissue preparation (Chapter 4).

**Aim 2:** To identify the relationship between key micro-CT imaging parameters and SNR and rCNR for ex-vivo organs and whole human fetuses.

This was achieved and is outlined in chapters 3 and 6.

**Aim 3:** To determine a clinically appropriate micro-CT scanning protocol with optimal SNR and rCNR, within a scan time of less than 30 minutes and to eliminate detector saturation.

This was the main aim of the thesis and has been established (Chapter 6).

**Aim 4:** To determine the relative contributions of fetal demographics and imaging parameters to image quality for post-mortem fetal micro-CT imaging.

This work found that maceration was the strongest predictor of image quality (Chapter 7), using specific ROI methodology (developed in Chapter 6).

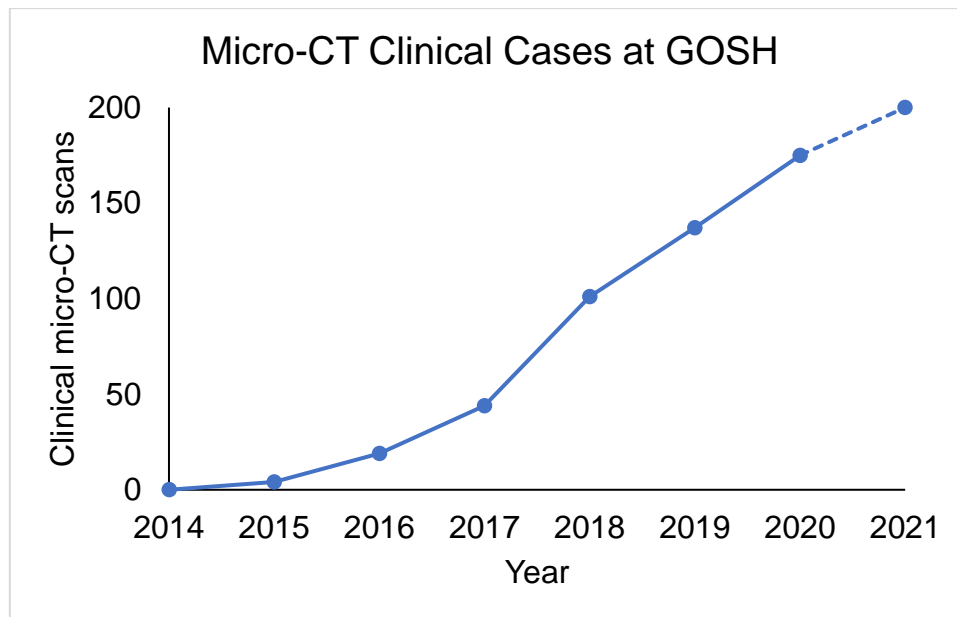
**Aim 5:** To qualitatively explore parental opinion of micro-CT following miscarriage, particularly around acceptability, the main benefits, and concerns.

Preliminary parental perceptions of Micro CT following miscarriage were positive, (Chapter 8).

## **9.2 How has this technique changed local clinical practice?**

At the start of this doctoral study in 2018 the proof of principle of using micro-CT for human fetal post-mortem imaging had been demonstrated [74, 121, 122, 125]. Over the past three years the technique has been optimised into a clinical protocol, and was introduced into clinical service at Great Ormond Street Hospital for Children (GOSH) for fetal autopsy [90].

As referring hospitals became aware of the technique, partly through consenting into the studies presented here, the number of clinical referrals has increased year on year, with a predicted 200 clinical cases in this calendar year, (Figure 9.1).



**Figure 9.1 Clinical micro-CT referrals for human fetal post-mortem imaging have increased throughout the course of this thesis, with projected numbers for 2021**

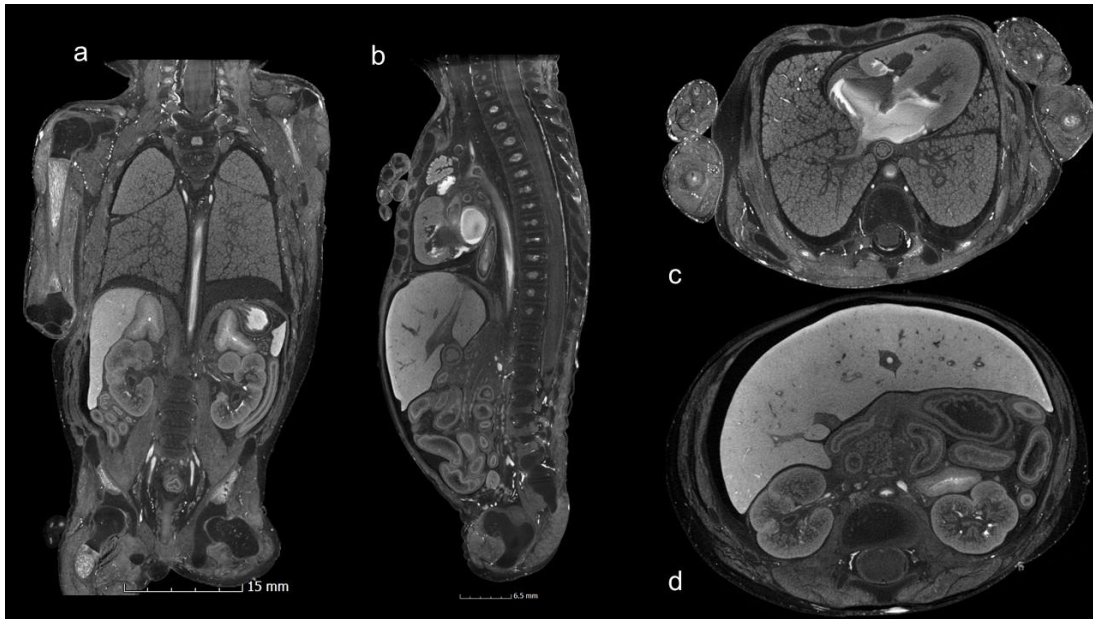
This increased uptake of a non-invasive imaging test demonstrates parental acceptability and the unmet clinical need, validating the need for this test and thesis. We have received no complaints from parents following the introduction of this technique, and importantly no negative feedback regarding discoloration following iodine.

### **9.3 Limitations of this thesis**

Several limitations of this thesis have been identified, aside from those specifically identified in each chapter.

#### **9.3.1 Other imaging techniques and contrast agents**

Throughout this thesis, immersion in a solution of I<sub>2</sub>KI was used to provide soft tissue contrast, (Figure 9.2), after being identified in the literature review, (chapter 2), as the most suitable contrast agent. Other contrast agents are available including OT and PTA but were not tested.



**Figure 9.2** High resolution images depicting the torso in coronal plane (a) and sagittal plane (b), and axial images of the chest (c) and abdomen (d) of a 16-week gestation fetus weighing 90 g

PCI is also being developed as an alternative to employing exogenous contrast agents to demonstrate soft tissue details non-invasively. Although this has been proven in enabling assessment of intra-operative tissue margins in the excision of breast tumours [103], further advances in this technology may prove this to be a suitable technique in the future.

Optimisation in fetal immobilisation would also be required, although the lack of contrast agent would minimise tissue distortion. Once iodinated, fetal tissue stiffens, providing resistance to compression when immobilising the fetus. Without this iodination and accompanying rigidity, movement artefacts could be caused, thereby reducing diagnostic capability.

Other methods of increasing the speed of contrast administration were also not investigated in detail. It is possible that iodination in a pressurised chamber, or with an agitator at the bottom, could speed up the iodination time. Inherently the clinical

protocol that has been developed is one that could be carried out in any hospital with access to a micro-CT scanner without other specialist preparation equipment.

### **9.3.2 Qualitative assessment of parental views following post-mortem imaging techniques**

Although the results of chapter 8 demonstrated an overwhelmingly positive attitude towards micro-CT and its use in identifying the causes of early pregnancy loss, the studies participants had not been offered micro-CT and had no direct personal experience of the technique.

When recruiting for this study the Miscarriage Association's social media account and email contacts were used to contact participants to take part in the focus groups. Due to the small number (<300) of parents who had undergone micro-CT at our centre (GOSH), and the large number of miscarriages estimated to occur each year in the UK (>180,000) [178], it is unsurprising that the small number of participants had any experience of this technique.

The general themes identified during this thematic analysis were aligned with other less- or non-invasive post-mortem imaging techniques [1, 8, 16, 37, 38, 162] demonstrating a need for the expansion of these options for parents. Therefore, whilst this does not detract from the overwhelmingly positive response to the micro-CT technique from its participants it does indicate further work by listening to parents' voices who have direct experience of a clinical micro-CT service.

### **9.3.3 Diagnostic accuracy studies**

A diagnostic accuracy study for micro-CT did not form part of this thesis, but has been reported elsewhere, led by the GOSH post-mortem imaging group [160].

There were several difficulties in a direct comparison of conventional invasive and micro-CT non-invasive techniques and their diagnostic accuracy.

Firstly, it was considered unethical to withhold the choice of micro-CT from parents who had declined conventional autopsy, which resulted in larger numbers choosing

micro-CT. Secondly, a conventional autopsy was not performed if the pathologist considered there would be no added benefit. Therefore, in the diagnostic accuracy study of 268 cases reported elsewhere [160], whilst 221/268 (82.5%) parents consented to both micro-CT and invasive autopsy, only 29/221 (13.1%) proceeded to autopsy under the pathologist's direction. The pathologist thought that there would be no added value from further invasive investigation, inherently validating the choice and availability of micro-CT for early pregnancy loss.

47/268 (17.5%) parents chose only external examination of the fetus and micro-CT and refused more invasive techniques. If micro-CT had not been available, these parents are likely to have declined all other available autopsy choices. Of those cases who underwent micro-CT alone, 25% showed fetal structural abnormalities, and confirmation of the antenatal ultrasound imaging findings in >80%, with additional anomalies also demonstrated through micro-CT [160].

Therefore, a true diagnostic accuracy study was not possible, as parents were unwilling to consent to the definitive autopsy test, but parental uptake does demonstrate a need for the use of micro-CT in this cohort.

#### **9.4 Future clinical integration**

Education and training are important factor in developing such a service [168, 179, 180], and post-mortem imaging has now developed to be a speciality within radiology over the past decade.

The micro-CT protocol [90] developed throughout this thesis could be taught to a relatively wide range of professional medical backgrounds within 1-2 months of suitable training, with similar associated running costs to a medical CT scanner [75, 160].

Although availability and access to specialist centres may be a practical barrier in the short term [58, 64, 75, 90, 126, 160, 174-176], along with awareness of the technique and its benefits within the medical community [44, 58, 64, 75, 90, 126, 160, 174, 175],



dissemination is continuing to raise awareness of the technique among the medical community.

It is equally important to raise awareness through increased public engagement. Due to the sensitive nature of the topic, it is essential to ensure that the information is delivered in a sensitive and caring manner appropriate to parents at this most traumatic of times. Therefore, engagement with multiple pregnancy loss charities within the UK, (Miscarriage Association and SANDS) has continued both before and throughout this thesis in ensuring the language used in consent forms, questionnaires and plain English statements is appropriate and accessible. This ensures that parents are made aware of the benefits and challenges of all the techniques available.

By demonstrating that micro-CT provides a suitable alternative to the invasive autopsy procedure among pathologists [160], its uptake into other centres could reduce the invasive technique workload within the early pregnancy loss cohort, whilst simultaneously providing parents with greater choice to investigate their loss.

## **9.5 Future research direction**

### **9.5.1 Evaluation of the additional diagnostic yield of micro-CT following miscarriage**

Micro-CT has been shown to provide sufficient confidence in the autopsy results for pathologists to decline further invasive investigation, despite consent from the parents [160].

In an initial diagnostic accuracy trial of micro-CT vs antenatal ultrasound, a high concordance was reported in 219/266 (82%) [160]. However, this study only analysed overall agreement (normal / abnormal), not detailed analysis by organ or specific abnormality. There is clearly a need for a detailed comparative evaluation between these techniques to identify what the value of micro-CT in this setting.

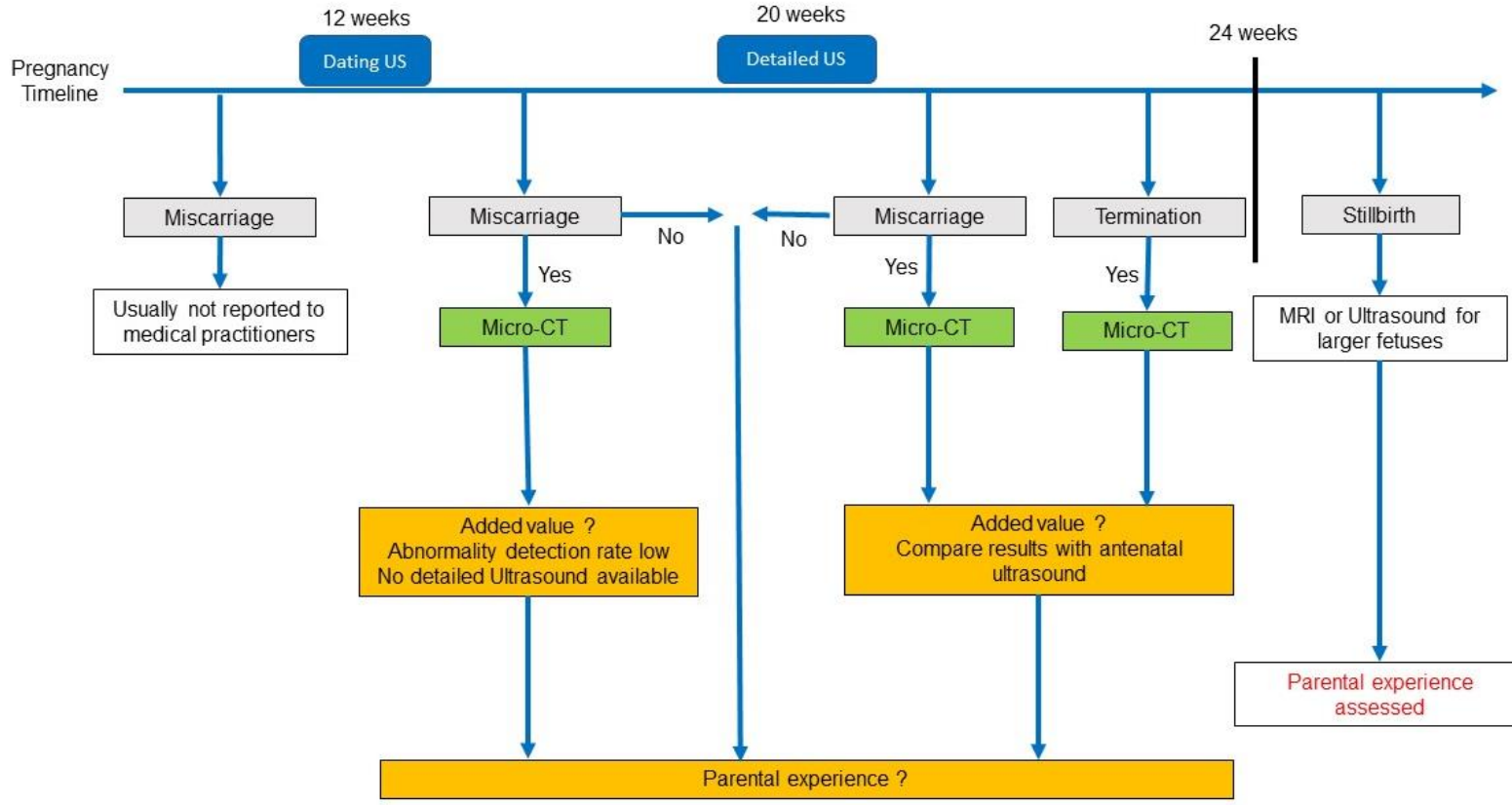
An ultrasound scan is usually performed at 12 weeks of pregnancy to confirm the pregnancy and provide a dating estimation, commonly called the dating scan. In the

UK, this is usually followed by a further ultrasound scan at 20 weeks to identify any abnormalities commonly called the anomaly scan (Figure 9.3).

Unfortunately, many miscarriages occur before the 20-week scan, and any post-mortem investigation could provide added value in determining the cause of death. As micro-CT is the only current imaging examination that can provide suitably high-resolution imaging in a manner acceptable to a larger number of parents, this may be the group most helped by micro-CT despite a true comparative study not being available [2, 44, 90, 126, 160, 162, 176].

Miscarriages that occur after the anomaly ultrasound scan at 20 weeks could be compared directly with the antenatal ultrasound in a direct comparison, to evaluate its potential value in this setting. In the setting of terminations of pregnancy following the anomaly scan, the diagnostic yield of micro-CT above and beyond antenatal ultrasound should be determined.

A single large study could be performed to capture all these events, to evaluate the true diagnostic yield of this new technique as well as acceptability in certain circumstances, (Figure 9.3).



**Figure 9.3** Flow diagram to identify the added diagnostic yield and value at differing stages of pregnancy loss as well as assessment of the parental experience

### **9.5.2 Ongoing public, patient involvement and experience**

The focus groups in Chapter 9 demonstrated the overwhelmingly positive opinion of micro-CT, with several patient-centric and societal benefits being raised by the participants.

They gave useful guidance on how to conduct trials of parental experience in future. As the main limitation of that study was that none of the participants had experience of clinical micro-CT, the next logical step is to evaluate the experience of parents who have this experience, either consenting to micro-CT or declining it as part of their care, and their subsequent positive and negative experiences of the service.

Feedback was identified in how parents would like trials, regarding patient experience, to be completed which will be invaluable in identifying the most suitable methodology, the questions to ask and the approach to take in this sensitive subject and at an extremely traumatic time in the parent's life.

This work will inform future provision of a micro-CT service and ensure the most appropriate method of service delivery is utilised, whilst also providing further evidence for the investment in this technology within other clinical specialist centres.

### **9.5.3 Ongoing engagement through pregnancy loss charities**

It is essential that healthcare research has patients and their voices at its centre. Whilst pregnancy loss is challenging, it is essential that knowledge surrounding these events are developed. Autopsy is proven to provide the highest diagnostic yield, yet the argument for less- or non-invasive techniques has been made. There is a wide array of options for parents to choose between when determining how they wish to investigate their loss and it is important that they are fully informed to be able to make the most appropriate personal choice.

Therefore, the information must be delivered in a format that is acceptable to parents at this time from a variety of backgrounds and religions. Charities are at the forefront of this work (e.g., Miscarriage Association, SANDS) and excel at being the first point of contact for information in a format that is acceptable and accessible to most parents.

They remain central to the future development of this micro-CT technique; the ability to contact large diverse groups of patients is invaluable as a researcher.

## **9.6 Conclusion**

The work presented in this thesis has made a significant contribution to the lives of parents who consented to micro-CT as part of a fetal autopsy investigation, where otherwise they may have been underserved or declined all other available autopsy choices. It has grown into an active clinical service and there is now sufficient experience to be able to take this work forwards in terms of accuracy, yield, and direct parental experience.

# 10, Appendix 1 Nature Protocols paper

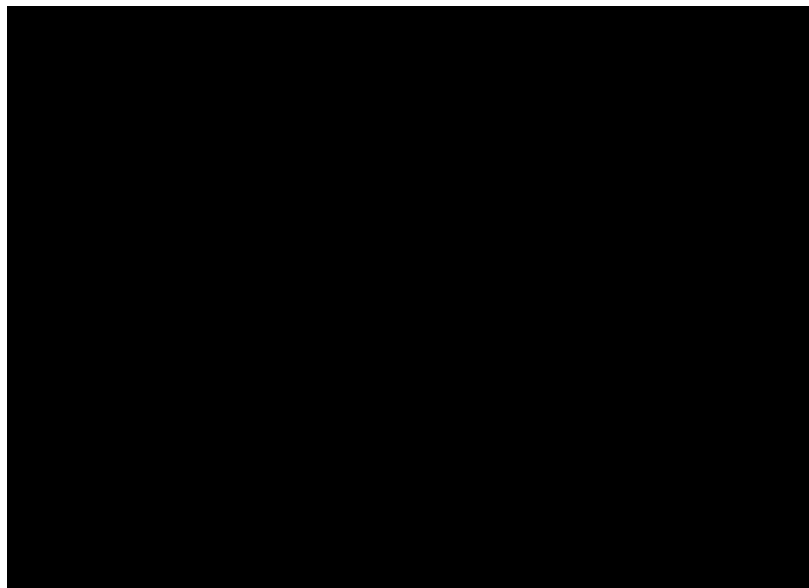


## Human fetal whole-body postmortem microfocus computed tomographic imaging

Ian C. Simcock<sup>1,2,3</sup>, Susan C. Shelmerdine<sup>1,2,3</sup>, J. Ciaran Hutchinson<sup>2,3,4</sup>, Neil J. Sebire<sup>2,3,4</sup> and Owen J. Arthurs<sup>1,2,3</sup>✉

Perinatal autopsy is the standard method for investigating fetal death; however, it requires dissection of the fetus. Human fetal microfocus computed tomography (micro-CT) provides a generally more acceptable and less invasive imaging alternative for bereaved parents to determine the cause of early pregnancy loss compared with conventional autopsy techniques. In this protocol, we describe the four main stages required to image fetuses using micro-CT. Preparation of the fetus includes staining with the contrast agent potassium triiodide and takes 3–19 d, depending on the size of the fetus and the time taken to obtain consent for the procedure. Setup for imaging requires appropriate positioning of the fetus and takes 1 h. The actual imaging takes, on average, 2 h 40 min and involves initial test scans followed by high-definition diagnostic scans. Postimaging, 3 d are required to postprocess the fetus, including removal of the stain, and also to undertake artifact recognition and data transfer. This procedure produces high-resolution isotropic datasets, allowing for radio-pathological interpretations to be made and long-term digital archiving for re-review and data sharing, where required. The protocol can be undertaken following appropriate training, which includes both the use of micro-CT techniques and handling of postmortem tissue.

### Introduction



<sup>1</sup>Department of Clinical Radiology, Great Ormond Street Hospital for Children, London, UK. <sup>2</sup>UCL Great Ormond Street Institute of Child Health, Great Ormond Street Hospital for Children, London, UK. <sup>3</sup>NIHR Great Ormond Street Hospital Biomedical Research Centre, London, UK. <sup>4</sup>Department of Histopathology, Great Ormond Street Hospital for Children, London, UK. ✉e-mail: [Owen.Arthurs@gosh.nhs.uk](mailto:Owen.Arthurs@gosh.nhs.uk)

# 11, Appendix 2 Ethics



## Health Research Authority

London - Camberwell St Giles Research Ethics Committee

Level 3, Block B  
Whitefriars  
Lewins Mead  
Bristol  
BS1 2NT

**Please note: This is the favourable opinion of the REC only and does not allow the amendment to be implemented at NHS sites in England until the outcome of the HRA assessment has been confirmed.**

19 February 2017

Dr Owen John Arthurs  
NIHR Clinician Scientist and Consultant Paediatric Radiologist  
Great Ormond Street Hospital NHS Foundation Trust for Children  
Department of Radiology  
Great Ormond Street Hospital  
Great Ormond Street  
WC1N 3JH

Dear Dr Arthurs

<b>Study title:</b>	Optimisation of paediatric and perinatal post mortem imaging protocols
<b>REC reference:</b>	13/LO/1494
<b>Protocol number:</b>	12RP07
<b>Amendment number:</b>	Amendment #1, 16/09/2016
<b>Amendment date:</b>	24 January 2017
<b>IRAS project ID:</b>	131395

The above amendment was reviewed on 10 February 2017 by the Sub-Committee in correspondence.

### Ethical opinion

The members of the Committee taking part in the review gave a favourable ethical opinion of the amendment on the basis described in the notice of amendment form and supporting documentation.

### Approved documents

The documents reviewed and approved at the meeting were:

<i>Document</i>	<i>Version</i>	<i>Date</i>
Covering letter on headed paper [Rationale for Substantial Amendment]		19 January 2017
Notice of Substantial Amendment (non-CTIMP) [AmendmentForm_ReadyForSubmission]		24 January 2017
Participant consent form [GOSH Consent Form]	3	16 January 2017
Participant consent form [PMI single A4 consent form]	3	23 January 2017
Participant information sheet (PIS) [2016 MIA and Imaging Leaflet review]	3	23 January 2017

### Membership of the Committee

The members of the Committee who took part in the review are listed on the attached sheet.

### Working with NHS Care Organisations

Sponsors should ensure that they notify the R&D office for the relevant NHS care organisation of this amendment in line with the terms detailed in the categorisation email issued by the lead nation for the study.

### Statement of compliance

The Committee is constituted in accordance with the Governance Arrangements for Research Ethics Committees and complies fully with the Standard Operating Procedures for Research Ethics Committees in the UK.

We are pleased to welcome researchers and R & D staff at our Research Ethics Committee members' training days – see details at <http://www.hra.nhs.uk/hra-training/>

<b>13/LO/1494:</b>	<b>Please quote this number on all correspondence</b>
--------------------	---

Yours sincerely



**Mr John Richardson**  
Chair

E-mail: [nrescommittee.london-camberwellstgiles@nhs.net](mailto:nrescommittee.london-camberwellstgiles@nhs.net)

*Enclosures:* *List of names and professions of members who took part in the review*

*Copy to:* *Mrs Thomas Lewis, Division of Reserach and Innovation, UCL ICH*  
*Ms Emma Pendleton*



London - Camberwell St Giles Research Ethics Committee

Attendance at Sub-Committee of the REC meeting on 10 February 2017

Committee Members:

<i>Name</i>	<i>Profession</i>	<i>Present</i>	<i>Notes</i>
Dr Ana Bajo	Research Psychologist	Yes	
Mr John Richardson	Retired Director of COREC: former Ecumenical Officer for Churches Together in South London	Yes	

Also in attendance:

<i>Name</i>	<i>Position (or reason for attending)</i>
Mr Alex Martin	REC Assistant

## 12, Appendix 3 Post-mortem Examination Consent Form

Your wishes about the post-mortem examination of your baby/child

*All sections MUST be completed to prevent delay.*

*The examination of your baby/child will take place at*

*Great Ormond Street Hospital NHS Foundation Trust.*

*London WC1N 3JH*

*0207 829 7906.*

<b>Mother</b>	<b>Baby/Child</b>
<b>Last name</b>	<b>Last name</b>
<b>First name(s)</b>	<b>First name(s)</b>
<b>Address</b>	<b>Date of birth</b>
	<b>Date of death (if liveborn)</b>
<b>Hospital no.</b>	<b>Hospital no.</b>
<b>NHS no.</b>	<b>NHS no.</b>
<b>Date of birth</b>	<b>Gender (if known)</b>
<b>Consultant</b>	<b>Consultant</b>
<b>Father/Partner</b>	<b>Address</b> (if different from the mother's)
<b>Last name</b>	
<b>First name(s)</b>	
<b>Preferred parent to contact, tel. no.:</b>	
<b>Religion:.....</b>	
<b>Other notes: language, interpreter .....</b>	

**How to fill in this form:**

- Please show what you agree to by writing **YES** in the relevant boxes.  
Write **NO** where you do not agree.
- Record any variations, exceptions, and special concerns in the Notes to the relevant section or in Section 5.
- Sign and date the form. The person taking consent will also sign and date it.

**Changing your mind**

After you sign this form, there is a short time (*Up to 48 Hours*) in which you can change your mind about anything you have agreed to. If you want to change your mind you must contact:

**[Name]** ..... **[tel.]** .....

**before [time]..... on [day] ..... [date] .....**

**Please be assured that your baby/child will always be treated with care and respect. Any investigations listed below are only undertaken according to your specific wishes.**

**Section 1: Your decisions about a post-mortem examination** *Select one of these four options.*

***The extent of examination that is carried out is up to you according to the options below. Each option describes all the tests that will take place. However, for some patients, if it is felt that a more limited examination can adequately answer the questions raised, the examination may not include some of the components. This depends on the specific features and history for each patient and is therefore at the discretion of the Consultant Pathologist responsible. However, we will NEVER perform more extensive investigations than you have agreed to.***

**A complete / full post-mortem.** This is the standard approach and may provide the most information in some cases. It includes an external examination, then via two or more incisions, examining all the internal organs, examining small samples of tissue under a microscope, a range of imaging techniques as appropriate (E.g., X-rays, CT, Micro CT, MRI, ultrasound) and medical photographs. Tests may also be done for infection and other problems. The placenta where relevant will also be examined.

**I/We agree to a complete / full post-mortem examination.**

**with Micro CT examination** (This involves using a contrast solution which may cause discolouration)

OR

**A minimally invasive post-mortem examination.** This includes an external examination, a range of imaging techniques as appropriate (E.g., X-rays, CT, Micro CT, MRI, ultrasound), medical photographs and examination of the internal organs of the body that you agree to, usually via a “key-hole surgery” approach. This will only involve a small incision for the endoscope; no large incisions will be made. The placenta will also be examined. In some cases, it may be possible to take small tissue biopsies under imaging guidance alone to answer certain specific questions.

**I/We agree to a minimally invasive post-mortem examination.**

**with Micro CT examination** (This involves using a contrast solution which may cause discolouration)

OR

**A limited post-mortem.** This may give less information than a complete/full or minimally invasive post-mortem examination but depending on the circumstances can often adequately answer specific questions. A limited post-mortem includes an external examination, examining the internal organs in the area(s) of the body that you agree to, examining small samples of tissue under a microscope, and imaging and medical photographs. Tests may also be done for infection and other problems and the placenta will also be examined where relevant.

I/We agree to a limited post-mortem examination.

Please indicate what can be examined:                      head                      chest      and  
neck

abdomen

placenta Only

other

.....

**OR**

**An external / imaging post-mortem.** This may give less information than a complete/full or minimally invasive post-mortem examination but depending on the circumstances can often adequately answer specific questions. An external post-mortem includes an examination of the outside of your baby/child's body plus a range of imaging techniques as appropriate (E.g., X-rays, CT, Micro CT, MRI, ultrasound) and medical photographs but no incisions will be made, or biopsies taken. The placenta will also be examined.

I/We agree to an external post-mortem examination with / without MRI

**With Micro-CT examination** (This involves using a contrast solution which may cause discolouration)

---

***Whatever type of post-mortem examination you have chosen above, you can also choose to agree to additional imaging tests, over and above those required for the PM report, to help teaching and research that may improve post-mortem examinations in the future:***

*There is a separate information sheet which will give you more information about this.*

**I/We agree to additional imaging tests for use in teaching, quality control and research (E.g., X-rays, CT, Micro CT, MRI, ultrasound).**

**Section 2: Tissue samples**

With your agreement, the tissue samples taken for examination under a microscope will be kept as part of the medical record (in small wax blocks and on glass slides). This is so that they can be re-examined to try to find out more if new tests or new information become available. This could be especially useful if you would like further tests in the future.

**I/We agree to the tissue samples being kept as part of the medical record for possible re-examination.** *If consent is not given, you must note below what should be done with the tissue samples. See page 8 Item 7 for more information.*

**Dispose of all tissue samples respectfully**

**Return to Hospital for a later burial / cremation / collection**

**Notes to Sections 1 and 2 if required .....**

**Section 3: Keeping tissue samples for training professionals and for research**

*Section 3 covers additional separate consent that you may decide to give. It will not affect what you have already agreed to above, what is done during the post-mortem, or the information you get about your baby’s condition, but it may be helpful for others in the future.*

With your agreement, the tissue samples may also be examined for quality assurance and audit of pathology services to ensure that high standards are maintained.

**I/We agree to the tissue samples being kept and used for quality assurance and audit.**

Tissue samples, medical images and other information from the post-mortem can be important for training health professionals. Identifying details are always removed when items are used for training.

**I/We agree to anonymised tissue samples, images and other relevant information from the post-mortem being kept and used for professional training.**

Tissue samples, medical images and other relevant information from the post-mortem can also be useful in research into different conditions and to try to prevent more deaths in the future. All research must be approved by a Research Ethics Committee.

**I/We agree to tissue samples, images and other relevant information from \_\_\_\_\_ the \_\_\_\_\_ post mortem being kept and used for ethically approved medical research.**

Occasionally extra tissue samples may be useful for research to help other parents and professionals in the future. These small extra samples are taken at the same time as the routine postmortem samples and are not identifiable when used.

**I/We agree to additional tissue samples being taken for teaching, quality control, audit and research.**

#### **Section 4: Genetic testing**

To examine the baby/child's chromosomes or DNA for a possible genetic disorder or condition, the pathologist takes small samples of skin, other tissue and/or samples from the placenta (afterbirth). With your agreement, this material will be kept as part of the medical record so that it can be re-examined to try to find out more if new tests or new information become available. This will be done on a request only basis.

**I/We agree to the genetic material being stored as part of the medical record \_\_\_\_\_ for possible examination. See Section 8 Item 6 for more information.**

**I/We agree to genetic testing of samples of skin, other tissue and/or the placenta.**



*If samples should not be taken from any of these, please note this below. This will mean we will not contact you if the material is requested by a geneticist.*

### **Section 5: Keeping one or more organs for diagnostic purposes**

In most cases, all the organs will be returned to your baby's/child's body after the post-mortem examination. But occasionally the doctors may recommend keeping one or more organs for longer, to carry out further detailed examination to try to find out more about why your baby/child died. This might take some weeks and so could affect the timing of your baby/child's funeral. The person who discusses the post-mortem with you will tell you if it is likely.

**I/We agree to further detailed examination of the organ(s) specified below:**

**Any organ**

**The following organ(s).....**

If you agree to further detailed examination, you also need to decide what should be done with the organs after the examination.

**I/We agree to donate the organ(s) to be used to train health professionals.**

**I/We agree to donate the organ(s) to be used for ethically approved medical research.**

**I/We want the hospital to dispose of the organ(s) respectfully as required by law.**

**I/We want the organ(s) returned to the funeral director we appoint for separate**

**cremation or burial.**

**I/We want to delay the funeral until the organ(s) have been returned to my/our baby's body.**

If you agree to donate one or more organ(s), any residual tissue will be sensitively disposed when they are no longer needed. This will be carried out in accordance with the HTA standards (usually after a minimum of one year).

If you change your mind about this donation at any time in the future, and want to withdraw your consent, please contact the hospital and ask for the mortuary department.

**Notes to Section 5 if required .....**

You can withdraw consent for any of the options in section 3 at any time in the future. To do so, please contact the hospital and ask for the person who has signed the consent takers statement. Alternatively, you can ask for the mortuary manager who can document any changes in your consent.

**Section 6: Consent from person(s) with Parental Responsibility**

I/We have been offered written information about post-mortem examinations.

I/We understand the possible benefits of a post-mortem examination.

My/Our questions about post-mortem examinations have been answered.

**Mother's name (Print):** ..... **Signature** .....

**Other person with Parental Responsibility: name (Print)**.....

**Signature** .....

**Date** ..... **Time** .....

**Section 7: Consent taker's statements** *To be completed and signed at the time of signing.*

I have read the written information offered to the parents/those with Parental Responsibility.

I believe that the parent(s)/those with Parental Responsibility has/have sufficient understanding of a post-mortem and (if applicable) the options for what should be done with tissue and organs to give valid consent.

I have recorded any variations, exceptions and special concerns.

I have checked the form and made sure that there is no missing or conflicting information.

I have explained the time period within which parents can withdraw or change consent, and have entered the necessary information at the beginning of this form.

Name ..... Position/Grade .....

Department..... Contact details (Ext/Bleep).....

Signature..... Date ..... Time .....

**Interpreter's statement (if relevant)**

I have interpreted the information about the post-mortem for the parent(s)/those with Parental Responsibility to the best of my ability and I believe that they understand it.

Name ..... Contact details .....

Signature ..... Date ..... Time .....

**Section 8: Notes for the consent taker**

1. "Responsibility for obtaining consent should not be delegated to untrained or inexperienced staff. Anyone seeking consent for hospital post-mortem examinations, should have relevant experience and a good understanding of the consent procedure. They should have been trained in dealing with bereavement and in the purpose and procedures of post-mortem examinations. Ideally, they should have also witnessed a post-mortem examination." (Human Tissue Authority, Code of Practice B, 2017).
2. Consent must be given by those with Parental Responsibility.
3. Written information about post-mortems should be offered to all Parents/those with Parental Responsibility before you discuss the form with them.
4. If the parents/those with Parental Responsibility have a specific request that you are not sure about, contact the pathologist **before the form is completed.**
5. Make sure that an appropriate time and date are entered in the *Changing your mind* section at the beginning of the form, and the parent(s)/those with Parental Responsibility understand what to do if they change their minds. The post-mortem should not begin unless this section is completed. **It is your responsibility to**

**ensure that, if the parent(s)/ those with Parental Responsibility change their minds, they will be able to contact the person or department entered on this form.** If the parents do not want a copy of the form, they should still be given written information about changing their minds.

6. Write the mother's or the baby/child's hospital number in the box at the foot of each page of the form. For a baby who was born dead at any gestation use the mother's hospital number; for a baby who was born alive use the baby's hospital number.
7. **Sections 2, 3 and 4: Tissue samples and genetic material** If the parents/those with Parental Responsibility do not want tissue samples or genetic material kept as part of the medical record, explain the different options for disposal (below) and note their decisions in the relevant section.  
  
If disposal is requested, it will usually take place a year later. This is to ensure that the family have the opportunity to ask for further testing. Our experience shows that this often happens 6-8months later. The options are disposal by a specialist hospital contractor; Returned to Hospital for a later burial / cremation / collection by chosen funeral director; or release to the parents themselves. They cannot be returned to the body but can accompany in a small box, this option may delay collection of their baby/child.
8. Send the completed form to the relevant pathology department, offer a copy to the parent(s)/those with Parental Responsibility, and put a copy into the mother's (for a stillbirth or miscarriage) or the baby/child's medical record.
9. Record in the clinical notes that a discussion about the post-mortem examination has taken place, the outcome, and any additional important information.
  - **Possible further examination of one or more organs.** If the organ is donated for research, after research sampling is completed, the residual tissue will be sensitively disposed of unless specific instructions from the family are documented. **If you already know that this is recommended,** discuss this, and also explain how it might affect funeral arrangements.
  - **If the pathologist recommends further examination after the post-mortem has begun,** they will contact you or the unit. The parents/those with Parental Responsibility should then be contacted as soon as possible to discuss their wishes and to explain how keeping the organ might affect funeral arrangements.

## 13, Appendix 4 Thesis Common Methods

### Potassium tri-iodide instructions

Iodination of the specimens/fetuses is key to identifying internal soft tissue structures. As indicated within chapter 2, precise measurement of the concentration of this solution was imperative to optimise the iodination and reduce tissue distortion, with higher concentration solutions resulting in increased tissue deformation and shrinkage. Therefore, the following instructions create a 5% I<sub>2</sub>KI solution to which 10% formalin is added, to restrict autolysis of the specimen, in a ratio of 1:1 to create 2.5% I<sub>2</sub>KI solution.

A spillage kit should be available to ensure safe decontamination of the area should a spillage occur.

Personal safety was ensured by the wearing of apron, eye protection and gloves and preparation completed in an adequately ventilated laboratory.

1, 100g of potassium iodide (KI) and 50g Iodine (I<sub>2</sub>) solid is weighed out.

2, 100g of KI is placed into a 1 litre conical flask and 100 ml of distilled water is added along with a magnetic stirrer.

3, The mouth of the conical flask is covered with parafilm to stop any spillage and placed on the electric controller of the magnetic stirrer.

4, The speed of the magnetic stirrer is adjusted as required to dissolve the KI, approximately 5 minutes duration.

5, Once dissolved, the parafilm cover is removed to allow the addition of 50 g of I<sub>2</sub>.

6, The total liquid volume is increased up to 1,000 ml by the addition further distilled water (approximately 750 ml).

7, The vessel is then again placed on the magnetic stirrer and the speed slowly increased and maintained until all the I<sub>2</sub> is dissolved, approximately 10 minutes. Minor sediment may remain at the bottom of the flask.

8, The liquid should then be poured into an opaque 1 litre Duran container and stored in a locked dark cupboard until required.

9, Dilution with 10% (wt/vol) formalin (ratio 1:1) results in a total iodine content of 63.25 mg/mL (iodine mass of  $2.49 \times 10^{-4}$  mol / mL).

Potassium tri-iodide liquid and vapour permanently marks work surfaces and should be stored in a secure container. Sodium thiosulphate (4% w/v) solution can be used to remove any discolouration from work surfaces.

To create differing concentrations as described within this thesis the following amounts of KI and I<sub>2</sub> should be added at steps 2 and 4 of the instructions, Table 13.1. This will create double the required concentration which is then diluted (ratio 1:1) with 10% formalin to arrest further tissue degradation and the appropriate concentration of I<sub>2</sub>KI acquired.

**Table 13.1 amount of KI and I<sub>2</sub> required for differing concentrations of I<sub>2</sub>KI**

I <sub>2</sub> KI concentration / %	KI / g	I <sub>2</sub> / g	Dissolved in water / ml	Diluted with 10% formalin / ml
1.25	50	25	1000	1000
2.5	100	50	1000	1000
3.75	150	75	1000	1000
5.0	200	100	1000	1000

## **13.2 Equipment**

### **13.2.1 Introduction**

Several common techniques utilising specific equipment were employed to scan both ex-vivo animal organs and whole human fetuses throughout this thesis to develop and optimise the clinical methodology and to minimise any artefacts. These methods are described here and explain the standardised methodology used throughout.

These methods are used and described in several publications originating from this thesis [90, 127, 141, 160, 175].

All micro-CT imaging was completed on either a Med-X or 225ST X-TH (Nikon Metrology, Tring, UK) micro-CT scanners, depending on availability between 2018 and 2021. Both scanners have equivalent targets and detectors, except that the 225ST X-TH is able to achieve higher kilovoltages, but no kilovoltages above 130kV, were used during this thesis. Projection images acquired by the scanner were reconstructed using modified Feldkamp filtered back-projection algorithms with proprietary software (CTPro3D; Nikon Metrology, Tring, UK) and post processed using VG Studio Max 3.4 (Volume Graphics GmbH, Heidelberg, Germany).

Due to the difference in shape and size of the animal organs and human fetal specimens a flexible technique to wrap and immobilise these specimens was developed and used throughout this thesis. The materials used are listed below.

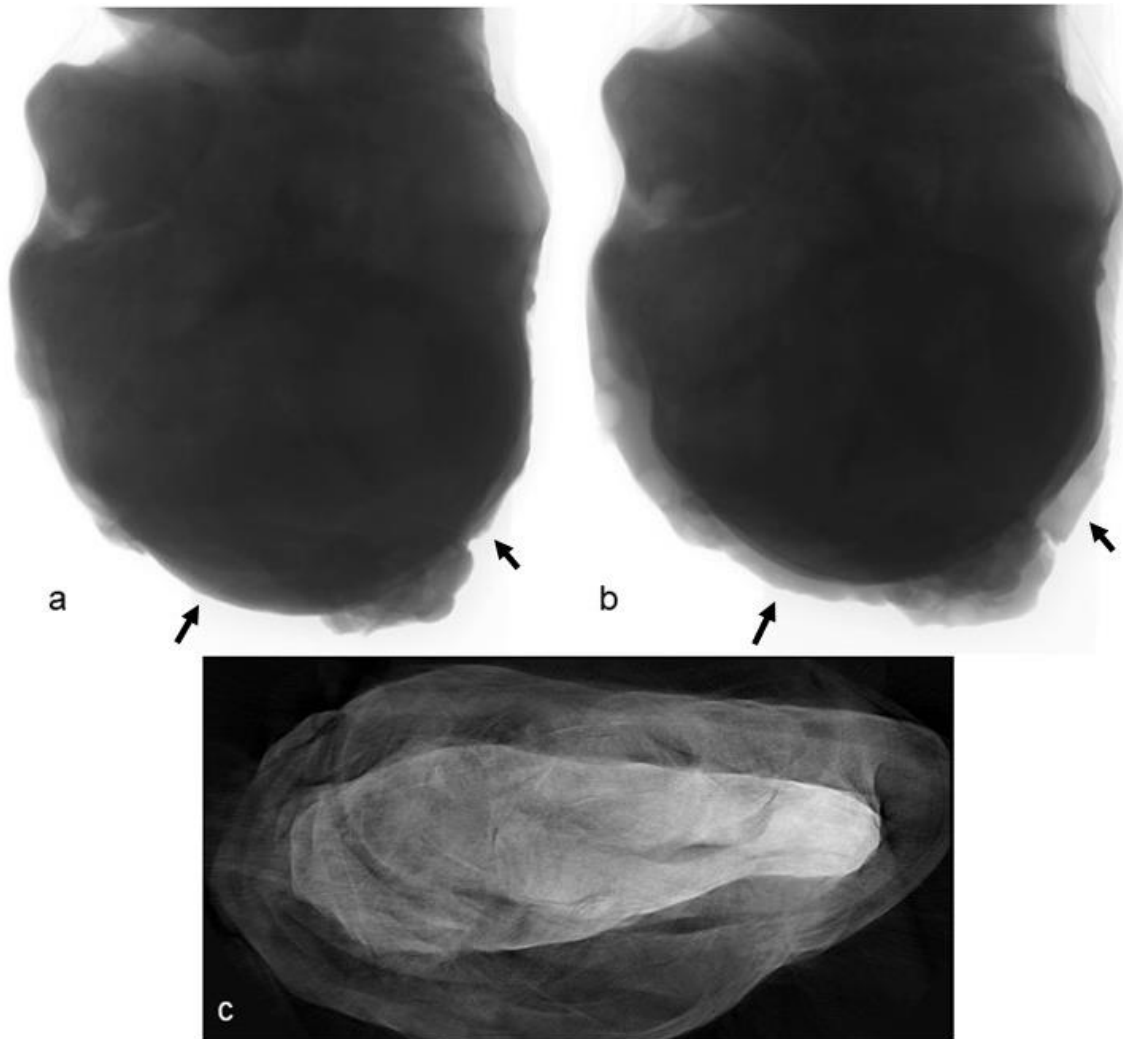
### **13.2.2 Parafilm M**

Parafilm M (Bemis, Oshkosh, WI) is a semi-transparent sealing film composed of waxes and polyolefins that is impermeable to liquids and once stretched, attaches to itself or non-biological substances, but does not bind directly to biological specimens.

It can be stretched in any direction and is sufficiently flexible to encase a wide variety of shapes yet remain intact. This allows wrapping of a specimen in a spiral to fully



encase the tissue and ensure no fluid leaks into the micro-CT scanner itself. This can cause fluid to pool within the wrapping and remain in contact with the tissue. This can affect the ability to reconstruct the image data due to inconsistencies in the tissue outline from the first and last image, (Figure 13.1). Therefore, an absorbent material must be placed within the parafilm wrapping to wick away excess fluid from being in contact with the specimen outline and eliminate this artefact.



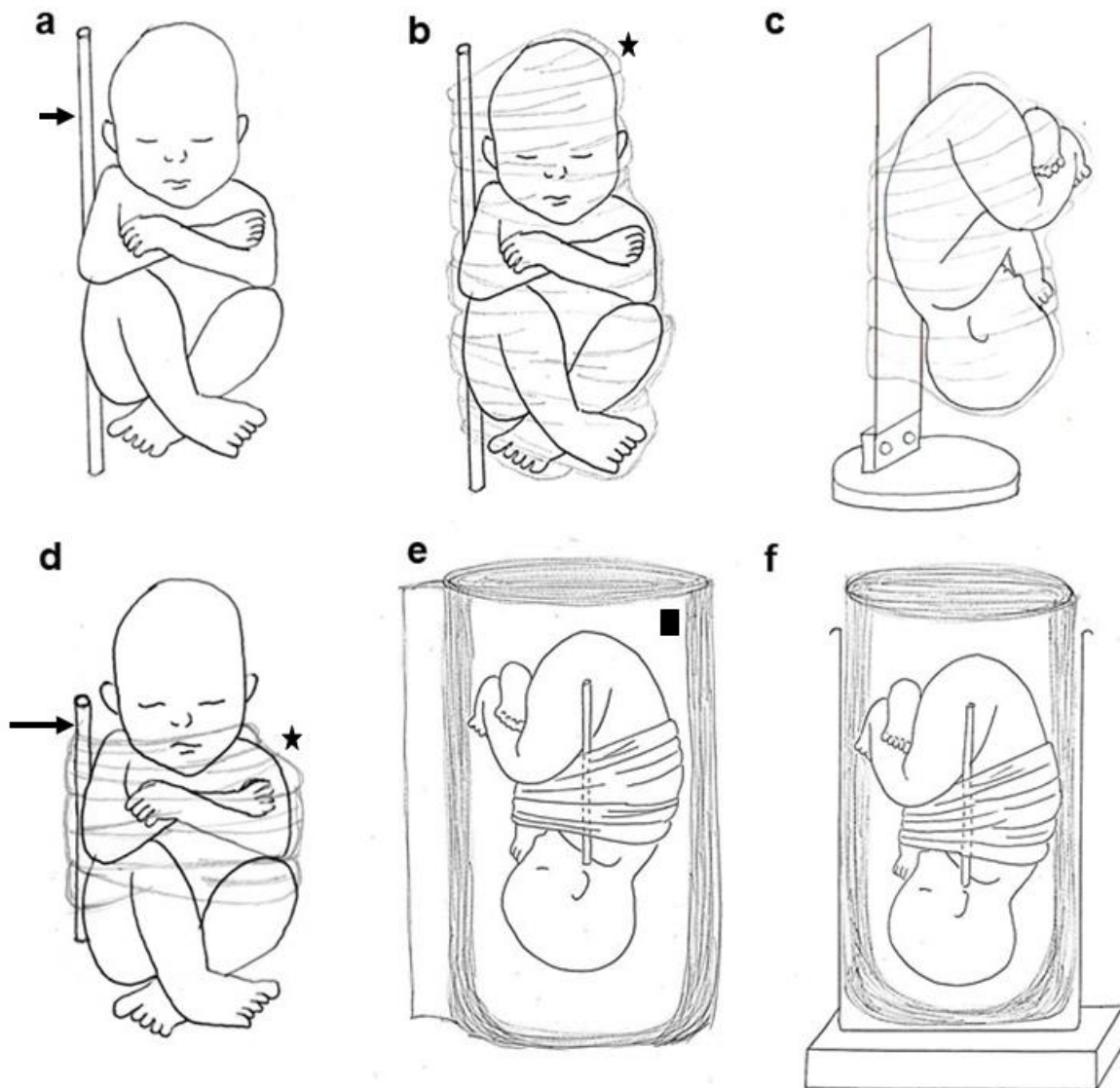
**Figure 13.1** Pooling of excess  $I_2KI$  is shown between the first (a) and last (b) images (indicated by arrows), distorts the tissue outline, affecting image reconstruction (c)

Parafilm M wrapping causes no damage to the specimen itself when removed as it cannot bind to the tissue itself and the ability to place Parafilm M in direct contact with the specimen also allows control over the pressure exerted when wrapping it. This

reduces any possible deformation of the specimen/fetus as it can be precisely controlled.

Parafilm M can also be used to bind and support the specimen upon a carbon fibre plate if sufficiently small, or to be used to immobilise within a container if the specimen is larger. It can be cut to the required length to reduce waste and expense and is semi-transparent, allowing for visualisation of the tissue whilst wrapped, (Figure 13.2).

Parafilm M is also less dense in comparison to iodinated tissue and is therefore not easily visible on the micro-CT images.



**Figure 13.2 Small fetus positioning (a-c). Large fetus positioning (d-f), carbon fibre rod (arrow), parafilm M (star) and absorbent padding (square) [90], with permission**

### 13.2.3 Absorbent padding

These pads are commonly used to soak up small leakages and are more radiolucent in comparison to iodinated tissue such as parafilm. They can be placed around the specimen to assist in immobilisation within a container and reduce excess pressure during wrapping. Although opaque, palpation of anatomical structures can still be completed to assist in the correct alignment of the fetuses limbs, head, and body, (Figure 13.2) with permission.

This padding can also be placed around small specimens to allow excess fluid from the fetus to be wicked away from the tissue itself and ensure accurate image reconstruction.

#### **13.2.4 Carbon fibre rod**

Carbon fibre is less dense, thereby not creating artefacts in comparison to iodinated tissue when placed in the scanning field but is able to be observed following image reconstruction. Carbon fibre rods, length 50 mm and diameter 1 mm were consistently placed on the right-hand side of the fetus alongside the head and torso and secured in place with parafilm. This aids in anatomical orientation following scanning, (Figure 13.2).

#### **13.2.5 Carbon fibre plate**

Carbon fibre plates (length 100 mm, width 20 mm) are attached to a base plate that can be secured in a central position within the micro-CT scanner. These are sufficiently stiff to support small fetuses/specimens being attached to it without slippage or movement occurring, (Figure 13.2). This allows them to be positioned closer to the x-ray source due to minimal excess packing, thus permitting higher resolution imaging.

#### Common positioning methods for all fetuses

Correct immobilisation of the fetus is vital to ensure no movement artefacts during scanning and requires the correct method of immobilisation to provide maximal resolution and eliminate artefacts.

Fetuses <80 mm should be scanned using the small fetus technique, whilst fetuses >80 mm should be scanned using the large fetus technique. If a large fetus (>80 mm) is positioned using the “small fetus” method, movement artefact will be observed through slippage. If a small fetus is positioned using the “large fetus” method, a scan is possible, but will require increased scanning time due to difficulties in accurately positioning them centrally within the x-ray beam.

### **13.3 Fetal size differences**

Regardless of the size of the fetus, the head, body and limbs were gently manipulated to align in the anatomical position for ease of identification following imaging, with the umbilical cord coiled on the abdomen away from the external genitalia to aid in the determination of sex.

#### **13.3.1 Small fetuses**

The carbon fibre plate, body alignment and umbilical cord were positioned as previously indicated and these fetuses were mounted using a 100 mm carbon fibre plate.

A small rectangle of absorbent material was cut to completely wrap the fetus longitudinally with a 1 cm overlap, leaving 2 cm of material clear of the fetus at the top and bottom. This was then wrapped around the fetus and secured in place with a length of parafilm which was wrapped continually around the fetus in a spiral motion until the wrapping was completely secured. The excess material was then folded over the fetus and secured in place with parafilm.

Once wrapped, palpation of the fetus ensured correct alignment of the head, body, and limbs and if required the wrapping was partially removed to allow repositioning.

Flat areas of fetal anatomy were identified and positioned against the carbon fibre plate to reduce anatomical deformation. Inversion of the fetus also ensured the largest anatomical area, the head, was placed inferior, to reduce slippage during scanning. The fetus was positioned sufficiently high on the carbon plate to ensure no anatomy projected over the metal fastenings. Parafilm M was then used to secure the fetus to the carbon fibre plate with care taken to not over tighten this wrapping and cause anatomical distortion, (Figure 13.2).

Finally, the fetus and carbon fibre was positioned centrally in the micro-CT scanner to ensure the most time efficient protocol was completed.

### **13.3.2 Large fetuses**

Fetuses >80 mm in length were too large to be supported by the carbon fibre plate without movement occurring due to slippage, and instead were scanned within a suitably sized container situated on the micro-CT turntable.

As with smaller fetuses they were also wrapped in an absorbent material which was cut longitudinally to allow 3 cm material clear of the head and 10 cm clear of the feet with sufficient material laterally to roll the fetus 2-3 times.

The carbon fibre rod, body alignment and umbilical cord was positioned as previously indicated.

The fetus was then rolled longitudinally in the absorbent material and inserted into the container with the head towards the bottom of the container, and 10 cm of material protruding from the top. This excess was then folded over and tucked back into the container to provide added cushioning and to further immobilise the fetus. This also helped to position the fetus straight within the container, which allowed a more time efficient scanning. Parafilm M was then placed over the top of this excess material and secured in place to ensure no movement occurred during scanning, (Figure 13.2).

The micro-CT turntable was used to position the fetus within the x-ray beam, with a radiolucent padded material used to separate the fetus clear of the turntable.

### **13.4 Stain removal**

The skin of the fetus was stained a darker colour following iodination and it was important to remove this prior to returning to the fetus to the parents to limit any alteration to the fetus. This was achieved by immersing the fetus in sodium thiosulphate solution 4% (wt/vol) at room temperature for several days [58]. This process does not remove the iodine, but instead allows the sodium thiosulphate.

## 14, Appendix 5 Data analysis guide

The following is a step-by-step guide using the two relevant software packages (VGStudio Max 3.4 and Image-J) to replicate the quantitative data analysis described in chapter 7.

### 14.1 VGStudio Max software

After scanning the fetus according to the individual experimentation a VGStudio Max file is created containing the 3D volume. This requires loading into VGStudio Max and exporting as an image stack of tif files following the steps below.

Open VGStudio Max software and load the required dataset.

*“File” – “Import” – “VGI file”.*

*“Next” – “map to” – “16-bit unsigned” – “histogram”.*

This may take several minutes; completion is noted by the “completion bar” in the bottom right-hand corner of the screen.

Once the data has been mapped, the background must be rendered black.

*Right mouse click on the image -“Background” – “black”*

Window the image accordingly using the histogram located on the right-hand side of the screen to ensure the air surrounding the fetus is black and sufficient contrast is visible within the anatomy to visualise anatomical differences.

Next, save the data file as a stack of tif images according to the voxel dimensions and pixel size, this will allow Image-J to analyse the data correctly. The voxel dimensions and pixel size are located by double clicking on the volume tree on the right-hand side of the screen.

*“File” – “export” – “Image stack” and ensure it is a tif stack*

Use the following naming mask to ensure correct analysis by Image-J, Experiment x Fetus number x X-coordinates x Y-coordinates x Z-coordinates x resolution in  $\mu\text{m}$ , (e.g., 130kv\_265\_846x1120x1999x0.08170000)

*“Save” - “No” and “Cancel” to the extra VGStudio Max volumes.*

**Note:** No alterations to the histograms should be completed to ensure the widest range of data is utilised within the analysis.



## 14.2 Image-J software - saving smaller volumes of interest

The whole fetal volume is a large file and whilst only the phantom and liver volumes are required for the SNR and rCNR calculations, the data size can be reduced, and subsequent speed of calculations increased by eliminating excess anatomical areas.

*Open Image-J software.*

A suitable micro-CT data set should be selected with sufficiently high image quality to visualise the liver and phantom clearly, to allow segmentation of these structures. These require loading into Image -J.

*“File” – “Import” – “Image sequence”*

Scroll through the loaded volume and manually note the start and end positions of the liver and phantom. It is necessary to save these volumes separately so the following step should be performed separately for the liver and phantom.

*“Image” – “Stacks” – “Tools” – “Slice Keeper” – and enter start and end as required for each volume with an increment of 1.*

*“File” – “Save as” – “tif stack” – and name either “ks-liver” or “ks-phantom”.*

This step can be completed by running the “keepstacks macro” in Python and for a single patient required approximately 2.5 hours.

### 14.3 Mask creation for segmentation

Creation of a mask for the liver and phantom volumes allows identical volumes to be applied to multiple datasets ensuring a consistent approach to the data analysis. These steps need to be completed separately for the liver and phantom volume.

Load either liver or phantom volume previously saved as a keepstacks into Image-J and adjust the brightness to enable the anatomy to be clearly visualised.

*“File”–“Import”–keep stacks tif volume previously saved.*

*“Image”–“Adjust”–“Brightness”*

Choose the kidney shaped tool to draw around individual slices – and draw around the first slice of liver using the left-hand mouse button to trace the anatomy. This should be completed every 10 slices throughout the volume.

*“Ctrl-T” to save each ROI before advancing 10 slices and repeating*

Select all the ROI throughout the volume and interpolate to fill in the gaps between the 10 slices.

*“Ctrl-A”-“more”-“sort”-“more”-“interpolate”*

Individual ROI slice errors should be identified by and deleted before repeating the above steps to redraw and re-interpolate the new volumes. Then select all ROI and save as a single ROI volume, name as “phantomROI” or “liverROI”.

*“Ctrl-A”–“more”–“Save”*

Select all ROI’s again and ensure that they are combined together.

*“more”–“fill” (if required double click dropper symbol and white at the front).*

Note the values within the ROI volume, there should be a single figure. This must be entered at the next stage to recognise the volume as a single entity. The same value must be entered for both minimum and maximum values and make take a couple of attempts for the software to accept the values.

*“Image”–“Adjust”–“Threshold” and fill in the values that are noted for within the single volume.*

*“Apply”–deselect “calculate threshold for each image”*

These volumes should be saved as either “segmentation-liver” or “segmentation-phantom” as appropriate.

*“File”–“Save as”*

*“Image”–“Type”–“32bit”*

*“Threshold”–“Auto”*

*“Process”- “Math”–“NaN background” and repeat for “Subtract” (255)*

*“Save as”–“segmentation-liver or phantom again.*

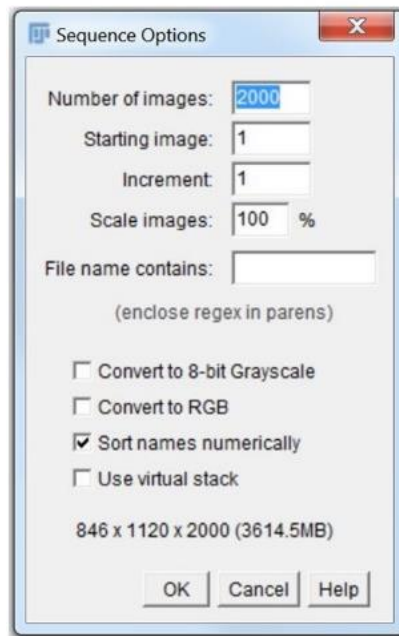
These 2 files must remain within the file for the python coding to access. All other files must be saved within a separate “holding” file during automated processing using the python coding.

## 14.4 Filter application

A filter must then be applied to the saved segmented volumes separately and to separately save the individual volumes for the organ and phantom.

The segmented volumes must first be loaded into Image-J

*Load Image-J – “File” – “Import” – “Image Sequence” – and choose the stack of tif images saved from VG Studio, ensuring the following choices in figure 14.1 are selected.*



**Figure 14.1** Number of images can be used to ensure the correct data file is selected

Next, a filter is applied.

*“Process” – “Filters” – “3D Median” – and select 2 for all factors.*

Following this separate volumes are required to be saved for the organ and phantom. Therefore, the start and end positions of each volume should be identified by viewing the volume in the axial plane.

## 14.5 Image-J – calculation of mean and standard deviation

These steps allow calculation of the mean and standard deviation for both the liver and phantom for each micro-CT acquisition which is used to calculate the corresponding SNR and CNR.

*Load Image-J*

“File”–“Import”–“Image Stacks”– and select segmentation volume

This volume should be changed to 32-bit data,

*“Image” – “Type” – “32-bit”*

The background outside the volume should be made dark and converted to be “Not a Number” (NaN) whilst the liver values must equal one.

“Image”–“Adjust”–“threshold”-choose “dark background” and no other options.

*“Process”–“Math”–“NaN background”–“Yes to all”*

*“Process”–“Math”–“Subtract”–“255”*

To ensure completion of this step, move the cursor over the volume and the background and a zero and a NaN should be observed.

Save these volumes as “segmentation\_liver” or “segmentation\_phantom”

*“File”-“Save as”*

Next it is necessary to add the individual volumes of each experiment to the segmented volumes to calculate the mean and standard deviation values of individual experiments.

*“Process”–“Image Calculator”–select segmented volume”–“add”–“individual experiment”–“create”–“32-bit float result”–“yes to all”*

You can now visualise the image by adjusting the histogram range to 0-255.

*“Image”–“Adjust”–“Brightness and Contrast”–“Set”–“0 and 255”–“OK”*

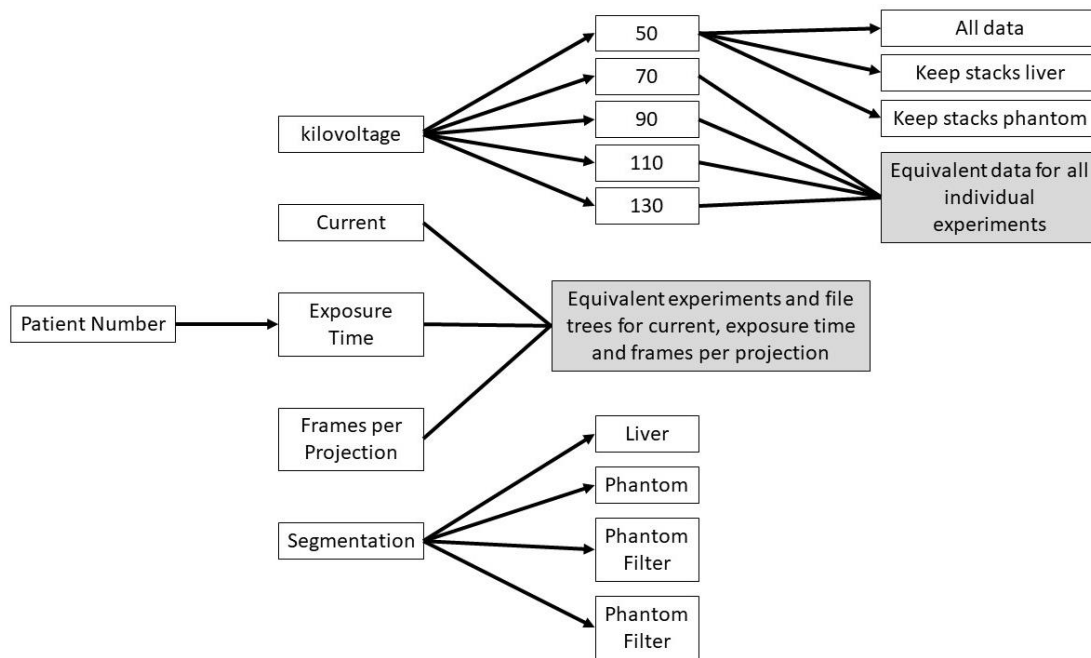
Now you are able to visualise a histogram, with associated values for the selected volume.

*“Ctrl and H” or “Analyse”–“select stack histogram”–“OK”*

Note the mean and standard deviation of the entire volume.

These steps can be automated using the Python coding.

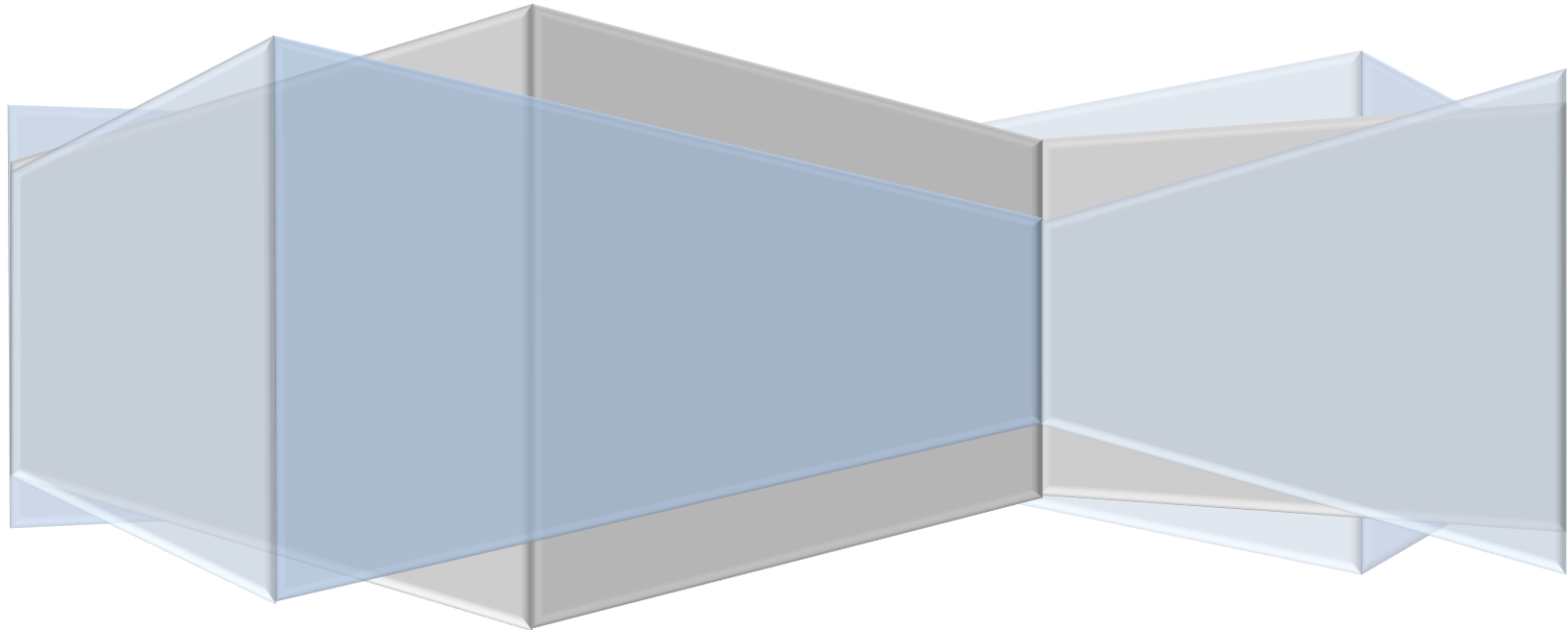
It is essential for the correct automation of the associated Python coding that the data is saved in the correct format and file tree, (Figure 14.2).



**Figure 14.2 Correct labelling and arrangement of the file tree will be automated data processing as demonstrated**

15, Appendix 6 Focus group recruitment

**NIHR** | Great Ormond Street  
Hospital Biomedical  
Research Centre





Following the tragic miscarriage of a baby, as well as coping with their loss, parents want to know why their baby died. Answers may only be provided by investigating what happened by carrying out a post-mortem examination (autopsy) of the baby, to tell whether there is a risk that existing children or future pregnancies will be affected.

Traditional autopsy often involves a large procedure like an operation, in which all parts of the body can be examined in detail, which requires a large incision. This approach is useful in answering these questions in around 30-40% of all cases. However, for a range of reasons, the majority of parents do not currently agree to this investigation being carried out, a main reason being their dislike of a large incision being made on the body.

Recently, our research has shown that by performing detailed imaging tests (including MRI, CT, ultrasound, and x-rays), and carrying out tests that do not require any cuts to the baby (such as blood tests and examining the placenta) we can find out almost the same amount of information, without needing to make an incision. We have also shown that it is possible to take similar samples to a full autopsy using a 'keyhole surgery' approach through a much smaller incision. However, these imaging tests can only provide accurate answers in babies older than 20 weeks gestation.

A new clinical test called Micro-CT has now been developed to provide high detail 3D images of the internal organs on much smaller babies (less than 20 weeks gestation) without any cuts being made. Our studies have shown that it can provide answers in a similar number of cases as conventional autopsy, although it involves temporary skin discoloration.

By taking part in our focus group, we hope you will tell us what you think of this new technique and how it could help parents who suffer from miscarriage in future.

We hope that by working together to develop this project, we will be able to maximise the amount of useful information given to clinicians and parents for each individual family's circumstance. Thank you for attending our focus group on Micro-CT.

## Timetable of Focus Group

Time	Duration	
12.00	30 mins	Arrival: drinks will be provided
12.30	10 mins	Introductions from the focus group team
12.40	10 mins	Short presentation on Micro-CT imaging test
12.50	1 hour 40 mins	Focus group interaction
14.30	30 mins	Drinks and light snacks
15.00		Close of meeting

### Focus Groups to consider:

1. Micro CT – opinions and acceptability
2. Main benefits and barriers
3. How to recruit participants – a sensitive approach
4. Opinions about who could most benefit

## References

1. Hutchinson JC, Shelmerdine SC, Lewis C, Parmenter J, Simcock IC, Ward L, et al. Minimally invasive perinatal and pediatric autopsy with laparoscopically assisted tissue sampling: feasibility and experience of the MinImAL procedure. *Ultrasound Obstet Gynecol.* 2019;54(5):661-9.
2. Shelmerdine SC, Hutchinson C, Lewis C, Simcock IC, Sekar T, Sebire NJ, et al. A pragmatic evidence-based approach to post-mortem perinatal imaging. *Insights in Imaging.* 2021;12(101).
3. Quenby S, Gallos ID, Dhillon-Smith RK, Podesek M, Stephenson MD, Fisher J, et al. Miscarriage matters: the epidemiological, physical, psychological, and economic costs of early pregnancy loss. *The Lancet.* 2021;397(10285):1658-67.
4. Tommy's. Pregnancy loss statistics in UK in 2019 2019 [Available from: <https://www.tommys.org/baby-loss-support/pregnancy-loss-statistics>].
5. Royal College of Obstetricians and Gynaecologists. Miscarriage and ectopic pregnancy 2021 [Available from: <https://www.rcog.org.uk/en/patients/fertility/miscarriage-ectopic/>].
6. MacWilliams K, Hughes J, Aston M, Field S, Moffatt FW. Understanding the Experience of Miscarriage in the Emergency Department. *J Emerg Nurs.* 2016;42(6):504-12.
7. The Lancet. Miscarriage: worldwide reform of care is needed. *The Lancet.* 2021;397(10285).
8. Lewis C, Hill M, Arthurs OJ, Hutchinson C, Chitty LS, Sebire NJ. Factors affecting uptake of postmortem examination in the prenatal, perinatal and paediatric setting. *BJOG.* 2018;125(2):172-81.
9. Brier N. Understanding and managing the emotional reactions to a miscarriage. *Obstetrics and Gynecology.* 1999;93(1):151-5.
10. Blackmore ER, Côté-Arsenault D, Tang W, Glover V, Evans J, Golding J, et al. Previous prenatal loss as a predictor of perinatal depression and anxiety. *British Journal of Psychiatry.* 2018;198(5):373-8.
11. Engelhard IM, van den Hout MA, Arntz A. Posttraumatic stress disorder after pregnancy loss. *General Hospital Psychiatry.* 2001;23:62-6.
12. Lok IH, Yip AS, Lee DT, Sahota D, Chung TK. A 1-year longitudinal study of psychological morbidity after miscarriage. *Fertil Steril.* 2010;93(6):1966-75.
13. Horey D, Flenady V, Conway L, McLeod E, Yee Khong T. Decision influences and aftermath: parents, stillbirth and autopsy. *Health Expect.* 2014;17(4):534-44.
14. Banno C, Sugiura-Ogasawara M, Ebara T, Ide S, Kitaori T, Sato T, et al. Attitude and perceptions toward miscarriage: a survey of a general population in Japan. *J Hum Genet.* 2020;65(2):155-64.
15. Bardos J, Hercz D, Friedenthal J, Missmer SA, Williams Z. A national survey on public perceptions of miscarriage. *Obstet Gynecol.* 2015;125(6):1313-20.
16. Lewis C, Riddington M, Hill M, Arthurs O, Hutchinson J, Chitty L, et al. Availability of less invasive prenatal, perinatal and paediatric autopsy will improve uptake rates: a mixed -methods study with bereaved parents. *BJOG.* 2019;126(6):754.
17. Gold KJ. Navigating care after a baby dies: a systematic review of parent experiences with health providers. *J Perinatol.* 2007;27(4):230-7.

18. Samuelsson M, Radestad I, Segesten K. A Waste of Life. Fathers' Experience of Losing a Child Before Birth. *Birth Defects Res C Embryo Today*. 2001;Jun(2):124-30.
19. Osborn M, Cox PG, Hargitai B, Marton T. Royal College of Pathologists. Guidelines on autopsy practice Neonatal death Royal College Path. 2019.
20. Michalski ST, Porter J, Pauli RM. Costs and consequences of comprehensive stillbirth assessment. *Am J Obstet Gynecol*. 2002;186(5):1027-34.
21. MBRRACE-UK Intrapartum Confidential Enquiry Report - Term, singleton, intrapartum stillbirth and intrapartum-related neonatal death. 2017.
22. Osborn M, Lowe J, Cox PG, Hargitai B, Marton T. Guidelines on autopsy practice. Fetal autopsy 2nd trimester fetal loss and termination of pregnancy for congenital anomaly. 2017.
23. Gordijn SJ, Erwich JJ, Khong TY. Value of the perinatal autopsy: critique. *Pediatr Dev Pathol*. 2002;5(5):480-8.
24. Opsjon BE, Vogt C. Explaining Fetal Death--What Are the Contributions of Fetal Autopsy and Placenta Examination? *Pediatr Dev Pathol*. 2016;19(1):24-30.
25. Nese N, Bulbul Y. Diagnostic value of perinatal autopsies: analysis of 486 cases. *J Perinat Med*. 2018;46(2):175-81.
26. Nayak SS, Shukla A, Lewis L, Kadavigere R, Mathew M, Adiga PK, et al. Clinical utility of fetal autopsy and its impact on genetic counseling. *Prenat Diagn*. 2015;35(7):685-91.
27. Rodriguez MA, Prats P, Rodriguez I, Cusi V, Comas C. Concordance between prenatal ultrasound and autopsy findings in a tertiary center. *Prenat Diagn*. 2014;34(8):784-9.
28. Hauerberg L, Skibsted L, Graem N, Maroun LL. Correlation between prenatal diagnosis by ultrasound and fetal autopsy findings in second-trimester abortions. *Acta Obstet Gynecol Scand*. 2012;91(3):386-90.
29. Dickinson JE, Prime DK, Charles AK. The role of autopsy following pregnancy termination for fetal abnormality. *Aust N Z J Obstet Gynaecol*. 2007;47(6):445-9.
30. Royal College of Obstetricians and Gynaecologists and Royal College of Pathologists. Fetal and Perinatal Pathology Report of a working party. 2001.
31. Blokker BM, Weustink AC, Wagenveld IM, von der Thusen JH, Pezzato A, Dammers R, et al. Conventional Autopsy versus Minimally Invasive Autopsy with Postmortem MRI, CT, and CT-guided Biopsy: Comparison of Diagnostic Performance. *Radiology*. 2018:180924.
32. Blokker BM, Wagenveld IM, Weustink AC, Oosterhuis JW, Hunink MG. Non-invasive or minimally invasive autopsy compared to conventional autopsy of suspected natural deaths in adults: a systematic review. *Eur Radiol*. 2016;26(4):1159-79.
33. Sieswerda-Hoogendoorn T, van Rijn RR. Current techniques in postmortem imaging with specific attention to paediatric applications. *Pediatr Radiol*. 2010;40(2):141-52; quiz 259.
34. NHS Implementation Sub-Group of the Department of Health Post Mortem Forensic and Disaster Imaging Group. Can Cross-Sectional Imaging as an Adjunct and or Alternative to the Invasive Autopsy be Implemented within the NHS. In: Health Do, editor. 2012.
35. Nijkamp JW, Sebire NJ, Bouman K, Korteweg FJ, Erwich J, Gordijn SJ. Perinatal death investigations: What is current practice? *Semin Fetal Neonatal Med*. 2017;22(3):167-75.

36. Breeze AC, Jessop FA, Whitehead AL, Set PA, Berman L, Hackett GA, et al. Feasibility of percutaneous organ biopsy as part of a minimally invasive perinatal autopsy. *Virchows Arch.* 2008;452(2):201-7.
37. Lewis C, Hutchinson JC, Riddington M, Hill M, Arthurs OJ, Fisher J, et al. Minimally invasive autopsy for fetuses and children based on a combination of post-mortem MRI and endoscopic examination: a feasibility study. *Health Technology Assessment.* 2019;23(46):1-104.
38. Lewis C, Latif Z, Hill M, Riddington M, Lakhanpaul M, Arthurs OJ, et al. "We might get a lot more families who will agree": Muslim and Jewish perspectives on less invasive perinatal and paediatric autopsy. *PLoS One.* 2018;13(8):e0202023.
39. Flach PM, Thali MJ, Germerott T. Times have changed! Forensic radiology--a new challenge for radiology and forensic pathology. *AJR Am J Roentgenol.* 2014;202(4):W325-34.
40. Lawn JE, Cousens S, Zupan J. 4 million neonatal deaths: When? Where? Why? *The Lancet.* 2005;365(9462):891-900.
41. Sonnemans LJP, Vester MEM, Kolsteren EEM, Erwich JJH, Nikkels PGJ, van Rijn RR, et al. Dutch guideline for clinical foetal-neonatal and paediatric post-mortem radiology, including a review of literature. *European Journal of Pediatrics.* 2018;177:791-803.
42. Sandaite I, Lombardi C, Cook AC, Fabietti I, Deprest J, Boito S. Micro-computed tomography of isolated fetal hearts following termination of pregnancy: a feasibility study at 8 - 12 week's gestation. *Prenat Diagn.* 2020.
43. McDowell AR, Shelmerdine SC, Carmichael DW, Arthurs OJ. High resolution isotropic diffusion imaging in post-mortem neonates a feasibility study. *British Journal of Radiology.* 2018;91.
44. Kang X, Carlin A, Cannie M, Sanchez TC, Jani JC. Fetal postmortem imaging: an overview of current techniques and future perspectives. *American Journal of Obstetrics and Gynecology.* 2020.
45. Kamphuis-van Ulzen K, Koopmanschap DH, Marcelis CL, van Vugt JM, Klein WM. When is a post-mortem skeletal survey of the fetus indicated, and when not? *J Matern Fetal Neonatal Med.* 2016;29(6):991-7.
46. Shelmerdine SC, Arthurs OJ, Gilpin I, Norman W, Jones R, Taylor AM, et al. Is traditional perinatal autopsy needed after detailed fetal ultrasound and post-mortem MRI? *Prenat Diagn.* 2019;39(9):818-29.
47. Shelmerdine SC, Sebire NJ, Arthurs OJ. Perinatal post-mortem ultrasound (PMUS): radiological-pathological correlation. *Insights Imaging.* 2019;10(1):81.
48. Di Paolo M, Maiese A, dell'Aquila M, Filomena C, Turco S, Giaconi C, et al. Role of post mortem CT (PMCT) in high energy traumatic deaths. *Clin Ter.* 2020;171(6):e490-e500.
49. Robinson C, Deshpande A, Richards C, Ruddy G, Mason C, Morgan B. Post-mortem computed tomography in adult non suspicious death investigation—evaluation of an NHS based service. *BJR Open.* 2019;26(1).
50. Grabherr S, Egger C, Vilarino R, Campana L, Jotterand M, Dedouit F. Modern post-mortem imaging: an update on recent developments. *Forensic Sci Res.* 2017;2(2):52-64.
51. Klein WM, Bosboom DG, Koopmanschap DH, Nievelstein RA, Nikkels PG, van Rijn RR. Normal pediatric postmortem CT appearances. *Pediatr Radiol.* 2015;45(4):517-26.

52. Addison S, Arthurs OJ, Thayyil S. Post-mortem MRI as an alternative to non-forensic autopsy in fetuses and children: from research into clinical practice. *The British journal of radiology*. 2014;87(1036):20130621.
53. Arthurs OJ, Thayyil S, Olsen OE, Addison S, Wade A, Jones R, et al. Diagnostic accuracy of post-mortem MRI for thoracic abnormalities in fetuses and children. *European Radiology*. 2014;24:2876-84.
54. Arthurs OJ, Taylor AM, Sebire NJ. Indications, advantages and limitations of perinatal postmortem imaging in clinical practice. *Pediatr Radiol*. 2015;45(4):491-500.
55. Morgan B, Adlam D, Robinson C, Pakkal M, Rutty GN. Adult post-mortem imaging in traumatic and cardiorespiratory death and its relation to clinical radiological imaging. *The British journal of radiology*. 2014;87(1036):20130662.
56. Forensic and Disaster Imaging Group. Can Cross-Sectional Imaging as an Adjunct and or Alternative to the Invasive Autopsy be Implemented within the NHS. 2012.
57. Votino C, Cannie M, Segers V, Dobrescu O, Dessy H, Gallo V, et al. Virtual autopsy by computed tomographic angiography of the fetal heart: a feasibility study. *Ultrasound Obstet Gynecol*. 2012;39(6):679-84.
58. Dawood Y, Strijkers GJ, Limpens J, Oostra RJ, de Bakker BS. Novel imaging techniques to study postmortem human fetal anatomy: a systematic review on microfocus-CT and ultra-high-field MRI. *Eur Radiol*. 2019.
59. Arthurs O, Thayyil S, Pauliah SS, Jacques TS, Chong WK, Gunny R, et al. Diagnostic accuracy and limitations of post-mortem MRI for neurological abnormalities in fetuses and children. *Clinical Radiology*. 2015;70:872-80.
60. Arthurs OJ, Thayyil S, Owens CM, Olsen OE, Wade A, Addison S, et al. Diagnostic accuracy of post mortem MRI for abdominal abnormalities in fetuses and children. *European Journal of Radiology*. 2015;84:474-81.
61. Leadbetter KZ, Vesoulis ZA, White FV, Schmidt RE, Khanna G, Shimony JS, et al. The role of post-mortem MRI in the neonatal intensive care unit. *J Perinatol*. 2017;37(1):98-103.
62. Norman W, Jawad N, Jones R, Taylor AM, Arthurs OJ. Perinatal and paediatric post-mortem magnetic resonance imaging (PMMR): sequences and technique. *The British journal of radiology*. 2016;89(1062).
63. Thayyil S, Sebire NJ, Chitty LS, Wade A, Chong WK, Olsen O, et al. Post-mortem MRI versus conventional autopsy in fetuses and children: a prospective validation study. *The Lancet*. 2013;382(9888):223-33.
64. Shelmerdine SC, Hutchinson JC, Arthurs OJ, Sebire NJ. Latest developments in post-mortem foetal imaging. *Prenat Diagn*. 2020;40(1):28-37.
65. Lombardi S, Scola E, Ippolito D, Zambelli V, Botta G, Cuttin S, et al. Micro-computed tomography: a new diagnostic tool in postmortem assessment of brain anatomy in small fetuses. *Neuroradiology*. 2019;61(7):737-46.
66. Jawad N, Sebire NJ, Wade A, Taylor AM, Chitty LS, Arthurs OJ. Body weight lower limits of fetal postmortem MRI at 1.5 T. *Ultrasound Obstet Gynecol*. 2016;48(1):92-7.
67. Arthurs OJ, Hutchinson JC, Sebire NJ. Current issues in postmortem imaging of perinatal and forensic childhood deaths. *Forensic Sci Med Pathol*. 2017;13(1):58-66.
68. Kang X, Cannie MM, Arthurs OJ, Segers V, Fourneau C, Bevilacqua E, et al. Post-mortem whole-body magnetic resonance imaging of human fetuses: a

- comparison of 3-T vs. 1.5-T MR imaging with classical autopsy. *Eur Radiol.* 2017;27(8):3542-53.
69. Thayyil S, Cleary JO, Sebire NJ, Scott RJ, Chong K, Gunny R, et al. Post-mortem examination of human fetuses: a comparison of whole-body high-field MRI at 9.4 T with conventional MRI and invasive autopsy. *The Lancet.* 2009;374(9688):467-75.
70. Handschuh S, Beisser CJ, Ruthensteiner B, Metscher BD. Microscopic dual-energy CT (microDECT): a flexible tool for multichannel ex vivo 3D imaging of biological specimens. *J Microsc.* 2017;267(1):3-26.
71. Shelmerdine SC, Langan D, Mandalia U, Sebire NJ, Arthurs OJ. Maceration determines diagnostic yield of fetal and neonatal whole body post-mortem ultrasound. *Prenat Diagn.* 2020;40(2):232-43.
72. Shelmerdine SC, Sebire NJ, Arthurs OJ. Perinatal post mortem ultrasound (PMUS): a practical approach. *Insights Imaging.* 2019;10(1):35.
73. Offiah CE, Dean J. Post-mortem CT and MRI: appropriate post-mortem imaging appearances and changes related to cardiopulmonary resuscitation. *The British journal of radiology.* 2016;89(1058):20150851.
74. Hutchinson JC, Shelmerdine SC, Simcock IC, Sebire NJ, Arthurs OJ. Early clinical applications for imaging at microscopic detail: microfocus computed tomography (micro-CT). *The British journal of radiology.* 2017;90(1075):20170113.
75. Shelmerdine SC, Simcock IC, Hutchinson JC, Aughwane R, Melbourne A, Nikitichev DI, et al. 3D printing from Microfocus Computed Tomography (micro-CT) in Human Specimens: Education and Future Implications. *The British journal of radiology.* 2018:20180306.
76. Alfiadi RJ, Haaga J, Meaney TF, MacIntyre WJ, Gonzalez L, Tarar R, et al. Computed Tomography of the Thorax and Abdomen; A preliminary report. *Radiology.* 1975;117(2):257-64.
77. French J, Gingles N, Stewart J, Woodhouse N. Use of magnetic resonance imaging (MRI) and micro-computed tomography (micro-CT) in the morphological examination of rat and rabbit fetuses from embryo-fetal development studies. *Reprod Toxicol.* 2010;30(2):292-300.
78. Seeram E. *Computed Tomography: Physical Principles, Clinical Applications, and Quality Control*: Elsevier; 2015.
79. Abdul Razak HR, Shaffiq Said Rahmat SM, Md Saad WM. Effects of different tube potentials and iodine concentrations on image enhancement, contrast-to-noise ratio and noise in micro-CT images: a phantom study. *Quant Imaging Med Surg.* 2013;3(5):256-61.
80. Wang J, Fleischmann D. Improving Spatial Resolution at CT: Development, Benefits, and Pitfalls. *Radiology.* 2018;289(1):261-2.
81. Flohr TG, Stierstorfer K, Suss C, Schmidt B, Primak AN, McCollough CH. Novel ultrahigh resolution data acquisition and image reconstruction for multi-detector row CT. *Med Phys.* 2007;34(5):1712-23.
82. Arthurs OJ, Guy A, Thayyil S, Wade A, Jones R, Norman W, et al. Comparison of diagnostic performance for perinatal and paediatric post-mortem imaging: CT versus MRI. *Eur Radiol.* 2016;26(7):2327-36.
83. Batiste DL, Kirkley A, Laverty S, Thain LM, Spouge AR, Gati JS, et al. High-resolution MRI and micro-CT in an ex vivo rabbit anterior cruciate ligament transection model of osteoarthritis. *Osteoarthritis Cartilage.* 2004;12(8):614-26.

84. Gignac PM, Kley NJ. Iodine-enhanced micro-CT imaging: methodological refinements for the study of the soft-tissue anatomy of post-embryonic vertebrates. *J Exp Zool B Mol Dev Evol.* 2014;322(3):166-76.
85. Gignac PM, Kley NJ, Clarke JA, Colbert MW, Morhardt AC, Cerio D, et al. Diffusible iodine-based contrast-enhanced computed tomography (diceCT): an emerging tool for rapid, high-resolution, 3-D imaging of metazoan soft tissues. *J Anat.* 2016;228(6):889-909.
86. Elliott JC, Dover SD. X-ray microtomography. *Journal of Microscopy.* 1982;126(May):211-3.
87. Paulus MJ, Gleason SS, Kennel SJ, Hunsicker PR, Johnson DK. High resolution xray Computed Tomography: An emerging tool for small animal cancer research. *Neoplasia.* 2000;2(1-2):62-70.
88. Holdsworth DW, Thornton MM. Micro-CT in small animal and specimen imaging. *Trends in Biotechnology.* 2002;20(8):S34-S9.
89. Schambach SJ, Bag S, Schilling L, Groden C, Brockmann MA. Application of micro-CT in small animal imaging. *Methods.* 2010;50(1):2-13.
90. Simcock IC, Shelmerdine SC, Hutchinson JC, Sebire NJ, Arthurs OJ. Human fetal whole-body postmortem microfocuss computed tomographic imaging. *Nature Protocols.* 2021;16(5):2594-614.
91. Gregg CL, Butcher JT. Quantitative in vivo imaging of embryonic development: opportunities and challenges. *Differentiation.* 2012;84(1):149-62.
92. Metscher BD. MicroCT for comparative morphology: simple staining methods allow high-contrast 3D imaging of diverse non-mineralized animal tissues. *BMC Physiol.* 2009;9:11.
93. Goulet R, Goldstein S, Ciarelli M, Kuhn J, Brown M, Feldkamp L. The relationship between the structural and orthogonal compressive properties of trabecular bone. *Journal of Biomechanics.* 1994;27(4):375-7 9-89.
94. Genant H, Gordon C, Jiang Y, Lang T, Link T, Majumdar S. Advanced Imaging of Bone Macro and Micro Structure. *Bone.* 1999;25:149-52.
95. Brockdorf K, Brunke O, Neuber D. NanoCT: Visualizing of Internal 3D-Structures with Submicrometer Resolution. *Microscopy and Microanalysis.* 2007;13(S02).
96. Houry BM, Bigelow EM, Smith LM, Schlecht SH, Scheller EL, Andarawis-Puri N, et al. The use of nano-computed tomography to enhance musculoskeletal research. *Connect Tissue Res.* 2015;56(2):106-19.
97. Bonse U, Hart M. *Applied Physics Letters.* 1965;6:155.
98. Bonse U, Hart M. *Applied Physics Letters.* 1965;7:99.
99. Pisano ED. Current status of full-field digital mammography. *Radiology.* 2000;214:26-8.
100. Pisano ED, Johnston ER, Chapman D, Geradts J, Iacocca MV, Livasy CA, et al. Human breast cancer specimens. diffraction-enhanced imaging. *Radiology.* 2000;214:895-901.
101. Bravin A, Coan P, Suortti P. X-ray phase-contrast imaging: from pre-clinical applications towards clinics. *Phys Med Biol.* 2013;58(1):R1-35.
102. Kotre CJ, Robson KJ. Phase-contrast and magnification radiography at diagnostic X-ray energies using a pseudo-microfocuss X-ray source. *The British journal of radiology.* 2014;87(1039):20130734.



103. Massimi L, Suaris T, Hagen CK, Endrizzi M, Munro PRT, Havariyoun G, et al. Detection of involved margins in breast specimens with X-ray phase-contrast computed tomography. *Sci Rep.* 2021;11(1):3663.
104. Dullin C, Ufartes R, Larsson E, Martin S, Lazzarini M, Tromba G, et al. muCT of ex-vivo stained mouse hearts and embryos enables a precise match between 3D virtual histology, classical histology and immunochemistry. *PLoS One.* 2017;12(2):e0170597.
105. de SJM, Zanette I, Noel PB, Cardoso MB, Kimm MA, Pfeiffer F. Three-dimensional non-destructive soft-tissue visualization with X-ray staining microtomography. *Sci Rep.* 2015;5:14088.
106. Du LY, Umoh J, Nikolov HN, Pollmann SI, Lee TY, Holdsworth DW. A quality assurance phantom for the performance evaluation of volumetric micro-CT systems. *Phys Med Biol.* 2007;52(23):7087-108.
107. Degenhardt K, Wright AC, Horng D, Padmanabhan A, Epstein JA. Rapid 3D phenotyping of cardiovascular development in mouse embryos by micro-CT with iodine staining. *Circ Cardiovasc Imaging.* 2010;3(3):314-22.
108. Sookpeng S, Butdee C. Signal-to-noise ratio and dose to the lens of the eye for computed tomography examination of the brain using an automatic tube current modulation system. *Emerg Radiol.* 2017;24(3):233-9.
109. El Ketara S, Ford NL. Time-course study of a gold nanoparticle contrast agent for cardiac-gated micro-CT imaging in mice. *Biomed Phys Eng Express.* 2020;6(3):035025.
110. Pauwels E, Van Loo D, Cornillie P, Brabant L, Van Hoorebeke L. An exploratory study of contrast agents for soft tissue visualization by means of high resolution X-ray computed tomography imaging. *J Microsc.* 2013;250(1):21-31.
111. Johnson JT, Hansen MS, Wu I, Healy LJ, Johnson CR, Jones GM, et al. Virtual histology of transgenic mouse embryos for high-throughput phenotyping. *PLoS Genet.* 2006;2(4):e61.
112. Bentley MD, Jorgensen SM, Lerman LO, Ritman EL, Romero JC. Visualization of three-dimensional nephron structure with microcomputed tomography. *Anat Rec (Hoboken).* 2007;290(3):277-83.
113. Dunmore-Buyze PJ, Tate E, Xiang FL, Detombe SA, Nong Z, Pickering JG, et al. Three-dimensional imaging of the mouse heart and vasculature using micro-CT and whole-body perfusion of iodine or phosphotungstic acid. *Contrast Media Mol Imaging.* 2014;9(5):383-90.
114. Metscher BD. MicroCT for developmental biology: a versatile tool for high-contrast 3D imaging at histological resolutions. *Dev Dyn.* 2009;238(3):632-40.
115. Quintarelli G, Zito R, JA. C. On Phosphotungstic acid staining I. *The Journal of Histochemistry and Cytochemistry.* 1971;19(11):641-7.
116. Hopkins TM, Heilman AM, Liggett JA, LaSance K, Little KJ, Hom DB, et al. Combining micro-computed tomography with histology to analyze biomedical implants for peripheral nerve repair. *J Neurosci Methods.* 2015;255:122-30.
117. Vickerton P, Jarvis J, Jeffery N. Concentration-dependent specimen shrinkage in iodine-enhanced microCT. *J Anat.* 2013;223(2):185-93.
118. Stephenson RS, Boyett MR, Hart G, Nikolaidou T, Cai X, Corno AF, et al. Contrast enhanced micro-computed tomography resolves the 3-dimensional morphology of the cardiac conduction system in mammalian hearts. *PLoS One.* 2012;7(4):e35299.

119. Ritman EL. Micro-computed tomography-current status and developments. *Annu Rev Biomed Eng.* 2004;6:185-208.
120. Tobita K, Liu X, Lo CW. Imaging modalities to assess structural birth defects in mutant mouse models. *Birth Defects Res C Embryo Today.* 2010;90(3):176-84.
121. Hutchinson JC, Arthurs OJ, Ashworth MT, Ramsey AT, Mifsud W, Lombardi CM, et al. Clinical utility of postmortem microcomputed tomography of the fetal heart: diagnostic imaging vs macroscopic dissection. *Ultrasound Obstet Gynecol.* 2016;47(1):58-64.
122. Hutchinson JC, Barrett H, Ramsey AT, Haig IG, Guy A, Sebire NJ, et al. Virtual pathological examination of the human fetal kidney using micro-CT. *Ultrasound Obstet Gynecol.* 2016;48(5):663-5.
123. Wong MD, Dorr AE, Walls JR, Lerch JP, Henkelman RM. A novel 3D mouse embryo atlas based on micro-CT. *Development.* 2012;139(17):3248-56.
124. Kim AJ, Francis R, Liu X, Devine WA, Ramirez R, Anderton SJ, et al. Microcomputed tomography provides high accuracy congenital heart disease diagnosis in neonatal and fetal mice. *Circ Cardiovasc Imaging.* 2013;6(4):551-9.
125. Lombardi CM, Zambelli V, Botta G, Moltrasio F, Cattoretti G, Lucchini V, et al. Postmortem microcomputed tomography (micro-CT) of small fetuses and hearts. *Ultrasound Obstet Gynecol.* 2014;44(5):600-9.
126. Hutchinson JC, Kang X, Shelmerdine SC, Segers V, Lombardi CM, Cannie MM, et al. Postmortem microfocus computed tomography for early gestation fetuses: a validation study against conventional autopsy. *American Journal of Obstetrics and Gynecology.* 2018;218(4):445.e1-.e12.
127. Simcock IC, Hutchinson JC, Shelmerdine SC, Matos JN, Sebire NJ, Fuentes VL, et al. Investigation of optimal sample preparation conditions with potassium triiodide and optimal imaging settings for microfocus computed tomography of excised cat hearts. *American Journal of Veterinary Research.* 2020;81:326 - 33.
128. Novo Matos J, Garcia-Canadilla P, Simcock IC, Hutchinson JC, Dobromylskyj M, Guy A, et al. Micro-computed tomography (micro-CT) for the assessment of myocardial disarray, fibrosis and ventricular mass in a feline model of hypertrophic cardiomyopathy. *Scientific Reports.* 2020;10(1).
129. Simcock IC, Shelmerdine SC, Hutchinson C, Matos JN, Sebire NJ, Arthurs OJ. Optimisation soft tissue preparation for high quality micro computed tomography. *Tomography for Scientific Advancement Symposium; University of Warwick, Coventry, UK.*2018.
130. Matos JN, Garcia-Canadilla P, Simcock IC, Hutchinson C, Dobromylskyj M, Guy A, et al. Micro-computed tomography (micro-CT) for the assessment of myocardial disarray in a feline model of hypertrophic cardiomyopathy. *Tomography for Scientific Advancement; London, UK* 2020.
131. Tan TJ, Garcia--Cañadilla P, Bijnens B, Dejea H, Bonnin A, Tran V, et al. Using micro-CT and X-PCI to visualise coronary morphology and ventriculo-coronary arterial connections in the setting of pulmonary atresia with intact ventricular septum. *Medical Careers Conference; London, UK*2018.
132. Simcock IC, Matos JN, Sebire NJ, Arthurs OJ. Optimisation of Iodination and Tissue Distortion for Micro-CT of Renal Specimens. *Tomography for Scientific Advancement Symposium; Southampton, UK.*2019.
133. Olivares AL, Pons MI, Mill J, Matos JN, Garcia P, Cerrada I, et al. Shape analysis and computational fluid simulations to assess feline left atrial function and

- thrombogenesis. *Functional Imaging and Model of the Heart*; Stanford University, California, USA2021.
134. Aslanidi OV, Nikolaidou T, Zhao J, Smaill BH, Gilbert SH, Holden AV, et al. Application of micro-computed tomography with iodine staining to cardiac imaging, segmentation, and computational model development. *IEEE Trans Med Imaging*. 2013;32(1):8-17.
  135. Liu X, Tobita K, Francis RJ, Lo CW. Imaging techniques for visualizing and phenotyping congenital heart defects in murine models. *Birth Defects Res C Embryo Today*. 2013;99(2):93-105.
  136. Pelizzo G, Calcaterra V, Lombardi C, Bussani R, Zambelli V, De Silvestri A, et al. Fetal Cardiac Impairment in Nitrofen-Induced Congenital Diaphragmatic Hernia: Postmortem Microcomputed Tomography Imaging Study. *Fetal Pediatr Pathol*. 2017;36(4):282-93.
  137. Liu X, Francis R, Kim AJ, Ramirez R, Chen G, Subramanian R, et al. Interrogating congenital heart defects with noninvasive fetal echocardiography in a mouse forward genetic screen. *Circ Cardiovasc Imaging*. 2014;7(1):31-42.
  138. Cox PG, Jeffery N. Reviewing the morphology of the jaw-closing musculature in squirrels, rats, and guinea pigs with contrast-enhanced microCT. *Anat Rec (Hoboken)*. 2011;294(6):915-28.
  139. Montaldo P, Addison S, Oliveira V, Lally PJ, Taylor AM, Sebire NJ, et al. Quantification of maceration changes using post mortem MRI in fetuses. *BMC Med Imaging*. 2016;16:34.
  140. Simcock I, Shelmerdine SC, Hutchinson C, Sebire NJ, Arthurs OJ. Tissue preparation optimisation for post-mortem human fetal micro computed tomography. *European Congress of Radiology*; Vienna, Austria 2019.
  141. Simcock IC, Shelmerdine SC, Arthurs OJ, Sebire NJ. Effect of body weight on iodination for human foetal post-mortem microCT imaging. *Insights Into Imaging*. 2021;12(Suppl 2):75.
  142. Simcock IC, Shelmerdine SC, Langan D, Sebire NJ, Arthurs OJ. Optimisation of Human Post-Mortem Micro-CT Service - Iodination and Image Quality Predictors. *International Paediatric Radiology Conference*; Marseille, France2021.
  143. Hutchinson JC, Ashworth M, Heazell AE, Levine S, Sebire NJ. Effects of intrauterine retention and postmortem interval other on bodyweight. *Ultrasound in Obstetrics and Gynecology*. 2016;48:574-8.
  144. Baker JN, Windham JA, Hinds PS, Gattuso JS, Mandrell B, Gajjar P, et al. Bereaved parents' intentions and suggestions about research autopsies in children with lethal brain tumors. *J Pediatr*. 2013;163(2):581-6.
  145. Rankin J, Wright C, Lind T. Cross sectional survey of parents' experience and views of the postmortem examination. *British Medical Journal*. 2002;324:816-8.
  146. Meaney S, Gallagher S, Lutomski JE, O'Donoghue K. Parental decision making around perinatal autopsy: a qualitative investigation. *Health Expect*. 2015;18(6):3160-71.
  147. Holste C, Pilo C, Pettersson K, Radestad I, Papadogiannakis N. Mothers' attitudes towards perinatal autopsy after stillbirth. *Acta Obstet Gynecol Scand*. 2011;90(11):1287-90.
  148. Snowdon C, Elbourne DR, Garcia J. Perinatal pathology in the context of a clinical trial: attitudes of bereaved parents. *Arch Dis Child Fetal Neonatal Ed*. 2004;89(3):F208-11.

149. Simcock IC. Coding Quantitative Data. Academic Involvement Group - ORCHID; Great Ormond Street Hospital 2020.
150. Schindelin J, Arganda-Carreras I, Frise E, Kaynig V, Longair M, Pietzsch T, et al. Fiji: an open-source platform for biological-image analysis. *Nat Methods*. 2012;9(7):676-82.
151. Simcock IC. Development of Micro-CT for Human Fetal Post-mortem Imaging. Clinical Academic Careers Evening; Great Ormond Street Hospital 2018.
152. Simcock IC. Guidelines for Imaging Small Fetuses Under 20 Weeks Gestation in Microcomputed Tomography. Allied Health Professionals in Research; Great Ormond Street Hospital, London, UK 2019.
153. Simcock IC, Shelmerdine SC, Sebire NJ, Arthurs OJ. Micro-CT of Early Gestation Fetuses: Technique, Tips & Tricks. European Congress of Radiology; Vienna 2020.
154. Simcock IC. Development of a clinical micro-CT service for human fetal post-mortem imaging. Great Ormond Street Hospital Conference; Great Ormond Street Hospital, London UK 2021.
155. Genest DR, Singer DB. Estimating the Time of Death in Stillborn Fetuses\_ III; External Fetal Examination. a Study of 86 Stillborns. *Obstetrics and gynecology*. 1992;80:593-600.
156. Shelmerdine SC, Hickson M, Sebire NJ, Arthurs OJ. Post-Mortem Magnetic Resonance Imaging Appearances of Feticide in Perinatal Deaths. *Fetal Diagn Ther*. 2019;45(4):221-9.
157. Genest DR. Estimating the Time of Death in Stillborn Fetuses II. Histologic Evaluation of the Placenta; a Study of 71 Stillborns. *Obstetrics and gynecology*. 1992;80:585-92.
158. Genest DR, Williams MA, Greene MF. Estimating the Time of Death in Stillborn Fetuses I. Histologic Evaluation of Fetal Organs; an Autopsy Study of 150 Stillborns. *Obstetrics and gynecology*. 1992;80:575-84.
159. Huda W, Scalzetti EM, Levin G. Technique Factors and Image Quality as Functions of Patient Weight at Abdominal CT. *Radiology*. 2000;217:430-5.
160. Shelmerdine SC, Simcock IC, Ciaran Hutchinson J, Guy A, Ashworth MT, Sebire NJ, et al. Post-mortem micro-CT for non-invasive autopsies: Experience in > 250 human fetuses. *American Journal of Obstetrics and Gynecology*. 2020.
161. Kang X, Sanchez TC, Arthurs OJ, Bevilacqua E, Cannie MM, Segers V, et al. Postmortem fetal imaging: prospective blinded comparison of two-dimensional ultrasound with magnetic resonance imaging. *Ultrasound Obstet Gynecol*. 2019;54(6):791-9.
162. Lewis C, Simcock IC, Arthurs OJ. Improving uptake of perinatal autopsy. *Prenat Diagn*. 2021;33(2):129-34.
163. Simcock IC, Lewis C, Shelmerdine SC, Sebire NJ, Arthurs OJ. Focus Group Findings – Parental feedback on micro-CT imaging following miscarriage. National Institute for Health Research Academy Conference; Leeds, UK 2020.
164. Simcock IC, Lewis C, Shelmerdine SC, Sebire NJ, Arthurs OJ. Knowing the answers gives you hope moving forward: parental views on micro-CT scanning following miscarriage. United Kingdom Imaging and Oncology Conference; Liverpool, UK 2021.
165. Simcock IC, Lewis C, Shelmerdine SC, Sebire NJ, Arthurs OJ. "I just wanted answers": parental views on micro-CT scanning following miscarriage. *International*

Society of Radiographers and Radiographical Technologists World Congress; Dublin, Ireland 2021.

166. Wiener L, Sweeney C, Baird K, Merchant MS, Warren KE, Corner GW, et al. What do parents want to know when considering autopsy for their child with cancer? *J Pediatr Hematol Oncol*. 2014;36(6):464-70.

167. Breeze AC, Jessop FA, Set PA, Whitehead AL, Cross JJ, Lomas DJ, et al. Minimally-invasive fetal autopsy using magnetic resonance imaging and percutaneous organ biopsies: clinical value and comparison to conventional autopsy. *Ultrasound Obstet Gynecol*. 2011;37(3):317-23.

168. Sauvegrain P, Carayol M, Piedvache A, Guery E, Bucourt M, Zeitlin J. Low autopsy acceptance after stillbirth in a disadvantaged French district: a mixed methods study. *BMC Pregnancy Childbirth*. 2019;19(1):117.

169. Braun V, Clarke V. Using thematic analysis in psychology. *Qualitative Research in Psychology*. 2006;3(2):77-101.

170. McHaffie HE, Fowlie PW, Hume R, Laing IA, Lloyd DJ, Lyon AJ. Consent to autopsy for neonates. *Arch Dis Child Fetal Neonatal Ed*. 2001;85:F4-F7.

171. Heazell AE, McLaughlin MJ, Schmidt EB, Cox P, Flenady V, Khong TY, et al. A difficult conversation? The views and experiences of parents and professionals on the consent process for perinatal postmortem after stillbirth. *BJOG*. 2012;119(8):987-97.

172. Feroz A, Ibrahim MN, McClure EM, Ali AS, Tikmani SS, Reza S, et al. Perceptions of parents and religious leaders regarding minimal invasive tissue sampling to identify the cause of death in stillbirths and neonates: results from a qualitative study. *Reprod Health*. 2019;16(1):53.

173. Sirkia K, Saarinen-Pihkala UM, Hovi L, Sariola H. Autopsy in children with cancer who die while in terminal care. *Medical and Pediatric Oncology*. 1998;30:284-9.

174. Shelmerdine SC, Hutchinson JC, Kang X, Suich JD, Ashworth M, Cannie MM, et al. Novel usage of microfocus computed tomography (micro-CT) for visualisation of human embryonic development-Implications for future non-invasive post-mortem investigation. *Prenat Diagn*. 2018;38(7):538-42.

175. Shelmerdine SC, Singh M, Simcock IC, Calder AD, Ashworth M, Beleza A, et al. Characterization of Bardet–Biedl syndrome by postmortem microfocus computed tomography (micro-CT). *Ultrasound, Obstet Gynecol*. 2019;53:129-34.

176. Kang X, Cos T, Guizani M, Cannie MM, Segers V, Jani JC. Parental acceptance of minimally invasive fetal and neonatal autopsy compared with conventional autopsy. *Prenat Diagn*. 2014;34(11):1106-10.

177. Simcock IC. Developing non-invasive imaging to investigate fetal death. Biomedical Research Centre / Institute of Child Health Showcase Event; Wellcome Institute, London, UK 2019.

178. Tommy's. Miscarriage statistics 2021 [Available from: <https://www.tommys.org/baby-loss-support/miscarriage-information-and-support/miscarriage-statistics#general>].

179. Spierson H, Kamupira S, Storey C, Heazell AEP. Professionals' Practices and Views regarding Neonatal Postmortem: Can We Improve Consent Rates by Improving Training? *Neonatology*. 2019;115(4):341-5.

180. Cullen S, Mooney E, Casey B, Downey P. An audit of healthcare professionals' knowledge regarding perinatal autopsy. *Ir J Med Sci*. 2019;188(2):583-5.

